The University Of Sheffield.

Model Predictive based load frequency control studies in a deregulated environment

Eyefujirin Evans Ejegi

A thesis in Partial Fulfilment of
the requirements for the degree of
Doctor of Philosophy

Automatic Control and Systems Engineering
University of Sheffield
April 2017

Abstract

A fundamental objective in power system operations is to ensure reliablity and quality supply, and one key action that aids the accomplishment of this objective is the load frequency control (LFC). Primarily, LFC is an automatic action that aims to restore system frequency and net tie line power between a control area (CA) and its neighbours to their scheduled values; these quantities deviate when there is an imbalance between active power demand and supply in a synchrononus interconnection. This thesis aims to investigate a model predictive control (MPC) technique for LFC problems in a deregulated power system environment which has become a challenging task. In deregulated power interconnections, generation companies (GenCos) and distribution companies (DisCos) exist in each CA, and a transmission system operator (TSO) in each area is responsible for grid reliability. Each TSO handles LFC in its CA and ensures that market participants (GenCos and DisCos) in other CAs have an unbiased and open access to its network. As a result, there has been a rise in cross-border transactions between GenCos and DisCos for bulk energy and load matching (LM) and consequently large frequency fluctuations recently. DisCos can participate in LFC by making bilateral LM contracts with GenCos. An extensive review of the LFC literature, in terms of strengths and weaknesses of different control techniques, is presented to identify the key gaps. The review reveals that MPC can bring some benefits in the deregulated environment but its strengths are underexploited.

Beginning with a small-scale system to provide insights into deregulated system modelling and predictive control design, a centralised MPC (CMPC)-based LFC scheme is proposed for a 2-area deregulated power system with measured (contracted) and unmeasured (uncontracted) load changes, where the areas are assumed to equally rated. The 2-area deregulated system is developed by incorporating bilateral LM contracts in the well known traditional LFC model as a new set of information. It is assumed that DisCos handle contracted load changes via bilateral LM contracts with GenCos and a TSO handles any variations outside the LM contracts (uncontracted) via a supplementary control scheme which represents the CMPC. The CMPC algorithm is developed as a tracking one, with an observer to provide estimates of the system states and uncontracted load changes. Also, input and incremental state constraints, which depict limits on LFC control efforts and generation rate constraints (GRC) respectively,

are considered. A simulation comparison of the proposed CMPC solution and optimal linear quadratic regulator (LQR) demonstrates the efficacy of CMPC. Developing deregulated LFC models for larger systems with complex topologies and a large number of CAs/market participants could be laborious. Therefore, a novel generalised modelling framework for deregulated LFC is further proposed. The key benefits of the generalised framework is that it provides a relatively easy and systematic procedure to develop deregulated LFC benchmark systems irrespective of the interconnection size, topology and number of market participants. It also offers the flexibility of accommodating LFC studies where CAs have either equal (often assumed) or unequal (more pragmatic) rated capacities. A 7-area deregulated benchmark model is developed from the generalised framework to illustrate its usage and significance, and the importance of incorporating area rated capacities is demonstrated via simulations. In addition, a 4-area benchmark model is developed to provide a reader with more insight into how the generalised formulation can be applied to develop LFC models for an arbitrary network.

Furthermore, to demonstrate the scalability of an MPC design procedure, the CMPC proposed previously is extended to examine the LFC problem of the 7-area system. Key novelties here are CAs are assumed to have unequal rated capacities, some GenCos do not participate in supplementary control, and the control input to each GenCo is computed separately rather than a single lumped input for each CA which is the norm in previous deregulated LFC studies. The separate control inputs is to ensure that the input constraints of each GenCo is accounted for in the CMPC in addition to their GRCs and this is achieved by incorporating the area participation factors of the GenCos explicitly in the CMPC cost function. A test conducted on the 7-area benchmark confirms the benefits of this new approach. CMPC shows great potential for deregulated LFC in terms of multiple inputs coordination, effective disturbance rejection and constraints handling; however it is unrealistic for practical interconnections were CAs are operated by different organisations and have large geographical separations.

This limitation is addressed by investigating a distributed MPC (DMPC) technique for rejecting incremental load changes, convenient for a finite number of control areas (subsystems), and therefore represents a more practical control architecture for LFC in multi-area systems. The proposed DMPC is non-cooperative and developed to operate using output feedback, where distributed observers using local measurements are developed to provide uncontracted load changes and subsystem states' estimates to local MPCs. Moreover, the DMPC, unlike other non-cooperative schemes, is simple and devoid of extensive offline parameter tuning. Using the 4-area and the 7-area benchmarks models developed as test systems for the proposed DMPC, some comparisons of simulations results, regulation cost and discussions are provided between the proposed DMPC and alternative MPC schemes.

Dedication

Dedicated to the almighty God

Acknowledgement

Firstly, I am grateful to ALMIGHTY God for his grace upon my life and for providing me with the mental amplitude to achieve such a feat. I also appreciate HIM for granting me good health from the inception of my PhD studies to this very end.

My gratitude also goes to my main supervisor, Dr Anthony Rossiter and my second supervisor, Dr Paul Trodden for their immeasurable supports, good guidance and constructive criticism which helped developed the requisite skills and experience for my PhD degree.

Finally, my profound appreciation goes to my wife, Mrs Alero Alice Ejegi, my daughters Oritsemisan Purity Ejegi and Utseoritselaju Pelia Ejegi, my Parents and Sisters for their constant prayers and words of encouragement during the course of my studies.

Contents

List of Tables

List of Figures

Abbreviations and Acronyms

AC	Alternating current.
ACE	Area Control Error.
AGC	Automatic Generation Control.
AVR	Automatic Voltage Regulator.
CA	Control Area.
CMPC	Centralised Model Predictive Control.
dDMPC	densed Distributed Model Predictive Control.
DeMPC	Decentralised Model Predictive Control.
DMPC	Distributed Model Predictive Control.
DisCo	Distribution Company.
DPM	DisCo Participation Matrix.
ED	Ecomomic Dispatch.
FACTS	Flexible Alternating Current Transmission Systems
GDB	Governor Dead Band.
GenCo	Generation Company.
GRC	Generation Rate Constraints.
HVDC	High Voltage Direct Current.
ISO	Independent System Operator.
LFC	Load Frequency Control.
LM	Load Matching.
LMI	Linear Matrix Inequality.
LQR	Linear Quadratic Regulator.
MAS	Maximal Admissible Set.
MPC	Model Predictive Control.
PFC	Primary Frequency Control.
RES	Renewable Energy Sources.
sDMPC	sparse Distributed Model Predictive Control.
SFC	Secondary Frequency Control.
TFC	Tertiary Frequency Control.
TranCo	Transmission Company.
TSO	Transmission System Operator.
UC	Unit Commitment.
UCTE	Union for the Coordination of the Transmission of Electricity.
VIU	Vertically Integrated Utility.

Chapter 1

Introduction

This chapter prepares the ground for the work reported in this document which concerns load frequency control (LFC) problems within a deregulated electricity environment. In the first place, typical controls associated with power system operations will be briefly discussed. Next, the concept of load frequency control in the power system environment will be introduced. Furthermore, the motivation for the current work will be stated. Beyond these, the main objectives of the current work will be presented, and finally the contents of the subsequent chapters of this thesis will be outlined.

1.1   Power system Control

Electrical power interconnections comprise of a wide range of components systematically coupled together to form a large-scale, complex and high-order multivariable dynamical system that can generate, transmit and distribute electrical energy over a large geographical area [2]. Despite the compexity of interconnected power systems, reliability, economy and quality supply (stable voltage and frequency) are of utmost importance, and these make the operation of power systems very challenging; reliability, economy and quality supply can be achieved through strategic planning, modelling, analysis and design of suitable control systems. In power system operations, load fluctuations and other forms of disturbance result in a number of dynamic phenomena which present themselves at different timescales due to the difference in characteristics of the components that made up the interconnection. Figure 1.1 shows typical dynamic phenomena exhibited by power networks and some important controls, adapted from [1]. Lightning propagation in high voltage transmission lines as depicted in the schematic diagram of Figure 1.1 is observable in the timescale of typically a fraction of a microsecond to few milliseconds and exhibits the fastest dynamics. Moreover, overvoltages (surge) from switching operations in transmission and distribution lines exhibits dynamics in the timescale

of a fraction of tens of microseconds to tens of milliseconds. Much slower phenomena are boiler actions and daily load cycles with dynamics spanning a few minutes to several hours, typically. In terms of controls, flexible alternating current transmission system (FACTS) control schemes are one of the fastest as they act in the timescales of a millisecond to less than a second, typically. FACTS controllers are mainly used to influence the electrical characteristics of power transmission networks in order to improve power transfer capabilities [4].

Protection systems are also considered to be fast and their function is to isolate faulty components from the network; their timescale of operation, typically, is few milliseconds to around a second. Automatic voltage control (AVC) operates in a timescale of several milliseconds to a few seconds. The role of the AVC is to maintain the terminal voltage of a generator at the set value via the automatic control of the current fed to the generator field winding by a field exciter, and this is one of the most important mechanism for voltage control in most power networks [5]. Furthermore, frequency deviations in power systems, which occur when there is an imbalance between the total active power generated across the network and power consumed (including active power losses), is mainly addressed in three control levels, namely, primary frequency control (PFC), secondary frequency control (SFC) and tertiary frequency control (TFC) shown in Figure 1.1. A PFC scheme, which typically operates in a timescale of a second to tens of seconds, is essentially the local action of turbine governing systems in power plants and its function is to quickly, if it is within its ability, reject unacceptable disturbances and keep the frequency close to the nominal value (e.g 50Hz in Europe). PFC is a proportional control strategy and thus leaves some frequency offset behind. SFC which is the subject of this report, operates in the timescale of few seconds to around ten minutes, and it plays the important role of eliminating the frequency offset left behind by PFC schemes. It restores system frequency to the nominal value by regularly adjusting load reference settings of the turbine governing system of selected power plants, and therefore their output power. SFC is traditionally an integral control scheme.

Unlike PFC which operates at a local level (installed in generating plants operating at different locations), SFC operates at the control area (CA) level, i.e., a single SFC scheme operates within a power system CA or territory; the other controls in Figure 1.1 that are relatively faster than PFC also operates locally. In multi-area systems consisting of two or more CAs interconnected via tie lines, generation-load imbalance results in changes in net tie line power exchanges, and SFC also acts to restore net tie line flows to their scheduled values. TFC is the slowest among the aforementioned frequency control levels, and it typically functions to support PFC and SFC for disturbances beyond their capabilities. TFC action deploys a replacement power reserve to compensate for disturbances and restore PFC and SFC reserves to pre-disturbance values, making PFC and SFC reserves available for future contigencies. TFC actions are mostly based on operator's manual interventions and are system-wide with respect to a control area. Much slower actions in power systems are economic operations, which

could span from an hour to a day. Economic dispatch (ED) and unit commitments (UC) fall under this category, with UC actions being relatively slower. ED operation involves allocating the total power demand amongst a number of online power generating facilities to minimize the cost of power production while satisfying operational and transmission constraints [5]. On the other hand, UC operation determines the hourly operational schedule of generating units, i.e., the order in which generating units are brought online or shutdown over a period of time, typically a day [2], so that the total daily operational cost is minimized; UC is an extention of the EC operation to generating units [5]. In addition to the timescales shown in Figure 1.1, an important consideration in stability and control system design studies (to enhance stable operation), especially with respect to modelling details, is the size of disturbance involved [6]. Generally, disturbances (perturbations) affecting power systems are classified into small-disturbance (small-signal) and large-disturbance (large-signal). In small-signal studies, the magnitude of system perturbations considered is such that phenonema of interest can be studied via a linearization of governing mathematical models, while in large-signal studies (mainly severe system disturbance whose effect could trigger protections), the nonlinear characteristics of the system must be considered in the system equations.

Another key aspect in power system studies is the overlap existing between different phenomena and control hierarchies as seen from Figure 1.1. As an example, a dynamic perturbation in the voltage control loop, depending on the magnitude, could impact on the frequency control loop. However, automatic voltage control loop whose major time constant is contributed by generator field is much faster than the frequency control loop whose time constant depends on turbine actions and mechanical inertia constants[1] of generating units [7, 8]. Hence, for small system perturbations, transients associated with automatic voltage control disappear much faster and have negligible impact on power system frequency control; this is principally true for other control loops in power systems [9]. Thus, although successful operation and control of power systems appear complicated at a glace, the various phenomena to be addressed occur at a different time intervals. This timescale feature permits power system control engineers to consider mainly the model of components relevant to a dynamic phenomenon of interest in simulation studies and the design of the various power system control schemes [2, 10–12]. Consequently, the control architecture for a power system is hierarchical, consisting of a number of decoupled control loops operating at separate time frames [9]. The work in this report is focused on secondary-level small-angle frequency control whose boundary of operation is indicated by the grey bar in Figure 1.1, where linear models are used and coupling effects of other controls (except PFC loop) are neglected.

---

[1]Time constant of turbines and generator inertia constant are much larger than that of generator field.
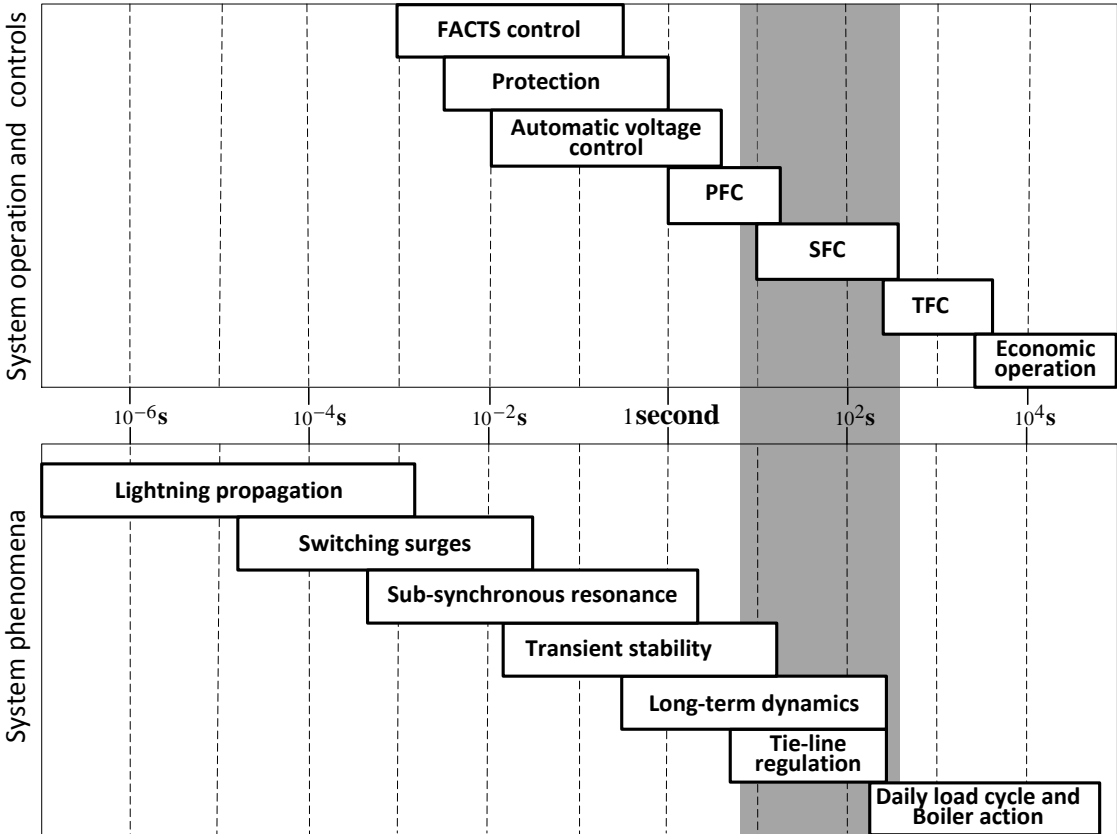
Figure 1.1: Schematic diagram of the time scale of some dynamic phenomena in power system and controls. Adapted from [1].

1.2 Load Frequency Control

Most modern day national and regional electrical power supply systems comprise of control areas (CA) interconnected via alternating current (AC) and/or high voltage direct current (HVDC) tie lines. AC interconnections, also known as synchronous interconnections, require that all CAs operate at a single frequency, and they are the most common type of interconnections; discussions in this document are focused on AC interconnections. A control area basically represents a territory where the strength of electrical interconnections within that area is stronger than the tie-lines linking it to neighbouring CAs, and consequently such area is characterized by a single frequency; a CA could be an entire country or a region within a country. To stably and reliably operate a power system and supply electrical energy of a good quality, a precise matching of total active power generation in the interconnection and load (including active power losses) at every instant in time is required. In power system operations, load variations occur throughout the day mostly due to errors in load forecast,

and since electricity cannot easily and conveniently be stored in bulk quantities, an active and continuous regulation scheme is required to constantly act to maintain system balance [2].

Power system studies have shown that an instantaneous imbalance between the total mechanical input power and the overall electrical output power of generators synchronized to the grid causes a speed-up/slow-down of their rotors and hence deviation in system frequency. This happens because the various synchronous generators (and motor loads which are frequency sensitive) in operation instantaneously compensate for the imbalance, using the stored inertia of their rotors. Consequently, there is a decrease in their angular speed (deficiency in the mechanical input power) or an increase (excess mechanical input power), and because of the direct proportionality between angular speed and frequency, there is a corresponding decrease or increase in frequency. Usually, the frequency settles at a new value, where the system finds a balance. Here, the mechanical input power is related to active power generation and the electrical output power is essentially what is consumed by system loads[2]. The instantaneous response here represents an uncontrolled natural response of synchronous machines.

If the magnitude of the frequency deviation (the magnitude of the difference between the nominal frequeny and the new value) exceeds a given thresold, PFC is activated. The thresold for PFC activation is prescribed by coordinating authorities in various jurisdications, e.g., the Union for the Coordination of Transmission of Electricity (UCTE) system in Europe requires PFC to be activated if frequency deviation exceeds ± 20mHz [5]. PFC is the first line of defense against further frequency rise or drop exceeding the set thresold. As mentioned in Section 1.1, PFC is the local action of turbine governors in power plants synchronized to grids, which senses a change in turbine speed (the turbine speed of an online generator is proportional to grid frequency) and adjust the flow of steam (steam power plants) or water (hydro power plants) to the turbine to regulate its speed, and hence network frequency.

The turbine governors of generators on PFC use a droop control mechanism, where for a fixed load reference setting, active power demand and nominal frequency, generating plants operate with some spinning reserve, i.e., they operate at levels between their upper and lower power limits. This droop mechanism allows generators online to automatically adjust their outputs (upward/downward) and collectively share the load increment/decrement at a unique frequency. A limitation of PFC is that it is vanilla proportional control scheme and needs some steady-state error to operate. Consequently, PFC keeps the system frequency at some offset away from the nominal frequency and this is undesirable. Hence additional control action is required to restore frequency to its nominal value and this is the function of the secondary frequency control. In power system, secondary frequency control is also known as load frequency control (LFC).

---

[2]When there are renewable energy sources (RES), the total active power generation includes power contributions from RES

Thus, LFC is a strategy used to re-establish PFC reserve[3], and restore system frequency and the net interchange power between a control area and adjacent neighbours their scheduled values. In electrical power industries, within each CA, the weighted CA frequency error (product of the frequency error and bias setting) is added to the net interchange error to obtain an area control error (ACE). A nonzero ACE is indicates an active power imbalance and so ACE magnitude is an index for evaluating frequency regulation performance of a CA, and traditionally, it is used as a control reference for LFC [6, 13]. LFC schemes restore system balance by sending a raise or lower signal to properly equipped online generators that are maintaining unloaded reserve capacity, and operating at a level above their minimum outputs; this also means adjusting load reference setpoints of turbine governors. Within an area, LFC is executed centrally through automatic generation control (AGC), and it is traditionally an integral control scheme. While PFC is the responsibility of every CA in a synchronous interconnection during active power imbalances, the CA where the disturbance originated is responsible for load frequency control. LFC in power systems is categorised as an operational reserved service, and power industries place a high premium on LFC because of its technicality, cost relevance in relation to other operational services, and also because of its relationship with power supply and demand. Unlike other operational services, rules for LFC provision are well documented in national electricity Acts [14].

1.2.1 Insight on frequency control based on speed-drop characteristic

One way of illustrating the concept of PFC and LFC is by considering the equivalent speed-droop characteristic of synchronised generating units in a power network as shown in Figure 1.2. It is assumed that the equivalent speed-droop characteristic of generating units is linear over the range of load and frequency variations considered. Note that the speed of synchronised generating units is proportional to the grid frequency.

Assume that at a nominal operating condition, the equivalent speed-droop characteristic of generating units online is given by the curve AA' of Figure 1.2. This nominal condition represents turbine governors operating at a fixed load reference setting. Thus every point on the curve AA' represents different frequency-load pair which is obtainable at the fixed load reference setting. For the nominal case, when the total generation matches load, the grid frequency is stabilised at its nominal value, which is shown in Figure 1.2 as the point 'a' on curve AA' ; the coordinate of the point is (P^D, f^0), where f^0 is the nominal (scheduled) grid frequency and P^D is the total load connected to the grid at the nominal frequency. Note that $P^D = P^M$ at the nominal frequency, where P^M is the total power generated in the grid.

When an additional load is added to the network at the nominal operating condition, there is a corresponding decrease in angular speed of synchronised generating units (and thus grid

---

[3]PFC spinning reserve is replaced to ensure its availability in the case of future disturbances.
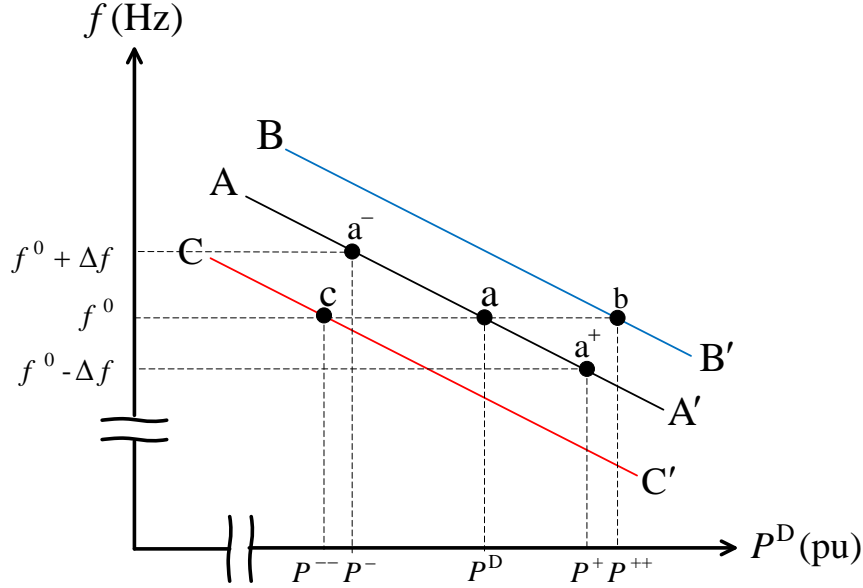
Figure 1.2: Idealised equivalent speed-droop characteristic illustrating PFC and LFC concepts

frequency). Consequently, via the droop mechanism in each generating unit, there is an increase in turbine power output, preventing the grid frequency from declining further. Assume the frequency settles at a new value $f^0 - \Delta f$, $\Delta f > 0$ after the intervention of the droop mechanism; this corresponds to a total generation $P^M = P^+$ and the point 'a$^+$' on the curve AA'. The incremental power generation in the grid as a result of the action of droop mechanisms is $\left| P^+ - P^D \right|$. Similarly, when load is withdrawn from the network which is originally operating at point 'a' on the curve AA', synchronised generating units speed-up and droop mechanisms intercept further increase in frequency, steering the grid, for example, to the equilibrium point 'a$^-$' corresponding to a frequency $f^0 + \Delta f$ and a total generation $P^M = P^-$. The decremental power generation in this case is $\left| P^D - P^- \right|$. This action of droop mechanisms whereby the the total power generation is regulated along a fixed load reference setting speed-droop curve to intercept a sudden rise or dip in grid frequency, and stabilise the frequency at a non-nominal value, is termed primary frequency control. As stated earlier, PFC, and hence the droop mechanism, is a proportional control scheme and thus stabilises the grid frequency at some offset away from the nominal value f^0; this is apparent in Figure 1.2.

For the increase in network load case (operating point 'a$^+$'), in order to restore grid frequency to the nominal value, the curve AA' must be shifted to the position BB' (blue curve) shown in Figure 1.2. For the decrease in network load case (operating point 'a$^-$'), the curve AA' must be shifted to the position CC', corresponding to the red curve in Figure 1.2, to restore the grid frequency to the nominal value. The shift in the curve AA' (black), giving rise to either curve BB' (blue) or curve CC' (red) can be achieved by changing the load reference setting of a turbine governor. This action is what is known as LFC. Note that the three curves (AA',

BB' and CC') are parallel. From Figure 1.2, the LFC action resulting in a shift from AA' to BB' corresponds to an incremental generation of $|P^{++} - P^{+}|$ while the action giving rise to curve CC' corresponds to a decremental generation of $|P^{-} - P^{--}|$. It is vital to mention that the slope of the speed-droop characteristic is the turbine-governor droop or simply droop; see Section 2.1.1 for mathematical expressions.

1.3 Research Motivation

The motivation for this work stems from the major restructuring that electrical power supply industries are experiencing globally [15], and associated technical issues [16]. In the past, power supply industries were vertically integrated where, within a CA, a large central electric utility has a monopoly franchise to own and operate the main parts of an electrical power system, namely generation, transmission and distribution, and also operational support services (LFC, voltage control, etc). Under this monopolistic and regulated framework, electric utilities were obligated to serve local consumers only and tie-lines between neighbouring CAs were mainly to provide mutual support in terms of reserve sharing and not for bulk inter-area trades [17]. Furthermore, the uncertainties in load variations and other disturbances were small, power flow patterns were highly predictable and electric utilities could satisfactorily control their large power plants. Therefore, the simple classical proportional-integral (PI) controller used by these utilities for load frequency control was adequate.

The ongoing deregulation and restructuring of power supply industries has altered the mode of planning and operation of interconnected power systems and created numerous challenges [2]. The main parts of an electricity supply system - generation, transmission and distribution - and also operational support services have been unbundled and new business entities (also known as market participants) have been created. Typically within a CA, the generation part is decomposed into a number of private generation companies (GenCos) each operating its own power station, and competing with each other and with GenCos in neighbouring CAs to sell power; distribution is divided into a number of distribution companies (DisCos) each owning and operating the different sections of the distribution network, and competing to sell power to consumers. A DisCo can purchase electrical power from any GenCo in its area and across CA boundaries. The transmission layer within a CA or service territory remains a natural monopoly and owned by a transmission company (TranCo). An independent entity known as a transmission system operator (TSO) has emerged in each CA territory to ensure a reliable transmission system operation. The TSO, in the new framework, handles operational support services (including LFC) which are now commonly known as ancillary services, ensures that market participants (GenCos and DisCos) in neighbouring CAs have open and an unbiased access to its transmission facilities and also coordinates power transactions. The TSO does

not own a generating plant and must procure LFC reserve capacity from its local GenCos competing/bidding to sell incremental (or decremental) power. DisCos can also contribute to LFC by making load matching (LM) contracts with GenCos in any area.

The advent of deregulation and open transmission access has not only led to an explosion in the volume of inter-area (cross-border) power transactions, it has created a degree of freedom for GenCos and DisCos in any area to bypass grid operators (TSO in this case) and make power contracts. The large number of inter-area power contracts have resulted in a reduced predictability in load variations and other grid distrurbance, and a highly uncertain and non-repetitive power flow patterns. Electrical energy flows in interconnected networks are guided by physical network laws (ohm's and Kirchhoff's law) and may not flow according to agreed "contract paths", hence in the deregulated environment, disturbances of irregular patterns intermittently propagate to TSOs' networks, with the TSOs having no advance knowledge of such grid disturbances. Currently, power grids are being operated with reduced security margins due to economic pressures in the power market; the strong overlap between power market[4], the physical network and system control is creating large frequency oscillations in the new (deregulated) environment [17–21]. These technical issues, created by deregulation, as well as the poor coordination existing between control areas in power networks, present a greater challenge for a secure and reliable grid operation [11, 22]. Therefore obtaining satisfactory control performance with classical PI controllers, whose gains obtained heuristically through lengthy tuning and field testing are fixed, is difficult.

This challenge is evident in the number of major electric grid blackouts experienced in recent times; for example, the Northeast blackout (August 14, 2003); the Sweden-Denmark blackout (September 23, 2003); the Italy blackout (September 28, 2003) and the biggest in history, the Indian blackout (July 30 & 31, 2012); the blackout in Turkey (March 31, 2015) [23–25]. These blackouts indicate the need for a thorough review of all problems associated with power system control, coordination, real-time information exchange between CAs and instability. The blackouts have shown that a novel system modelling incorporating power contract data and more efficient control strategies are required to ensure improved system security, reliability and power quality in the new environment. Power system experts have recommended a review of LFC strategies in most post-blackout [26]; large frequency deviations resulting from poor coordination and information exchange between control areas has also been reported as part of the root cause of the recent blackouts [27]. The LFC problem in today's power system has further been reinforced by the high penetration of renewable energy resources (RES) with no inertial support, and whose contribution to power demands cannot be precisely predicted; smaller power plants with low inertias are being introduced by some GenCos. Hence, there has been a reduction in the inertia per unit generation available in most power networks.

---

[4]Market participants are inclined towards maximising profits.

Significant frequency deviations can damage turbine blades due to vibratory stress, degrade the performance of power plant auxiliaries and overload tie lines. This can lead to a cascaded tripping of frequency relays and subsequently an unstable condition for the power grid [18]. Frequency deviations could make power plants work inefficiently, hence resulting in higher emissions which can have a negative impact on the environment [19]. Moreover, most faulty conditions in power networks present themselves as frequency deviations; by reducing typical frequency fluctuations to very small ripples, frequency deviations resulting from a fault can be detected early [7].

Several works have been published on the LFC issue. These works have adopted control strategies ranging from standard classical control techniques to modern control strategies such as optimal linear quadratic regulator (LQR), robust control and intelligent control methods. Nonetheless, the majority of the works were focused on vertically integrated power system structure. Some publications have considered LFC in a deregulated environment, but the strategies have either yielded a very high order controller and/or neglect practical system constraints, as the strategies lack constraints handling capabilities. In view of the above mentioned challenges in the deregulated environment, the current work considers the development of novel centralised and distributed model predictive control (MPC) based LFC schemes that possess some qualities specified by the IEEE system control subcommittee [12]:

- Simple structure: A straightforward and systematic procedure is followed in the design of the MPC based LFC schemes to ensure easy understandability, maintainability and reliability, and ultimately making the schemes attractive to electric power industries. Naturally, the underlying concept of MPC schemes is simple, and it has found extensive applications in petrochemical, food, and other related industries. It has also been used in the past to meet specialised control needs of electric power plants [28].

- Constraints handling: Important practical system limits such as generation rate constraints (GRC) and constraints on power plant inputs will be considered. One of the strongest points of MPC strategies, which industrial practioners found attractive, is its ability to dynamically enforce constraints, and this capability will be be deployed in this work.

- Scalable and adaptable to structural change: With minor modifications, the predictive control scheme should be able to cope with the removal or addition of a subsystem (CA) within the large interconnected power system. Furthermore, it should be flexible enough to cope with various types of power transactions in the deregulated environment.

- Non-centralised and coordinated: One of the contributions of this work will be to develop a distributed MPC (DMPC) scheme for LFC. This quality is important because today's

power system consists of a number of CAs having large geographical separations, and it is pragmatic to control such power interconnections in a non-centralised fashion.

- Meet basic LFC objectives: The control schemes should be able to restore system frequency and net tie line flows to their scheduled values, cope with a wide range of load fluctuations and make control decisions that are economical and optimal in some sense. Note that MPC algorithms take control decisions at every sampling instant by optimising predicted future behaviour of the system involved.

1.4 Aims and objectives

The main aim of this thesis is to investigate the use of an advanced process control method in power systems load frequency control problem, specifically a predictive control technique, to effectively coordinate the rising number of local and cross-border load matching (LM) power contracts amongst power system business entities and reject the various unmeasured disturbances in currently expanding deregulated power system interconnections. Furthermore, by considering the realistic control architecture where each CA has its own locally operating LFC scheme (a predictive controller in this case), this thesis will also examine the possibility of obtaining an improved system-wide control performance through a coordination and exchange of information between CAs. A new modelling framework will be developed through a modification of the traditional LFC models to incorporate power contract data between GenCos and DisCos. The contract data are modelled by extending the concept of a disco participation matrix (DPM) which was proposed for a 2-area deregulated system in [29]. In addition, deregulated LFC benchmark models of different sizes will be developed, and predictive control frameworks using area control error (ACE) measurements only will be proposed and implemented on the deregulated LFC benchmark systems.

LFC schemes currently in use in power industries use ACE measurements, and using a similar information in the predictive control schemes will aid practical implementability. The hypothesis here is that this aim can be achieved via predictive control for the following reason. Power system LFC is a multivariable control problem and predictive control technology has distinguished itself in various fields of application (oil refineries, petrochemicals, food processing, etc.) as an effective means of handling multivariable control problems [28]. Furthermore, practically important constraints/nonlinearities such as generation rate constraints (GRC) and control input limits [6, 12, 30], can easily and systematically be incorporated into MPC framework. It has been shown that the conventional PI based LFC and linear optimal control LFC strategy could result in oscillatory responses, and an unstable condition in some cases, in the presence of GRC [31, 32]. Control signals from predictive control regulators are typically obtained from an optimisation and hence are economically optimal in some sense; this property

could lead to some cost reduction in LFC. One limitation that has been identified in predictive control schemes is the computational time involved in the optimisation steps. However, LFC is a relatively slow process and there is no peculiar control or ecomonic purpose served by hastening the LFC action [12].

Key objectives

The key objectives to achieving the aim of this thesis are as follows:

1. Highlight the key strengths and weaknesses of current load frequency control methods and thus provide a platform for future studies.

2. Propose, for the 2-area deregulated LFC model developed in [29], a centralised MPC based load frequency control scheme which incorporate physical system limits/nonlinearites such as GRC and power plants' input constraints, and demonstrating the efficacy of the centralised MPC in constraints handling through simulations.

3. Propose a novel generalised LFC modelling framework that effectively captures the various power transactions in the deregulated environment, by modifying the traditional LFC modelling framework. The generalised formulation can be easily used to develop benchmark models for multi-area power networks irrespective of their topologies, and having an arbitrary number of interconnected CAs, GenCos and DisCos, for LFC simulation and control design studies in the deregulated environment. Also, studies where interconnected CAs either have equal (often assumed in the literature) or unequal capacity ratings can be accommodated.

4. Illustrate how one can utilised the generalised framework by developing a 7-area deregulated benchmark system from the framework and also providing simulation evidence to demonstrate the significance and effectiveness of the generalised framework.

5. Demonstrate scalability of MPC algorithms by extending the proposed centralised MPC algorithm to the developed 7-area deregulated benchmark systems and considers a more logical scenario where GenCos and DisCos have their private choices. The MPC problem is modified such that the control input of each GenCo is considered rather than a lumped control input for each CA which is the common practice in the deregulated LFC literature. With this approach, the input constraints of each GenCo can be accounted for.

6. Propose a practically implementable non-cooperative distributed model predictive control scheme for LFC and compare its performance with centralised and decentralised MPC schemes, on a developed 4-area benchmark system and also on the 7-area system to demonstrate scalability. GRC and input constraints are taken into consideration.

The proposed control schemes (centralised, distributed, etc) are developed to operate using output feedback, where a central observer (the centralised MPC studies) and distributed observers (the distributed MPC studies), using area control error measurements, provide MPC controllers with state and unmeasured disturbance estimations.

1.5 Supporting publications

This thesis is supported by the following publications

Conference papers

1. **E.E. Ejegi**, J.A. Rossiter, and P. Trodden (2014). A survey of techniques and opportunities in power system automatic generation control. *United Kingdom Automatic Control Conference - UKACC,* Loughborough, UK

2. **E.E. Ejegi**, J.A. Rossiter, and P. Trodden (2015). Model predictive load frequency control of a two-area deregulated power system. *European Control Conference - ECC,* Linz, Austria.

3. **E.E. Ejegi**, J.A. Rossiter, and P. Trodden (2016). Generalized model for load frequency control studies in a deregulated environment. *European Control Conference - ECC,* Aalborg, Denmark.

4. **E.E. Ejegi**, J.A. Rossiter, and P. Trodden (2016). Distributed model predictive load frequency control of a deregulated power system. *United Kingdom Automatic Control Conference - UKACC,* Belfast, Northern Ireland, UK.

Journal papers to be submitted

1. **E.E. Ejegi**, J.A. Rossiter, and P. Trodden (xxxx). Predictive load frequency control of an interconnected power system after deregulation.

2. **E.E. Ejegi**, J.A. Rossiter, and P. Trodden (xxxx). Distributed predictive control for power system load frequency control after deregulation.

1.6 Outine of the thesis

The work presented in this document comprises of 8 chapters. A summary of each of them and key contributions is presented here.

Chapter 2 The fundamentals of load frequency control, including definitions, structures and key concepts, are presented. The framework of LFC reported in this chapter is based on the traditional vertically integrated utilities (VIUs) where a large central utility owns and operates the generation, transmission and distribution facilities within its own service area (control area). Furthermore, a discussion of power system deregulation and restructuring, and the main market structures for the provision of LFC in the deregulated paradigm, is provided. Finally, a survey of the control techniques which have been suggested for power system load frequency controls is given. Different control schemes have been grouped and a summary of their strengths and weaknesses, in the context of applications, is provided. The summary is a useful starting point for determining where future control research is likely to bring great benefits to the structurally changing large scale interconnected power systems. A portion of this chapter appear in [33] and its a key **contribution** in this thesis.

Chapter 3 A theoretical background on the different predictive control architectures, namely, centralised, decentralised and distributed predictive control architectures, is presented. The basic attributes of the different predictive control architectures are emphasised. The chapter concludes with a summary of the key points to note about predictive control and its suitability to power system LFC problem.

Chapter 4 This chapter proposes a centralised model predictive control based LFC scheme for a 2-area deregulated power system with measured (contracted) and unmeasured (uncontracted) load variations. The contracted load changes (with values agreed in advance) represent bilateral LM contracts between GenCos and DisCos, while the uncontracted changes represent real time load variations resulting from DisCos that have not procured an LM contract and variations from unavoidable LM contract violations. The proposed MPC design problem is formulated as a tracking one where state and input constraints, representing GRC and input constraints respectively, are systematically included. Furthermore, the scheme is developed to work as output feedback, where an observer is designed to estimate system states and uncontracted load variations from ACE measurements. Simulations are provided, based on comparisons with optimal linear quadratic regulator (LQR), to demonstrate the efficacy of the proposed MPC based LFC scheme. This chapter is based on the work in [34] and its a key **contribution** in this thesis.

Chapter 5 In Chapter 4, a 2-area deregulated benchmark model is utilised in the studies to emphasise clarity in terms of the key steps in developing LFC models which incorporate power transactions; the procedure could become burdensome as the number of control areas, market participants and complexity of a network's topology increase. Hence, this chapter proposes a novel generalised modelling framework for LFC simulations and control design studies in a deregulated environment. The key advantage of this formulation is that it can accommodate

LFC studies in a realistic environment, where interconnected control areas (CAs) have different rated capacities. In addition, it can be used to develop benchmark LFC models for muti-area networks of an arbitrary size, topology, having any number of GenCos and DisCos. The significance and effectiveness of this formulation is demonstrated using a 7-area deregulated benchmark model developed from the generalised framework, which is a modification of the CIGRE-7 machine test system. A 4-area deregulated model is also developed to provide more insight into how one can use the generalised framework, and to use as a case study model in Chapter 7. A portion of this chapter is appears in [35, 36] and its a key **contribution** in this thesis.

Chapter 6 In this chapter, we propose a more generic centralised MPC based supplementary control (LFC) scheme for the 7-area deregulated benchmark model developed in Chapter 5. The proposed scheme is developed to coordinate measured (contracted) load variations and rejected unmeasured (uncontracted) load variations. The predictive control scheme receives state and unmeasured disturbance estimates from an observer using ACE measurements, and steady state target information from a target calculator. In the scheme presented in Chapter 4 and other LFC schemes in the literature, a single (lumped) supplementary control signal is generated for each CA of the system when there is an active power imbalance, and the lumped signal is spit up according to the different participation factors of committed GenCos in the CA and each strand of the splitted signal serves as the control input to their speed governors[5]. This approach may result in violations of generator's input constraints, especially during transients. Here, we absorbed the participation factors into the MPC optimisation and send separate control signals to each GenCo and thus, accounting for their individual input constraints. Furthermore, GRC of each GenCo on supplementary control is included in the MPC design. A more logical scenario where interconnected CAs have unequal capacity ratings and some GenCos opting out of supplementary control is considered, and simulation results are provided to demonstrate the effectiveness of the proposed scheme. This chapter is based on the work in [36] and its a key **contribution** in this thesis.

Chapter 7 This chapter focuses on developing a new distributed control scheme for LFC problems in deregulated power systems, capable of providing acceptable dynamic performance and good constraint handling capabilities. To this end, a non-cooperative distributed model predictive control (DMPC) algorithm is developed and tested on the 4-area and the 7-area deregulated benchmark models developed in Chapter 5; two different benchmark models are utilised here to show scalability. The DMPC scheme is developed to operate using output feedback, where distributed observers using local area control error measurements supply each

---

[5]In this thesis, a GenCo is represented by a single generator model consisting of a governor and turbine model connected

local MPC scheme with state and unmeasured disturbance estimations. The DMPC here, unlike other non-cooperative schemes, is simple and devoid of extensive offline parameter tuning. Some comparisons and discussions are provided between the DMPC and alternative model predictive control schemes. This chapter is based on the work in [37, 38] and its a key **contribution** in this thesis.

Chapter 8 A summary of the original contribution of this thesis, and some concluding remarks, are presented. Finally, possible directions for future work are stated.

Chapter 2

Background to frequency control and literature review

In Chapter 1, it was stated that electric power systems exhibit a wide range of dynamic phenomena occurring at different time scales (ranging from very fast to very slow dynamics) when perturbed, and various fast and slow acting controls have been developed to control these phenomena and ensure satisfactory operations. It was also emphasised that the time scale feature of power systems means that one can focus on components closely associated with a phenomenon when developing models for control system studies, and that this thesis is focused on small-angle load frequency control (LFC). As stated in Section 1.4, an aim of this thesis is to investigate the efficacy of predictive control schemes as a LFC strategy in a deregulated power system environment, where a key objective is to propose a novel generalised deregulated LFC modelling framework via the modification of the age-long traditional LFC model[1].

Consequently, this chapter, firstly, provides the mathematical fundamentals of the traditional LFC modelling framework; Chapter 3 is dedicated to providing the mathematical fundamentals of predictive control. Also in this chapter, important definitions and key concepts in this subject are highlighted and some previously explained concepts in Chapter 1 are reiterated for completeness. Moreover, the ongoing deregulation and operational restructuring in power industries globally and the main market structures that have emerged for energy and frequency regulation are discussed. A detailed survey of the control techniques which have been applied to load frequency control of power systems is presented. Based on objective 1 in Section 1.4, different control approaches have been categorised and a summary has been given of the context of application and strengths and weaknesses. Such a summary is an effective starting point for determining where future control research is likely to bring the most benefit to the

---

[1]The traditional framework here also means the vertically integrated utility structure.
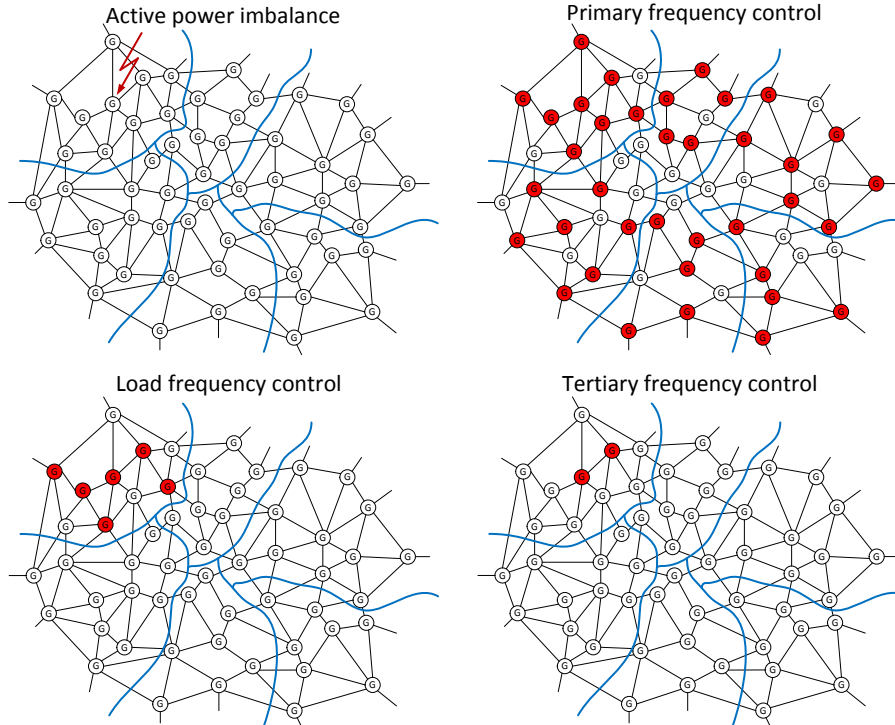
Figure 2.1: Illustration of the main control stages in frequency control

emerging large scale and interconnected structures in the power supply market. A portion of this chapter appears in [33] and it is a key **contribution** in this thesis.

This chapter is organised as follows: Section 2.1 gives an overview of frequency control and develops the mathematical model for LFC studies in the VIU (traditional) environment; Section 2.2 discusses power system deregulation and the market structures for LFC that have emerged; Section 2.3 presents a summary of issues that have been studied in LFC to date; Section 2.4 presents an extensive survey of LFC design, groups them into different control techniques and summarises their main strengths and weaknesses in a tabular form; Section 2.5 reports other LFC studies which do not exactly fall into control techniques discussed in Section 2.4, and are mainly focused on analysis.

Section 2.6, concludes this chapter by briefly stating the key message in each section (Sections 2.1-2.5), their importance to this thesis, and how they relate to the aims and objectives of this thesis.

2.1 Traditional LFC scheme

In synchronous power networks, frequency is a common denominator, and as stated in Section 1.2, a secure and reliable operation requires that frequency should remain fairly constant across

the network. The constancy of frequency is dependent on the balance between net active power supplied by generators in the interconnection and the overall system load (including losses) [6]. If the total load (demand) connected to the network exceeds the active power supply, kinetic energy is extracted from the inertial storage of synchronized generators and frequency sensitive loads (e.g AC motors) to compensate for the excess load. Consequently, the machines decelerate and hence the system frequency declines. Conversely, if the net active power supply exceeds consumer demands, the excess electrical power is taken up by online generators and frequency sensitive loads. This speeds up the machines and results in a frequency rise. The main control stages for addressing frequency deviations - primary frequency control (PFC), load frequency control (LFC) and tertiary frequency control (TFC) - are in general dimensioned according to the time of action (rapidity), volume of active power reserve they deploy and duration of deloyment of the power reserve [39]. For example, in the continental European synchronous interconnection, a total of 3000 MW (volume) of active power is reserved for PFC; this must be activated within few seconds (rapidity) following an active power imbalance, and PFC reserve must be emptied in the duration of a few seconds to a maximum of 30 seconds [40].

Furthermore, PFC is the joint responsibility of the different control areas that are part of an interconnection, that is, irrespective of the control area where a disturbance occurred, primary control reserves are activated in every location to minimize the risk of overloading some transmission corridors [2]. Load frequency control which acts to eliminate the frequency offset left after the proportional control action of PFC and restores an area net tie line flow to its scheduled value, is the responsibility of the CA where a disturbance had occurred; this is to ensure that the steady state net power interchanges between neighbouring CAs are maintained at their scheduled values. TFC reserves are only activated (often manually) to support and replace LFC in the case of major disturbances. The TFC reserves are left running until generating units are re-scheduled to accommodate the new situation [41]. Tertiary reserves are provided by large generating units in the area where the disturbance had occurred. The frequency control stages are illustrated in Figure 2.1, where the network is partitioned into six control areas; the blue lines indicate CA boundaries and the red circles indicate generators providing various reserves.

In power system LFC via automatic generation control (AGC), the slow manual TFC actions are often not considered; this is because, TFC reserve utilisation is complementary to electrical energy production scheduling which is done based on offline economic optimisations [9]. The basic structure of a traditional LFC scheme is shown in Figure 2.2. The structure consists of a PFC loop, a LFC loop and the main elements/components whose characteristics effect power system frequency control. The various frequency control loops as well as the other components shown in Figure 2.2 are discussed in detail in the following subsections, with some definitions re-emphasised for completeness.
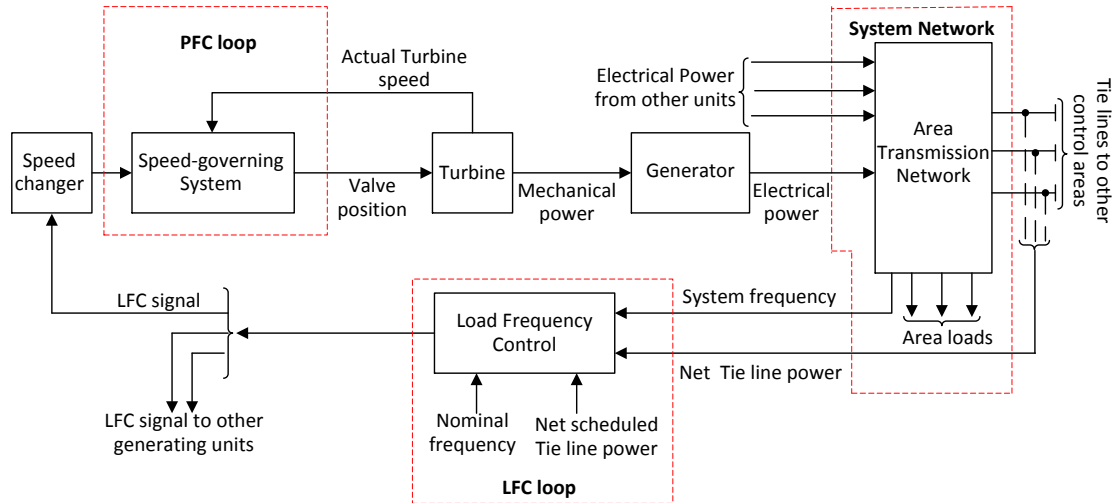
Figure 2.2: The basic schematic of frequency control in power system. Normal system operation is assumed and hence the tertiary frequency control loop is not included.

This section is organised as follows: Section 2.1.1 develops the dynamic model of the PFC loop; Section 2.1.2 presents the dynamic model of the turbine system; Section 2.1.3 presents the network dynamic model of a control area (CA) which incorporate the equivalent inertia of generating units in the CA, equivalent damping of frequency sensitive loads, total area generation and load increments. The resulting model is also known as the CA swing equation; Section 2.1.4 presents mathematical expressions of the LFC loop; Section 2.1.5 presents a complete LFC block for a typical VIU area, by combining the models presented in the Sections 2.1.1-2.1.4; Section 2.1.6 presents simulation examples to demonstrate the concept of frequency control in the VIU environment; Section 2.1.8 summarises what has been presented in this section. Note that with every LFC framework, the primary frequency control loop (PFC) is embedded as a static feedback loop. However, as will be demonstrated in the simulation example presented in Section 2.1.6, the PFC loop alone cannot restore frequency and tie line flows to their scheduled value, as emphasised in Sections 1.2 and 2.1.

2.1.1 Primary frequency control loop

A PFC loop is important to enable turbines to operate in a stable manner; it is the speed governing system of a turbine. For a fixed governor load reference setpoint, the PFC loop continuously compares the turbine actual speed with its scheduled speed (proportional to the nominal frequency) and using the speed error (proportional to frequency error) to adjust the governor valve position and hence steam flow into steam turbines (or gate position and hence

water flow into hydroturbines); the speed error will only exist when there is a generation-load mismatch. This action, also known as droop control, regulates the turbine output power in the direction of the system disturbance. The PFC loop intercepts frequency drifts as quickly as possible when a disturbance exceeding a given thresold occurs. A schematic of the turbine governing system is shown in Figure 2.3, and resulting block representation is shown in Figure 2.4.
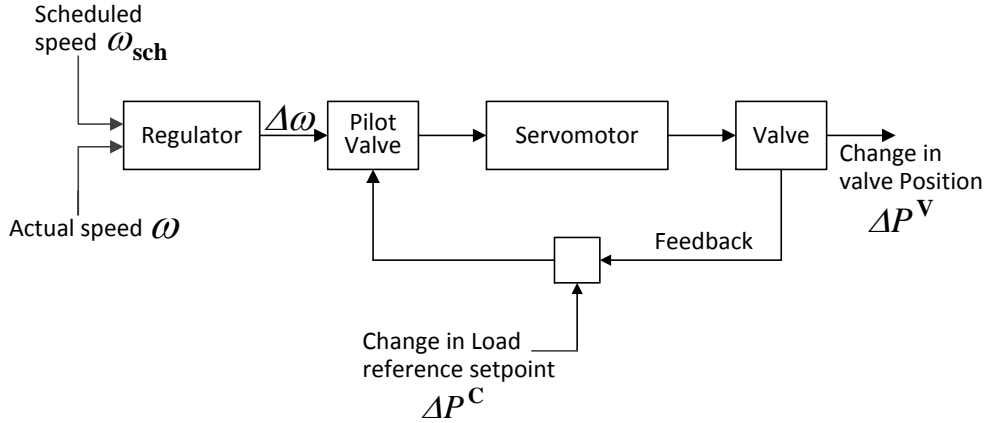
Figure 2.3: Schematic of a steam turbine speed governing system. Adapted from [2], with steam flow feedback neglected.
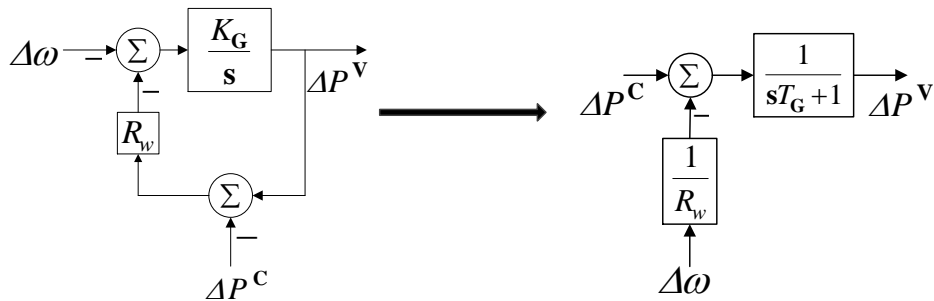
Figure 2.4: Transfer function representation of the turbine governing system.

The turbine governing system model presented here is of the General Electric electro-hydraulic without steam feedback type and this is adequate for most large scale analysis [42] . In addition, turbine governors have dead bands, which allows them to be insensitive to frequency deviations below a set threshold deadbands. The dead band is also not considered in the model and this is usually not an issue in large-scale system studies [42]. In studies where the prime concern is the performance of the turbine governor itself, it may be necessary to consider dead bands [42]. Furthermore, because frequency control reserves are either incremental or decremental power/energy, variables in Figure 2.3 and 2.4 have been expressed as deviations centred around

their nominal values. For small disturbances, the mathematical model of the turbine speed governing system shown in Figure 2.3 and 2.4 is:

$$\Delta \dot{P}^{\mathrm{V}} = \frac{1}{T_{\mathrm{G}}}(\Delta P^{\mathrm{C}} - \Delta P^{\mathrm{V}} - \frac{1}{R}\Delta f) \tag{2.1}$$

where $T_{\mathrm{G}} = \dfrac{1}{K_{\mathrm{G}} R_w}$ in seconds is the time constant of the speed governing system; R_w in Hz/pu MW is the droop; $R = \dfrac{R_w}{2\pi}$ in Hz/pu MW is the scaled droop; K_{G} is the amplification gain of the servomotor. The droop R_w is the percentage change in angular speed required to cause a 100% valve movement (from fully open to fully closed) when the load reference setpoint is fixed. It is important to note that turbine valve position, ideally, has the unit of displacement; however, the ultimate interest here is the resulting change in electrical power generation. Therefore, ΔP_{v} which corresponds to the change in the governor valve position is expressed in pu MW. Also, the change in load reference setpoint ΔP^{C} is also expressed in pu MW; ΔP^{C} is zero for PFC since the load reference setpoint is fixed. The power quantities are measured in per-unit as this is the practice in power system analysis; it helps to bring generating plants' quantities such as current, voltage, power, etc, of different ratings to within the same range, and this helps to simplify calculations and provide an intuitive perception of the performance of generating units [2]. For frequency control studies, power quantities (generation and loads) are divided by the total megawatt rating of a CA to obtain their per-unit (pu) equivalents [7, 43].

2.1.2 Turbine dynamic model

The turbine dynamics are crucial in frequency control studies. The turbine converts changes in steam flow (water flow), due to a change in valve position (gate position), to a mechanical power/torque that drives generating units and change their outputs. Depending on the type of turbine considered, its characteristics, as well as model representation, are different. The various types of turbines and their models as suggested by an IEEE committee can be found in [42]. In this report, we consider the non-reheat steam turbine; its configuration as well as the transfer function block is shown in Figure 2.5.

Generation rate constraint (GRC) nonlinearity is included in Figure 2.5 as this is very important in LFC studies [5, 12, 30, 42]. GRC imposes a limit on the speed at which a thermal generating unit can change its output power. A thermal unit changing its output too rapidly would encounter thermal and mechanical stresses which could reduce its lifespan. From the transfer function block representation in Figure 2.5, the turbine dynamics, assuming small perturbation is given as:
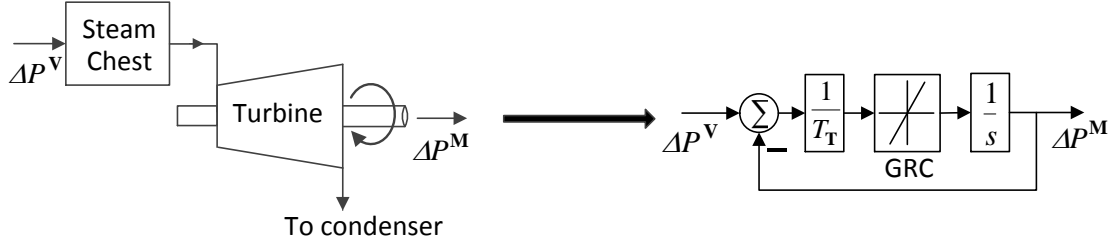
Figure 2.5: Schematic of a non-reheat steam turbine [3]. The transfer function block includes a GRC nonlinearity

$$\Delta\dot{P}^{\mathrm{M}} = \mathrm{sat}_{\Delta\dot{P}^{\mathrm{M}}}\left\{\frac{1}{T_T}(\Delta P^{\mathrm{V}} - \Delta P^{\mathrm{M}})\right\} \tag{2.2}$$

In (2.2), $\mathrm{sat}_{\Delta\dot{P}^{\mathrm{M}}}$ denotes the generation rate constraint. ΔP^{M} represents the change in mechanical output power of the turbine. Note that this thesis considers only steam turbines. Again, the primary concern is the resulting change in the electrical power output of the generating units, hence ΔP^{M} is expressed in pu MW.

2.1.3 System network representation

To obtain the dynamic representation of the system network, the transmission network in Figure 2.2 is considered as that of the ith control area (CA). Furthermore, it is assumed that the different generators synchronized to the network within a CA form a coherent group, that is, the generators will swing in unison in response to a disturbance; this assumption is commonplace in frequency control studies. Consequently, a single frequency can be defined for a control area. Now, consider the scenario when there is an increase in the total real load connected to the Area i network, ΔP_i^{D}, MW. As a result of the load increase, generating units on LFC, synchronized to Area i network, will receive a raise signal from the area control centre and thus increment their electrical output power. Let ΔP_i^{G} MW denote the total generation change in the ith CA; assuming the losses in generating units are negligible [8], then $\Delta P_i^{\mathrm{G}} = \Delta P_i^{\mathrm{M}}$, where ΔP_i^{M}, MW denotes the total change in mechanical output power of the turbines. Henceforth, ΔP_i^{M} MW will represent the total generation change in the ith CA. The total generation change ΔP_i^{M}, assuming an increase, will be consumed in four ways:

1. To reject the total load change (load increase) ΔP_i^{D} MW

2. Restore the area kinetic energy W_i^{E} that was "borrowed" instantaneously to compensate for ΔP_i^{D}.

3. For multi-area system, ΔP_i^{D} results in a drift in net tie line power flow of a CA from its scheduled value. Hence, part of the total generation change is consumed via a change (an increase) in the net tie line power flow $\Delta P_i^{\mathrm{tie}}$ of the ith CA; the convention here is that ΔP^{tie} MW is positive for power flow out of a CA.

4. Frequency sensitive loads (e.g synchronous motors) reduce their active power consumptions when frequency declines due to a load increase, ΔP_i^{D} . Hence, there is an increase in the power consumed by these loads when there is a total generation increase.

Points 2 and 4 in Section 2.1.3 will be briefly discussed in Sections 2.1.3.1 and 2.1.3.2; a power balance expression based on incremental changes for the ith CA will be stated in Section 2.1.3.3 and the incremental tie line dynamics will be developed in Section 2.1.3.4.

2.1.3.1 Area kinetic energy

When there is a sudden increase in load in a network, a corresponding increase in the output power of the turbines, and hence power output of generating units cannot happen instantaneously. Therefore, there is an instantaneous extraction of kinetic energy from the rotors of generating units. When the generating units eventually respond to the LFC signal and change their power outputs, the area kinetic energy is restored at a rate[2] expressed as

$$\Delta P_i^{\mathrm{E}} = \frac{d}{dt}\{W_i^{\mathrm{E}}\} = \frac{d}{dt}\left\{W_i^0\left(\frac{f^0 + \Delta f_i}{f^0}\right)^2\right\} \tag{2.3}$$

where ΔP_i^{E} is the incremental kinetic power; f^0 is the nominal speed/frequency; W_i^0, MWsec, is the area kinetic energy at the nominal frequency; Δf_i is the frequency deviation in the ith CA. The squared term (2.3) indicates that the area kinetic energy is proportional to the square of the instantaneous speed of machines and hence frequency. For small disturbance, $\Delta f_i \ll f^0$ and (2.3) can be stated as

$$\Delta P_i^{\mathrm{E}} \approx \frac{2W_i^0}{f^0}\frac{d}{dt}\{\Delta f_i\} \tag{2.4}$$

2.1.3.2 Frequency sensitivity of loads

As frequency increases due to ΔP_i^{M}, motor loads increase their power consumptions by an amount given as:

$$\Delta P_i^{\star} = \frac{\partial P_i^{\mathrm{D}}}{\partial f^0}\Delta f_i = D_i \Delta f_i \tag{2.5}$$

---

[2]Power is the rate of change of energy.

Here, constant D_i MW/Hz, is the rate at which area i load changes with frequency. For small frequency deviations it is assumed that the load frequency characteristic , $\dfrac{\partial P_i^{\mathrm{D}}}{\partial f^0} = D_i$ is linear and can be considered to be approximately constant [7, 8]. D_i is also known as the equivalent damping of the ith CA.

2.1.3.3 Control area power balance

The incremental power balance expression of the ith CA based on the total generation change in the ith CA can be stated by collecting (2.4), (2.5) and points 1 and 3 of Section 2.1.3:

$$\Delta P_i^{\mathrm{M}} = \Delta P_i^{\mathrm{D}} + \frac{2W_i^0}{f^0}\frac{d}{dt}\{\Delta f_i\} + \Delta P_i^{\mathrm{tie}} + D_i\Delta f_i \tag{2.6}$$

The expression in (2.6) is in the megawatt (MW) unit. Dividing through (2.6) by the rated capacity (total megawatt rating) of the ith CA, P_{r_i} MW gives:

$$\Delta P_i^{\mathrm{M}} = \Delta P_i^{\mathrm{D}} + H_i\dot{\Delta f_i} + \Delta P_i^{\mathrm{tie}} + D_i\Delta f_i \tag{2.7}$$

Terms ΔP_i^{M}, $\Delta P_i^{\mathrm{tie}}$ and ΔP_i^{D} are now pu MW and $H_i = \dfrac{2W_i^0}{f^0 P_{r_i}}$. The term H_i, pu sec, is the equivalent intertia constant of the ith CA. For a single area system, $\Delta P_i^{\mathrm{tie}}$ is excluded from (2.7). The expression (2.7) is also known as the swing equation of the ith CA. Taking the laplace transform of (2.7) and rearranging gives:

$$\Delta f_i = \frac{1}{sH_i + D_i}(\Delta P_i^{\mathrm{M}} - \Delta P_i^{\mathrm{D}} - \Delta P_i^{\mathrm{tie}}) \tag{2.8}$$

2.1.3.4 Net tie line deviation dynamics

Before deriving the dynamic equation governing the active power flow across a tie line, we state, clearly, the following assumptions which are implicit in most LFC literature [7]:

1. The tie line between any two CA is assumed to be purely inductive, that is, the tie line power flow is lossless.

2. In the frequency control timescales, it is assumed that the voltage control loops (faster) are able to maintain node voltages at their nominal values, which is unity in per-unit representation.

3. Finally, small angle disturbance is assumed (this permits linearisation).

These assumptions hold throughout the thesis and one or more of them may be repeated subsequently for convenience. The dynamics of the net incremental tie line power flow of the ith CA are:

$$\Delta \dot{P}_i^{\text{tie}} = \sum_{j \in \mathcal{A}_i^{\text{Ne}}} \Delta \dot{P}_{ij}^{\text{tie}} \tag{2.9}$$

where $\Delta P_{ij}^{\text{tie}}$ is the incremental tie line power flow from area i to a neigbouring area j; $\mathcal{A}_i^{\text{Ne}}$ is an index set of the neighbours of the ith CA. Note that net tie line flows are assumed to be out of a CA. At nominal frequency, the tie line flow from area i to j is:

$$P_{ij}^{\text{tie},0} = \frac{|V_i|\,|V_j|}{X_{ij}} \sin(\delta_i^0 - \delta_j^0) \tag{2.10}$$

$P_{ij}^{\text{tie},0}$ is the nominal tie flow from area i to j; V_i and V_j are respectively the equivalent terminal bus voltages[3] of area i and j; δ_i^0 and δ_j^0 are the equivalent nominal swing angle of area i and j respectively, and are measured in radians (rad). As stated in Section 1.1, this thesis is focused on small disturbance analysis, for which the interaction between voltage control loops and the frequency control loop is negligible. Moreover, it is assumed in this work that the voltage control loops are effective enough to keep the bus voltages at their nominal values. Hence, the nomalised values of $|V_i|$ and $|V_j|$ are unity. X_{ij} is the reactance of the line linking area i and j. Assume the disturbance, ΔP_i^{D}, causes the tie flow to deviate by a small amount, $\Delta P_{ij}^{\text{tie}}$, from its nominal value, then (2.10) can be written as:

$$P_{ij}^{\text{tie},0} + \Delta P_{ij}^{\text{tie}} = \frac{1}{X_{ij}} \sin\big((\delta_i^0 + \Delta \delta_i) - (\delta_j^0 + \Delta \delta_j)\big) \tag{2.11}$$

$\Delta \delta_i$ and $\Delta \delta_j$ are incremental swing angles of the ith and the jth CAs respectively, and are also measured in radians. Note that $\Delta \delta_i$ and $\Delta \delta_j$ are small because we are concerned with small-angle frequency control. Assuming the following holds for small angles in radians: $\Delta \delta_i \Delta \delta_j \approx 0$; $\sin(\Delta \delta_i) \approx 0$; $\cos(\Delta \delta_i) \approx 1$; $\sin(\Delta \delta_j) \approx 0$; $\cos(\Delta \delta_j) \approx 1$, then (2.11) becomes:

$$\Delta P_{ij}^{\text{tie}} = Y_{ij}(\Delta \delta_i - \Delta \delta_j) \tag{2.12}$$

where $Y_{ij} = \frac{1}{X_{ij}} \cos(\delta_i^0 - \delta_j^0)$. Similarly, the power flow from area j to i can be written as:

$$\Delta P_{ji}^{\text{tie}} = Y_{ji}(\Delta \delta_j - \Delta \delta_i) = -Y_{ij}(\Delta \delta_i - \Delta \delta_j) \tag{2.13}$$

---

[3]The coherency assumption implicitly implies that generating units within a control area are connected to a single bus for which a single bus voltage, V_i, swing angle, δ_i and frequency, f_i, can be defined.

Here, $Y_{ji} = Y_{ij}$ since the line reactance is constant in both directions and cosine is an even function, i.e., $\cos(\delta_i^0 - \delta_j^0) = \cos(\delta_j^0 - \delta_i^0)$. From (2.12) and (2.13), the following relationship exists:

$$\Delta P_{ji}^{\text{tie}} = -\frac{P_{r_i}}{P_{r_j}}\Delta P_{ij}^{\text{tie}} = -\alpha_{ij}\Delta P_{ij}^{\text{tie}} \qquad (2.14)$$

The term α_{ij} is the rated capacity ratio between area i and j. Taking the time derivative of 2.12 and substituting the resulting expression into 2.9 gives:

$$\Delta \dot{P}_i^{\text{tie}} = \sum_{j \in \mathcal{A}_i^{\text{Ne}}} T_{ij}(\Delta f_i - \Delta f_j) \qquad (2.15)$$

The expression in (2.15) represents the incremental net tie line dynamics of the ith CA. $T_{ij} = 2\pi Y_{ij}$ is the synchronizing coefficient between area i and j. Taking the laplace transform of (2.15) gives:

$$\Delta P_i^{\text{tie}} = \sum_{j \in \mathcal{A}_i^{\text{Ne}}} \frac{T_{ij}}{s}(\Delta f_i - \Delta f_j) \qquad (2.16)$$

From (2.8) and (2.16), a transfer function block can be obtained for the network, and this is shown in Figure 2.6.
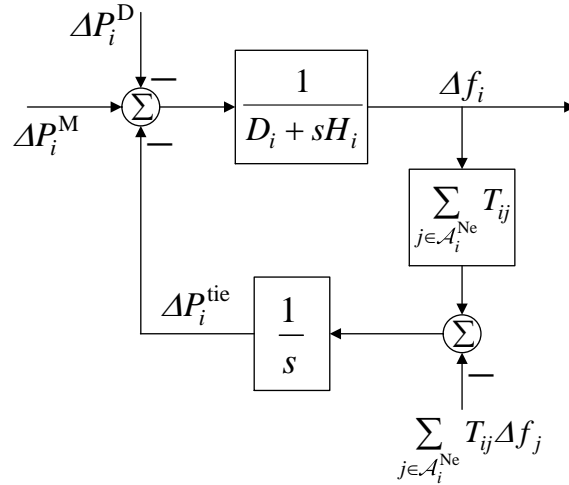
Figure 2.6: Transfer function block representation of area i network

2.1.4 Load frequency control loop

The PFC loop is a mere proportional controller whose control action is proportional to the turbine speed error and hence network frequency deviation. Therefore, the PFC loop only rejects grid disturbances and keeps system frequency close to the nominal value. PFC actions and the active power imbalance in the interconnection also induce changes in load flows on tie lines, i.e., there is a deviation in the net interchange power between control areas from scheduled values. Since an active power imbalance is a perpetual and unavoidable phenomenon in power systems, the LFC loop works continuously via automatic generation control to eliminate imbalances, and restore the frequency and net tie line power in its CA to their scheduled values. The LFC loop within a control area (the ith control area for example) utilises a linear combination of the frequency deviation, Δf_i and the deviation in the net tie line power flow, ΔP_i^{tie} measurements to estimate the value of the active power imbalance (either suplus or deficit), and in turn sends a control signal (a raise or lower command) to generating units on LFC within its own area; this translates to changing the load reference setpoint of a turbine governor via the speed changer as shown in Figure 2.2. The linear combination of the pair $(\Delta f_i, \Delta P_i^{\text{tie}})$, known as the area control error (ACE), is:

$$\text{ACE}_i = \beta_i \Delta f_i + \Delta P_i^{\text{tie}} \tag{2.17}$$

where β_i pu/Hz, is the frequency bias setting of the ith CA. As the LFC action involves changing the load reference setpoints of turbine governors, the signal from the LFC loop in the ith CA can be expressed as:

$$\Delta P_i^{\text{C}} = \Omega_i(\text{ACE}_i) \tag{2.18}$$

where the $\Omega_i(\bullet)$ is a function which represents the load frequency or secondary level controller. Traditionally, $\Omega_i(\bullet)$ is an integral control scheme. The LFC signal ΔP_i^{C} is distributed to generating units on LFC according to participation factors, γ, which are obtained via an economic dispatch (ED) process[4] . As an example, the LFC signal to a given generating unit k, in area i , $\Delta P_{i,\text{k}}^{\text{C}}$, whose participation factor is $\gamma_{i,\text{k}}$, can be expressed as:

$$\Delta P_{i,\text{k}}^{\text{C}} = \gamma_{i,\text{k}} \Delta P_i^{\text{C}} \tag{2.19}$$

where $\sum_{\text{k} \in \mathcal{S}_i} \gamma_{i,\text{k}} = 1$ must hold for each area executing LFC since the total disturbance in a control area must be rejected. $\mathcal{S}_i$ is the index set of generating units equipped with LFC

---

[4]The ED for LFC may be performed on an hourly basis or less.
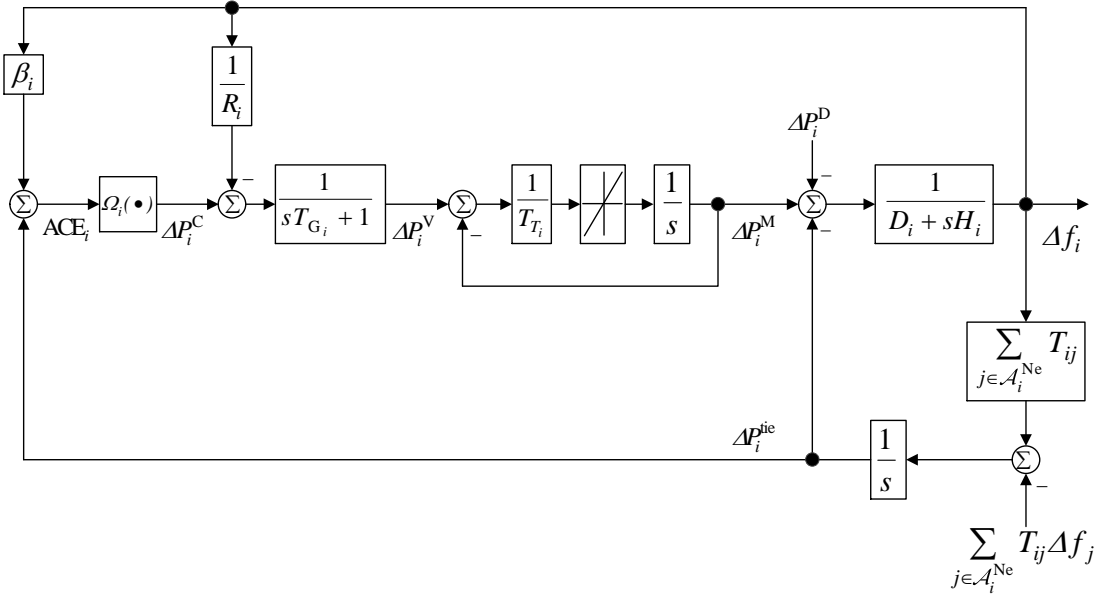
Figure 2.7: A complete transfer function representation for LFC in the ith CA

facilities in the ith CA; $0 \leq \gamma_{i,k} \leq 1$. For generating units equipped with LFC facilities but not participating in LFC at a given instant, $\gamma_{i,k} = 0$.

2.1.5 Complete frequency control block in the ith area

Sections 2.1.1-2.1.4 presented the mathematical equations required for a typical LFC study in the VIU framework. The important equations needed to model a typical control area in the VIU framework are: (2.1) turbine governing system dynamics; (2.2) turbine dynamic model; (2.8) incremental power balance of the ith CA; (2.16) incremental net tie line dynamics; (2.17) area control error; (2.18) load frequency controller. In a VIU framework, a single electric utility owns and operates generation, transmission and distribution facilities within a control area. As a result, the utility can provide a LFC service by activating the LFC reserve of any power plant of its choice, and what matters is that an incremental/decremental power is experienced by the network. Therefore, looking at a control area from the system level (a system-wide view) appears as though a single large generating unit is serving energy and providing the LFC service. Consequently, in the VIU framework, we may represent a control area by an equivalent generating unit connected to a single bus; such a representation is acceptable since we are not interested in the intermachine oscillations within each CA [6, 44]. A complete transfer function block representation for the ith control area is shown in Figure 2.7.
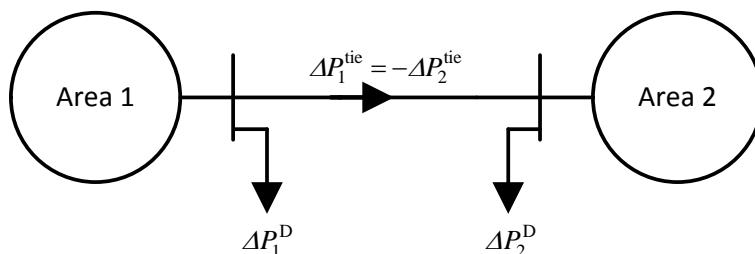
Figure 2.8: A single line diagram of 2-area power system

Table 2.1: Parameter of a 2-area traditional LFC framework

Area, i	H_i (pu s)	D_i (pu/Hz)	T_{G_i} (s)	T_{T_i} (s)	R_i (Hz/pu)	β_i (pu/Hz)	T_{ij} (pu/Hz)
1	0.1667	0.015	0.07	0.4	2.73	0.36	$T_{12} = 0.25$
2	0.1247	0.016	0.08	0.3	3	0.42	$T_{21} = 0.25$

2.1.6 Simulation example

Hence forth, power quantities such as load change and generation unit outputs use the unit "pu (per-unit)" rather than "MW pu (megawatt per-unit)".

2.1.6.1 2-area traditional LFC scheme

To make the concept of LFC in the traditional power system environment completely transparent, a simulation study of a 2-area LFC problem using the traditional integral controller is carried out. For clarity's sake, equal area rated capacities are assumed for the 2-area traditional system, i.e., α_{ij} in (2.14) is equal to one, where $i = 1$ and $j = 2$ for the 2-area example. Furthermore, because we are considering a 2-area system, each area has only one neighbour, i.e., $\mathcal{A}_1^{\text{Ne}} = \{2\}$ and $\mathcal{A}_2^{\text{Ne}} = \{1\}$. It can also be seen from (2.9) that $\Delta P_1^{\text{tie}} = \Delta P_{12}^{\text{tie}}$ and $\Delta P_2^{\text{tie}} = \Delta P_{21}^{\text{tie}}$; since $\alpha_{12} = 1$, from (2.14), $\Delta P_1^{\text{tie}} = -\Delta P_2^{\text{tie}}$. A single line diagram of a 2-area system is shown in Figure 2.8, and the transfer fuunction representation of LFC in the traditional power system environment is shown in Figure 2.9; the turbine GRC nonlinearity has been dropped. The system parameters are shown in Table 2.1 and are obtained from [22]. For the simulation, the following integral controllers are used for each area: $\Omega_1(\bullet) = -\dfrac{0.18}{s}$; $\Omega_2(\bullet) = -\dfrac{0.15}{s}$. The integral gains were obtained by trial and error method. It is assumed that a step disturbance of 0.05pu occurred in area 1 after 10s, i.e., $\Delta P_1^{\text{D}} = 0.05$pu. Figures 2.10-2.13 show the responses obtained with primary frequency control (PFC) only and PFC with a load frequency controller (secondary-level frequency control). For the PFC only scenario, the integral gains were set to zero.
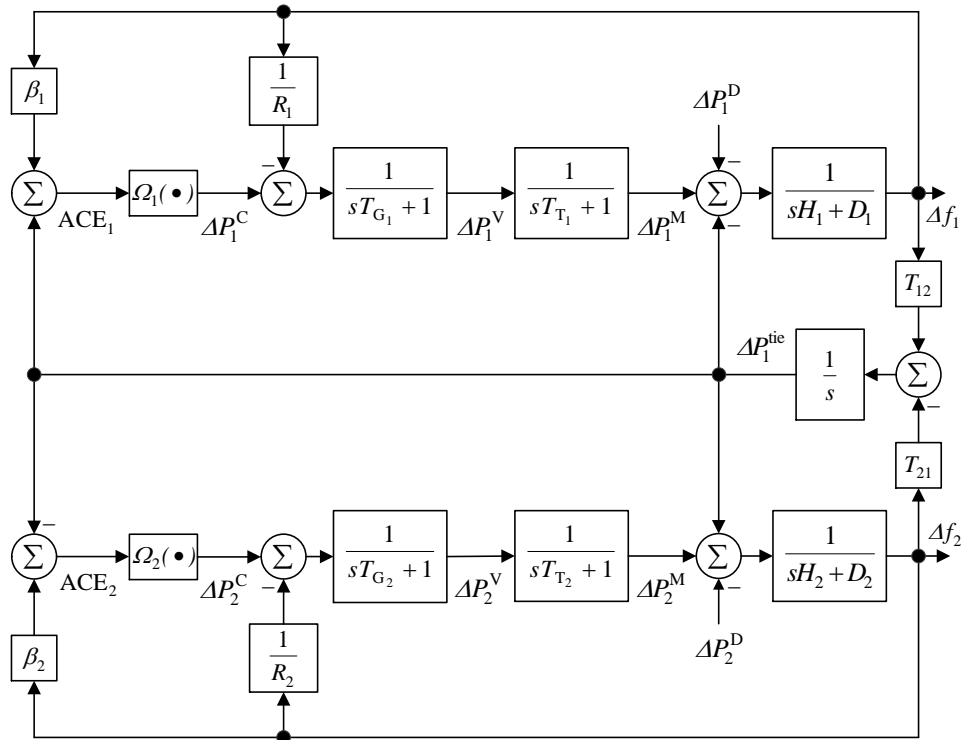
Figure 2.9: A Transfer function diagram of a 2-area traditional power system LFC framework.
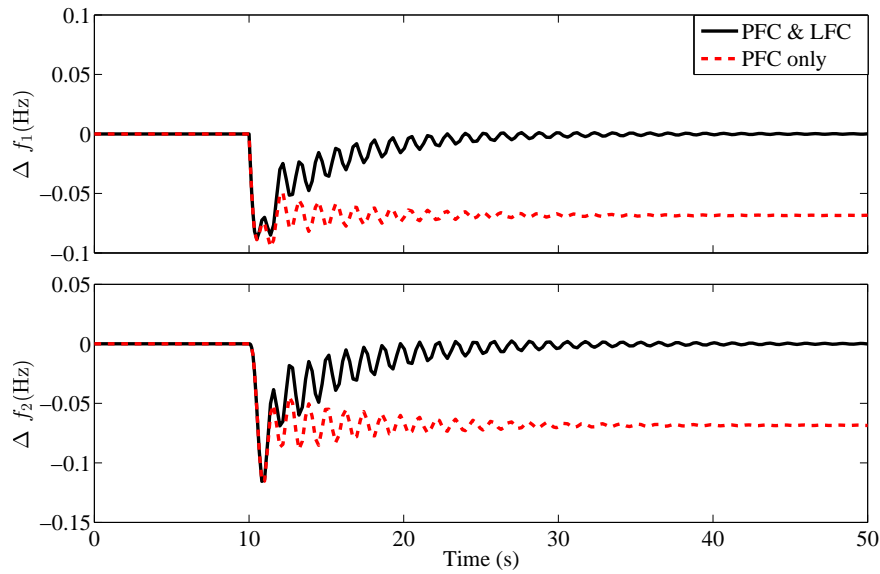
Figure 2.10: Frequency deviation in Area 1 and 2 in the VIU framework. As seen, PFC alone could not eliminate the frequency deviations due to the disturbance in area 1
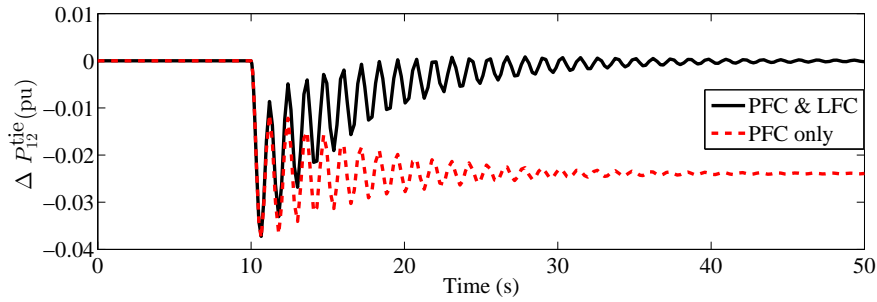
Figure 2.11: Deviation in the net tie line power flow from area 1. As seen, without LFC, $\Delta P_{12}^{\text{tie}}$ settled at a nonzero value.
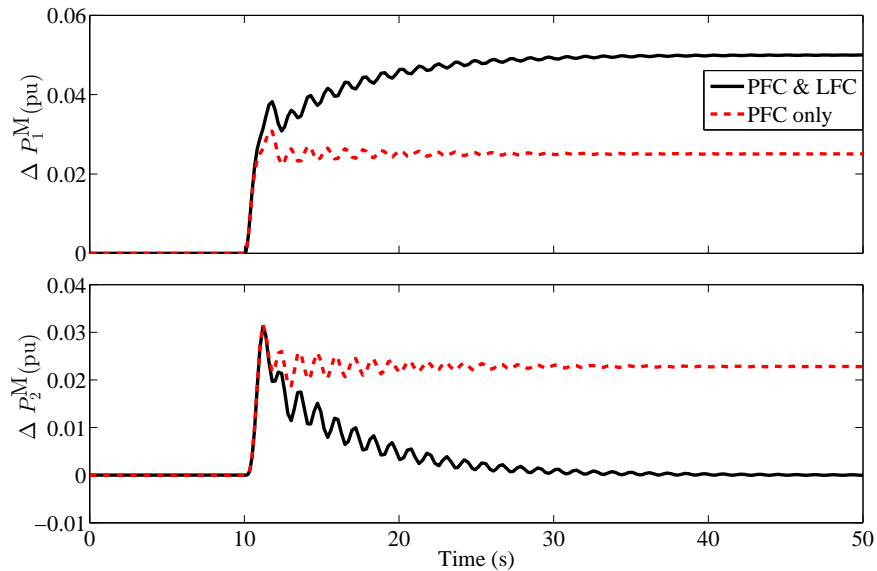
Figure 2.12: Incremental power output of Area 1 and 2. As seen, PFC only cannot activate sufficient power to completely reject the load disturbance.

2.1.6.2 Discussion

Simulation was carried for two scenarios - PFC only and then PFC with an integral load frequency controller. Figures 2.10, 2.11, 2.12 and 2.13 are the frequency deviation, net incremental tie line power, incremental power generation and area control error, respectively, in area 1 and 2; the red dotted lines in the figures indicate PFC only while the black lines are the responses of PFC and LFC working together. Recall from Sections 1.2 and 2.1 that the traditional aim of LFC is to drive frequency deviations, net incremental tie line powers and thus area control errors to zero. As seen from Figures 2.10 and 2.11, there was an instantaneous drop in frequency in both areas and a deviation in the tie line flow when a load disturbance occurred after 10s in area 1. Also, it can be observed that PFC only could not restore frequency and net tie line flows to their scheduled value. This is because, PFC loops in both areas, being a mere proportional control scheme, could not control the generating units
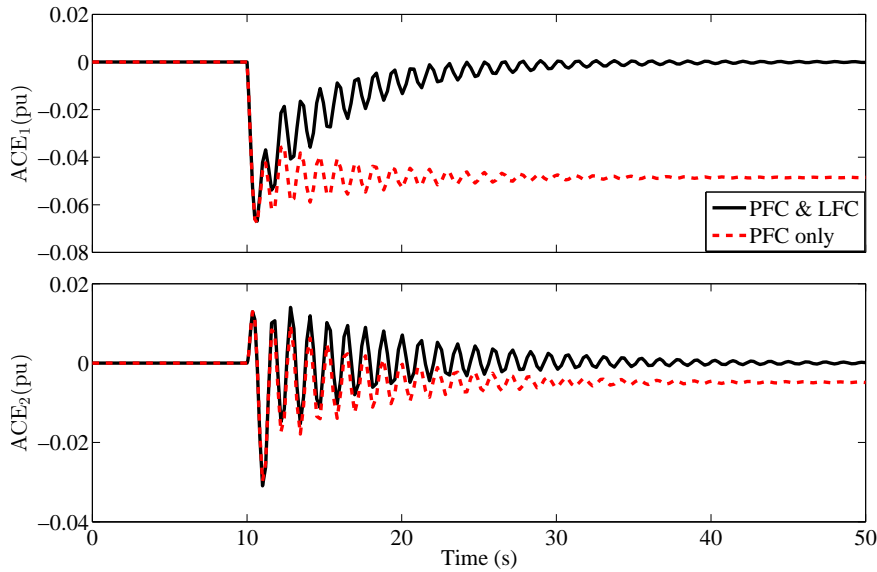
Figure 2.13: Area control error in Area 1 and 2. With PFC only, the ACEs are nonzero and this is undesirable.

to track the change in demand, as demonstrated in Figure 2.12. The ACEs of both areas under PFC only also settle at a nonzero value, as seen in Figure 2.13.

On the other hand, with a secondary-level controller, that is the LFC loop, the frequency and tie line errors are eliminated, as shown by the black lines in Figures 2.10 and 2.11 respectively. Also, the ACE of both areas were driven to zero by the LFC loop, see Figure 2.13. This was possible because the LFC loop in area 1, at steady state, regulated area 1 output power to track the load change as illustrated in Figure 2.12; it was emphasised in Section 2.1 that it is the responsibility of the CA where a disturbance occurred to provide LFC reserve at steady state. During transient, there was a power flow from area 2 to 1 as seen in Figure 2.11; the response in Figure 2.11 is the incremental flow from area 1 to 2, and thus the negative tie flow during transient indicates that there was a power transfer from area 2 to 1. This flow from area 2 to 1 can also be observed from the behaviour of ΔP_2^{M} in Figure 2.12 during transient, where there was a sudden increase in power output after 10s, which then gradually converged to zero as area 1 ramped up its power output to track the load change.

2.1.7 Incorporating renewables into LFC models

This thesis assumes that each control area consists of only conventional generation sources (steam generating plants considered) supplying energy and reserves. However, renewables are increasingly being introduced in power generation mix globally primarily due to environmental concerns, and their impacts on frequency control have received keen attention recently [45]. The existence of renewables such as wind and solar generation systems create an extra source of variability to the power networks which are traditionally variable in nature [22]. This is

because their power outputs mainly depends on weather conditions and seasons which are completely uncontrollable.
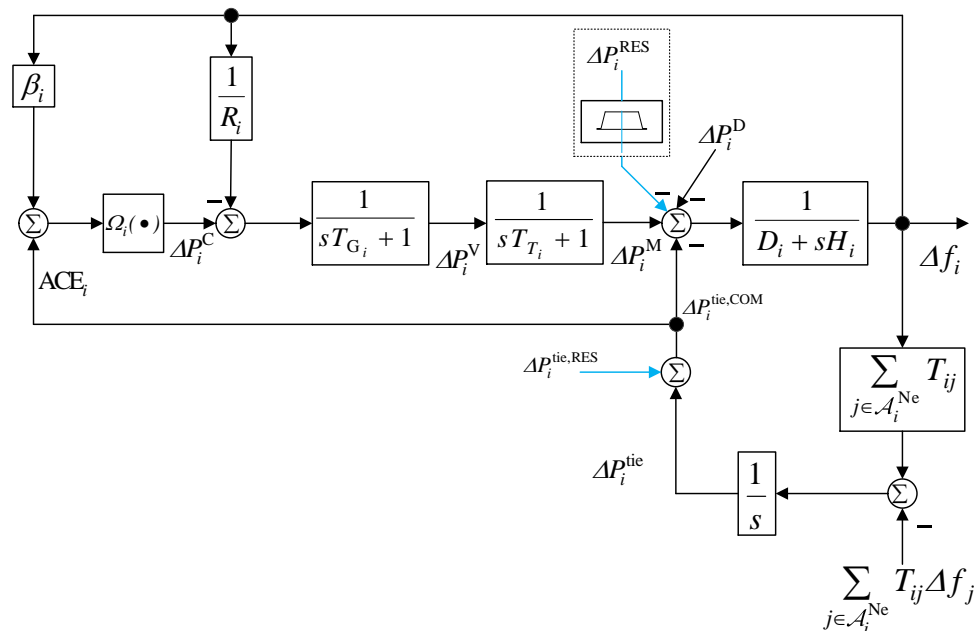
Figure 2.14: LFC model accounting for RES power fluctuation.

The frequency fluctuations created by renewables depend on the level of penetration of renewables with regards to the total electrical power production of the interconnection. Power grids with large inertia (energy largely supplied by conventional sources) relative to the level of penetration of renewables can absorb the power variability due to the existence of renewables and the impact of renewables on the LFC strategy may be negligible. However, for high penetration of renewables, LFC structure must be modified to account for the power fluctuation dynamics of renewable energy sources (RES).

The power fluctuations resulting from renewables in a control area usually comprise of fast components from individual renewable generation sources and a slow component resulting from the collective fluctuations of all renewables within a control area . It has been shown that the operational impacts of fast components of power fluctuations of renewables are mostly absorbed by large thermal and mechanical time constants of thermal generating units synchronised to the network [46]. On the other hand, the slow components contribute, negatively, to power imbalance and thus unacceptable frequency fluctuations, and therefore must be considered in the LFC scheme. One approach of taking into account the existence of renewables in LFC studies is to introduce additional signals into the conventional LFC model as shown by the blue lines of Figure 2.14, where $\Delta P_i^{\mathrm{RES}}$ represents the total power fluctuations due to RES in the ith CA and $\Delta P_i^{\mathrm{tie,RES}}$ is the deviation in net tie line power due to RES in the ith area.

Hence, the modified net tie line flow deviation in the ith area $\Delta P_i^{\text{tie,COM}}$ as well as the ACE in the presence of renewables are:

$$\Delta P_i^{\text{tie,COM}} \quad = \quad \Delta P_i^{\text{tie,RES}} + \Delta P_i^{\text{tie}} \tag{2.20}$$

$$\text{ACE}_i \quad = \quad \beta_i \Delta f_i + \Delta P_i^{\text{tie,COM}} \tag{2.21}$$

Note that in Figure 2.14, the turbine GRC has been omitted and it is assumed that renewables are not participating in LFC. A number of modern wind turbine generators, which are the most utilised renewables, are being equipped with active power control capabilities to enable them provide inertial support, primary frequency control and LFC in power networks [47]. The inertial support and primary frequency control are achieved typically using wind turbine generator torque control while LFC is achieved using pitch angle control. For more details on the participation of wind turbines in power system LFC, see [47, 48].

2.1.8   Summary

In summary, this section has provided the mathematical background/definitions for the LFC problem in the traditional power system environment. Simulation evidence were provided to demonstrate that PFC loops alone are incapable of restoring grid frequency and net tie line power to their scheduled value when a disturbance occurs in the network, and that an LFC loop (also known as secondary level frequency control loop) is required to restore active power balance in an interconnected network. Since the main focus of this thesis is the LFC problem in the deregulated environment, the following section will discuss the ongoing deregulation in power industries, the market structures for LFC and energy that have emerged, and the overall effect on load frequency control services.

2.2   Power system deregulation

This section provides a background of the framework of LFC services as electric industries transit from a monopolistic and regulated structure towards a competitive and deregulated structure. Power industries, during the early days, operated a vertically integrated utility (VIU) structure where a utility held a monopoly franchise granted by the government, giving it the exclusive rights to perform the key power system functions such as generation, transmission and distribution within its CA. In exchange for lack of competition, a VIU had to provide electricity to all consumers within its CA, and not just to those that it may perceived to be financially rewarding. Under this regime, price for power/energy was regulated by the
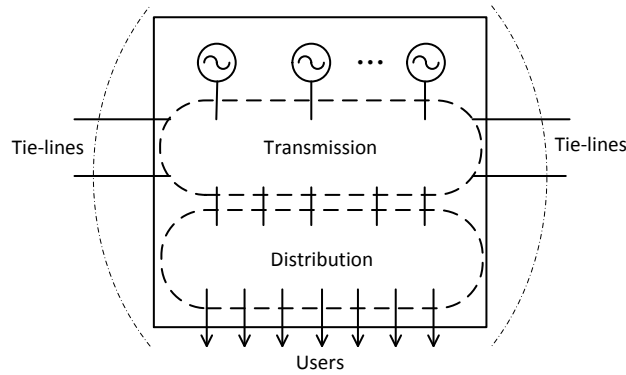
Figure 2.15: Vertically Integrated Utility Structure

government. The LFC within a CA, as well as other operational reserved services, was provided by the VIU since it owns and controls all of the generating equipment and system infrastructure within its territory [13, 49]. Figure 2.15 depicts the structure of the VIU, where everything within a rectangular box represents a single company. LFC studies in the VIU framework have appeared in numerous conference proceedings and technical journals and a comprehensive summary is available in [12, 13, 50] and their references.

In the period from mid-1980s onward, many countries decided to deregulate and restructure their power industries [2, 15]; the central notion was to provide a more effecient framework to deliver cheap and reliable power to customers. The key steps in the process is the unbundling of the functions performed by VIUs, and the allocation of these functions to private business entities/separate companies. Thus in a typical CA, business entities such as Generation Companies (GenCos), a Transmission Company (TranCo) and Distribution Companies (DisCos) have been created. This has given birth to a competition in power generation, an open access policy on transmission, and a competition at the distribution level. The several GenCos in a CA may compete/bid to sell power/energy to DisCos within and across CA boundaries, and each DisCo has the liberty to contract with GenCos within and outside its CA to meet its loads. Figure 2.16 shows a typical deregulated structure, where each rectangular box denotes a private entity; the dash-dot curved lines represent CA boundaries. In most regions, the TranCo is natural monopoly due to the cost and importance of the transmission infrastructure; TranCo owns and maintains transmission facilities, but may not be involved in transmission grid operations.

Furthermore, an independent entity known as a transmission system operator (TSO) has emerged in each CA, and its functions among others are to ensure a non-discriminatory access to the transmission grid by all GenCos, guarantee the reliability and security of its CA, manages transmission congestion, and coordinate power transactions/contracts between GenCos
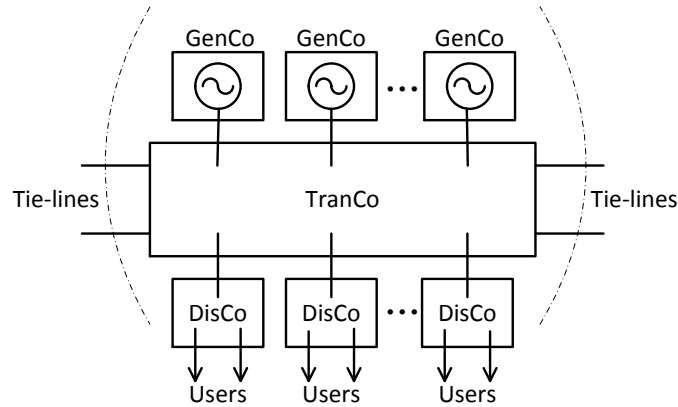
Figure 2.16: Deregulated Structure

(seller) and DisCos (buyer); a TSO essentially operates the transmission grid of its CA. In some jurisdictions, a TranCo performs the duties of a TSO in its CA, and an example is the National Grid Electricity Transmission plc in England and Wales [51]. Note that the term TSO is used mainly in the European power industries; in the United States, a TSO's equivalent is known as an Independent System Operator (ISO), hence TSO and ISO will be used interchangeably in this chapter. In the new environment, the TSO provides LFC and other operational reserved services which are on the whole referred to as ancillary services [52]. Unlike the VIU that owns and controls generation resources, and provides LFC services from its unloaded reserved capacity, the TSO providing LFC in the new environment does not own any generating unit. Hence, TSOs rendering LFC services have to procure/purchase reserved capacity from a GenCo/GenCos, and a GenCo is not obligated to sell LFC capacity to the TSO. This new paradigm is expected to change the LFC framework used in the VIU environment, since LFC reserves are now procured through bidding/contract from a competitive electricity market. Since incremental energy reserves are required to provide LFC services, the competitive market structure for energy within a given jurisdiction is also binding on the procurement of LFC reserves [53]. Issues bordering on LFC framework in the deregulated environment have been discussed in [13, 54–56].

In general, a number of market structures exist around the globe for the provision of energy and hence LFC services. Nonetheless, three primary market structures can be identified, and these structures are briefly discussed in the Section 2.2.1-2.2.3:

2.2.1 Poolco-based LFC market

In the poolco-based LFC market, GenCos that have the willingness and capability to quickly adjust their power outputs, submit incremental (and also decremental) bids to the TSO, indicating how much upward (and downward) regulation they can provide at a given price. The poolco structure can be one-sided or two-sided [57]. In the one-sided structure, the TSO, based on demand forecasts, dispatches the GenCos that have indicated interest in LFC without considering bids from DisCos. In the two-sided structure, the TSO takes bids from GenCos (incremental/decremental generation) and DisCos (amount of load following needed and the price they are willing to pay), and matches the bids based on some market rules. An example of the one-sided structure is the England-Wales system while the two-sided is practiced in California and New York State [49]. From a control system point to view, both poolco structures are similar as the TSO, only, controls the participating GenCos from a central location to ensure that active power balance is maintained. The poolco-based LFC is also equivalent to the traditional LFC framework since generators are controlled by a single entity, the TSO [55].

2.2.2 Bilateral-based LFC market

In the bilateral-based LFC, a DisCo in any control area goes into bilateral contracts in advance with Gencos within or across its CA boundaries for load matching (LM)[5], based on the DisCos' anticipated demand variation pattern, and then supply their contractual obligations to the TSO for coordination in real time operations. In this structure, it is the responsibility of the GenCos and DisCos to provide a communication path to exchange contract data along with measurements to perform LM functions. In the bilateral LFC, a GenCo changes its power output to closely match a DisCo's load change provided it does not exceed the contracted value, and a DisCo is obligated to monitor its load to avoid contract violations. Hence, the TSO has no obligation to provide LFC. Bilateral transactions are allowed in California [49].

2.2.3 Mixed LFC market

In practice, it may be impossible to provide LFC through bilateral transactions only as a generating unit providing LM service could malfunction or a DisCo load could exceed contracted values. Therefore, a mixed LFC market, incorporating poolco and bilateral structures, could be made to work [49, 54]. In such an arrangement, GenCos and DisCos within and across CA boundaries negotiate a bilateeral LM contract, while the TSO secure LFC reserve commitments from GenCos (Poolco structure) to cater for load variations occurring in real-time operation, either due to GenCos and DisCos violating contracts, power losses or variations from DisCos that have not purchased an LM contract. In this work, the load variations handled by a TSO

---

[5]LM can be understood from the perspective of load following.

in the mixed framework is denoted as uncontracted load changes. The TSO must secure the reserve for the uncontracted load change from GenCos in its own area [55]; the reason is to maintain steady state net incremental tie line flows, based on cross-border LM contracts, at contractual (scheduled) value.

In summary, this section discussed the ongoing structural changes occuring in power industries, from the VIU structure to the deregulated structure, and the resulting market structures for LFC services. Note that the deregulation picture painted here may not be applicable to all countries/regions.

2.3   A summary of the evolution of LFC studies

This section provides a snapshot of key issues that have been considered in LFC studies to date; a detailed review of the LFC literature is presented in Section 2.4. To avoid misconception, note this: some publications use the term automatic generation control (AGC) to refer to LFC action since it is a supplementary control action that *automatically* regulates active power output levels of generating units within a control area (CA). The inclusion of other components such as economic dispatch control, environmental dispatch control, security dispatch control, etc., as part of an AGC scheme and its definition has also been recommended [58], with LFC being the main component of any AGC system. However, most publications that used the term AGC essentially carried out studies on LFC and did not include the other recommended components. Studies that attempt to incorporate, for example, economic dispatch into the main component of AGC [59, 60] mostly emphasised the term economic dispatch as part of the publication title. For this reason, and for the purpose of uniformity, this thesis will mostly use the term LFC to report publications that have used either the LFC or AGC nomenclature, and the term AGC will only be used when it is absolutely necessary.

For over six decades, LFC of an interconnected power system has been studied, and a mountain of research papers and books exist on the subject; an exhaustive review has been reported in [50, 61, 62]. One of the earliest issues considered in LFC was about providing a theoretical dynamic analysis of LFC performance which had hitherto been static [63], and the study utilised the conventional integral controller. As the demand for power increases, more efficient use of generation facilities became important; there was the need to expand power system facilities and intall larger power plants. Researchers within the power system community raised the issue of reduced stability margins with the increasing load and the size of power generating infrastucture.

Consequently, a number of LFC studies based on optimal control theory to improve stability margins and system reliability were suggested [43, 64–66]. Some early studies on LFC also

considered the effect of practical nonlinearities in power plants such as generation rate constraints (GRC) [31, 32, 67] and governor dead band (GDB) [68–70]; discrete variable structure based LFC studies, accounting for the simultaneous effect of GRC and GDB, was reported in [71]. LFC studies devoted to the issue of variation in system parameters/changes in system operating conditions have also been reported; sensitivity studies on the effect of variations in system parameters such as turbine and governor time constants, droop, control area capacity ratio, equivalent area damping and inertia constants on LFC performance was reported in [67]. Furthermore, LFC schemes based on variable structure control technique [32], adaptive control and self tuning methods [72, 73], robust method [74] and intelligent schemes [75, 76] to cope with parameter uncertainties and power plant nonlinearities have been proposed. The IEEE standard definitions of terminologies specific to automatic generation control and revised versions of the definitions were reported in [58, 77, 78], while comprehensive transfer function models of various types of speed governors and turbines of power generating units were provided in [42] . The LFC studies reported above are based on the vertically integrated utility structure (VIU).

With the deregulation and restructuring in power industries that commenced in the middle of 1980s, starting from Chile and the UK, and spreading to other parts of the world [15, 51], more attention has been focused on reformulating and implementing LFC in the deregulated enviroment. The modifications required in the well tested VIU LFC dynamic framework to account for various types of power procurement contracts within the deregulated environment, were suggested in [29, 55, 56]; the concept of a DisCo participation matrix (DPM) was proposed in [29] to aid the visualization and implementation of bilateral contracts among GenCos and DisCos in a two area power system. The DPM has since formed the nucleus of most LFC work in the deregulated environment, and some deregulated LFC studies based on robust control techniques [79, 80], optimal control [81, 82], internal model control (IMC) based PID [83], linear active disturbance rejection method [84] and intelligent control techniques [85–87] have been reported.

Furthermore, power system deregulation has necessitated the need for an open communication infrastucture, as opposed to the dedicated communication channels used in VIU, to support the bilateral contracts and the growing array of ancillary services, including third party LFC; open communication causes random delays/data losses, and the need to include their effects in deregulated LFC studies was demonstrated in [88]. Also, a number of robust LFC schemes accounting for communication delays have been proposed [89, 90]. Recently, the increase in penetration of renewable energy sources such as wind and photovoltaic systems in power systems, driven by environment concerns, has had detrimental impacts on network frequency globally [91]. The is mainly due to the variability of renewable energy sources and the lack of inertial support from them. Consequently LFC design accounting for uncertainties in wind generation have been reported in [92–96].

Another important issue that has been considered in both VIU and the deregulated power system LFC studies is the architecture of the control system. Traditionally, LFC in multi-area networks is based on a decentralised architecture where integral based LFC loop in each area controls the frequency and net interchange power of that area without communicating with LFC loops in neighbouring control areas [97]. A number of advanced control methods proposed for multi-area LFC to obtain improved performance and security margins over traditional integral schemes were based on a centralised control architecture [43, 82, 98–101]. These centralised schemes provided satisfactory LFC performance; however, it has been argued that the centralised LFC schemes for multi-area network are impracticable due to the large geographical separations in power networks, organisational constraints, and issues associated to centralised computation, actuation, modelling and collection of data [102, 103]. Hence centralised LFC schemes for multi-area systems may be used as control benchmarks.

To emulate the traditional LFC architecture, decentralised LFC schemes based on advanced control strategies have been reported [72, 83, 104–111]. Depending on the strength of couplings between each subsystem representing a control area, some form of coordination and exchange of information between the LFC loop in each area may be necessary. It has been demonstrated that decentralised control designs may result in highly sub-optimal performance/ unstable conditions in a strongly coupled interconnection [112]. A typical example is the synchronous nordic multi-area power system where, in recent years, increasing incidents of frequency violations have been observed [113]; each area TSO in the nordic multi-area system uses a PI based LFC scheme that operate independently of each other. To address the issue of lack of coordination and communication between CAs, a number of distributed LFC designs, mainly based on model predictive control strategies, have been proposed [102, 112, 114–116]. These distributed model predictive control (DPMC) LFC schemes utilised local MPC in each control area that solves a system-wide optimisation (cooperative DMPC) or an area-wide/local optimisation (noncooperative DMPC), and exchange relevant information with neigbouring control areas to improve system-wide performance.

In summary, this section provided a concise overview of the main issues that are considered in LFC studies and highlights control methods/technique that have been applied to power system LFC problems.

2.4 Extensive survey of the LFC literature

In this section, an up-to-date and a thorough review of the LFC literature is presented, and an attempt is made to categorise LFC studies based on control design techniques. LFC works are reviewed under the following design techniques: Section 2.4.1 focuses on conventional technique; Section 2.4.2 focuses on linear optimal control and related techniques; Section 2.4.3

focuses on internal model control (IMC) LFC technique; Section 2.4.4 focuses on adaptive control and self-tuning techniques; Section 2.4.5 discusses model predictive control LFC technique; Section 2.4.6 discusses robust LFC technique; Section 2.4.7 focuses on intelligent control techniques. It is important to state that such a categorisation of LFC design techniques is not always an easy task in reality as some LFC studies in the literature combine more than one control technique in their proposed LFC design. A summary of the main strengths and weaknesses of each of the techniques is presented in Tables 2.2-2.8.

2.4.1 Conventional LFC scheme

Conventional PID control are mostly based on graphical design methods which are developed in the frequency domain. These are the simplest, and well understood, controller design methods and are very easy to implement on practical systems, especially for single loops. The earliest LFC studies/implementations were based on this method. Numerical studies on the effect of large disturbances on LFC performance considering nonlinear tie line flows have been reported in [117, 118], while [97, 119] investigated the effect of different frequency bias settings on LFC performance. The studies [97, 117–119] were based on conventional integral control based LFC. However, despite or because of their simplicity, conventional methods are not well suited to multivariable systems. Furthermore, they are mainly designed for nominal operations with no constraint violations and thus could become ineffective during a change in operating point. It has also been shown that conventional integral controllers may result in a degraded LFC performance in the presence of power plant nonlinearities [31, 32]. To improve the performance of conventional LFC schemes, an extended PI based LFC scheme was proposed in [120]; the scheme substituted the conventional integral term with a convolution integral which contains an exponential decay function. The superiority of the extended PI scheme over conventional PI, in the presence of GRC nonlinearity, was demonstrated on a single machine system. A summary of the key strengths and weaknesses of the conventional LFC schemes is provided in Table 2.2.

2.4.2 Linear optimal control and related LFC techniques

An optimal control technique is a control design framework whose primary philosophy is to determine a control policy that can steer a dynamical system at the lowest possible cost. The most common problem considered in optimal control is the linear quadratic regulator (LQR) problem. Optimal control uses a cost function to specify plant control objectives, and the cost function is optimised assuming a known dynamical model of the plant. The solution is a set of controller gains suitable to achieve the defined objectives. The LQR technique has been applied to LFC problems both in the traditional (VIU) framework [65, 121] and the deregulated power system environment [81, 82].

Table 2.2: A summary of the strengths and weaknesses of conventional LFC schemes

Technique	Strengths	Weaknesses
Conventional LFC [97, 117–120]	They are simple, and hence very easy to understand and maintain.	They are SISO based, and hence could perform poorly in the multivariable power system environment. Also, its capability to cope with GRC and other constraints is poor [31, 32]. The control architecture is mainly decentralised, and hence could result in a poor performance/unstable conditions in a strongly coupled multi-area network [112]. They mainly considered VIU and may be difficult to implement in the deregulated environment. System uncertainty not considered.

The work [65] formulated the LFC problem as a load tracking rather than a regulation problem, where the controller was designed to track predicted load variations. Simulation results, using a 2-area traditional test system, show that the LFC requirements were met. Practical power systems have control areas with a mix of different types of turbine. Recently, the LFC problem of a single-area traditional power system, with a mix of thermal, hydro and gas turbines was reported [121]. An optimal output feedback controller was designed for the LFC problem and the simulation conducted shows that the controller offers a satisfactory dynamic performance; the effect of GRC nonlinearity on controller performance, as well as parameter variations, was also studied.

A reduced order observer based LQR scheme for LFC in the deregulated environment was reported in [81], while [82] proposed an LQR scheme in the deregulated environment where a mix of hydro, thermal and gas generating units in each CA was considered. In [104], a decentralised state feedback LFC scheme, based on eigenstructure assignment, was proposed in a deregulated electricity environment, and tested on a 2-area and 4-area power system. The compliance of the proposed scheme to CPS1 and CPS2 NERC performance standards was also established. Functional observers (FOs) are known to possess a much simpler structure (and lower order) than full state or reduced state observers [122], though at the expense of estimation performance. Recently, linear state feedback LFC schemes based on FOs have been reported [123–125]. A 2-area traditional LFC based on quasi-decentralised FOs was proposed in [123]; the scheme uses a local FO, and each FO uses some output information from its neighbour to estimate a state feedback law. Simulation results were provided to demonstrate its efficacy.

Moreover, a quasi-decentralised traditional LFC scheme based on a FO approach was proposed in [124], where it was demonstrated, in the presence of GRC and GDB nonlinearities, that a FO based LFC scheme possesses a comparable performance with full order state observer based LFC. A multi-area LFC scheme using electric vehicles to support thermal generating

Table 2.3: The strengths and weaknesses of Linear optimal control and related LFC schemes

Technique	Strengths	Weaknesses
LFC based on Linear optimal and control related method [65, 81, 82, 104, 121, 123–125]	These schemes are simple and systematic. They can cope with the multivariable nature of power systems, and have also been considered in the deregulated environment.	They lack constraints handling capabilities and therefore may give poor performance in the presence of generation rate constraints [32]. Also, the schemes do not consider system uncertainty explicitly. Mainly centralised and decentralised and could result in a poor performace/instability in strongly interactive networks [112]

units in providing LFC power was proposed in [125]. The scheme uses distributed FOs to reconstruct the control input signal in each local area. The efficacy of the proposed scheme was demonstrated on a 3-area, 4-area and 6-area network where the areas are interconnected via a mix of AC / HVDC lines and thyristor controlled phase shifters.

The LFC schemes reported here generally have a simple structure and the methodology is systematic. Also, it is cost and computationally efficient, from a practical implementation point of view. However, the schemes also have several weaknesses. The emphasis is on optimality for the given linear model and thus it may not cope well with unmodelled dynamics and parameter variations. Moreover there is no explicit constraint handling incorporated and thus this capability is poor. The key strengths and weaknesses of the schemes discussed here is summarised in Table 2.3.

2.4.3 Internal model control (IMC) based LFC technique

The IMC principle relies on the fact that if a control system encapsulates the model of the process to be controlled (implicitly or explicitly), then a better control can be achieved. Recently, LFC schemes based on the IMC principle have been proposed [106, 126, 127]. A PID based LFC, synthesised from a two-degree-of freedom IMC scheme, was proposed in [126] for a single and multi-area network. The author utilised two controllers, one for setpoint tracking and the other for disturbance rejection, to obtain an overall controller, which was subsequently approximated with a PID controller. A decentralised PID-based LFC for a multi-area system was proposed in [106], where the controller gains were tuned via an IMC strategy. A two-degree-of-freedom IMC scheme for the LFC of a single area-single machine network, considering uncertainties in system parameters, was reported in [127]. The scheme used a reduced order model as the internal model, and similar to the scheme reported in [126], introduced two controllers in the IMC scheme, one for disturbance rejection and the other for setpoint tracking. The IMC schemes reported here provided good LFC performance; however, these schemes are

Table 2.4: A summary of the strengths and weaknesses of IMC-based LFC

Technique	Strengths	Weaknesses
IMC-based LFC [106, 126, 127]	These schemes are simple, systematic, and can be cope with the multivariable characteristics of power systems.	The schemes lack constraints handling capability, and therefore cannot handle generation rate constraints and constraints on inputs to the speed governor. Their performance is strongly linked to the accuracy of the internal model. Also, the IMC-based schemes were foused on VIU power systems. The schemes are largely single area [126, 127], and the only mult-area scheme [106] ignores interactions/coupling between CAs.

based on the traditional power system. Furthermore, their performance rely strongly on the accuracy of the internal model. They also lack explicit constraints handling capabilites, e.g. the schemes may not be able to handle generation rate constraints and constraints on inputs to the speed governor. A summary of the strengths and weaknesses of the IMC-based schemes is provided in Table 2.4.

2.4.4 Adaptive control and self-tuning LFC techniques

Adaptive control is one of the methods for handling parametric uncertainties in engineering systems. Many nonlinear systems can be modelled effectively by a number of linear systems whose parameters change from one operating point to another. Adaptive control takes advantage of *a posteriori* estimates of parameter values and adapts the control law for each operating condition. Numerous LFC solutions based on model reference adaptive control (MRAC) [72, 128] and self-tuning (STC) adaptive control [73, 129–131] methods have been presented in the literature.

A decentralised robust output feedback, based on a reference model, for a 3-area power system LFC has been presented in [72]. For each control area, an adaptive observer is designed to estimate the states and parameters of the plant using local input-output data; these estimates are combined linearly with states of a reference model to construct a local robust feedback adaptive control law for each area. Simulation results reveal that the proposed strategy is suitable for LFC under system parameter variations. Also, a decentralised model reference adaptive control for the LFC of a multi-area power system was proposed in [128]. The scheme was designed to ensure the frequency fluctuation, under the combined effect of load change, parameter variations and GRC, converges to a small range within the target frequency. The results obtained reveal that the controller works well under those conditions. Furthermore, the development of a self tuning adaptive LFC for the Hungarian power system was described in

Table 2.5: A summary of the strengths and weakensses of adpative and self-tuning schemes

Technique	Strength	Weakness
LFC based on MRAC [72, 128] and STC [73, 129–131].	These schemes work well for some limited conditions in terms of coping with parameter uncertainties	Online parameter estimation could be computationally time consuming, hence unlikely to be practical for large dimension systems. Also, a biased parameter estimate could be detrimental to system control.

[131]. It was reported that the controller has been in use in the Hungarian power system since June 1981.

The adaptive schemes proposed so far have performed well in meeting the LFC requirements, under the given simulation environments. An attribute of the adaptive schemes above is the fact that they perform well under parametric uncertainties. However, a common feature of the scheme above is the online parameter estimation, which could be computationally time consuming, and hence slow for large scale power systems control. Also, a failure in the parameter estimation module or a biased parameter estimate can be detrimental to a power system operations and control, especially in this stringent new power system environment. Also, most of the schemes rely on driving the steady state error between the reference plant and the actual plant to zero without considering transient performance, during which large frequency deviations can occur. The key strengths and weaknesses of the schemes presented here are summarised in Table 2.5.

2.4.5 LFC based on model predictive control technique

Model predictive control are a family of computer control algorithms which utilise an internal dynamic model of the plant, similar to the IMC philosophy, to optimise the predicted future behaviour [132]. MPC schemes are formulated as a constrained optimisation problem which is solved online for system control. The attraction towards MPC stems from its systematic and explicit constraints handling capability, the simplicity of the underlying concept, and its ability to make decisions that are economical and optimal in some sense. A survey on its industrial acceptance can be found in [28]. Several authors have applied MPC to various aspects of power system [133, 134]. Unsurprisingly therefore, LFC schemes, based on a centralised MPC (CeMPC) architecture [96, 100, 101, 113, 135, 136], decentralised MPC (DeMPC) [108, 137, 138], distributed MPC (DMPC) architecture [102, 112, 115, 116, 139] and hierarchical [140, 141] have been proposed.

In the CeMPC schemes [96, 100, 101, 113, 135, 136], there was an implicit assumption that power system data from the different CAs, that is required for LFC, can be telemetered to a single location. From an organisational viewpont, it means that an entire interconnection is managed by a single TSO. This is not realistic as in most power systems, different sections (CAs) of the interconnection are managed by separate TSOs. The European network controlled by 41 TSOs from 34 countries across Europe is a typical example [142]. Apart from the organisational obstacle to implementing centralised MPC in a multi-area system, the communication requirements/cost of data telemetering from different CAs having large geographical separations to a central location, and the associated computational load may be relatively high. Hence, centralised schemes [96, 100, 101, 113, 135, 136, 143] may largely serve as a performance benchmark. A scheme combining CeMPC and sliding mode control for the LFC of a 3-area network is also available in the literature [99], where it was shown that the scheme can provide acceptable LFC performance in the presence of random time delays between the controller and generator governor.

The DeMPC schemes reported [108, 137, 138] assume that the separate CAs of the grid can be controlled independently of the others, i.e. each TSO uses local information in its MPC algorithm to maintain system balance within its territory. Decentralised strategies for LFC mostly translate to high savings in communication infrastructure and a reduced computational load, and this is the practice in most interconnected networks, e.g. the European grid [144]. Nonetheless, it has been shown that in highly interconnected systems, a decentralised control can be overly sub-optimal or sometimes lead to unstable conditions [112]. This is because, the coupling effect between each subsystem is neglected. A typical example is the synchronous nordic power system where, in recent years, increasing incidents of frequency deviations have been observed [113]. Note that there has been a high penetration of renewable energy sources in the nordic power system, and each TSO in the synchronous nordic system operates its own PI based LFC using local data only.

DeMPC based LFC schemes with compliance to CPS1 and CPS2 NERC standards have also been reported [145, 146]. In [145], a decentralised MPC based LFC which comply to CPS1 and CPS2 operating standards was proposed. To prevent the unncessary maneuvering of generating units, the predictive control scheme was designed to take control actions when the level of compliance to NERC standards was low to prevent violation of the standards. Simulation was performed on a 3-area system to demonstrate the effectiveness of the proposed scheme. A wedge-shape MPC based LFC that complies to NERC CPS1 and CPS2 control performance standard was proposed in [146]. The wedge control philosophy incorporated in the MPC scheme was to reduce the number of generating units' reversal and hence wear and tear. The wedge control concept involves varying the settings of constraints on control input changes in real time, such that generating units' power remain unchanged in some instances.

The superiority of the proposed scheme over conventional PI control was demonstrated on a 3-area network.

In DMPC based LFC schemes [102, 112, 114–116], each local MPC based LFC scheme communicates, interatively [102, 112] or non-iteratively [114–116], with the MPC controller of dynamic neighbour. This information shared between dynamic neighbours is incorporated in each area based MPC optimization to achieve an overall systemwide performance close to a centralised MPC. DMPC has also been applied in frequency regulation problems in a mult-terminal HVDC grid [147], and a comparative study of non-centralised MPC schemes for LFC was reported in [139].

In the hierarchical scheme [140], MPC is utilised as an upper layer scheme which provides an optimal correction to the ACE signal received by a traditional PI controller. The use of energy units such as plug-in hybrid electric vehicles (PHEVs) in V2G mode, a combined-heat-and-power generation (CHP) unit and controllable loads to provide LFC services was investigated in [141]. The scheme uses a hierarchical framework where an aggregator, utilising an MPC strategy, receives an LFC setpoint from a TSO, and in turn splits the signal amongst units (PHEVs, CHP and controllable loads) while honouring their constraints.

However, as the application of MPC in the LFC problem is relatively new, the majority of these schemes [96, 101, 102, 108, 112–116, 135–139, 147] explored the capabilities of MPC in the traditional VIU framework. They represented the generating units within a CA with a lumped model as described in Section 2.1.5 (which is reasonable when a single company owns and operates all the generation facilities within a CA). This was the practice of LFC studies reported before deregulation [63]; in the new environment, each GenCo is represented by a single generating unit. Also in the VIU environment, load disturbances in a CA affect other CAs through the tie-lines only, while in the deregulated environment, they affect not only through the tie-lines, but also through various possible inter-area bilateral load matching (LM) contracts, making the disturbance rejection problem more challenging [84]. The other work [100, 143] studied LFC in a 2-area deregulated network using centralised MPC. As would been seen later, the definition of area control error in the deregulated environment is modified to account for bilateral LM contracts. Also, with the exception of the CeMPC studies [96, 101, 113, 136], GRC nonlinearity has often been ignored in the predictive control based LFC design. Therefore, more work on LFC in the deregulated environment, accounting for GRC nonlinearity, as well as constraints on control inputs, is required. A summary of the main strengths and weaknesses of the predictive control based LFC schemes is provided in Table 2.6.

Table 2.6: The key strengths and weaknesses of current predictive control based LFC summarised

Technique	Strengths	Weaknesses
LFC based on Predictive control [96, 101, 102, 108, 112–116, 135–141, 145–147]	Work well under multivariable conditions, systematic and good constraints handling.	Existing proposals not exploit potential of MPC or up to date power system structure (deregulated power system structure). Most of the schemes often ignore generation rate constraints.

2.4.6 LFC based on robust technique

Robust control methods are techniques that focus on how best to handle uncertainties. The philosophy is based on designing a controller to be able to deal with not only the nominal plant (imperfect model), but a family of plants in the neighbourhood (uncertainties) of the nominal plant and also, to reject unknown disturbances and cope with time delays. A number of robust schemes, largely focused on parameter uncertainty and time delays, have been reported in the literature [74, 79, 80, 84, 89, 90, 109–111, 148–155]. The decentralised LFC of a four-area system using $\mu-$synthesis and analysis was described by [74]. A sequential design approach was adopted where the controllers are designed in steps, from one area to the another. At each step, the information of the previous controller(s) are incorporated in the design of the next controller. Simulation results verify the effectiveness of the proposed method. A H_∞ control design for LFC of a four-area deregulated system was described by [110], and the controller was synthesised using LMI technique. The results obtained, under some variation in system parameters, show that the proposed method outperforms a PI based LFC.

Furthermore, in [79, 80], decentralised robust LFC schemes were proposed; the study [79], used a mixed H_2/H_∞ control strategy, while [80] combined a mixed H_2/H_∞ with neural networks. In both schemes, simulations were conducted on a three-area deregulated framework, under parameter uncertainties and GRC conditions, to demonstrate their effectiveness. An LFC scheme based on the concept of active disturbance rejection control (ADRC) was proposed by [148]. A three-area test system, consisting of a reheat, non-reheat and hydraulic turbine units, was considered. The ADRC technique is based on designing an extended observer to estimate (online) uncertainties that are inherent in power system operations. This estimation is embedded in the control law to decouple the system from the actual uncertainties. Simulation results show that the proposed strategy met the LFC requirements. A linear active disturbance rejection control scheme for LFC, with an anti-GRC feedback loop was proposed in [84] and its efficacy was demonstrated on a 4-area deregulated system. A two-layer active disturbance rejection control LFC scheme was proposed in [149] and tested on a 2-area system; the first layer

comprises of a generalised state observer and an equivalent input disturbance compensator to handle disturbances and uncertainties, and the second layer uses a state-feedback scheme to ensure system stability and reference tracking.

In [109], a robust decentralised PID controller was proposed for LFC of a multi-area system in the presence of parameter uncertainties, where Kharitonov's method was utilised to identify a family of plants and stability boundary locus method was used to obtain stabilising gains for the plants, while [150] presented a fractional order PID-based LFC scheme for a single area interval system and applied Kharitonov's method to obtain controller gains that ensure system stability within the parameter interval considered. In [111], a decentralized PI-based LFC based on sliding mode control strategy was presented, and tested on a 3-area system with matched and unmatched parameter uncertainties. A Robust LFC scheme based on H_∞ technique, to minimise frequency and tie line flow deviations, was reported in [151]. In the work, unmodelled dynamics, system nonlinearities and undesirable tieline flows were represented as a bounded sector of uncertainties. The superiority of the scheme over a traditional PI based LFC was demonstrated on a 2-area system. In [152], robustness analysis on a single generating unit supplying power in a single area network, based on a number of existing robust techniques, was used to show that unmodelled dynamics could have a more negative impact on LFC performance than parameter variations. A configuration to overcome the effect of GRC was also presented.

For the LFC problem considering communication delays, [153] considered an LMI approach to design an LFC scheme to achieve robustness against delays in ACE signal, where the effectiveness of the scheme was tested on a 3-area system. The work [154, 155] investigated the delay-dependent stability of PI-based LFC scheme; [154] focused on a traditional LFC model with delays, and calculated the delay margin using a Lyapunov stability criterion for time delays and LMI methods, and also showed the relationship between the delay margin and controller gains; [155] considered a deregulated LFC model, and provided an improved and a more computational efficient stability criterion for calculating delay margin, revealed the interactions between delay margins of different CAs, and demonstrated how the delay margin could be used as additional performance index for controller tuning. Also, a delay-dependent robust method was presented in [89] for the analysis/synthesis of a PID-based LFC scheme, where the delay margin was obtained by minimising a robust performance index. Also in [89], consideration was given to the impact of both delays and disturbances, and the robustness against delays below the delay margin was demonstrated on a 3-area system under traditional and deregulated scenarios. In [90], a delay-distribution-dependent H_∞ LFC was proposed, where the probability distribution characteristic of the communication delay was considered in a single area LFC problem.

Table 2.7: A summary of the key strengths and weaknesses of robust-based LFC designs

Technique	Strengths	Weaknesses
Robust LFC considering either parameter uncertainty or time delays [74, 79, 80, 84, 89, 90, 109–111, 148–155].	Works well under multivariable conditions and handles uncertainties within the design bounds.	Some lead to high order fixed gain controller, hence may be impractical for large dimensions. Generally, they are highly conservative and therefore control performance may be less than what is achievable. Also, they lack constraint handling capabilities and are not distributed.

A unique feature of the above techniques is their ability to cope with MIMO systems. Also, they work well under the bounds of uncertainty considered, e.g., the range of parameter variations for which the controller was designed or the delay margin for work focused on robustness against time delays. However, some of the strategies above mainly yield high order controllers, which may preclude practical implementability in the rapidly expanding deregulated power environment. Furthermore, the proposed methods do not demonstrate systematic constraint handling capabilities. In general, robust schemes are highly conservative and therefore may suffer performance degradation for uncertainties not captured. A summary of the strengths and weaknesses of robust based methods is given in Table 2.7.

2.4.7 Intelligent control based LFC techniques

Under the intelligent control techniques, discussions are focused on fuzzy based LFC in Section 2.4.7.1, neural network based LFC in Section 2.4.7.2 and neuro-fuzzy LFC schemes in Section 2.4.7.3. A summary of their strengths and weaknesses is provided in Table 2.8

2.4.7.1 Fuzzy logic based LFC

Fuzzy logic strategies have gained considerable attention in the control system community. A literature survey on fuzzy logic controller can be found in [156]. Fuzzy controllers execute control based on the degree of "True or False" selected from a membership function rather than the crisp value of "True or False". It is commonly applied in the control of ill-defined, nonlinear and hard to model systems [157]. Fuzzy control schemes have been considered for LFC [75, 87, 94, 158–163]. In [158], a fuzzy gain scheduling PI controller for LFC of a 4-area system, with GRC and GDB nonlinearities, was presented. The areas consist of three reheat turbine thermal units and one hydro unit. This controller uses fuzzy logic to effectively change the controller gains as the system parameters change. Simulation results

showed that the proposed controller achieved the main LFC objectives. A Takagi-Sugeno (T-S) type fuzzy inference system approach was considered in [75] to design an adaptive gain scheduling scheme for conventional PI and a linear optimal controller in a two area LFC. The gains of the controllers were adjusted online by the fuzzy system. Simulation results reveal that the controllers can achieve LFC requirements, under nominal and off-nominal conditions.

Furthermore, [159] proposed a version of fuzzy gain proportional and integral (FGPI) controller for the LFC of a 2-area system. A higher number of membership functions (MFs) were chosen as compared to [158] and universe of discourse used to represent the PI gains were also chosen to be different. Simulation results show an improved performance as compared to [158]. In the deregulated power system, large system disturbances will be common due to the increased number of power transactions, competition and open transmission access. This, if not suitably controlled, can cause cause the governor valve to saturate and create large overshoots and sustained oscillations in nominal frequency and tie line power interchange. The design of a robust LFC to handle such disturbances, using T-S fuzzy logic and LMIs, has been described by [160]. The method considered both the governor valve position nonlinearity and plant parametric uncertainty, and incorporated both into the design procedure. Simulation results, using a 2-area test system, show that the proposed controller achieved its objectives.

In [94], a fuzzy logic control based LFC was proposed for a power network with high penetration of wind energy; the fuzzy controller parameters were tuned using a particle swarm optimisation (PSO) technique, and its effectiveness was demonstrated on a 3-area system, while a PI-based LFC, tuned online by a combination fuzzy logic and PSO was proposed in [161], and efficacy demonstrated using an experimental setup. In [164], a multi-area LFC scheme based on direct-indirect adaptive fuzzy control technique was proposed. The adaptive fuzzy control law consists of three parts: a primary control term, a term that uses fuzzy logic to approximate unknown parameters and nonlinearities such as GRC and GDB, and an auxiliary control part to attenuate errors due to fuzzy approximation and to attain H_∞ tracking performance. The superiority of the proposed scheme over a traditional LFC scheme was demonstrated on a 3-area system. A 2-area LFC scheme, based on a type-2 fuzzy logic, was proposed in [87], and its effectiveness was demonstrated in the presence of GRC and model parameter uncertainty. Recently, a quasi-oppositional harmony search-based fuzzy logic LFC was proposed in [162], and tested on a 4-area deregulated power system, while a type-2 fuzzy logic scheme combined with a classical PD controller was reported in [163] for a 2-area system, taking into account nonlinear communication delays.

The above fuzzy schemes proved to be suitable for power system nonlinearity and plant parameter uncertainties. However, the rules used by the proposed methods for obtaining the knowledge FLCs are not systematic. Furthermore, structural properties of a control system such as stability, controllability, sensitivity analysis and robustness cannot be systematically

studied in the proposed FLCs system. For instance, the author in [160] demonstrated robustness by using Lyapunov's theory in conjunction with a LMI but the approach was highly conservative, complex and supported by "sufficient rather than necessary conditions" which makes it lack flexibility to control complicated and large systems like the power grid. Other weaknesses with fuzzy logic approaches are the lack of a standardised methodology for deciding on the membership functions. As an example, [159] used seven triangular membership functions for the PI gains while [158] used two exponential-type curves for the same gains. Finally, most of the fuzzy methods proposed were completely centralised and could only be used as benchmarks.

2.4.7.2 Neural network based LFC

Artificial neural network (ANN) schemes mimic the human brain, which has the ability to learn certain patterns, store them and use them to make deductions when a similar pattern is presented. It is capable of handling nonlinearities and parametric uncertainties, and has been used in LFC [76, 95, 165–167]. In [165] a neural network (NN) scheme was presented to monitor the operation of an adaptive LFC scheme The NN, which operates in parallel with the adaptive scheme, was trained offline. Simulations were conducted to show the superiority of the proposed framework over a purely adaptive control based LFC. The application of a centralised multi-layer perceptron ANN scheme to the LFC of a 4-area system with three reheat steam turbines and one hydro turbine was described by [76]. Simulation results, under load perturbations and GRC, reveal that the ANN scheme outperforms a conventional integral controller.

A PID based LFC scheme, tuned by an ANN framework was proposed in [166]. The neural network scheme was trained under different load pertubations to obtain a set of PID gains. Simulation results indicate that the proposed controller possesses a better transient performance than a conventional PID scheme. A multilayer perceptron neural network based LFC for a 3-area system was reported in [167]. The inputs to the neural network are the area load perturbations, tie-line and frequency deviations. Simulation results, with GRC considered, also reveal its superiority over a conventional integral controller. A neural network based integral sliding mode control scheme was proposed in [95] for LFC, where uncertainty due to the wind energy penetration was considered; GRC nonlinearity was also considered and represented as part of system uncertainties. The total system uncertainty was captured by a radial basis function network, and simulation was performed on a 2-area system.

A common feature in the neural network schemes proposed above is their ability to provide good dynamic performance in the face of parametric uncertainties and nonlinearities. However, these nice properties of the neural network schemes must be acquired through some learning process. The performance of the ANN scheme is a function of the amount of labelled pattern

in its memory base. To obtain an acceptable performance, a large data base of examples, reflecting all possible system operating conditions, must be used for training. Potentially unrealistic amounts of data, computer memory and disk space will be required to achieve this for a large interconnected system. During training, a large amount of CPU processing power and time must also be sacrificed.

This is a general limitation of ANN technique for control of large scale power interconnections. Also, a neural network operates as a black-box and analyzing its functionality and what has been learned is difficult. The large number of neurones in the hidden layers needed to capture system complexity is also an issue. Most of the ANN scheme proposed used a centralised control which assumes the information from different areas, such as the frequency deviation, can be collected to one location. This is impractical for current geographically expansive power systems.

2.4.7.3 LFC based on hybrid intelligent scheme (neuro-fuzzy)

The neuro-fuzzy technique combines the learning ability of the neural network strategy and human-mimicry feature of the fuzzy logic strategy to synthesise controllers. Some AGC problems using the hybrid controller have been reported in the literature. A fairly recent work on LFC of a 2-area deregulated power system using hybrid intelligent controller was presented in [168]. The scheme, based on an adaptive neuro-fuzzy inference system, was trained offline under various load conditions, using PSO optimal gain scheduling, to obtain an array of integral gains for the two control areas. Simulation results show that the proposed controller achieves faster response to load disturbances than a PSO adaptive integral controller.

A hybrid LFC which combines fuzzy logic, genetic algorithm (GA) and ANN was reported in [169]. The scheme utilised GA to determine the FLC parameters and the parameters were in turn used to train an ANN controller. Simulation results, using a single-area test system, show a superior dynamic performance over a coventional PI scheme. A hybrid neuro-fuzzy LFC scheme was presented in [170] and tested on a 3-area system in the presence of GRC nonlinearity.

Peculiar to the hybrid schemes discussed here is their insensitivity to changing loads, hence, they provide a robust LFC performance. Also, they worked well with limited a priori knowledge of the test system used. However, selecting the optimal number of neurones needed in the ANN schemes is unresolved. The verification of structural properties of a control system such as stability, controllability, sensitivity analysis and robustness is difficult with these hybrid controllers. The issue of how to extract knowledge from a fuzzy method, is also transfered to the neuro-fuzzy methods.

Table 2.8: A summary of the strengths and weaknesses of Intelligent control based LFC

Technique	Strengths	Weaknesses
Intelligent LFC (fuzzy [75, 87, 94, 158–163], neural network [76, 95, 165–167] and neuro-fuzzy [168–170]).	Handles uncertainties and nonlinearity. Intelligent techniques work well for small scale systems	The construction of rules and tuning is impractical/not systematic for large scale interconnected networks. Analysis such as stability, controllability, controller robustness, etc., is difficult. Also, constraints handling capability is weak.

2.5 Other LFC studies

This section reports other work on LFC which do not exactly fall under the LFC design techniques discussed in Section 2.4; some work reported here are more focused on LFC system analysis rather than controller design. Designing and implementing a frequency control scheme in practice is challenging as a number of design issues such as tolerable bounds of frequency fluctuations and ACE, impact of restructuring and deregulation, penetration of renewable energy, indices for frequency control performance measures, etc. must be considered, and this will vary from one jurisdiction to another. Furthermore, achieving a compromise between frequency regulation cost, reliability, power consumers' satisfaction, etc. has to be considered.

In [171], a methodology for re-designing frequency control in AC networks was proposed. The work described a number of steps to achieve an optimal strategy in terms of cost of control, network security, reliability and markets, and it was stated that the proposed strategy resulted in over an 80% reduction in generator movements in the South African network without a serious impact on custumers or network reliability. For the first time, an analytic framework for the formulation and evaluation of frequency control performance in LFC was developed in [172] using concepts from probability and random processes. The framework developed was considered as a generalisation of the NERC CPS1 and CPS2 frequency performance measures, which had hitherto lacked an analytical basis. In [173], it was shown, using a 4-area network implemented with a virtual power system, that frequency fluctuations during transients increase and last longer as the number of generating units on LFC decreases. A framework to quantify the impact of uncertainties arising from renewable generation, load variations, and noise in communication channels on AGC systems was developed in [92], where approximate probability expressions were obtained for system frequency and ACE.

The feasibility of procuring load following services through a bilateral contract between generating units and customers in a deregulated power environment was reported in [174]. The authors suggested a decentralised framework for load following by considering a local PI control

loop on each generator on bilateral load following contract, and provided a model description. Two frameworks for load following in a deregulated energy market were reported in [175]. The first considered a self-providing mechanism where DisCos negotiate bilateral contracts with GenCos for load following, and actual power imbalances are telemetered to a control centre for the independent system operator (ISO) to dispatch generators according to contracts; the second focused on the pool model where the ISO procures load following services from a competitive market. The efficacy of both schemes, implemented using reset controllers, were demonstrated using IEEE-30 bus test system. A tool to enable a generator to optimally allocate its resources to energy market, LFC market and market for reserves, and maximise profit while satisfying its technical constraints was presented in [176]. The tool utilised a mixed-integer mathematical programming technique.

The increasing integration of wind power into existing power system [177] has raised interests in the consideration of wind systems in LFC studies. A flatness-based approach was proposed in [93], for the LFC of a multi-machine system with high penetration of wind energy. The approach splits an n machine system into n linear controllable systems, equipped local controllers that track system operating points using reference reference information determined by a global level economic dispatch scheme. A strategy to enable a wind farm connected to AC network via HVDC line to participate in LFC was reported in [178]. A droop control loop was introduced in the HVDC rectifier which senses deviations in grid frequency, and regulates the flow on the HVDC line via the HVDC control of the power delivered by the wind farm. In [179], MPC was suggested for LFC of microgrids through the coordinated control of blade pitch angle of wind turbine generators and plug-in hybrid electric vehicles (PHEVs), where it was shown that such coordinated control reduces the number of PHEVs participating in LFC.

As described in Section 2.3, communication delay is an important issue that should be considered in practical LFC studies as large delays can result in poor control performance. An LFC scheme capable of thwarting time delays injected by a hacker into the LFC system was reported in [180]. It was stated that such time delays could result in an unstable condition. The reported scheme was designed by augumenting a state feedback controller with an online time delay estimator to obtain a modified controller that can handle injected time delays. A graphical method for determining stabilising PI gains for a single area LFC with a time delay was reported in [181]. The work utilised a stability boundary locus technique to display controller parameters in a two dimensional PI-parameter space, and hence obtained the region of stabilisation via simulations. An event-triggered LFC scheme for a multi-area system, accounting for communication delay, is presented in [182], to obtain reduced communication between sensors and controller, and stability conditions under event-triggering were established. Modelling and stability analysis of the AGC system of a smart grids using cognitive radio (CR) network as the networking and communication infrastructure was reported in [183]. The key challenge here is the data loss, delays and hence instability that could arise when a primary

user of the CR network randomly interrupts a secondary user, and this work provided sufficient conditions for the stability of AGC when an interruption occurs.

In any control design, such as the design of an LFC scheme, it is important that Engineers utilise a suitable simplified system model as this would result in significant savings in hardwares/computer memory used in processing control actions. In [184], a simulation scheme relevant to AGC studies was developed. The key objective was to achieve high computational efficiency in AGC simulations, by representing the AGC model using algebraic equations as opposed to traditional dynamic models. A two-stage procedure for the identification of transfer function models for LFC purposes was reported in [185]. The first stage utilises a bandwidth limited frequency response (FR) identification procedure to obtain a FR with reduced noise level and hence reduce model order, and the second stage computes the transfer function from the filtered FR obtained in the first stage.

Recently, nature inspired/intelligent optimisation techniques have been considered in tuning controller gains in LFC schemes. In [186], a three-degree-of-freedom integral derivative based LFC was proposed for a two-area deregulated power system, where the parameters of the three controllers were optimised using biogeography-based optimisation strategy. The superiority of the scheme over a two-degree-of-freedom and a single-degree-of-freedom integral derivative schemes was also shown. A PID based LFC scheme was proposed for a 2-area network in [187], where the controller gains were optimized to obtain improved performance using lozi map-based chaotic optimization method. Moreover, a PID based LFC whose gains were tuned using particle swarm optimisation method was proposed in [85], and tested on a four-area deregulated system. A fractional order PID LFC scheme, tuned by a bacterial foraging technique, was reported in [86], and tested under GRC condition.

In [188], a quasi-decentralised unscented transform-based LFC scheme was reported. The work included excitation systems to the conventional LFC model, avoided aggregation assumptions, and utilised magnitude and phase measurements of system variables. A cooperative control scheme based on differential games was reported in [189] for a multi-area LFC problem, and its superiority over the traditional PI control and linear quadratic regulator (LQR) was demonstrated. The authors in [190] proposed a distributed LFC framework for a 4-area network, consisting of battery storage systems, heat pumps and traditional power plants. The work used state feedback regulators whose gains were determined in real time using an iterative gradient method; some comparison results between the proposed scheme, a centralised and a decentralised LFC were provided. A PI-based LFC scheme based on the method of inequalities and principle of matching, and taking GRC into account, was proposed in [191] for a single area system. In a letter presented in [192], critical load level information was used to provide adaptive LFC participation factors under rapid demand fluctuations to prevent violating transmission line load limits. In [193], a stability-equation method, accounting for

governor backlash nonlinearities, was reported for the analysis and design of LFC of a 2-area network. The scheme uses harmonic-balance equations and a characteristic equation to obtain a parameter plane where stable integral gains are obtained.

2.6 Conclusion

This chapter provided a large amount of fine detailed information on power system frequency control, and therefore, summarising the key message in this chapter, and how it leads/relates to the main aim and objectives of this thesis is important. Recall from Section 1.4 that this thesis aims to investigate the use of predictive control technique in the LFC problem of deregulated (new) multi-area power interconnections, and two of the key objectives stated to achieving the aim of this thesis are:

- To highlight the key strengths and weaknesses of existing LFC techniques and hence where new work is required.

- Develop a generalised LFC modelling framework that incorporate the various power transactions (market structures for LFC), by modifying the traditional LFC modelling framework.

To present the key message of this chapter and reconcile it with the main aim of the thesis and the two objectives itemised above in this section, the following three questions are posed: (i) What are the major themes covered in this chapter? (ii) Why are the themes important? (iii) How does the thesis use the themes? These three questions are discussed in detail in Sections 2.6.1-2.6.3.

2.6.1 What are the major themes covered in this chapter?

The main part of this chapter (Sections 2.1-2.5) covered three major themes enumerated next:

1. Section 2.1 focused on developing LFC mathematical modelling framework in the traditional (VIU) environment and also presented simulations to illustrate frequency control concepts in the VIU environment. This will be referred to as **theme 1.**

2. Section 2.2 discussed power system deregulation and restructuring, and described the three main market structure (poolco, bilateral and mixed market structures) for procuring LFC services in the new environment. This will be referred to as **theme 2.**

3. Sections 2.3-2.5 focused on discussing existing research work on LFC. This will be referred to as **theme 3.**

2.6.2 Why are the themes important?

Themes 1 and 2 (Traditional LFC modelling and market structures for LFC)

Theme 1 and theme 2 are important in developing the generalised LFC model which is a key objective and one of the contributions in this thesis. Since the generalised deregulated LFC model will be developed via the modification of the traditional LFC modelling framework, it was important to describe in detail the LFC model in the traditional environment, and that was what Section 2.1 served. The main equations from Section 2.1 that will be utilised are: (2.1) turbine governing system dynamics; (2.2) turbine dynamic model; (2.8) incremental power balance of the ith CA; (2.16) incremental net tie line dynamics; (2.17) area control error; (2.18) load frequency controller.

Furthermore, since the modification must reflect the various market structures (power transactions) in the new environment, it was also important to understand the LFC procurement mechanisms in each of the market structures (Section 2.2.1 poolco, Section 2.2.2 bilateral and Section 2.2.3 mixed market structures), and hence the purpose of Section 2.2.

Theme 3 (Existing research work on LFC)

As stated in Section 2.6.1, theme 3 covers Sections 2.3-2.5 which are focused on existing work on LFC. The importance of Section 2.3 was to provide a snapshot of the different issues/studies that have been considered in LFC studies from the early days to this day. The earliest amongst the studies concentrated on understanding LFC performance from a theoretical and dynamic viewpoint as previously LFC utilisation in the industry lacked good theoretical basis and analysis had been static [63]. Other issues are consideration of GRC and GDB, parameter uncertainties, obtaining unified terminologies specific to automatic generation control, the effect of deregulation, uncertainties resulting high penetration of renewable sources and from communication delays, and control system architectures (centralised, decentralised and distributed). Control techniques that have been considered in LFC were also highlighted.

Section 2.4 focused on control design and provided a detailed and up-to-date survey of LFC designs in the literature, grouped them according to different control techniques (Sections 2.4.1-2.4.7) and summarised the key strengths and weaknesses of each of the control techniques; the summary of their strengths and weaknesses can be found in Tables 2.2-2.8. Section 2.4 is very important as it serves the purpose of revealing where new work is required, and that is another key objective of this thesis.

Section 2.5 discussed existing contributions in LFC studies which are mainly analysis rather than controller design, and this is important to provide a complete picture of LFC works rather than providing discussions from a control design perspective only.

2.6.3 How does the thesis use the themes?

Themes 1 and 2 (Traditional LFC modelling and market structures for LFC)

Although already obvious from Section 2.6.2, the deregulated LFC benchmark models which will be developed and used in later chapters are based on incorporating the market structures for LFC procurements (theme 2) into the traditional LFC model (theme 1). These models include the 2-area model in Chapter 4 and the generalised LFC model proposed in Chapter 5 (from which a 7-area benchmark model will be developed). The 7-area deregulated LFC model will be used in Chapters 5, 6 and 7 while a new 4-area model will be developed and also used in Chapter 7 only. These are in line with key objectives 2-6 stated in Section 1.4.

Theme 3 (Existing research work on LFC)

Here, we drop further discussions of Sections 2.3 and 2.5 and focused on the detailed LFC review provided in Section 2.4 as it provided the roadmap (revealed the gaps) leading to the main aim and key objectives, and hence contributions of the thesis. To identify the key gaps, some of which form the basis of this thesis, the existing studies in LFC under a number of control techniques were discussed in Section 2.4, and as stated before, the strengths and weaknesses were identified. The strengths and weaknesses were examined based on the following minimum specifications of a good LFC design in today's power systems:

Minimum specifications of a good LFC design

- C_1: Simple, reliable and systematic design.

- C_2: Systematic and effective constraints handling capability.

- C_3: Distributed control architecture.

- C_4: Multivariable capability (MIMO).

- C_5: Robust against system uncertainties.

To reveal at a glance the strengths and weaknesses of the different techniques, a simplified comparison of the techniques based on the minimum specifications (C_1, C_2, C_3, C_4 and C_5) has been presented in Table 2.9, where the checkmark ($\checkmark$) indicates a strength, the xmark ($\times$) indicate a weakness and the double dagger ($\ddagger$) indicates a technique whose strength and weakness with respect to a given LFC specification is subjective. Further comments on each technique have also been provided in Table 2.9.

Table 2.9: LFC techniques comparison based on specifications of a good design

Techniques	Specifications of a good LFC					Further comments
	C_1	C_2	C_3	C_4	C_5	
Conventional	✓	✗	✗	✗	✗	Has not been investigated in the deregulated environment. Schemes mainly decentralised and may result in poor performance in highly interactive networks.
Linear optimal	✓	✗	✗	✓	✗	Has been considered in the deregulated environment. Existing designs are mainly centralised and quasi-decentralised.
IMC	✓	✗	✗	✓	✗	Has not been investigated in the deregulated environment. Mostly centralised and considered for single area system.
MRAC and STC	✗	✗	✗	✓	✓	Mainly investigated in the VIU environment. Online parameter estimation could be a challenge for large scale applications.
Predictive control	‡	✓	✓	✓	‡	Simplicity and robustness are subjective. Existing MPC based LFC that were designed to be robust [96, 138] are not simple and may be impracticable on large scale systems, while those that rely on the inherent robustness of nominal MPC are simple, reliable and systematic. Existing schemes have mainly investigated LFC in the VIU environment. No distributed scheme for deregulated system exists. Schemes mostly ignores GRC nonlinearity.
Robust	✗	✗	✗	✓	✓	Generally conservative. Most schemes result in high order controllers.
Intelligent	✗	✗	✗	✓	✓	Neural network LFC designs lacks transparency. Training/rule constructions could be impracticable for large scale systems. Not easily scalable and structurally adaptable.

From Table 2.9, it can be seen that no single control technique/existing studies meet the minimum specification for today's LFC. For example, apart from predictive control based schemes, others lack a systematic and effective constraints handling capability. Furthermore, schemes that are effective in handling uncertainties (MRAC and STC, robust based LFC and intelligent LFC schemes) could be too complex for large scale networks. Moreover, with the exception of some predictive control based LFC [102, 112, 114–116], other techniques considered a centralised or decentralised control architecture. However, the majority of the predictive control schemes are focused on the traditional power system, and hence more work is needed in predictive control application (distributed) in the deregulated power environment. Exploiting the constraint handling capability of predictive control scheme by considering both GRC and input constraints in the deregulated environment is also important. Note that a few predictive control based LFC schemes developed to be robust are in the literature; however they could be too complex for large scale networks.

Therefore, from a control design perspective, none of the existing studies/techniques meet the minimum specifications of a good LFC design in a present day power system such as robustness to system uncertainties, simple/systematic design, effective and systematic handling of various constraints, distributed architecture and MIMO capability, and as stated in [12], a continuous enhancement of LFC schemes is expected as progress is made in process control technology. However, a logical objective of any LFC scheme should be to find a method which enables an effective compromise.

Furthermore, simplicity (for computational efficiency), constraint handling (for economic and physical safety reasons) and distributed control architecture (for practical implementability and handling of interactions between area) should be key in any future LFC design. The effects of deregulation should also be adequately captured in any proposed LFC scheme. Finally, LFC schemes should regulate the power output of a generating unit in a manner that minimises cost in terms of wear and tear, suggesting an advantage to use optimal or optimisation based control technique such as predictive control, which this current work intends to utilise. Specifically it is noted that a key obstacle going forward is the potentially large scale nature of the problem and thus research is required to determine the best way of creating a simple, distributed, and hence practical, control strategy.

Chapter 3

Background on model predictive control

In Section 1.4 of Chapter 1, it was established that the main aim of this thesis is to investigate the efficacy of predictive control techniques (also known as model predictive control) in the load frequency control (LFC) problem of power systems in the deregulated environment. One of the relevant technical backgrounds needed to comprehend the deregulated LFC studies presented in Chapters 4-6, which include having an understanding of the basic concept of LFC in the traditional power system environment, has been presented in Chapter 2, where a comprehensive discussion of existing works on LFC to justify the aim of this thesis was also provided. Since predictive control is the technique considered in this thesis, it will be useful from a reader's viewpoint to also provide some technical background on predictive control.

Thus, the goal of this chapter is to present the basic concept of the model predictive control (MPC) technique, and discuss the main components of a typical MPC. The discussion of the main components of the MPC, which includes a mathematical description of each of the components, is initially focused on a centralised MPC (CMPC) architecture. Thereafter, the discussion of MPC is extended to a decentralised MPC (DeMPC) and a distributed MPC (DMPC) architecture, where their (DeMPC and DMPC) main attributes are emphasised. Some concluding remarks on the MPC architectures as well as a discussion of the suitability of predictive control schemes to the power system LFC problem is provided.

This chapter is organised as follows: Section 3.1 provides a brief discussion of the underlying concept of any MPC scheme; Section 3.2 focuses on the CMPC architecture and its key attributes, and provides a mathematical description of the main components of a CMPC algorithm; Section 3.3 discusses DeMPC, where a mathematical descriptions of the basics of DeMPC is provided and its key attributes are highlighted; Section 3.4 focuses on DMPC, provides its mathematical descriptions and discusses its key attributes; Section 3.5 provides some

concluding remarks on the different MPC architectures by summarising their advantages and drawbacks in Table 3.1, and briefly discusses the suitability of MPC to the LFC problem.

3.1 The basic concept of MPC

Model predictive control (MPC) is a model based process control technology that has been successfully employed in industrial settings; a description of some industrial MPC packages in existence during the last decades, and the features that reconcile them with important industrial process control issues is available in [28, 194, 195]. Within the context of power system, MPC has been applied to control the boiler system of a fossil-fired power station [196, 197], coordinated control of voltage in power networks [133, 198], dynamic load balancing of a power system portfolio and wind turbine applications and its coordination with plug-in electric vehicles [199–201].

The attraction towards MPC, particularly in the industrial settings, stems from simultaneously offering the following vital advantages [202]: (i) effective in controlling multivariable systems where interactions between output variables, disturbance and input variables could exist, (ii) explicit and systematic handling of constraints on system input, states and outputs, (iii) MPC schemes can be designed and coordinated with an upper layer that calculates optimal operating setpoints and (iv) the predictive property of MPC could help anticipate a future potential problem in a system.

The basic concept behind any MPC scheme is the same and this is stated in the following. At a given sampling instant, a model of the process/system is used to predict its future behaviour, based on the availability of estimates or measurements of the current state of the process and assuming the existence of a finite sequence of future control moves or policy. Then, given a desired behaviour (target) of the process and limits (constraints), and a sequence of control moves that causes the predicted behaviour to approach the desired behaviour in an optimal manner are determined such that the system constraints are not violated; this is done via an optimisation of a predicted cost. Only the first (current) control move of the optimised sequence of control moves is applied to the process, and to embed feedback in the MPC strategy, the entire process (prediction of future behaviour and calculation of optimal control moves based on a desired behaviour) is repeated at subsequent sampling instants when new state measurements/estimates are available.

The principle of repitition in MPC where a new sequence of control/policy is recalculated as new information becomes available is termed as receding horizon, and this can help reduce the mismatch between the predicted and desired process behaviour, and offers the MPC some degree of inherent robustness against model uncertainty [203]. It is important to emphasise that every MPC scheme requires a model of a process, and in many cases, a perfect model

of the process may not be required to achieve an acceptable control performance, as the receding horizon principle will handle some process-model mismatch (uncertainty). Hence a control designer should aim at using the simplest model that provides accurate enough system predictions [132].

3.2 Centralised MPC

This section discusses the main components of a typical MPC problem and provides key mathematical descriptions of the components. The discussions here are focused on a centralised MPC problem. Furthermore, the presentation here is restricted to a nominal MPC, where the control problem is based on a linear time invariant (LTI) system with no form uncertainty [203]. Typically, MPC algorithms have three major components, namely a model to predict future system behaviour, a set of system constraints and a cost function which provides a measure of predicted performance. Each of these components are discussed in detail in Sections 3.2.1-3.2.3.

3.2.1 Prediction model

Here, a discrete time (DT) LTI state space model representation is considered, as it is in line with the power system models used in this thesis, and this can be expressed as:

$$
\begin{aligned}
x_{k+1} &= Ax_k + Bu_k \\
y_k &= Cx_k
\end{aligned}
\tag{3.1}
$$

where $k \in \mathbb{Z}_{\geq 0}$ is a non-negative integer which indicates the sampling number and $\mathbb{Z}_{\geq 0}$ denotes the set of non-negative integer. $x_k \in \mathbb{R}^{n_x}$ is a vector of system's states, $u_k \in \mathbb{R}^{n_u}$ is a vector of control inputs and $y_k \in \mathbb{R}^{n_y}$ is a vector of system outputs. Unless otherwise stated, the model of (3.1) represents information in the current sampling time, that is, $x_{k/k} = x_k$. For clarity of presentation, this chapter assumes that the state variables are measurable. Furthermore, it is assumed that the system (A, B) is controllable and (A, C) is observable. Note that it is implicitly assumed here that the model of a given system represented in a continuous time format can be discretised and utilised for the MPC design.

3.2.2 Constraints

As previously mentioned, a key strength of the MPC technique is that system constraints can be explicitly considered during the design phase, and through the repetitive online optimisation,

constraint violation can be prevented. Here it is assumed that the system is subjected to linear constraints on the input and states. The input constraints can be expressed as:

$$u^{\min} \ \leq \ u_k \ \leq \ u^{\max} \qquad\qquad k \in \mathbb{Z}_{\geq 0} \qquad\qquad (3.2)$$

where $u^{\min}$ and $u^{\max}$ denote the lower and upper limits of the input constraints respectively. The expression in (3.2) can be further written as a single inequality:

$$\begin{bmatrix} I \\ -I \end{bmatrix} u_k \leq \begin{bmatrix} u^{\max} \\ -u^{\min} \end{bmatrix} \qquad\qquad k \in \mathbb{Z}_{\geq 0} \qquad\qquad (3.3)$$

Similarly, constraints on the state variable can be expressed as:

$$x^{\min} \ \leq \ x_{k+1} \ \leq \ x^{\max} \qquad\qquad k \in \mathbb{Z}_{\geq 0} \qquad\qquad (3.4)$$

where $x^{\min}$ and $x^{\max}$ denote the lower and upper limits of the state constraints respectively. State constraints can be further written as a single inequality:

$$\begin{bmatrix} I \\ -I \end{bmatrix} x_{k+1} \leq \begin{bmatrix} x^{\max} \\ -x^{\min} \end{bmatrix} \qquad\qquad k \in \mathbb{Z}_{\geq 0} \qquad\qquad (3.5)$$

The input and state constraints of (3.3) and (3.5) respectively can be combined to obtain a more compact inequality representation given as:

$$G_x x_{k+1} + F_u u_k \leq h \qquad\qquad k \in \mathbb{Z}_{\geq 0} \qquad\qquad (3.6)$$

$$G_x = \begin{bmatrix} \mathbf{0} \\ \mathbf{0} \\ I \\ -1 \end{bmatrix} ; F_u = \begin{bmatrix} I \\ -I \\ \mathbf{0} \\ \mathbf{0} \end{bmatrix} ; h = \begin{bmatrix} u^{\max} \\ -u^{\min} \\ x^{\max} \\ -x^{\min} \end{bmatrix} \qquad\qquad (3.7)$$

The matrix $G_x \in \mathbb{R}^{2(n_u+n_x)\times n_x}$, $F_u \in \mathbb{R}^{2(n_u+n_x)\times n_u}$ and $h \in \mathbb{R}^{2(n_u+n_x)}$. Note that the dimension of I (identity matrix) and $\mathbf{0}$ (zero matrix) in (3.3), (3.5) and (3.7) depend on the context of usage. Also, there could also be a constraint on the rate of change of the input $(u_{k+1} - u_k)$ and the system output y_k, and these constraints could be easily incorporated into (3.6); however they are not considered here. A description of how to represent output and rate of change of input constraints can be found in the MPC textbooks [132, 204]. Some literature represents

(3.2) and (3.4) in the generalised set membership form $u_k \in \mathbb{U}$ and $x_k \in \mathbb{X}$ respectively where $\mathbb{U}$ (assumed to be a convex and compact set) and $\mathbb{X}$ (assumed to be a closed and convex set) are input and state constraint sets. For a regulation MPC problem, it is commonplace to assume that $\mathbb{U}$ and $\mathbb{X}$ contain the origin in their interior.

3.2.3 Cost function

For a regulation MPC problem, where the objective is to steer the system states to the origin while maintaining a tolerable control effort, an open loop quadratic cost is minimised at each sampling instant and this can be written as:

$$J(x_k, u_k) = \sum_{t=0}^{\infty} \frac{1}{2} \left\{ x_{k+t+1}^T Q\, x_{k+t+1} + u_{k+t}^T R\, u_{k+t} \right\} \tag{3.8}$$

where $Q = Q^T \succeq 0$ (positive semidefinite and symmetric) and $R = R^T \succ 0$ (positive definite and symmetric) are the weighting matrices on the states and inputs in the MPC cost. The cost function of (3.8) has an infinite horizon which implies that the model of (3.1) must be simulated forward over an infinite time steps, that is, an infinite prediction horizon must be considered $\{x_{k+1/k}, x_{k+2/k}, x_{k+3/k}, \ldots, x_{\infty/k}\}$. In addition, the cost function of (3.8) must be minimised over an infinite sequence decision variables which are the control inputs $\{u_{k/k}, u_{k+1/k}, u_{k+2/k}, \ldots u_{\infty/k}\}$. However, in the absence of the constraints of (3.6), it has been shown [204] that the cost function (3.8) can be minimised in a finite number of steps by an optimal linear state feedback law given as:

$$u_k = -K x_k \tag{3.9}$$

The control law of (3.9) is known as a linear quadratic regulator (LQR). However, when the constraints (3.6) are present, an explicit optimal state feedback law of the form (3.9) does not exist. Thus, under the constraints scenario, MPC computes a feedback control law, by minimising the cost (3.8) based on system predictions, subject to system constraints (3.7), where the constraint minimisation problem is solved online at each sample instant when new state estimates/measurements are available, and after each minimisation, the first control action in the sequence is injected into the plant. The MPC law in the constraint case is nonlinear.

As the cost function (3.8) to be optimised employs an infinite horizon, the optimisation problem encountered by the MPC scheme is, in general, intractable. However, it has been shown that the infinite horizon cost (3.8) to be minimised can be reduced to a finite-dimensional optimisation problem by utilising the dual mode control concept [205].

3.2.3.1 Dual mode concept

In the context of MPC, dual mode control entails splitting the infinite horizon minimisation problem into two parts or modes, namely a finite horizon constrained optimisation problem (stage cost mode / mode 1) and an infinite horizon unconstrained optimisation problem (terminal cost mode / mode 2). Hence in dual mode, (3.8) can be expressed as

$$
J(\mathrm{x}_k, \mathrm{u}_k) \;=\; \overbrace{\sum_{t\,=\,0}^{n_c\,-\,1} \frac{1}{2} \{\mathrm{x}_{k+t+1}^T Q\, \mathrm{x}_{k+t+1} + \mathrm{u}_{k+t}^T R\, \mathrm{u}_{k+t}\}}^{J_S(\text{ stage cost, constrained})}
$$
$$
+ \underbrace{\sum_{t\,=\,0}^{\infty} \frac{1}{2} \{\mathrm{x}_{k+n_c+t+1}^T Q\, \mathrm{x}_{k+n_c+t+1} + \mathrm{u}_{k+n_c+t}^T R\, \mathrm{u}_{k+n_c+t}\}}_{J_T(\text{Terminal cost, unconstrained})} \tag{3.10}
$$

where n_c is the number of degrees of freedom in the input; it is also the prediction horizon in this case. Since the terminal cost is unconstrained, there is no guarantee that the system predictions will satisfy constraints beyond n_c. Using very large n_c might be beneficial but this could lead to a computationally expensive optimisation. However, it has been shown that if a terminal constraint is imposed on the state at the end of mode 1 x_{k+n_c}, which requires that it lies in a maximal admissible set (MAS) $\mathcal{S}_{\max}$ that is positive invariant, then the system evolution in mode 2 under the feedback law $\mathrm{u}_k = -K\mathrm{x}_k$ would guarantee the satisfaction of system constraints. In this context, a positive invariant set, in simple terms, is one that has a property such that when a state $\mathrm{x}_{k/k}$ enters the set, it subsequent evolution $\mathrm{x}_{k+i/k} \ \forall i > 1$ remains in the set. A more detailed treatment on this can be found in [132, 203]. Thus with the set $\mathcal{S}_{\max}$ constructed, an optimal unconstrained state feedback control law such as (3.9) is valid under the mode 2. In the following section, the complete MPC problem is developed.

Remark 3.2.1. *The cost function (3.8) represents the case where the state vector x_k is to be driven to zero. For the case where the output y_k is to be driven to the origin, the weighting matrix on the state Q can be replaced with $\mathrm{C}^T Q\mathrm{C}$, and the formulation presented in Section 3.2 remains valid.*

3.2.4 Complete MPC problem

In this section, open loop predictions based on stage cost and terminal cost are presented.

Stage cost

To develop the complete MPC problem, firstly, state predictions are generated by evolving the prediction model of (3.1) n_c steps into the future based on the cost J_S in (3.10):

1. At $t = 0$ in mode 1 of (3.10), the prediction is the same as the state expression (3.1).

2. At $t = 1$, the state expression is

$$
\begin{aligned}
x_{k+2} &= Ax_{k+1} + Bu_{k+1} \\
&= A^2 x_k + ABu_k + Bu_{k+1}
\end{aligned}
\tag{3.11}
$$

3. At $t = 2$, the prediction is

$$
\begin{aligned}
x_{k+3} &= A^2 x_{k+1} + ABu_{k+1} + Bu_{k+2} \\
&= A^3 x_k + A^2 Bu_k + ABu_{k+1} + Bu_{k+2}
\end{aligned}
\tag{3.12}
$$

4. At $t = n_c - 1$, following the previous trends, the prediction is

$$
\begin{aligned}
x_{k+n_c} &= A^{n_c} x_k + A^{n_c-1} Bu_k + A^{n_c-2} B^2 u_{k+1} + A^{n_c-3} Bu_{k+2} \\
&\quad + \cdots + ABu_{k+n_c-2} + Bu_{k+n_c-1}
\end{aligned}
\tag{3.13}
$$

Therefore, the vector of predictions up to n_c can expressed as

$$
\underbrace{\begin{bmatrix} x_{k+1} \\ x_{k+2} \\ x_{k+3} \\ \vdots \\ x_{k+n_c} \end{bmatrix}}_{\underset{\to k}{x}} = \underbrace{\begin{bmatrix} A \\ A^2 \\ A^3 \\ \vdots \\ A^{n_c} \end{bmatrix}}_{P_x} x_k + \underbrace{\begin{bmatrix} B & 0 & 0 & 0 & \cdots & 0 \\ AB & B & 0 & 0 & \cdots & 0 \\ A^2 B & AB & B & 0 & \cdots & 0 \\ \vdots & \vdots & \vdots & \vdots & \vdots & \vdots \\ A^{n_c-1}B & A^{n_c-2}B & A^{n_c-3}B & A^{n_c-4}B & \cdots & B \end{bmatrix}}_{H_u} \underbrace{\begin{bmatrix} u_k \\ u_{k+1} \\ u_{k+2} \\ \vdots \\ u_{k+n_c-1} \end{bmatrix}}_{\underset{\to k-1}{u}}
\tag{3.14}
$$

and a compact representation of the state prediction is:

$$
\underset{\to k}{x} = P_x x_k + H_u \underset{\to k-1}{u}
\tag{3.15}
$$

In (3.15), $\underset{\to k}{x}$ is the vector of state prediction; $\underset{\to k-1}{u}$ is the input sequence of control moves which is also known as the degrees of freedom in predictions. Note the following convention used throughout the thesis: $\underset{\to k-1}{u}$ indicates that the prediction starts from the current sampling

instant u_k; $\underset{\to k}{u}$ means that the prediction would start from the next sampling instant u_{k+1}. This convention is applicable to the system states and output predictions. The ouput prediction $\underset{\to k}{y}$ can be generated by multiplying each block element of the matrix $P_x \in \mathbb{R}^{n_x n_c \times n_x}$ and $H_u \in \mathbb{R}^{n_x n_c \times n_u n_c}$ by the model output matrix C in (3.1). Substituting (3.15) into J_S and performing a series of algebra, yields the stage predicted cost:

$$J_S = \frac{1}{2} \underset{\to k-1}{u}^T (H_u^T \mathbf{Q} H_u + \mathbf{R}) \underset{\to k-1}{u} + (H_u^T \mathbf{Q} P_x x_k)^T \underset{\to k-1}{u} + \frac{1}{2} \underbrace{x_k^T P_x^T \mathbf{Q} P_x x_k}_{\nu_1} \tag{3.16}$$

where $\mathbf{Q}$ and $\mathbf{R}$ are block diagonal matrices of Q and R respectively. The system constraints in the first n_c steps based on (3.6) are:

$$\underbrace{\begin{bmatrix} G_x & \mathbf{0} & \cdots & \mathbf{0} \\ \mathbf{0} & G_x & \cdots & \mathbf{0} \\ \vdots & \vdots & \ddots & \vdots \\ \mathbf{0} & \mathbf{0} & \cdots & G_x \end{bmatrix}}_{G_d} \begin{bmatrix} x_{k+1} \\ x_{k+2} \\ x_{k+3} \\ \vdots \\ x_{k+n_c} \end{bmatrix} + \underbrace{\begin{bmatrix} F_u & \mathbf{0} & \cdots & \mathbf{0} \\ \mathbf{0} & F_u & \cdots & \mathbf{0} \\ \vdots & \vdots & \ddots & \vdots \\ \mathbf{0} & \mathbf{0} & \cdots & F_u \end{bmatrix}}_{F_d} \begin{bmatrix} u_k \\ u_{k+1} \\ u_{k+2} \\ \vdots \\ u_{k+n_c-1} \end{bmatrix} \leq \underbrace{\begin{bmatrix} h \\ h \\ h \\ \vdots \\ h \end{bmatrix}}_{h_d} \tag{3.17}$$

$$G_d \underset{\to k}{x} + F_d \underset{\to k-1}{u} \leq h_d \tag{3.18}$$

Substituting the prediction of (3.15) into (3.18) gives:

$$F_S \underset{\to k-1}{u} \leq h_S \tag{3.19}$$

where $F_S = G_d H_u + F_d$ and $h_S = h_d - G_d P_x x_k$.

Terminal cost

As stated in Section (3.2.3.1), the evolution of the model (3.1) in mode 2 is governed by an optimal unconstrained state feedback control law; thus from the cost function J_T in (3.10),

1. At $t = 0$, the following expressions exist

$$u_{k+n_c} = -K x_{k+n_c} \tag{3.20}$$

$$\mathbf{x}_{k+n_c+1} = (A - BK)\mathbf{x}_{k+n_c} = \varPhi\mathbf{x}_{k+n_c} \tag{3.21}$$

2. At $t = 1$, the input and state predictions are

$$\mathbf{u}_{k+n_c+1} = -K\mathbf{x}_{k+n_c+1} = -K\varPhi\mathbf{x}_{k+n_c} \tag{3.22}$$

$$\mathbf{x}_{k+n_c+2} = \varPhi^2\mathbf{x}_{k+n_c} \tag{3.23}$$

3. At $t = 2$, the expressions for the input and state are

$$\mathbf{u}_{k+n_c+2} = -K\mathbf{x}_{k+n_c+2} = -K\varPhi^2\mathbf{x}_{k+n_c} \tag{3.24}$$

$$\mathbf{x}_{k+n_c+3} = \varPhi^3\mathbf{x}_{k+n_c} \tag{3.25}$$

The mode 2 predictions extends to infinity; by substituting these predictions into J_T in (3.10)

$$
\begin{aligned}
J_T &= \sum_{t=0}^{\infty} \frac{1}{2} \{\mathbf{x}_{k+n_c+t+1}^T Q\,\mathbf{x}_{k+n_c+t+1} + \mathbf{u}_{k+n_c+t}^T R\,\mathbf{u}_{k+n_c+t}\} \\
&= \frac{1}{2}\mathbf{x}_{k+n_c}^T \underbrace{\left[\left(\varPhi^T Q\varPhi + (\varPhi^T)^2 Q\varPhi^2 + \cdots \right) + \left(K^T RK + \varPhi^T K^T RK\varPhi + \cdots \right) \right]}_{P_f} \mathbf{x}_{k+n_c}
\end{aligned}
\tag{3.26}
$$

where $P_f \succeq 0$ (symmetric) is the terminal weight and represents the solution of the Lyapunov equation:

$$\varPhi^T P_f \varPhi = P_f - \varPhi^T Q\varPhi - K^T RK \tag{3.27}$$

Thus, the terminal cost function can be expressed as:

$$J_T = \frac{1}{2}\mathbf{x}_{k+n_c}^T P_f \mathbf{x}_{k+n_c} \tag{3.28}$$

Note that $\mathbf{x}_{k+n_c}$ is the n_cth block row of the state prediction (3.15) and can be expressed as:

$$\mathbf{x}_{k+n_c} = P_{n_c}\mathbf{x}_k + H_{n_c}\underset{\to k-1}{\mathbf{u}} \tag{3.29}$$

Substituting (3.29) into (3.28) yields the predicted terminal cost:

$$J_T = \frac{1}{2} \underset{\rightarrow k-1}{u}^T H_{n_c}^T P_f H_{n_c} \underset{\rightarrow k-1}{u} + (H_{n_c}^T P_f P_{n_c} x_k)^T \underset{\rightarrow k-1}{u} + \frac{1}{2} \underbrace{x_k^T P_{n_c}^T P_f P_{n_c} x_k}_{\nu_2} \qquad (3.30)$$

Terminal constraints

Although the terminal cost suggests that the terminal constraints should be infinite dimensional, it has been shown [132] that $\mathcal{S}_{\max}$ and hence the terminal constraints can be represented by a number of inequalities which is finite. Assume that $\mathcal{S}_{\max}$ defined as:

$$\mathcal{S}_{\max} = \{x \; : \; F_{\max}x \leq d_{\max}\} \qquad (3.31)$$

Since the requirement for satisfaction of constraints in mode 2 is that x_{k+n_c} must lie in $\mathcal{S}_{\max}$, the terminal constraints can be expressed as:

$$F_{\max}\left[P_{n_c}x_k + H_{n_c} \underset{\rightarrow k-1}{u} \right] \leq d_{\max} \qquad (3.32)$$

Here, (3.29) was substituted for x_{k+n_c}. Moreover, (3.32) can be expressed in the form:

$$F_T \underset{\rightarrow k-1}{u} \leq h_T \qquad (3.33)$$

where $F_T = F_{\max}H_{n_c}$ and $h_T = d_{\max} - F_{\max}P_{n_c}x_k$.

Combine the stage and terminal predicted costs

The MPC infinite horizon predicted cost is obtained by combining the stage and terminal mode predicted cost (3.16) and (3.30) respectively:

$$J(x_k, \underset{\rightarrow k-1}{u}) = \frac{1}{2} \underset{\rightarrow k-1}{u}^T S_f \underset{\rightarrow k-1}{u} + H_f^T \underset{\rightarrow k-1}{u} \qquad (3.34)$$

Here, $S_f = (H_u^T \mathbf{Q} H_u + \mathbf{R}) + H_{n_c}^T P_f H_{n_c}$ and $H_f = H_u^T \mathbf{Q} P_x x_k + H_{n_c}^T P_f P_{n_c} x_k$. The terms ν_1 and ν_2 in (3.16) and (3.30) respectively are dropped because they are not a function of the degrees of freedom $\underset{\rightarrow k-1}{u}$. Thus, the centralised MPC problem P_{CMPC} can be formally stated as follows

$$\text{P}_{\text{CMPC}}: \qquad\qquad \min_{\substack{\text{u} \\ \rightarrow k-1}} \{\frac{1}{2} \underset{\rightarrow k-1}{\text{u}}^T S_f \underset{\rightarrow k-1}{\text{u}} + H_f^T \underset{\rightarrow k-1}{\text{u}}\}$$

$$(3.35)$$

Subject to

$$F_D \underset{\rightarrow k-1}{\text{u}} \leq h_D$$

where

$$F_D = \begin{bmatrix} F_S \\ F_T \end{bmatrix}, \quad h_D = \begin{bmatrix} h_S \\ h_T \end{bmatrix}$$

Note that in some MPC literature, the terminal constraints (3.33) in the MPC problem is expressed in the form $\text{x}_{k+n_c} \in \mathcal{S}_{\max}$. It is important to emphasise that for the nominal case considered here, the use of an infinite horizon makes the cost $J(\text{x}_k, \underset{\rightarrow k-1}{\text{u}})$ a Lyapunov function and this property, together with a well-designed $\mathcal{S}_{\max}$, is used to guarantee closed-loop stability and recursive feasibility a priori [132].

Remark 3.2.2. *The dual mode formulation presented here is an open loop paradigm and other variants are available. Another formulation, which uses closed loop predictions utilises a perturbed control law* $\text{u}_{k+i} = K\text{x}_{k+i} + \text{c}_{k+i} \ \forall i = 0, \cdots, n_c - 1$ *in mode 1 and retains the feedback law (3.20) in mode 2. Under this closed loop paradigm (CLP),* $\text{c}_{k+i} \ \forall i = 0, \cdots, n_c - 1$ *replaces* $\underset{\rightarrow k-1}{\text{u}}$ *as the degree of freedom in prediction to handle constraints. Further discussions are available in [132]. With regard to a different approach that has also been adopted to guarantee stability and controller feasibility in centralised MPC problems, see [206].*

Remark 3.2.3. *The discussion presented in this chapter concentrates on a regulation problem where the MPC objective is to drive system states or outputs to zero. To address nonzero target tracking problems, the model of (3.1) is expressed as a deviation from state-state values, i.e,* x_k *is replaced by* $\text{x}_k - \text{x}_{ss}$*,* u_k *is replaced by* $\text{u}_k - \text{u}_{ss}$ *and* y_k *is replaced by* $\text{y}_k - \text{y}_{ss}$*, where* y_{ss} *is usually known and the pair* $(\text{x}_{ss}, \text{u}_{ss})$ *are supplied in real-time by a target calculator. Having made these adjustments, the procedure presented in Section 3.2 remains valid.*

3.2.5 Typical atttributes of a CMPC scheme

In general, centralised MPC schemes provide the best closed loop control performance in relation to other MPC architectures such as decentralised and distributed MPC which are discussed in Sections 3.3 and 3.4. This is because, a CMPC scheme has a global vision of the

controlled system. However, CMPC has several drawbacks when implemented on large scale systems [207], e.g. a large interconnected power network. Firstly, communicating systemwide information to a central location places a serious emphasis on speed of communication and network safety. Also, as online optimisation is associated with constrained MPC schemes, the computational/memory requirements are high for large scale operations.

In scenarios where high computational requirements are addressed through faster optimisation software [208], there could also be organisational obstacles in implementing CMPC if the different subsystems of the larger system are owned and operated by different entities; one example being the control areas within a large interconnected power system which are managed by different transmission system operators. Furthermore, CMPC schemes have low flexibility, as if a portion of a large scale system develops a fault or requires some form of maintenance, it may be necessary to halt the CMPC scheme for the entire system.

The CMPC scheme has a low fault tolerance capacity as it may lose its efficacy if any component of the control system (sensors, actuators, computer, communication system, etc) develops a fault. Finally, major modification of a CMPC scheme may be required if a new subsystem is introduced to the existing system, hence CMPC schemes are not easily adaptable to structural changes. Consequently, CMPC is often used as a control performance benchmark for other MPC architectures.

3.3 Decentralised MPC

In most control design problems involving large scale systems, it may be appropriate to partition the systemwide control task into a number of smaller local controls. In this situation, each local control scheme focuses on a subsystem (a section of the larger system), and the overall systemwide control is achieved by the aggregate control action of the local control schemes [204]. Therefore for DeMPC, a subsystem model of a lower-order is utilised for the MPC design, and it is assumed that the subsystem model, which represents the dynamics of a subsystem within the larger system, can be obtained by decomposing the model of the larger system.

3.3.1 Subsystem model

To obtain a subsystem model, assume that the model of (3.1) can be represented as:

$$
\underbrace{\begin{bmatrix} x_{k+1}^{[1]} \\ x_{k+1}^{[2]} \\ \vdots \\ x_{k+1}^{[i]} \\ \vdots \\ x_{k+1}^{[N]} \end{bmatrix}}_{x_{k+1}} = \underbrace{\begin{bmatrix} A_{11} & A_{12} & \cdots & A_{1i} & \cdots & A_{1N} \\ A_{21} & A_{22} & \cdots & A_{2i} & \cdots & A_{2N} \\ \vdots & \vdots & \vdots & \vdots & \vdots & \vdots \\ A_{i1} & A_{i2} & \cdots & A_{ii} & \cdots & A_{iN} \\ \vdots & \vdots & \vdots & \vdots & \vdots & \vdots \\ A_{N1} & A_{N2} & \cdots & A_{Ni} & \cdots & A_{NN} \end{bmatrix}}_{A} \underbrace{\begin{bmatrix} x_k^{[1]} \\ x_k^{[2]} \\ \vdots \\ x_k^{[i]} \\ \vdots \\ x_k^{[N]} \end{bmatrix}}_{x_k}
$$

$$
+ \underbrace{\begin{bmatrix} B_{11} & B_{12} & \cdots & B_{1i} & \cdots & B_{1N} \\ B_{21} & B_{22} & \cdots & B_{2i} & \cdots & B_{2N} \\ \vdots & \vdots & \vdots & \vdots & \vdots & \vdots \\ B_{i1} & B_{i2} & \cdots & B_{ii} & \cdots & B_{iN} \\ \vdots & \vdots & \vdots & \vdots & \vdots & \vdots \\ B_{N1} & B_{N2} & \cdots & B_{Ni} & \cdots & B_{NN} \end{bmatrix}}_{B} \underbrace{\begin{bmatrix} u_k^{[1]} \\ u_k^{[2]} \\ \vdots \\ u_k^{[i]} \\ \vdots \\ u_k^{[N]} \end{bmatrix}}_{u_k}
$$

$$
\tag{3.36}
$$

$$
\underbrace{\begin{bmatrix} y_k^{[1]} \\ y_k^{[2]} \\ \vdots \\ y_k^{[i]} \\ \vdots \\ y_k^{[N]} \end{bmatrix}}_{y_k} = \underbrace{\begin{bmatrix} C_{11} & \mathbf{0} & \cdots & \mathbf{0} & \cdots & \mathbf{0} \\ \mathbf{0} & C_{22} & \cdots & \mathbf{0} & \cdots & \mathbf{0} \\ \vdots & \vdots & \vdots & \vdots & \vdots & \vdots \\ \mathbf{0} & \mathbf{0} & \cdots & C_{ii} & \cdots & \mathbf{0} \\ \vdots & \vdots & \vdots & \vdots & \vdots & \vdots \\ \mathbf{0} & \mathbf{0} & \cdots & \mathbf{0} & \cdots & C_{NN} \end{bmatrix}}_{C} \underbrace{\begin{bmatrix} x_k^{[1]} \\ x_k^{[2]} \\ \vdots \\ x_k^{[i]} \\ \vdots \\ x_k^{[N]} \end{bmatrix}}_{x_k}
\tag{3.37}
$$

where N is the number of subsystems model that make up the system model (3.1), and it is assumed to be equivalent to the number of subsystems obtained by partitioning a large scale system. The variables $x_k^{[i]}$, $u_k^{[i]}$ and $y_k^{[i]}$ denote the state, input and output vector of an ith subsystem model. In (3.37), it assumed that the each subsystem output is decoupled, and the dimension of the matrix elements with the symbol $\mathbf{0}$ are context dependent. From (3.36) and (3.37), the ith subsystem model (lower-order) is:

$$
x_{k+1}^{[i]} = A_{ii}x_k^{[i]} + B_{ii}u_k^{[i]} + \sum_{\substack{j=1 \\ j \neq i}}^{N} \{A_{ij}x_k^{[j]} + B_{ij}u_k^{[j]}\}, \ y_k^{[i]} = C_{ii}x_k^{[i]}
\tag{3.38}
$$

where $x_k^{[i]} \in \mathbb{R}^{n_x^i}$, $u_k^{[i]} \in \mathbb{R}^{n_u^i}$ and $y_k^{[i]} \in \mathbb{R}^{n_y^i}$ are vectors of subsystem states, inputs and outputs respectively. The terms A_{ij} and B_{ij} are the state and input coupling/interaction matrix with dynamic neighbours j.

3.3.2 The DeMPC problem

In DeMPC, a local MPC problem is considered and in the local controller design phase, model predictions are made with a subsystem model in which the coupling terms are neglected. Thus, even though subsystems may be coupled via a network of energy, flow of materials or streams of information [209], the local MPC is designed to work independently, that is, it does not communicate with other local MPC schemes assigned to neighbouring subsystems. This is typically how load frequency control (LFC) is implemented in most interconnected power systems globally [210], although with a classical proportional-integral regulator. With a noninteracting subsystem model available, the design of each local MPC follows the philosophy of the CMPC design described in Section 3.2. Thus, the ith DeMPC problem $P_{i-\text{DeMPC}}$ can be stated for $k \geq 0$ as follows

$$P_{i-\text{DeMPC}} : \qquad \min_{\{u_{k/k}^{[i]}, \cdots, u_{k+n_c-1/k}^{[i]}\}} J_i(x_{k/k}^{[i]}, u_{t/k}^{[i]}) \qquad (3.39)$$

Subject to, $\forall t = \{k, k+1, \cdots, k+n_c-1\}$, $k \geq 0$

$$x_{t+1/k}^{[i]} = A_{ii} x_{t/k}^{[i]} + B_{ii} u_{t/k}^{[i]} \qquad (3.40)$$

$$x_{t+1/k}^{[i]} \in \mathbb{X}^{[i]} \subset \mathbb{R}^{n_x^i}, \ x_{k+n_c}^{[i]} \in \mathcal{S}_{\max}^{[i]}$$

$$u_{t/k}^{[i]} \in \mathbb{U}^{[i]} \subset \mathbb{R}^{n_u^i}$$

In the minimisation problem $P_{i-\text{DeMPC}}$, the local cost $J_i(x_{k/k}^{[i]}, u_{t/k}^{[i]})$ is defined as the standard quadratic MPC cost:

$$
\begin{aligned}
J_i(x_{k/k}^{[i]}, u_{t/k}^{[i]}) &= \frac{1}{2} \sum_{t=k}^{\infty} \{ {x_{t+1}^{[i]}}^T Q_{ii} \, x_{t+1}^{[i]} + {u_t^{[i]}}^T R_{ii} \, u_t^{[i]} \} \\
&= \frac{1}{2} \sum_{t=k}^{n_c-1} \{ {x_{t+1}^{[i]}}^T Q_{ii} \, x_{t+1}^{[i]} + {u_t^{[i]}}^T R_{ii} \, u_t^{[i]} \} + \frac{1}{2} {x_{k+n_c}^{[i]}}^T P_{f_{ii}} \, x_{k+n_c}^{[i]}
\end{aligned}
$$

where $P_{fii} = P_{fii}^T \succeq 0$. Here, it is assumed that the state at $k = 0$, that is $x_{0/0}^{[i]}$ is also contained in the set $\mathbb{X}^{[i]}$. Note that $\mathbb{X}^{[i]}$ and $\mathbb{U}^{[i]}$ are respectively the state and input constraints sets of the ith subsystem. $x_{t/k}^{[i]}$ denotes the state vector of the ith subsystem at sample time t measured at the kth sampling time; this definition is the same throughout the thesis where this representation is used. The prediction of (3.14) is equivalent to the expression in (3.40) for the ith subsystem.

3.3.3 Typical atttributes of a DeMPC scheme

The DeMPC scheme improves on some of the disadvantages of CMPC discussed in Section 3.2.5. Typically, issues associated with communication network such as speed and network security are almost insignificant since communication between subsystems is not required. Moreover, computational/memory requirements are relatively low since each local subsystem MPC optimises over local inputs only. The DeMPC architecture also offers improved flexibility as compared to CMPC as its inherent modular structure allows the maintenance of a subsystem and interruption of its local MPC only, while other local MPC schemes continue to operate. Furthermore, DeMPC has better fault tolerance capability; the failure of a component in a local control system does not drastically affect overall system performance [103, 211]. Also, DeMPC schemes have good structural adaptability properties as they can cope, better, with the removal or addition of a new subsystem [138, 211] .

However, these schemes have drawbacks. Firstly, extending the analyses employed in guaranteeing constraint satisfaction, recursive feasibility and stability in the centralised MPC to the DeMPC scheme, such as the careful design of MAS, terminal cost and the Lyapunov property of the centralised MPC cost, is difficult [212]. Hence, constraint satisfaction, recursive feasibility and stability cannot be guaranteed in the DeMPC scheme, although it may be retained in practice. Furthermore, since the coupling between subsystems are ignored in each local MPC design, there may be a systemwide performance degradation if the interactions/couplings between subsystems are strong. Hence DeMPC algorithms are best suitable for large scale systems in which the building blocks (subsystems) are weakly coupled. A work on DeMPC [213] considered the design of a decentralised MPC scheme using state feedback for nonlinear DT systems subject to asymptotically decaying disturbances. In the work, closed-loop stability was realised by including a contractive constraint in each local MPC optimisation problem. The contractive constraints ensure that the state trajectories associated with each subsystem are steered, forcefully, towards the origin in the face of disturbances and mutual interactions. For a discussion of other DeMPC schemes in the literature, please see [206, 212].

3.4 Distributed MPC

To improve the control performance of the DeMPC strategy when the coupling between subsystems are strong, each local MPC may need to communicate to achieve some coordinations amongst themselves. The resulting strategy, which now considers the coupling terms in (3.38), is called a distributed MPC (DMPC). It is important to note that a wide range of problems have been considered by researchers in the DMPC community, and a myriad of approaches with distinct properties, depending on the intended control goal, have reported in the literature. Consequently, categorising DMPC schemes in the literature, clearly, is a difficult task [212]. As an example, the couplings considered in DPMC problems are not restricted to states and inputs as (3.38) portrayed. Typically, couplings considered in DMPC problems could arise from five basic sources [103]. Firstly, there are dynamical systems whose subsystems are coupled via states only; in such a scenario, B_{ij} in (3.38) would be a null matrix. A natural example would be a multi-area power network where the main objective is to regulate frequency in each area and net tie line power using a distributed control strategy; the work in [114] is a typical example.

Furthermore, there are scenarios where only input couplings exit and A_{ij} in (3.38) would be a null matrix. Problems relating to input couplings are commonly encountered in chemical plants where changes in a manipulated variable (input) affects several controlled variables (output) or states; an example is the work reported in [209], where the efficacy of its DMPC proposal was demonstrated on a chemical process consisting of two continuous stirred tank reactors and a separator. Moreover, there are DMPC schemes developed for subsystems having decoupled dynamics but with coupled constraints; one work that considered this paradigm is [214]. A practical scenario is the multi-vehicle guidance and control problem where collision avoidance could be enforced through coupled constraints. One could also encounter a DMPC problem were the source of the coupling is the output of each subsystem. There are also situations where couplings originate from the objective function, that is, the subsystems are dynamically decoupled but are required to work together to achieve a common objective. A practical example could be a group of autonomous cars that are expected to follow a prespecified trajectory.

A more interesting example is the control of a group of autonomous cars that are expected to follow a prespecified trajectory while preserving a particular spatial pattern; this falls under what is known as formation control problems [215]. In this case, the requirement of preserving the spatial pattern can be implemented as coupled constraints and therefore, the DMPC problem will involve subsystems with decoupled dynamics, a coupled objective function and coupled constraints; the DMPC proposal in [216] considered this kind of problem. This shows that some DMPC schemes are designed to handle more than a single coupling source. It is worth mentioning that this section focuses on the basic philosophy of a typical DMPC scheme only

and deliberately avoid the finer details of DMPC algorithms. For a comprehensive overview of DMPC algorithms and applications, please see [103]. Another set of properties that can be used to describe and categorise DMPC algorithms are: (i) the protocol for information exchange between local MPC (ii) the cost function optimised by each local MPC. These properties are very important when the benefits of a proposed DMPC scheme are examined from a practical viewpoint[1], and they are described in the following sections.

3.4.1 DMPC algorithms based on information exchange protocols

Concerning information exchange protocols, DMPC algorithms can be categorised into two basic types.

3.4.1.1 Non-interative DMPC

In non-iterative DMPC algorithms, each local MPC scheme exchanges information with other local MPC schemes once within a control cycle/sample time to generate a local control law that is fed to the subsystem. This paradigm is common in practical systems where a controller performs a single calculation at a given time instant to obtain a control signal that is injected into the system. There are several DMPC proposals in the literature that are of the non-iterative type. For example, a pioneering work in the DMPC field [114] (see also [217]) proposed a non-iterative DMPC algorithm for a class of DT LTI unconstrained systems where subsystems are coupled via their states. The work uses state feedback and also falls under the non-cooperative DMPC category described in Section 3.4.2.1. A fairly recent work [218] proposed a non-iterative DMPC algorithm for DT LTI systems, where subsystems can be coupled via their states and inputs, and also considered state and input constraints; the scheme is of the non-cooperative DMPC type. For more examples on non-iterative schemes, please see [103].

3.4.1.2 Iterative DMPC

In iterative DMPC algorithms, each local MPC scheme exchanges information with other local MPC schemes multiple times within a control cycle to obtain a local control law for its subsystem; the communication between local MPC schemes within a sample time is terminated when some convergence conditions are met. Iterative approaches to DMPC designs come with an assumption that the sampling interval of the system is greater than the computational time needed to meet the converge condition. In situations when the system sampling interval does not allow for convergence, an iterative scheme has to be terminated prior to convergence of input and state trajectories. Typical papers on DMPC based on an iterative strategy are

---

[1]As an example, communicational constraints might prevent a proposal from being applied in practice.

[102, 219]. The iterative DMPC scheme proposed in [102] considered a DT LTI system where subsystems are coupled via inputs and subjected to input constraints only. Furthermore, the scheme falls under the cooperative DMPC category described in Section 3.4.2.2. In [219], the iterative DMPC scheme proposed considered a DT unconstrained LTI system described by an input-output model, where subsystems are coupled via inputs; the scheme can also be categorised under the non-cooperative DMPC type described in Section 3.4.2.1.

In general, iterative DMPC schemes tend to provide better systemwide performance compared to the noniterative schemes. However, the communication and computation overheads in iterative DMPC schemes are higher compared to their non-iterative counterparts and this could be a drawback [207].

3.4.2 DMPC algorithms based on cost function type

Regarding the type of cost function used, DMPC algorithms can be categorised into non-cooperative DMPC and cooperative DMPC. These are explained in the sequel.

3.4.2.1 Non-cooperative DMPC

In non-cooperative DMPC, each local MPC optimises a local cost or objective function, similar to the DeMPC scheme. Thus each local MPC considers the state and input trajectories of neigbouring subsystems as known disturbances affecting its output via the subsystem model, and one of the control responsibility of a local MPC is compensate of these disturbances with its optimal input sequence [204]. Some of the DMPC proposals mentioned in Section 3.4.1 are of the non-cooperative type. A key issue with a non-cooperative DMPC approach is that since the local MPCs have no idea of each other's objective function, there could be a conflict/competition between the local MPCs. From the perspective of game theory, the solution from non-cooperative strategies typically converges to a Nash equilibrium (NE). Depending on the system/process to be controlled, the NE may be unstable, thus resulting in systemwide instability. Furthermore, the NE may be stable but the resulting closed loop not stable. It could happen that the NE is stable and the system is also stable in closed loop. Please see [204, 220] for more details on non-cooperative approach and NE.

Thus, because of the tendency for a non-cooperative scheme to destabilise a system, additional constraints are usually incorporated in each local MPC problem to guarantee system stability and recursive feasibility [212]. Note that the analyses used in guaranteeing stability in CMPC are not directly applicable here in DMPC. In [114] (and also [217]), a non-cooperative, non-iterative DMPC scheme was proposed for DT LTI systems with state coupling. Stability was obtained in the scheme via the inclusion of a contractive constraint in each local MPC problem which prevents the Euclidean norm of the successor state of each subsystem from diverging;

the scheme does not guarantee stability a priori. Also, [218] presented a non-cooperative, non-iterative DMPC scheme for DT LTI constrained systems with state and input couplings; the work is based on the tube-based robust MPC strategy reported in [204]. Stability and convergence properties of the scheme are guaranteed by careful off-line design of weightings in each local cost, decentralised gains, terminal set and other tuning parameters which introduces some complexity.

One attractive feature of non-cooperative schemes is that each local MPC does not necessarily needs to know the dynamic models of neighbouring susbystems. A basic non-cooperative DMPC problem for the ith subsystem $\mathrm{P}_{i-\mathrm{nDMPC}}$ of (3.38) at $k \geq 0$ is stated as follows:

$$\mathrm{P}_{i-\mathrm{nDMPC}}: \qquad \min_{\{\mathrm{u}_{k/k}^{[i]}, \cdots, \mathrm{u}_{k+n_c-1/k}^{[i]}\}} J_i(\mathrm{x}_{k/k}^{[i]}, \mathrm{u}_{t/k}^{[i]}) \tag{3.41}$$

Subject to, $\forall t = \{k, k+1, \cdots, k+n_c-1\}$, $k \geq 0$

$$\mathrm{x}_{t+1/k}^{[i]} = A_{ii}\mathrm{x}_{t/k}^{[i]} + B_{ii}\mathrm{u}_{t/k}^{[i]} + \sum_{\substack{j=1 \\ j \neq i}}^{\mathrm{N}} \{A_{ij}\mathrm{x}_{t/k}^{[j]} + B_{ij}\mathrm{u}_{t/k}^{[j]}\}$$

$$\mathrm{x}_{t+1/k}^{[i]} \in \mathbb{X}^{[i]} \subset \mathbb{R}^{n_x^i}, \ \mathrm{x}_{k+n_c}^{[i]} \in \mathcal{S}_{\max}^{[i]}$$

$$\mathrm{u}_{t/k}^{[i]} \in \mathbb{U}^{[i]} \subset \mathbb{R}^{n_u^i}$$

The pair $(\mathrm{x}_{t/k}^{[j]}, \mathrm{u}_{t/k}^{[j]})$ $\forall t = \{k, k+1, \cdots, k+n_c-1\}$ $k \geq 0$, are the state and input trajectory of the jth neigbouring subsystems respectively.

3.4.2.2 Cooperative DMPC

In cooperative DMPC, each local MPC minimises a common cost function, which is essentially the systemwide cost (3.8). Consequently, each local MPC monitors the effect of its states and inputs on its own output as well as the outputs of other local MPC schemes. Since each local MPC minimises a systemwide cost, the control decision made by the local controllers represents an optimal compromise between the need of each subsystem. It has been shown that in an iterative-cooperative DMPC scheme, the MPC solutions can converge to a Pareto optimum if the sampling time of the system permits convergence of the iterative, cooperative algorithm, and thus providing a CMPC-like performance [209].

It is worthwhile to state that non-iterative, cooperative DMPC is not available since cooperation would require some negotiations between local controllers [212]. Examples of iterative,

cooperative DMPC schemes are the works presented in [102, 209] for DT LTI systems with input couplings and input constraints. It was shown that as the number of iteration within a sampling interval increases, the aggregate control actions of the local MPCs converge to a CMPC solution. Feasibility and stability guarantees, hinged on convexity properties, were demonstrated. The scenario where coupled input constraints are present was also considered in [209].

Typically, the systemwide cost considered in cooperative DMPC is taken as the convex combination of the local cost used in the non-cooperative DMPC case. Thus, a basic cooperative DMPC problem for the ith subsystem $\mathrm{P}_{i-\mathrm{cDMPC}}$ (3.38) can be stated, at $k \geq 0$, as follows:

$$\mathrm{P}_{i-\mathrm{cDMPC}} : \quad \min_{\{\mathrm{u}_{k/k}^{[i]}, \cdots, \mathrm{u}_{k+n_c-1/k}^{[i]}\}} \left\{ \rho_i \, J_i(\mathrm{x}_{k/k}^{[i]}, \mathrm{u}_{t/k}^{[i]}) + \sum_{\substack{j=1 \\ j \neq i}}^{\mathrm{N}} \{\rho_j \, J_j(\mathrm{x}_{k/k}^{[j]}, \mathrm{u}_{t/k}^{[j]})\} \right\} \qquad (3.42)$$

Subject to, $\forall t = \{k, k+1, \cdots, k+n_c-1\}$, $k \geq 0$

$$\mathrm{x}_{t+1/k}^{[i]} = \mathrm{A}_{ii}\mathrm{x}_{t/k}^{[i]} + \mathrm{B}_{ii}\mathrm{u}_{t/k}^{[i]} + \sum_{\substack{j=1 \\ j \neq i}}^{\mathrm{N}} \{\mathrm{A}_{ij}\mathrm{x}_{t/k}^{[j]} + \mathrm{B}_{ij}\mathrm{u}_{t/k}^{[j]}\}$$

$$\mathrm{x}_{t+1/k}^{[i]} \in \mathbb{X}^{[i]} \subset \mathbb{R}^{n_x^i}, \ \mathrm{x}_{k+n_c}^{[i]} \in \mathcal{S}_{\max}^{[i]}$$

$$\mathrm{u}_{t/k}^{[i]} \in \mathbb{U}^{[i]} \subset \mathbb{R}^{n_u^i}$$

The parameters $\rho_{1,\cdots}, \rho_i, \cdots, \rho_{\mathrm{N}}$ in (3.42) are used to specify the relative emphasis of each subsystem in the systemwide cost. Also, the convex combination of local costs requires that $\sum_{j=1}^{\mathrm{N}} \rho_i = 1$. With a few algebra steps, it can be shown that the cost function of (3.42) is equivalent to the centralised cost of (3.8) if the following definitions are considered:

$$Q = \begin{bmatrix} \rho_1 Q_{11} & & & & \\ & \ddots & & & \\ & & \rho_i Q_{ii} & & \\ & & & \ddots & \\ & & & & \rho_{\mathrm{N}} Q_{\mathrm{NN}} \end{bmatrix}, \ R = \begin{bmatrix} \rho_1 R_{11} & & & & \\ & \ddots & & & \\ & & \rho_i R_{ii} & & \\ & & & \ddots & \\ & & & & \rho_{\mathrm{N}} R_{\mathrm{NN}} \end{bmatrix}$$

In general, a cooperative DMPC could provide a better performance than noncooperative schemes if the algorithm is allowed to converge at each sample time. However, cooperative

schemes generally require that each subsystem supplies its dynamic model to the other sub-systems, and this may not be practicable especially when the subsystems are owned by different entities.

3.4.3 Typical attributes of a DMPC scheme

DMPC schemes, because of they are inherently modular, possess some of the positive attributes offered by the decentralised MPC scheme. Examples of the positive attributes are flexibility in maintenance of a subsystem within the larger system without a complete interruption of all local MPC schemes, fault tolerance and good structural adaptability [103, 211]. The computational requirements of DMPC and DeMPC schemes are similar since in both schemes, each local MPC optimises a cost over its local inputs [204].

Moreover, because the couplings between subsystems are explicitly modelled in the DMPC and local MPCs exchange state and input trajectories, the DMPC can provide a better control performance than the DeMPC, although not as good as the CMPC which is commonly used as a control performance benchmark. However, the key challenge in DMPC schemes is how to design the communication and coordination strategy between the local MPC schemes, and this would vary from one control application to another [207].

3.5 Conclusion

In this chapter, the fundamentals of model predictive control necessary to comprehend the load frequency control designs proposed in thesis have been presented. Specifically, three MPC architectures, namely CMPC, DeMPC and DMPC have been discussed and mathematical descriptions of each of these architectures have been provided. The attributes of the different architectures, in terms of advantages and disadvantages, are highlighted and a summary is provided in Table 3.1. From a control performance perspective, the best performance can be obtained from a CMPC as it has a global view of systemwide information, and the worst performance can be expected from a DeMPC since it ignores the interactions between subsystems; control performance comparisons of the three MPC architectures, each considered as the LFC scheme in a deregulated power network, are provided in Chapter 7 of this thesis.

The model predictive control technique is particularly suitable for power system LFC for the following reasons. The simplicity of the underlying concept of MPC indicates that MPC schemes can be easily understood and maintain, and thus have good reliability properties, and this is fundamentally important to any practical LFC [12]. Also, because of its constraints handling capability, equipment constraints such as generation rate constraints (GRC) and the limits on governor setpoints (also known as the limits on the control effort from a load frequency

Table 3.1: Attributes comparison of centralised, decentralised and distributed MPC

MPC architecture	Advantage	Disadvantage
CMPC	Provides the best performance and serves as a natural performance benchmark against DeMPC and DMPC. Explicit and systematic constraints handling and the underlying concept is simple.	Relatively high computation/communication requirements due to centralised computation/centralised information gathering. Low structural adaptability properties (for possible system expansion or reduction), low tolerance to faults in control system and poor flexibility in subsystem maintenance.
DeMPC	Low computational requirements and almost insignificant communication requirements. Good structural adaptability, fault tolerance endowment and flexibility in subsystem maintenance. Handles constraints and simple concept.	Control performance is generally lower than that of CMPC and DMPC. Usage of DeMPC Could result in instability when subsystems are strongly coupled.
DMPC	Handles constraints and simple underlying concept. Provides better performance than DeMPC. Computational requirements similar to DeMPC. DMPC schemes have good tolerance to faulty control system components. A subsystem can be shut-down for maintenance without a complete interruption of all local MPCs, lower communication requirements compared to CMPC.	Higher communication requirements than DeMPC. Lower control performance than CMPC. Design of the communication/coordination strategy could be tricky.

controller) can be explicitly considered, and this could help reduce LFC cost associated with equipment wear and tear and an increase in equipment lifespan.

Furthermore, distributed MPC based LFC can explicitly handle tie line interactions between control areas of an interconnected power system, and this is particularly important in the deregulated power system environment where competitive economic pressure and a large number of inter-area bilateral contracts is creating unpredictable flows across tie lines. Also, because

MPC solves an online optimisation problem to generate control actions, it steers a dynamical system in the most economic way, which could also result in cost savings in frequency regulation.

Chapter 4

The LFC of a 2-area deregulated system based on a centralised MPC

4.1 Introduction

It was emphasised in Section 1.4 that the main aim of this thesis is to investigate the potency of a model predictive control (MPC) based load frequency control (LFC) scheme in a deregulated power system environment, where deregulated LFC benchmark models would be obtained via the modification of the traditional LFC modelling framework, which was described in Section 2.1. Furthermore, the basics of model predictive control have been provided in Chapter 3, where a mathematical description of each of the main MPC architectures, namely centralised, decentralised and distributed MPC was presented.

It was also stated that a key strength of MPC is its ability to account for system constraints during the design phase. Chapter 5 proposes a new generalised deregulated LFC modelling framework for mult-area networks of any size; nonetheless, having a clear understanding of the key modifications steps required to obtain deregulated LFC models from the traditional framework is very important, and such transparency can be obtained by considering a small-scale network.

Hence, to demonstrate the constraints handling capability of MPC and to provide a transparent description of how the deregulated models considered in this thesis are developed, a centralised MPC (CMPC) scheme is proposed in this chapter for the LFC problem of a 2-area deregulated power system with measured (contracted) and unmeasured (uncontracted) load pertubations. The proposed MPC based LFC scheme is designed by posing the control problem as a tracking one with input and incremental state constraints representing limits on LFC control efforts (also known as limits on the change in load reference setpoint) and generation rate constraints (GRC) respectively. Finally, some comparisons are made betweeen the proposed CMPC based

LFC and optimal linear quadratic regulator to demonstrate the potency of MPC, especially in respect of constraints handling and disturbance rejection in the deregulated environment.

This chapter is based on the work in [34] and it is a key **contribution** in this thesis. The organisation of the chapter is as follows: Section 4.2 provides a summary of the main contributions of this chapter; Section 4.3 describes the developement of a 2-area deregulated LFC model; Section 4.4 provides the key design steps of the proposed CMPC; Section 4.5 presents simulation evidence and discussions; Section 4.6 closes this chapter with some concluding remarks.

4.2 Summary of the main contributions

This chapter makes the following contributions:

- Proposes a CMPC scheme for the LFC problem of a 2-area deregulated power system with contracted (measured) and uncontracted (unmeasured) load pertubations. The uncontracted load pertubation of an area represents the net load pertubations from entities that have either violated the LM contract or did not purchase LM contracts.

- The work here employs an observer to estimate system states as well as uncontracted load variations (which is assumed to be unmeasured) from ACE measurements, hence the proposed CMPC is output feedback

- GRC and limits on governor setpoints are included in the MPC design and simulations.

Note that throughout this thesis, it is assumed that there are no restrictions on the amount of incremental power each GenCo can provide at steady state.
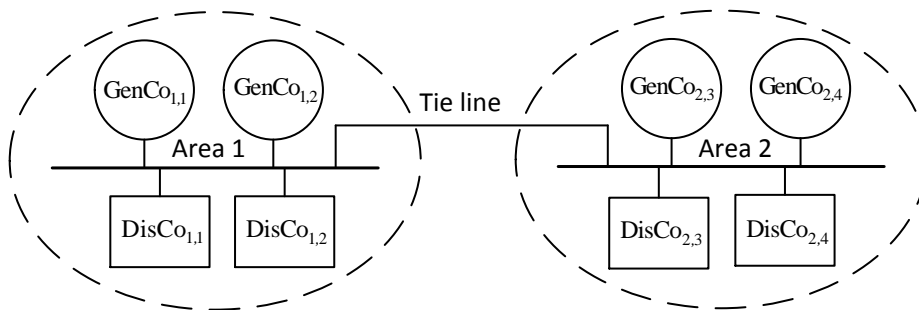
Figure 4.1: Single line diagram of a 2-area deregulated system

4.3 Deregulated LFC model of a 2-area system

This section presents the modification required in the traditional LFC model to incorporate the various power transactions in the deregulated environment. The formulation here is focused on a 2-area system whose single line diagram is shown in Figure 4.1. It is assumed, as in [29], that area 1 has two GenCos and two DisCos; the same applies to area 2. $\text{GenCo}_{i,\text{k}}$ represent the kth GenCo in the ith area, while $\text{DisCo}_{i,l}$ represents the lth DisCo in the ith area. The 2-area deregulated LFC framework is based on the transfer function block representation of Figure 4.2, which is a modification of Figure 2.9.

The equations presented in this section are based on Figure 4.2. In the deregulated environment, the total load change in each area, as shown in Figure 4.2, is:

$$\Delta P_1^{\text{D}} = \underbrace{\Delta P_{1,1}^{\text{L}} + \Delta P_{1,2}^{\text{L}}}_{\text{Contracted}} + \underbrace{\Delta P_1^{\text{U}}}_{\text{Uncontracted}} \tag{4.1}$$

$$\Delta P_2^{\text{D}} = \underbrace{\Delta P_{2,3}^{\text{L}} + \Delta P_{2,4}^{\text{L}}}_{\text{Contracted}} + \underbrace{\Delta P_2^{\text{U}}}_{\text{Uncontracted}} \tag{4.2}$$

The uncontracted load changes in each area (ΔP_1^{U} and ΔP_2^{U}) take a zero value if the total load changes in each area are supplied through bilateral LM contract only with no contract violations. From (2.14), the rated area capacity ratio between any two CAs linked by a tie line is $\alpha_{ij} = \dfrac{P_{r_i}}{P_{r_j}}$. In the context of the 2-area deregulated system studied here, equal area rated capacities are assumed, that is, the value of α_{12} in Figure 4.2 is taken to be unity.

The swing equations (4.3) and (4.4) presented the following section are slightly different from (2.8) as the load changes are separated into a contracted part $\Delta P_{i,l}^{\text{L}}$ and an uncontracted part ΔP_i^{U}. Also the change in the output of each GenCo in an area $\Delta P_{i,\text{k}}^{\text{M}}$ is considered separately rather the total change in power generation in a given control area, ΔP_i^{M}.

4.3.1 Modified swing equation

The swing equation governs the dynamic changes in frequency that occur in a control area, when there is an active power imbalance. A modified form of the swing equation of (2.8) for each area in the deregulated environment is:

$$\dot{\Delta f_1} = \frac{1}{H_1}(\Delta P_{1,1}^{\text{M}} + \Delta P_{1,2}^{\text{M}} - \Delta P_{1,1}^{\text{L}} - \Delta P_{1,2}^{\text{L}} - \Delta P_1^{\text{U}} - \Delta P_1^{\text{tie}} - D_1 \Delta f_1) \tag{4.3}$$

$$\dot{\Delta f_2} = \frac{1}{H_2}(\Delta P_{2,3}^{\mathrm{M}} + \Delta P_{2,4}^{\mathrm{M}} - \Delta P_{2,3}^{\mathrm{L}} - \Delta P_{2,4}^{\mathrm{L}} - \Delta P_2^{\mathrm{U}} - \Delta P_2^{\mathrm{tie}} - D_2 \Delta f_2) \tag{4.4}$$

Here, $\Delta P_{i,l}^{\mathrm{L}}$ pu denotes the contracted load change of lth DisCo in the ith control area; ΔP_i^{U} pu represents the total uncontracted load changes in the ith control area, which a TSO handles; $\Delta P_{i,k}^{\mathrm{M}}$ pu is the change in the output power of the kth GenCo in the ith CA; Δf_i Hz and $\Delta P_i^{\mathrm{tie}}$ pu are the frequency and the net tie line flow deviations in the ith CA respectively.
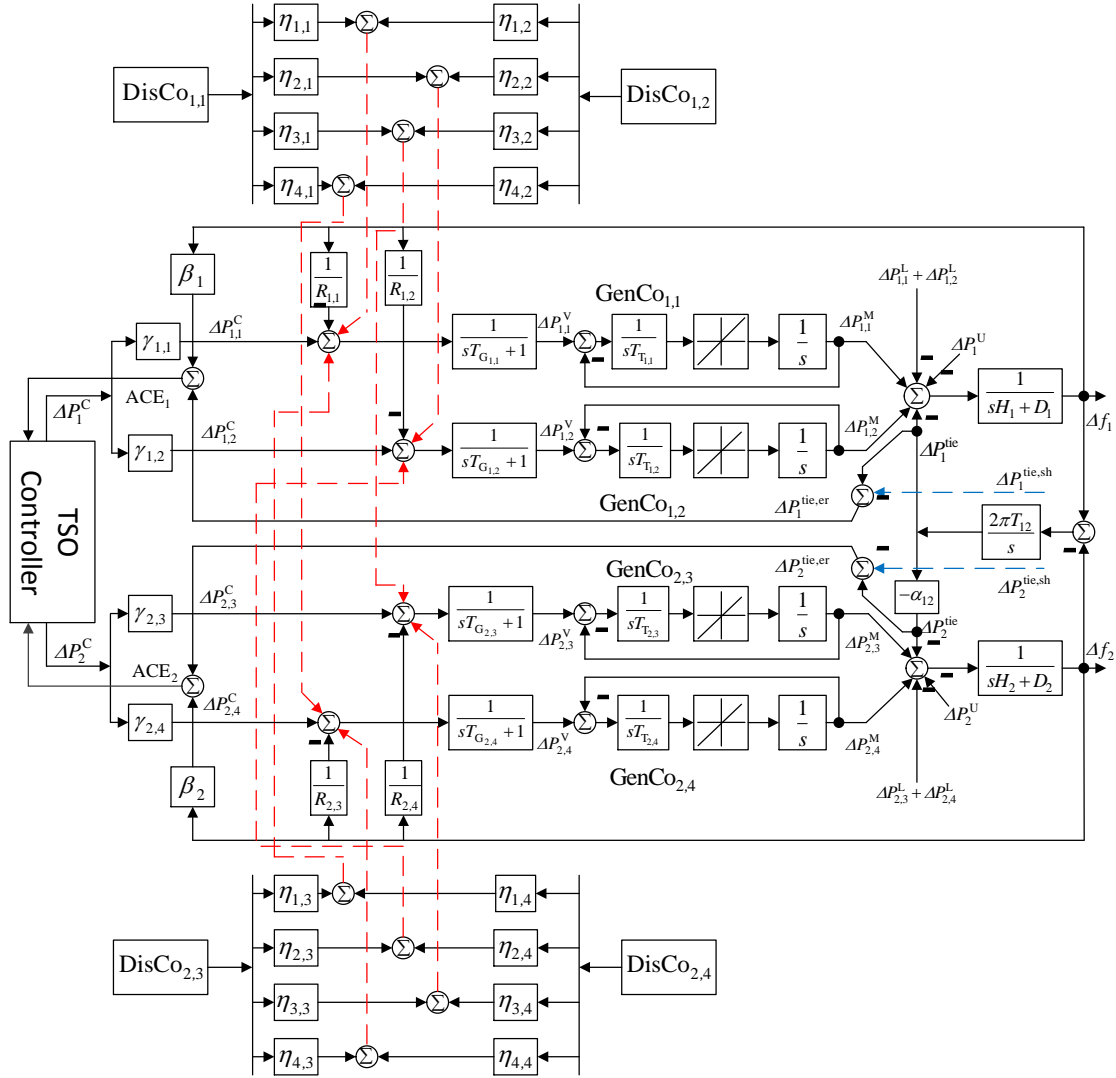
Figure 4.2: Transfer function block of a 2-area model of a deregulated power system.

4.3.2 Contracted LM signal

As emphasised earlier, a DisCo can opt to self-provide LFC via a bilateral LM contract with any GenCo, where in this case, a DisCo can send a contracted signal directly to any GenCo that has subscribed to the LM contract. The contracted signal from a DisCo to any GenCo based on the contracted load changes can be modelled using the concept of a DisCo participation matrix (DPM) proposed in [29]:

$$
\begin{bmatrix} S_{1,1} \\ S_{1,2} \\ S_{2,3} \\ S_{2,4} \end{bmatrix} = \begin{bmatrix} \eta_{1,1} & \eta_{1,2} & \eta_{1,3} & \eta_{1,4} \\ \eta_{2,1} & \eta_{2,2} & \eta_{2,3} & \eta_{2,4} \\ \eta_{3,1} & \eta_{3,2} & \eta_{3,3} & \eta_{3,4} \\ \eta_{4,1} & \eta_{4,2} & \eta_{4,3} & \eta_{4,4} \end{bmatrix} \begin{bmatrix} \Delta P_{1,1}^{\mathrm{L}} \\ \Delta P_{1,2}^{\mathrm{L}} \\ \Delta P_{2,3}^{\mathrm{L}} \\ \Delta P_{2,4}^{\mathrm{L}} \end{bmatrix} = \mathrm{DPM} \begin{bmatrix} \Delta P_{1,1}^{\mathrm{L}} \\ \Delta P_{1,2}^{\mathrm{L}} \\ \Delta P_{2,3}^{\mathrm{L}} \\ \Delta P_{2,4}^{\mathrm{L}} \end{bmatrix} \tag{4.5}
$$

The number of rows and columns of the DPM are equal to the number of GenCos and DisCos in the multi-area deregulated system respectively. The sum of the elements in each column of the DPM should be unity, that is $\sum_{k=1}^{4} \eta_{k,l} = 1 \ \forall l = \{1,2,3,4\}$. The entry in the DPM $\eta_{k,l}$ represents the fraction of the lth DisCo's total LM requirement contracted to the kth GenCo; the entries of the DPM are known as a contract participation factors. If $\eta_{k,l} = 0$, then there is no LM contract between GenCo k and DisCo l. Also, $0 \leq \eta_{k,l} \leq 1$.

The variable $S_{i,\mathrm{k}}$ is the total LM contractual obligation of the kth GenCo in the ith CA, e.g., $S_{2,3}$ is the LM contractual obligation of GenCo 3 in Area 2. The $S_{i,\mathrm{k}}$ of each GenCo is shown as the red dotted lines of Figure 4.2. Note that the information $S_{i,\mathrm{k}}$ is absent in the traditional LFC model. Thus with the contracted load change of each DisCo known, (4.5) can be used to compute the contracted incremental power each GenCo on LM contract must generate at steady state.

4.3.3 Modified speed governor dynamics

The speed governor, in the new framework, receives setpoints in the form of a raise or lower control pulse from a TSO as well as contracted signal from DisCos that have purchased LM contracts (red dotted lines in Figure 4.2) for LFC. The modified dynamics of the speed governing system of each GenCo based on the new information $S_{i,\mathrm{k}}$, is

$$
\Delta \dot{P}_{i,\mathrm{k}}^{\mathrm{V}} = \frac{1}{T_{\mathrm{G}_{i,\mathrm{k}}}} \left(\gamma_{i,\mathrm{k}} \Delta P_i^{\mathrm{C}} - \Delta P_{i,\mathrm{k}}^{\mathrm{V}} - \frac{1}{R_{i,\mathrm{k}}} \Delta f_i + S_{i,\mathrm{k}} \right) \quad \forall (i,\mathrm{k}) \in \mathcal{P} \tag{4.6}
$$

$$
\mathcal{P} \in \{(1,1),(1,2),(2,3),(2,4)\} \tag{4.7}
$$

The governor model considered here is the General Electric Electro-hydraulic governor without steam feedback [42]. The variable $\Delta P_{i,k}^{\mathrm{V}}$ pu is the change in governor output of the kth GenCo in the ith CA; ΔP_i^{C} is the ith area control signal from a TSO to cater for uncontracted load changes, $\Delta P_i^{\mathrm{C}} = 0$ if the entire load changes in the ith area are compensated for via bilateral LM contracts, with no violation of contract. Also, $\gamma_{i,\mathrm{k}}$ is the area participation factor of the kth GenCo in the ith CA. The area participation factor specifies the extent to which a GenCo can contribute in handling uncontracted load variations in its CA. Area participation factors of GenCos committed to supplying uncontracted load changes are known after the balancing market where incremental/decremental powers are traded have been cleared. See Table 4.1 for the definition of other parameters used in this section.

Within a control area, the participation factors of GenCos committed to providing reserve for uncontracted load variation must sum to unity. As an example from Figure 4.2, the following must hold:

$$\gamma_{1,1} + \gamma_{1,2} = 1, \quad \gamma_{2,3} + \gamma_{2,4} = 1, \quad 0 \leq \gamma_{i,\mathrm{k}} \leq 1 \tag{4.8}$$

The turbine equation (4.9) presented in the following section has the same form as the one presented in (2.2). However, (4.9) is written for a specific GenCo k in an area i and the set $\mathcal{P}$ which contains the pair (i, k) for the 2-area system is written alongside.

4.3.4   Turbine dynamics

The dynamics of the turbine of each GenCo is maintained as presented in (2.2), and it is restated here:

$$\Delta \dot{P}_{i,\mathrm{k}}^{\mathrm{M}} = \mathrm{sat}_{\Delta \dot{P}_{i,\mathrm{k}}^{\mathrm{M}}} \left\{ \frac{1}{T_{\mathrm{T}_{i,\mathrm{k}}}} \left(\Delta P_{i,\mathrm{k}}^{\mathrm{V}} - \Delta P_{i,\mathrm{k}}^{\mathrm{M}} \right) \right\} \quad \forall (i, \mathrm{k}) \in \mathcal{P} \tag{4.9}$$

where the set $\mathcal{P}$ is as defined in (4.7). The turbine equation represents a nonreat steam turbine [42], and the saturation nonlinearity $\mathrm{sat}_{\dot{P}_{i,\mathrm{k}}^{\mathrm{M}}}^{i}(\bullet)$ represents turbine GRC.

4.3.5   Net tie line flow deviation

The net tie line deviation dynamics is maintained as given in (2.15), and it is restated in the context of Figure 4.2 here:

$$\Delta \dot{P}_1^{\mathrm{tie}} = T_{12}(\Delta f_1 - \Delta f_2) \tag{4.10}$$

Since each area is assumed to have equal capacity rating, that is $\alpha_{12} = 1$, $\Delta\dot{P}_2^{\text{tie}} = -\Delta\dot{P}_1^{\text{tie}}$; T_{12} is the synchronising coefficient between area 1 and 2.

4.3.6 Scheduled net incremental tie line flow

For a given control area, the net scheduled incremental tie line flow, $\Delta P_i^{\text{tie,sh}}$ is determined by the magnitude of the inter-area bilateral LM contracts (from the DPM (4.5)) between the GenCos in one area and the DisCos in another area. For the 2-area deregulated system considered,

$$
\begin{aligned}
\Delta P_1^{\text{tie,sh}} &= \left\{ \begin{array}{c} \text{contracted incremental demands of DisCos} \\ \text{in area 2 from GenCos in area 1} \end{array} \right\} \\
&\quad - \left\{ \begin{array}{c} \text{contracted incremental demands of DisCos} \\ \text{in area 1 from GenCos in area 2} \end{array} \right\} \\
&= (\eta_{1,3} + \eta_{2,3})\Delta P_{2,3}^{\text{L}} + (\eta_{1,4} + \eta_{2,4})\Delta P_{2,4}^{\text{L}} \\
&\quad - (\eta_{3,1} + \eta_{4,1})\Delta P_{1,1}^{\text{L}} - (\eta_{3,2} + \eta_{4,2})\Delta P_{1,2}^{\text{L}}
\end{aligned}
\tag{4.11}
$$

$$
\begin{aligned}
\Delta P_2^{\text{tie,sh}} &= \left\{ \begin{array}{c} \text{contracted incremental demands of DisCos} \\ \text{in area 1 from GenCos in area 2} \end{array} \right\} \\
&\quad - \left\{ \begin{array}{c} \text{contracted incremental demands of DisCos} \\ \text{in area 2 from GenCos in area 1} \end{array} \right\} \\
&= (\eta_{3,1} + \eta_{4,1})\Delta P_{1,1}^{\text{L}} + (\eta_{3,2} + \eta_{4,2})\Delta P_{1,2}^{\text{L}} \\
&\quad - (\eta_{1,3} + \eta_{2,3})\Delta P_{2,3}^{\text{L}} - (\eta_{1,4} + \eta_{2,4})\Delta P_{2,4}^{\text{L}}
\end{aligned}
\tag{4.12}
$$

It is important to state that $\Delta P_1^{\text{tie,sh}} = -\Delta P_2^{\text{tie,sh}}$ because $\alpha_{12} = 1$. The flow convention assumed for each positive $\Delta P_i^{\text{tie,sh}}$ (as well as ΔP_i^{tie}) throughout this thesis is due to power flow out of the control area. An objective of LFC in the new environment is to ensure that ΔP_i^{tie} converges to $\Delta P_i^{\text{tie,sh}}$ at steady state.

4.3.7 Modified area control error

The modified ACE in the deregulated environment is

$$
\text{ACE}_i = \beta_i \Delta f_i + \Delta P_i^{\text{tie}} - \Delta P_i^{\text{tie,sh}} \quad \forall i \in \{1, 2\}
\tag{4.13}
$$

Note that the definition of ACE in the deregulated environment (4.13) is different from the traditional version of ACE (2.17).

4.3.8   State space model

A continuous time (CT) state space representation of the 2-area deregulated system can be written by collecting the following key expressions (4.3),(4.4),(4.6),(4.9),(4.10) and (4.13):

$$
\begin{aligned}
\dot{x} &= A^c x + B^c u + B^{dc} d + B^{bc} b \\
y &= Cx + Dd
\end{aligned}
\tag{4.14}
$$

$$
x = \begin{bmatrix} x_1 \\ \Delta P_1^{\text{tie}} \\ x_2 \end{bmatrix} ; \quad
x_1 = \begin{bmatrix} \Delta f_1 \\ \Delta P_{1,1}^{M} \\ \Delta P_{1,1}^{V} \\ \Delta P_{1,2}^{M} \\ \Delta P_{1,2}^{V} \end{bmatrix} ; \quad
x_2 = \begin{bmatrix} \Delta f_2 \\ \Delta P_{2,3}^{M} \\ \Delta P_{2,3}^{V} \\ \Delta P_{2,4}^{M} \\ \Delta P_{2,4}^{V} \end{bmatrix}
$$

$$
u = \begin{bmatrix} \Delta P_1^{C} \\ \Delta P_2^{C} \end{bmatrix} ; \quad
d = \begin{bmatrix} \Delta P_{1,1}^{L} \\ \Delta P_{1,2}^{L} \\ \Delta P_{2,3}^{L} \\ \Delta P_{2,4}^{L} \end{bmatrix} ; \quad
b = \begin{bmatrix} \Delta P_1^{U} \\ \Delta P_2^{U} \end{bmatrix} ; \quad
y = \begin{bmatrix} \text{ACE}_1 \\ \text{ACE}_2 \end{bmatrix}
$$

where x the vector of system states; u is the vector of control inputs (governor setpoints); d is the vector of contracted load changes; b is the vector of uncontracted load changes; y is the vector of area control error. The matrices A^c, B^c, B^{dc}, B^{bc}, C and D are available in Section A.1.

4.3.9   Summary

In summary, the procedure required to develop a deregulated LFC model from the traditional version has been described using the 2-area power system of Figure 4.1. The 2-area deregulated model developed in this section assumes that the rated capacity of area 1 is equal to that of area 2, that is, the value of α_{12} in Figure 4.2 was taken to be unity. The model will be used for the CMPC design (as prediction model) and also as a benchmark system to demonstrate the efficacy of the CMPC.

4.4 CMPC design for LFC

In this section, a description of the main design steps involved in developing a centralised MPC for the 2-area deregulated power system is provided. The target is to design an LFC scheme capable of coordinating contracted load changes, rejecting uncontracted disturbances, while accounting for GRC and input constraints. The key expressions needed in formulating a linear CMPC problem will be repeated here for convenience; Section 3.2 contains further details.

4.4.1 CMPC Prediction

To design the CMPC, consider a discrete time (DT) version of CT state space model (4.14)

$$
\begin{aligned}
x_{k+1} &= Ax_k + Bu_k + B^d d_k + B^b b_k \\
y_k &= Cx_k + Dd_k
\end{aligned}
\tag{4.15}
$$

The DT model (4.15) can be obtained from the CT model (4.14) using the zero-order hold method. Note the difference between k (index of a GenCo) and k (a sampling instant). To present (4.15) in the standard state space form of (3.1), consider the following steady state equivalent of (4.14):

$$
\begin{aligned}
x_{ss} &= Ax_{ss} + Bu_{ss} + B^d d_{ss} + B^b b_{ss} \\
y_{ss} &= Cx_{ss} + Dd_{ss}
\end{aligned}
\tag{4.16}
$$

Substracting (4.16) from (4.15), and assuming $d_k = d_{ss}$, $b_k = b_{ss}$, gives:

$$
\bar{x}_{k+1} = A\bar{x}_k + B\bar{u}_k; \quad \bar{y}_k = C\bar{x}_k
\tag{4.17}
$$

where $\bar{x}_k = x_k - x_{ss}$; $\bar{u}_k = u_k - u_{ss}$; $\bar{y}_k = y_k - y_{ss}$. The state space model (4.17) represents a deviation from steady state targets, and it is now in the form stated in (3.1). The deviation model serves to convert the MPC design problem from setpoint tracking into a regulation problem. Thus, similar to (3.15) of Section 3.2, a state prediction can be written:

$$
\underset{\rightarrow k}{\bar{x}} = P_x \bar{x}_k + H_u \underset{\rightarrow k-1}{\bar{u}}
\tag{4.18}
$$

The following $\underset{\rightarrow k}{\bar{x}}$, P_x, H_u and $\underset{\rightarrow k-1}{\bar{u}}$ are defined in Section 3.2.

4.4.2 CMPC Cost function

An open loop dual mode CMPC cost, and the corresponding standard quadratic compact form (after a series of algebra), similar to (3.10) and (3.34) respectively, are

$$
J(\bar{x}_k, \bar{u}_k) = \sum_{t=0}^{n_c-1} \frac{1}{2} \{\bar{x}_{k+t+1}^T Q \, \bar{x}_{k+t+1} + \bar{u}_{k+t}^T R \, \bar{u}_{k+t}\} + \frac{1}{2} \, \bar{x}_{k+n_c}^T P_f \bar{x}_{k+n_c} \tag{4.19}
$$

$$
J(\bar{x}_k, \, \underset{\rightarrow k-1}{\bar{u}}) = \frac{1}{2} \, \underset{\rightarrow k-1}{\bar{u}^T} S_f \, \underset{\rightarrow k-1}{\bar{u}} + H_f^T \, \underset{\rightarrow k-1}{\bar{u}} \tag{4.20}
$$

where Q , R and P_f are the state weighting matrix, input weighting matrix and terminal weight respectively; n_c is the prediction horizon. See Section 3.2 for the definition of the other terms P_f S_f, H_f^T.

4.4.3 Constraints

An economic operating point of most industrial systems are typically located at constraint boundaries and thus, a controller that can drive a system close to the constraint boundaries without violating them is often a preferred choice [28]. Online constraint handling is one of the most important features of the model predictive control. In the context of the 2-area LFC problem, input constraints and GRC are considered, and this is a key contribution in this chapter.

Input constraints

The input constraints are imposed to prevent excessive LFC actions, and can be stated as

$$
\underbrace{\begin{bmatrix} \Delta P_1^{C,\min} \\ \Delta P_2^{C,\min} \end{bmatrix}}_{u^{\min}} \leq \underbrace{\begin{bmatrix} \Delta P_1^{C} \\ \Delta P_2^{C} \end{bmatrix}}_{u_k} \leq \underbrace{\begin{bmatrix} \Delta P_1^{C,\max} \\ \Delta P_2^{C,\max} \end{bmatrix}}_{u^{\max}} \tag{4.21}
$$

With the definitions of $u^{\min}$, $u^{\max}$ and u_k in (4.21), the input constraints can be written similar to (3.3):

$$
\begin{bmatrix} I \\ -I \end{bmatrix} \bar{u}_k \leq \begin{bmatrix} u^{\max} - u_{ss} \\ u_{ss} - u^{\min} \end{bmatrix} \tag{4.22}
$$

Generation rate constraints

In computing LFC signals, it should be considered that there is a limit to the rate at which generating units can change their output. This is notably critical for steam generating units where rapid changes in power outputs could have damaging effect on turbines due to thermal and mechanical stresses. Another reason for GRC consideration, especially in thermal units, is rapid power demands would allow steam to exceed the volume that is required at steady state, to flow from the boiler system, resulting in a pressure reduction and formation of water droplets within the high velocity steam. These droplets, impinging on the turbine blades, could result in a gradual blade erosion, and can also create safety concerns [120, 221]. In the 2-area deregulated system, the GRC can be stated in CT format as:

$$
\underbrace{\begin{bmatrix} \Delta P_{1,1}^{\dot{\mathrm{M}},\min} \\ \Delta P_{1,2}^{\mathrm{M},\min} \\ \Delta P_{2,3}^{\mathrm{M},\min} \\ \Delta P_{2,4}^{\mathrm{M},\min} \end{bmatrix}}_{\Delta P^{\dot{\mathrm{M}},\min}} \leq \underbrace{\begin{bmatrix} \Delta \dot{P}_{1,1}^{\mathrm{M}} \\ \Delta \dot{P}_{1,2}^{\mathrm{M}} \\ \Delta \dot{P}_{2,3}^{\mathrm{M}} \\ \Delta \dot{P}_{2,4}^{\mathrm{M}} \end{bmatrix}}_{\Delta \dot{P}^{\mathrm{M}}} \leq \underbrace{\begin{bmatrix} \Delta P_{1,1}^{\dot{\mathrm{M}},\max} \\ \Delta P_{1,2}^{\mathrm{M},\max} \\ \Delta P_{2,3}^{\mathrm{M},\max} \\ \Delta P_{2,4}^{\mathrm{M},\max} \end{bmatrix}}_{\Delta P^{\dot{\mathrm{M}},\max}} \tag{4.23}
$$

Here, it is assumed that the four GenCos in the 2-area system are participating in the TSO supplementary LFC to address uncontracted load changes, that is, each GenCo has its $\gamma_{i,\mathrm{k}} > 0$. In practice, not all GenCo participates in a TSO's LFC; some GenCos may choose to participate in bilateral LM contracts only (bilateral LFC); some may choose to participate in a TSO's LFC (poolco LFC); some may have bilateral LM contracts with DisCos as well as participate in providing uncontracted load changes via a TSO's LFC action. In the case where only a selected GenCos participate in a TSO's LFC, GRC are only considered for those GenCos[1]; such a case is considered in Chapters 6 and 7. In DT, (4.23) can be expressed as

$$
t_s \Delta P^{\dot{\mathrm{M}},\min} \leq \underbrace{\left(\overline{\Delta P_{k+1}^{\mathrm{M}}} + \Delta P_{\mathrm{ss}}^{\mathrm{M}} \right)}_{\Delta P_{k+1}^{\mathrm{M}}} - \underbrace{\left(\overline{\Delta P_k^{\mathrm{M}}} + \Delta P_{\mathrm{ss}}^{\mathrm{M}} \right)}_{\Delta P_k^{\mathrm{M}}} \leq t_s \Delta P^{\dot{\mathrm{M}},\max} \tag{4.24}
$$

where $\Delta P^{\dot{\mathrm{M}},\max}$ and $\Delta P^{\dot{\mathrm{M}},\min}$ are vectors of limits on incremental generation rate and decremental generation rate respectively; $\overline{\Delta P_k^{\mathrm{M}}}$ is a deviation from steady state incremental generation target (similar to $\overline{\mathrm{x}}_k$ since ΔP_k^{M} is a system state); $\Delta P_{\mathrm{ss}}^{\mathrm{M}}$ is the steady state target value of the generation change (similar to x_{ss}). The scalar t_s is the sampling time; t_s is also used in obtaining the DT model (4.15) from the CT model (4.14). A relationship between $\overline{\Delta P_k^{\mathrm{M}}}$ and the vector of the complete system states and input can be written:

---

[1]The model predictive control scheme acts as the load frequency controller that would run on the TSO computer and in principle, the MPC only considers constraints on units under the TSO's control.

$$\overline{\Delta P_{k+1}^{\mathrm{M}}} = \mathrm{A^g}\overline{\mathrm{x}}_k + \mathrm{B^g}\overline{\mathrm{u}}_k; \quad \overline{\Delta P_k^{\mathrm{M}}} = \Gamma^{\mathrm{g}}\overline{\mathrm{x}}_k \tag{4.25}$$

where (4.25) is similar to the deviation model (4.17), and $\overline{\Delta P_k^{\mathrm{M}}}$ represents a deviation from a steady state generation target; $\mathrm{A^g} \in \mathbb{R}^{4\times 11}$ and $\mathrm{B^g} \in \mathbb{R}^{4\times 4}$ are matrices formed by extracting the rows corresponding to $\Delta P_{1,1}^{\mathrm{M}}$, $\Delta P_{1,2}^{\mathrm{M}}$, $\Delta P_{2,3}^{\mathrm{M}}$, and $\Delta P_{2,4}^{\mathrm{M}}$ from the A and B in (4.15) respectively. The matrix $\Gamma^{\mathrm{g}} \in \mathbb{R}^{4\times 11}$ is available in Section A.1. Thus, (4.24) can be stated as a single inequality:

$$\begin{bmatrix} \mathrm{A^g} - \Gamma^{\mathrm{g}} \\ \Gamma^{\mathrm{g}} - \mathrm{A^g} \end{bmatrix} \overline{\mathrm{x}}_k + \begin{bmatrix} \mathrm{B^g} \\ -\mathrm{B^g} \end{bmatrix} \overline{\mathrm{u}}_k \leq \begin{bmatrix} t_s\Delta P^{\dot{\mathrm{M}},\max} \\ -t_s\Delta P^{\dot{\mathrm{M}},\min} \end{bmatrix} \tag{4.26}$$

GRC and input constraints combined

The input constraints (4.22) and GRC (4.26) can be combined to obtain a compact inequality representation of both constraints (see Section 3.2.2):

$$G_c\overline{\mathrm{x}}_k + F_c\overline{\mathrm{u}}_k \leq h_c \tag{4.27}$$

Similar to the operation performed in (3.17), the constraints (4.27) can be recursively calculated n_c steps into the future to obtain an expression similar to (3.19):

$$\boldsymbol{F_c}\, \underset{\rightarrow k-1}{\overline{\mathrm{u}}} \leq \boldsymbol{h_c} \tag{4.28}$$

4.4.4 Observer design and steady state calculator

In the proposed CMPC based LFC, it is assumed that the system states x_k and uncontracted load changes b_k are unmeasurable and thus, an observer is employed, making the proposed CMPC output feedback; most predictive control based LFC assume perfect states and disturbance knowledge. In this current work, the estimates $\widehat{\mathrm{b}}_k$, and $\widehat{\mathrm{x}}_k$ are obtained using ACE measurements. To design the observer, b_k is modelled as integrated white noise and augumented with the state equation of (4.15) to obtain the expression:

$$\widehat{\xi_{k+1}} = \mathrm{A_o}\widehat{\xi}_k + \mathrm{B_o}\mathrm{u}_k + \mathrm{B_o^d}\mathrm{d}_k - \mathrm{L}(\mathrm{y}_k - \mathrm{C_o}\widehat{\xi}_k - \mathrm{Dd}_k) \tag{4.29}$$

$$\mathrm{A_o} = \begin{bmatrix} \mathrm{A} & \mathrm{B^b} \\ \mathbf{0} & 1 \end{bmatrix}; \mathrm{B_o} = \begin{bmatrix} \mathrm{B} \\ \mathbf{0} \end{bmatrix}; \mathrm{B_o^d} = \begin{bmatrix} \mathrm{B^d} \\ \mathbf{0} \end{bmatrix}; \mathrm{C_o} = \begin{bmatrix} \mathrm{C} & 0 \end{bmatrix}$$

where $\hat{\xi}_k = [\hat{x}_k^T \ \hat{b}_k^T]^T$; L is an observer gain computed such that $\rho(A_o - LC_o) < 1$. The zero matrix $\mathbf{0}$ is context dependent. The steady state pair (x_{ss}, u_{ss}) can be computed at every sampling instant when the observer provides the estimate of the uncontracted load changes $\hat{b}_k$, using the following consistency equation obtained from (4.16)

$$\begin{bmatrix} x_{ss} \\ u_{ss} \end{bmatrix} = \begin{bmatrix} I - A & -B \\ C & \mathbf{0} \end{bmatrix}^{-1} \begin{bmatrix} B^d d_{ss} + B^b b_{ss} \\ y_{ss} - D d_{ss} \end{bmatrix}; \quad b_{ss} = \hat{b}_k \qquad (4.30)$$

In (4.30), the following variables are known: y_{ss} is the vector of desired ACE value, which is zero for each area; $d_{ss} = d_k$ is the vector of contracted load changes which DisCos that have purchased LM contracts must supply to the TSO.

4.4.5 CMPC problem

Thus, the centralised MPC problem solved by the TSO (similar to (3.35)) at sampling instant $k \geq 0$ is stated as follows:

$$P_{\text{CMPC}}: \qquad \min_{\underset{\to k-1}{\overline{u}}} \left\{ \frac{1}{2} \overline{u}_{\to k-1}^T S_f \ \overline{u}_{\to k-1} + H_f^T \ \overline{u}_{\to k-1} \right\}$$

$$(4.31)$$

Subject to

$$\boldsymbol{F_c} \ \overline{u}_{\to k-1} \leq \boldsymbol{h_c}$$

The constrained minimisation problem P_{CMPC} is convex and thus can be solved easily using any suitable quadratic optimisation tool. The actual input to the benchmark system is $u_k = \overline{u}_k^* + u_{ss}$, where $\overline{u}_k^*$ is the first control move of the optimal sequence $\overline{u}_{\to k-1}$ computed at $k \geq 0$. Figure 4.3 shows the structure of the proposed scheme. Note that terminal constraints are not considered in this thesis.

Table 4.1: Parameters of the 2-area deregulated power system

	Area 1		Area 2	
	$\text{GenCo}_{1,1}$	$\text{GenCo}_{1,2}$	$\text{GenCo}_{2,4}$	$\text{GenCo}_{2,4}$
Governor time constant $T_{\text{G}_{i,k}}$ (s)	0.085	0.1	0.09	0.075
Turbine time constant $T_{\text{T}_{i,k}}$ (s)	0.54	0.375	0.28	0.45
Droop $R_{i,k}$ (Hz/pu)	3	3.9	4.2	3.5
Area participation factor $\gamma_{i,k}$	0.55	0.45	0.5	0.5
Frequency bias β_i (pu/Hz)	0.532		0.495	
Equivalent inertia constant H_i (pu s)	0.21		0.24	
Equivalent damping D_i (pu/Hz)	0.008		0.007	
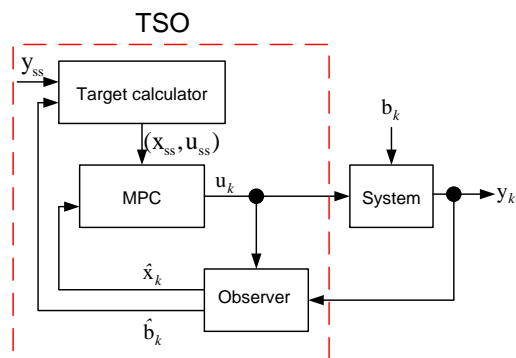
Figure 4.3: Block overview of the MPC scheme

4.5 Simulation and discussion

In this section, simulation evidence and some discussions are provided to demonstrate the efficacy of the proposed CMPC based LFC. The parameters of the 2-area deregulated power system are shown in Table 4.1; the selection of these parameters are guided by the ones used in [22]. Other parameters are: $T_{12} = 0.765$ pu/Hz; $t_s = 0.2$ s; $\left|\Delta \dot{P}^{\text{M}}_{i,k}\right| \leq 0.003$ pu/s (the same GRC for all GenCos); $\left|\Delta P^{\text{C}}_i\right| \leq 0.018$ (the same input constraints for each area). Both GRC and input constraints constraints are taken as hard constraints, and are imposed on the system during simulation. The state and input weightings of the MPC cost are $Q = 100\text{I}_{\text{x}}$ and $R = \text{I}_{\text{u}}$ respectively, where I_{x} is an identity matrix whose size is equal to the number of system states, and I_{u} is an identity matrix whose size is equal to the number of system inputs.

A prediction horizon $n_c = 50$ is used in (4.18) to obtain (4.20). To obtain the inequality constraint (4.28), the constraint at the current sample (4.27) is calculated n_y steps into the future, where $n_y = 5n_c$, and the input sequence $\underset{\rightarrow k-1}{\bar{\text{u}}}$ is truncated after n_c steps, making $\boldsymbol{F_c}$ in (4.28) a 'tall and thin' matrix. The choice n_y is to ensure recursive feasibility in some sense, since n_c was selected via tuning. Furthermore, for comparison purposes, an infinite horizon
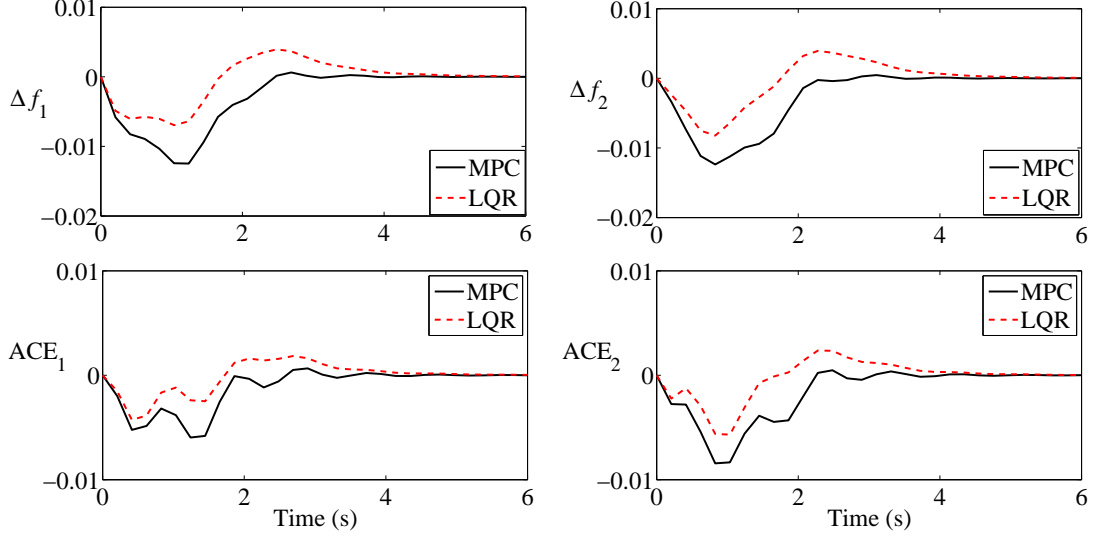
Figure 4.4: Frequency deviations Δf_i Hz and area control errors ACE_i pu in area 1 and 2 (case 1).

linear quadratic regulator (LQR) is also simulated, with the same Q, R, and initial states as the CMPC, and the results are presented alongside. Details of the LQR formulation are omitted as it is standard in the literature.

In the simulation, two cases are considered. The first considers the scenario where LFC is supplied through bilateral LM contract only with no contract violation. The second case considers the scenario where LFC is initially supplied via LM contract and then uncontracted load changes occur. The magnitudes of contracted and uncontracted load changes considered in this chapter and throughout the thesis are guided by the values utilised in [22, 222].

4.5.1 Case-1: Bilateral LFC with no uncontracted load changes

This section demonstrates the scenario where all DisCos self-provide LFC via bilateral transaction with no uncontracted load changes in the network. Under this condition, ΔP_1^{U} and ΔP_2^{U} in (4.1) and (4.2) respectively are zero and the control signals from the TSO (ΔP_1^{C} and ΔP_2^{C}) are expected to have a zero steady state value. The considered DPM in this case is

$$
\mathrm{DPM}=\begin{bmatrix} 0.4 & 0.25 & 0.1 & 0.3 \\ 0.2 & 0.25 & 0.2 & 0.25 \\ 0.1 & 0.25 & 0.5 & 0.2 \\ 0.3 & 0.25 & 0.2 & 0.25 \end{bmatrix}
\tag{4.32}
$$

Assuming each DisCo in area 1 has a contracted load change of 0.0035 pu and each DisCo in area 2 has a contracted load change of 0.002 pu. Using (4.5), the desired incremental generation of each GenCo at steady state can be calculated. Figure 4.4 shows the frequency deviations

(top) and ACE (bottom) of each control area. As expected, they both converged to zero since the DisCos catered for their total load changes via the bilateral LM contract and no violation of contracts.

Moreover, Figure 4.5 shows the change in the power output of each GenCo; the desired generation of each GenCo has been calculated and represented in Figure 4.5 as a black dotted line. It can be seen that each GenCo fulfilled their contractual obligation by tracking the desired incremental generation.

The generation rate of each GenCo is shown in Figure 4.6, where the black dotted lines are limit on incremental generation rate (upper bound) and decremental generation rate (lower
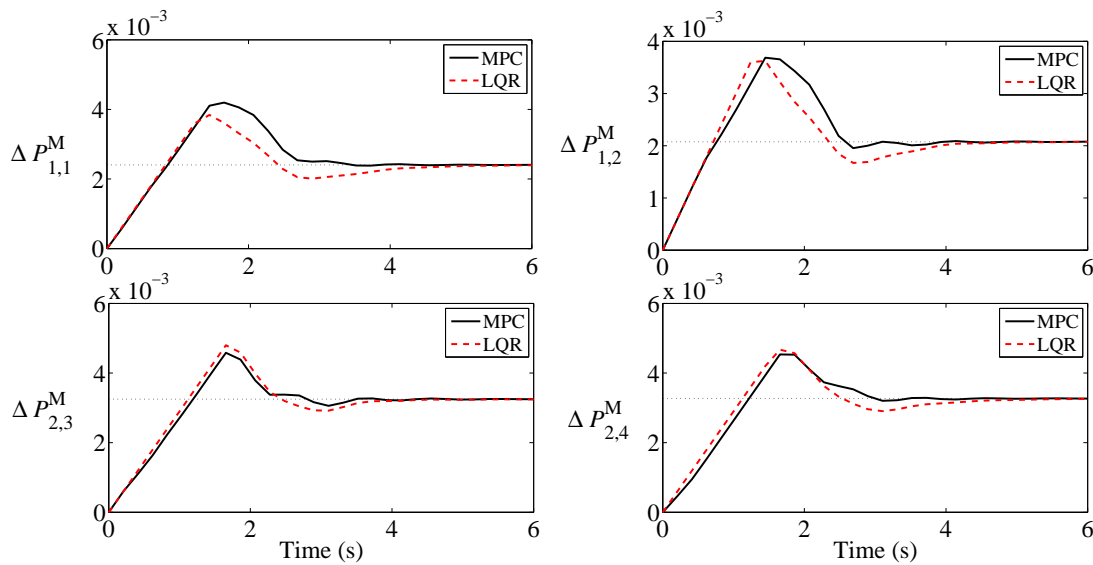
Figure 4.5: Change in the output power $\Delta P_{i,k}^{M}$ pu of GenCos in area 1 and 2 (case 1). Black dotted lines are the desired generation based on the DPM and contracted load changes.
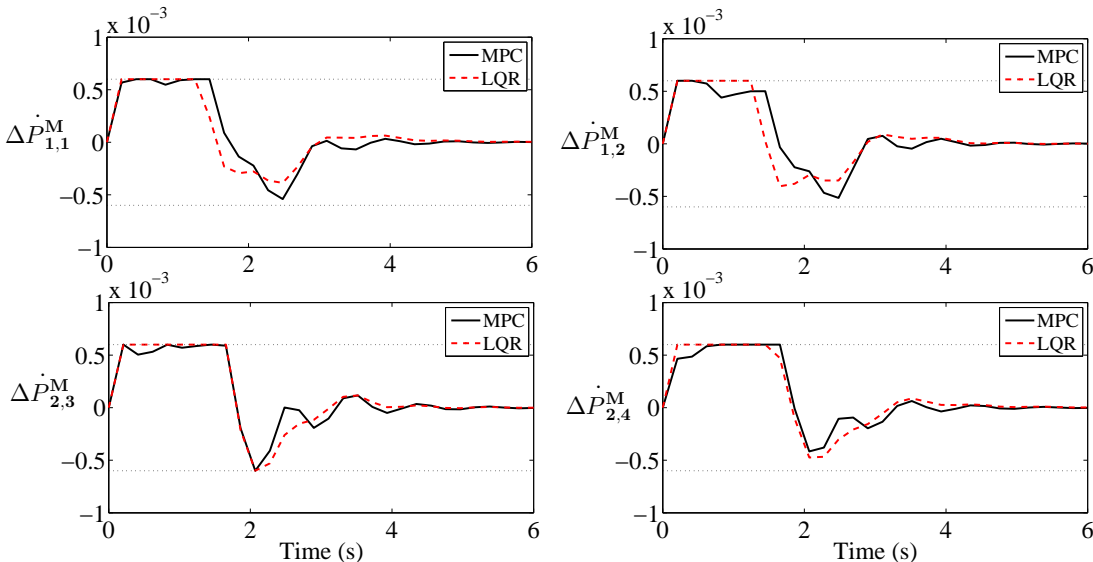
Figure 4.6: Generation rate of GenCos $\Delta \dot{P}_{i,k}^{M}$ pu/s in area 1 and 2 (case 1). The black dotted lines are the constraint bounds.
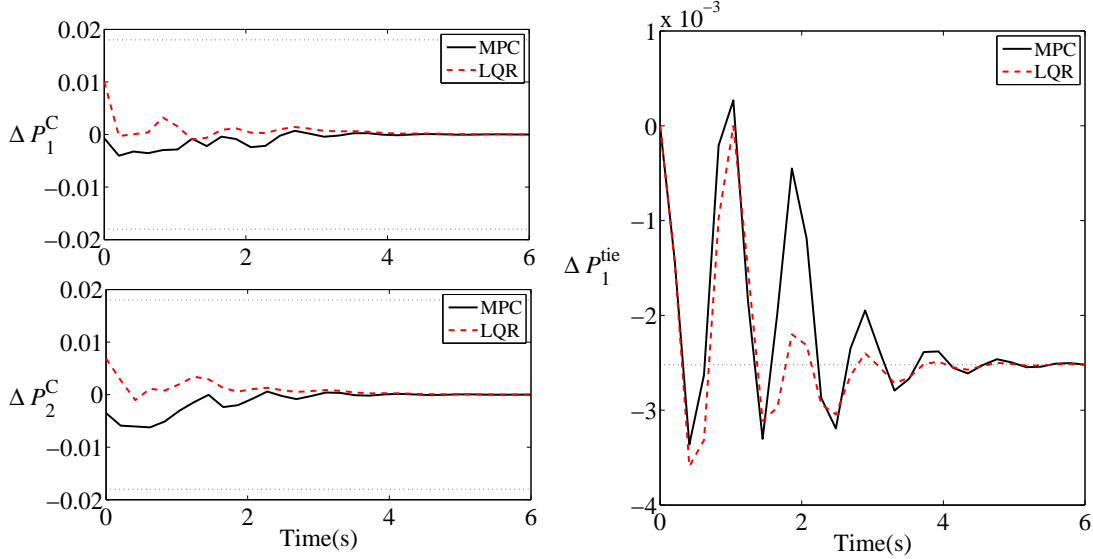
Figure 4.7: Control inputs ΔP_i^{C} in area 1 and 2, and net tie line deviation in area 1 $\Delta P_1^{\mathrm{tie}}$ pu (case 1). Left dotted lines: bounds on control inputs. Right dotted line: scheduled net incremental tie line flow of area 1 $\Delta P_1^{\mathrm{tie,sh}}$ pu based on inter-area bilateral LM contract.

Table 4.2: Uncontracted load changes in each area

Uncontracted change in area 1, ΔP_1^{U}	0.0107 pu	0 pu	-0.012 pu	0 pu
Time occurred in area 1 from 0 s	8.6 s	18.4 s	27.4 s	36 s
Uncontracted change in area 2, ΔP_2^{U}	-0.0107 pu	0 pu	0.012 pu	0 pu
Time occurred in area 2 from 0 s	9.6 s	18.8s	27.2s	36.2 s

bound). It can be seen that in most cases, LQR provided a more sustained saturation than the CMPC scheme. Finally, Figure 4.7 shows the control inputs in each area (left) and net tie line deviation in area 1 (right); the black dotted lines in the ΔP_i^{C} plots are the input constraints bounds, while the black dotted line in the $\Delta P_1^{\mathrm{tie}}$ plot is the scheduled net incremental tie line flow computed using (4.11) and its value is -0.00252 pu.

The control inputs converged to zero because no uncontracted load changes occurred; the area participation factors in Table 4.1 only affected the system behaviour during transients. Also, unlike in the traditional power system where the net tie line deviation is required to converge to zero (see Figure 2.11), $\Delta P_1^{\mathrm{tie}}$ in Figure 4.7 converged to a nonzero value. This is because DisCos in a CA can procure LFC in the form of LM bilateral contract from GenCos in another area. Note that $\Delta P_1^{\mathrm{tie}} = -\Delta P_2^{\mathrm{tie}}$ since equal area capacity is assumed. The negative value of $\Delta P_1^{\mathrm{tie}}$ (-0.00252 pu) indicates that area 1 is importing power. In general, there is no glaring advantage of using MPC over LQR in this case as the input constraints are not active and this is because the magnitudes of the contracted load changes are small; however, from Figure 4.5, LQR causes some undershoots and this is because of the more sustained saturation it exhibited in the GRC.

103
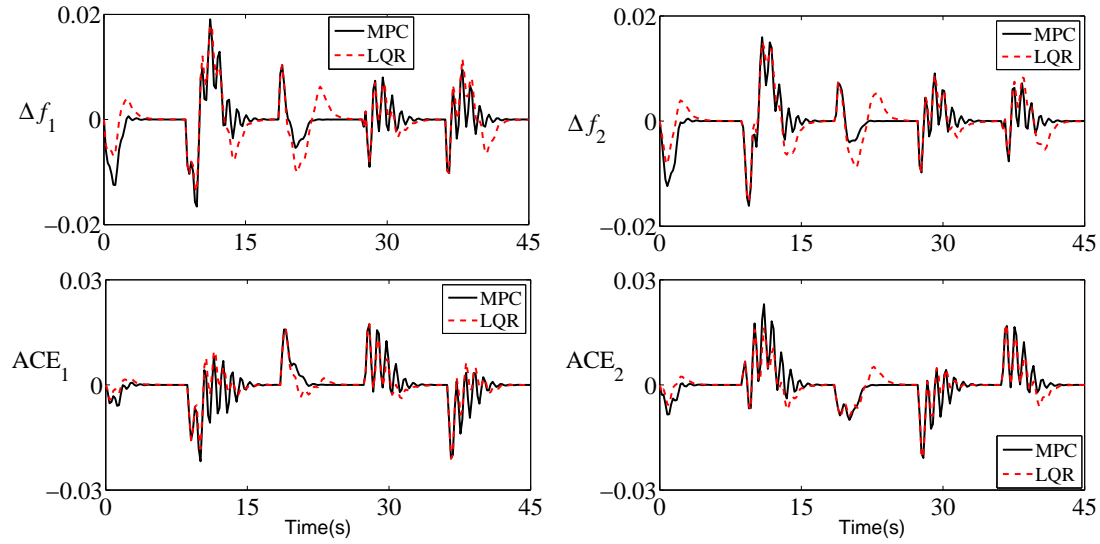
Figure 4.8: Frequency deviations Δf_i Hz and area control errors ACE_i pu in area 1 and 2 (case 2).
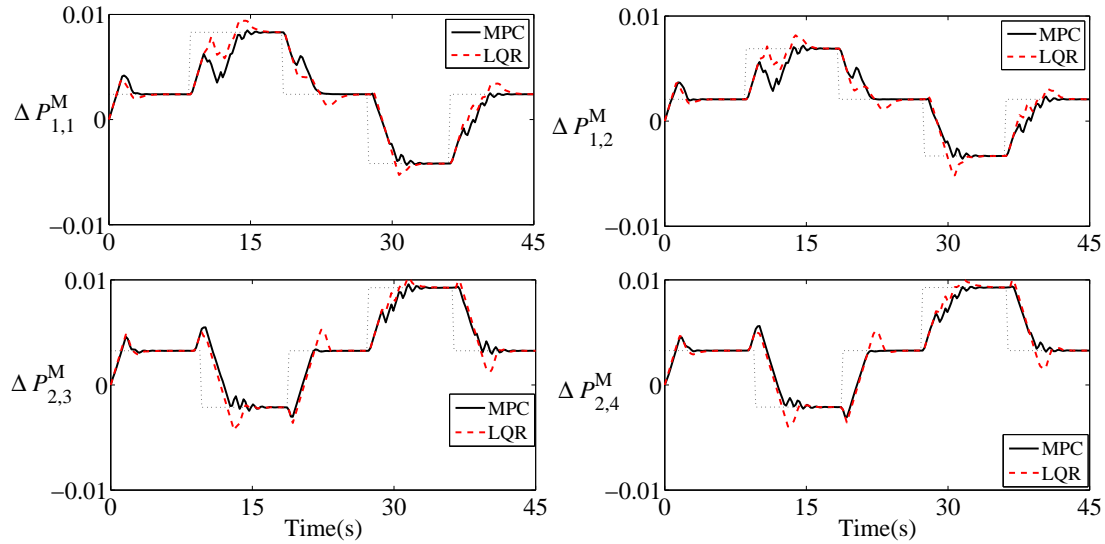
Figure 4.9: Change in the output power $\Delta P_{i,k}^{\text{M}}$ pu of GenCos in area 1 and 2 (case 2). Black dotted lines are the desired generation based on contracted load changes (computed using the DPM) and uncontracted load changes (computed using area participation factors)
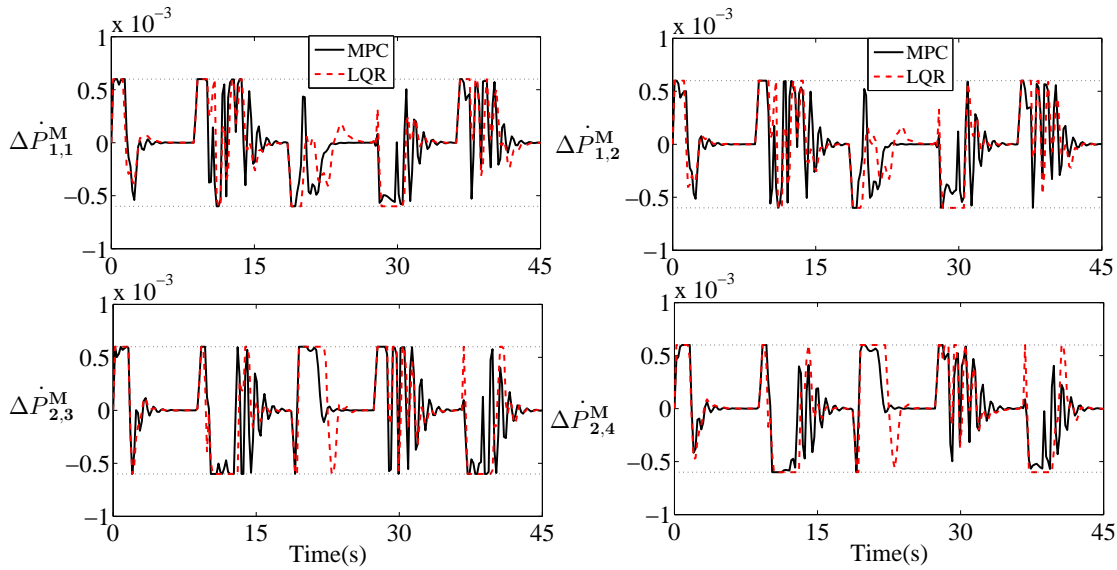
Figure 4.10: Generation rate of GenCos $\Delta \dot{P}_{i,k}^{M}$ pu/s in area 1 and 2 (case 2). The black dotted lines are the constraint bounds.
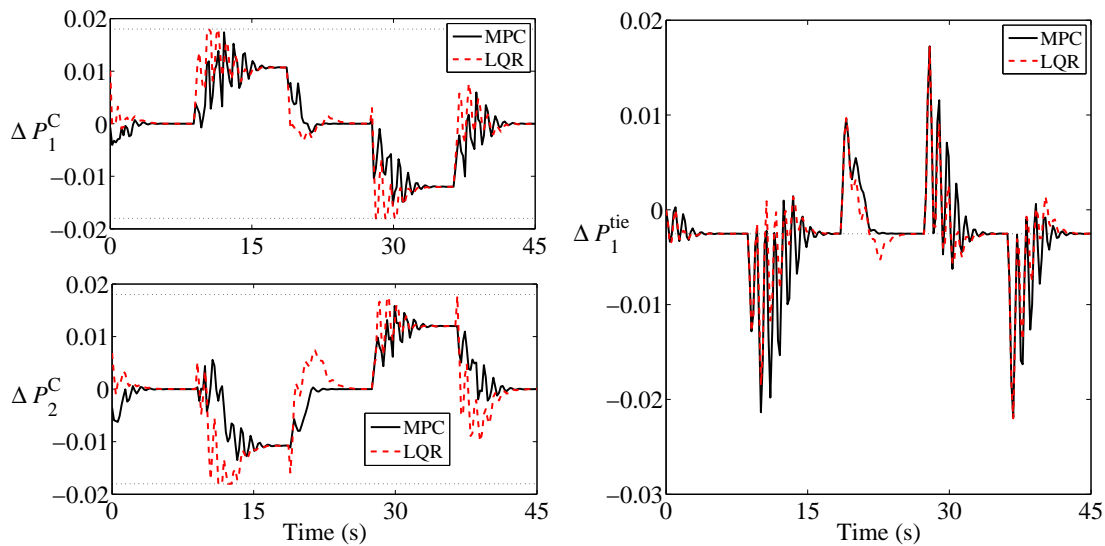
Figure 4.11: Control inputs ΔP_i^C in area 1 and 2, and net tie line deviation in area 1 ΔP_1^{tie} pu (case 2). Left dotted lines: bounds on control inputs. Right dotted line: scheduled net incremental tie line flow of area 1 $\Delta P_1^{tie,sh}$ pu based on inter-area bilateral LM contract.

4.5.2   Case-2 : Bilateral LFC with uncontracted load change

This section demonstrates the scenario were bilateral LM contracts exist between GenCos and DisCos and then uncontracted load changes occured. The same DPM and contracted load change assumed as in case-1 is used here. Under this condition, ΔP_1^U and/or ΔP_2^U in (4.1) and (4.2) are/is nonzero at some point. As previously stated, uncontracted load changes are handled by GenCos in the area where load changes occurred, and therefore, the net tie line deviation in this scenario is expected to be the scheduled value of case-1 (-0.00252 pu).

105

Furthermore, it is expected that GenCos would take up the excess power (uncontracted) according to their $\gamma_{i,k}$ values stated in Table 4.1. Assume uncontracted load changes occurred in each area whose values and time of occurrence is shown in Table 4.2. The desired change in generation of each GenCo has been calculated using the relationship in (4.5) as well as the area participation factor of each GenCo in Table 4.1. As an example, the desired value of $\Delta P_{1,1}^{\mathrm{M}}$ is given as:

$$\Delta P_{1,1}^{\mathrm{M}}(\text{desired}) = \sum_{l=1}^{4} \eta_{1,l}\Delta P_{1,l}^{\mathrm{L}} + \gamma_{1,1}\Delta P_{1}^{\mathrm{U}} \tag{4.33}$$

The frequency deviations (top) and ACE (bottom) of each area, under case-2, are shown in Figure 4.8. As expected, Δf_1, Δf_2, ACE_1 and ACE_2 converged to zero. Moreover, LQR resulted in more undershoots and overshoots and this is because it lacks systematic constraints handling. The change in power output of each GenCo is presented in Figure 4.9, where the black dotted lines are used to specify the desired generation of each GenCo. It can be seen from the change in power outputs that the CMPC tracks the desired generation more effectively as compared to the LQR; this is because, CMPC accounted for the generation rate constraints of each GenCo.

The generation rate of each GenCo is shown in Figure 4.10. It can be seen that the LQR spends more time in saturation than the CMPC, and this justifies the constraint handling capability of CMPC. Finally, the control inputs in each area (left) and net tie line deviation (right) in area 1 are shown in Figure 4.11. It can be seen that at the times when the uncontracted load change in each area is nonzero (see Table 4.2), the control signals are nonzero. Furthermore, CMPC performs better in terms of handling the input constraints.

For the net tie line deviation, the black dotted line is used to specify the scheduled net incremental tie line flow $\Delta P_1^{\mathrm{tie,sch}}$. The net tie line deviation $\Delta P_1^{\mathrm{tie}}$ always settles at the scheduled value (-0.00252 pu) at steady state, after uncontracted changes have been rejected, and this shows that each control area handled its own uncontracted load variations.

4.6 Conclusion

The main duty of a multi-area LFC (to eliminate active power imbalance in networks) is preserved in the deregulated environment, however with key modifications to the age-long traditional LFC framework. The basics of such modifications, which primarily consist of accounting for bilateral load matching contracts between GenCos and DisCos based on the concept of DisCo participation matrix, can be understood when a 2-area system is considered. Moreover,

this chapter has demonstrated via simulation, for a 2-area deregulated system, that by explicitly incorporating GRC and input constraints into a LFC design, a better LFC performance can be achieved, and that a predictive control technique may be a better choice for LFC in that respect. Also, it has been shown that predictive control can effectively reject uncontracted load changes and coordinate the transient behaviour of a system when contracted load changes occur.

It is vital to mention that the results presented in this thesis have not be compared with the integral control LFC scheme used in the industry. This is as a result of the difficulty in obtaining a suitable integral gain that can offer a sensible response for the deregulated LFC case. In a traditional power system structure, an equivalent machine model is used in each CA to represent generating units within that territory. Hence the load frequency control problem in a control area is SISO, as demonstrated in Section 2.1.6 using integral control. However, in the deregulated case, each generating unit in a CA (known as a GenCo and consists of a governor and a turbine model) is considered separately as opposed to an equivalent machine. Furthermore, local and cross-border bilateral contracts signals are introduced into the LFC model and thus, load disturbances impact on CAs not only through the tie-lines, but also through various possible bilateral load matching (LM) contracts. Consequently, the control problem considered in each area is multivariable (highly interactive) and obtaining integral gains using classical control method is difficult. No work in the literature has considered designing classical integral control scheme for deregulated LFC problems and the PI-based deregulated LFC schemes in the literature are largely based on intelligent methods [85, 170].

Chapter 5

Generalised LFC model in the deregulated framework

5.1   Introduction

In the previous chapter, it was emphasised that a 2-area benchmark system is a good choice of multi-area system to gain insights into the key modifications required to obtain a deregulated load frequency control (LFC) model from the traditional model described in Chapter 2. Thus, the previous chapter demonstrated the potency of predictive control based LFC on a 2-area deregulated benchmark system. However, realistic power system interconnections may consist of several (more than two) control areas (CAs) linked by tie lines. Furthermore, while the CAs within practical interconnections usually have unequal rated capacities, equal ratings were assumed for the 2-area system in the previous chapter. Hence, deregulated LFC studies involving more than 2-areas, where unequal area ratings are considered, are required.

While the 2-area study provided good insight into the key modifications required to develop a deregulated model, some steps presented in Section 4.3 such as determining the total LM contractual obligation of a GenCo $S_{i,\mathrm{k}}$, the net tie line flow dynamics of each area (4.10) and scheduled net incremental tie line flow (4.11) and (4.12) for large scale interconnections with several CAs, having numerous GenCos and DisCos in each CA that are making local and cross-border transactions may be burdensome. Moreover, accounting for the difference in rated capacities of control areas in deregulated LFC models, especially in a large scale type, might be tricky; previous works often assumed that CAs have equal rated capacities. Thus, it is necessary to develop a generic framework that provides a systematic procedure to develop realistic deregulated LFC benchmark models for interconnections of any size.

Therefore, in reference to the third objective of this thesis as stated in Section 1.4, this chapter proposes a novel generalised model for load frequency control studies in a deregulated environment. The key advantage of this formulation is that it can accommodate LFC studies in the more pragmatic case, where interconnected control areas (CAs) having different rated capacities, or when equal CA ratings are considered. The significance and effectiveness of this formulation is demonstrated using a 7-area deregulated network. The test network is a modification of the CIGRE-7 machine test system. The 7-area deregulated network will be used in Chapters 6 and 7 for control design studies. Moreover, an additional 4-area deregulated benchmark model is developed to demonstrate, further, the usefulness of the generalised formulation and to provide more insight into how one can utilise the generalised formulation to develop a LFC model for any choice of network. The 4-area model is used as one of the case study models in Chapter 7 to provide more evidence on the benefit of a distributed MPC scheme.

This chapter is based on the work in [35] and a part of [36] and its a key **contribution** in this thesis. The organisation of the chapter is as follows: Section 5.2 provides a summary of the main contributions of this chapter; Section 5.3 presents the generalised deregulated LFC framework; Section 5.4 applies the generalised framework to develop a 7-area deregulated benchmark model; Section 5.5 presents simulation evidence and discussions; Section 5.6 develops a 4-area deregulated benchmark model; Section 5.7 provides some concluding remarks.

5.2 A summary of the main contributions

The main contributions in this chapter are summarised below:

- Proposes a generalised formulation of a deregulated LFC model for an N control area network, which can accommodate studies where control areas either have unequal rated capacities or equal rated capacities.

- Develops a 7-area deregulated benchmark model by applying the proposed generalised model, and provides simulation evidence to demonstrate the importance of considering the difference in area rated capacities.

- A 4-area deregulated benchmark model is also developed to further demonstrate the usefulness of the generalised formulation, and to provide more insight into how the LFC model of any deregulated power network can be developed from the generalised formulation.

Note that the main reason for considering the difference in rated capacities is that in power system analysis, power quantities are usually expressed in their per-unit (pu) equivalent, that

is, they are expressed as a fraction of a base value. At the interconnection level of power systems, the rated capacity of a CA may be considered as the base in that area, and this value is likely to vary from one CA to the other. Thus, when there is bilateral LM contracts across CA boundaries, a change of base should be applied. If the difference in the rated capacities is not considered in the contract information, a GenCos on a LM contract may generate an incorrect amount of incremental power when it contracts with DisCos outside its CA leading to a power imbalance and consequently, frequency offsets in each area of the interconnected system. It is vital to emphasise that if GenCos contract with DisCos in their CA only (no contractual power flow across tie lines), or if power quantities are expressed in their actual megawatt values rather than in pu values, neglecting the difference in area rated capacities in LFC would not create a power imbalance in the network.

5.3 Generalised model

This section proposes a new generalised formulation for LFC studies in a deregulated power system; the generalised formulation is one contribution in this chapter. GenCos and DisCos within and across CA boundaries can bilaterally make a LM contract, and they are also responsible for having data channels to exchange the necessary contract data/information and measurements required to perform load matching functions. In theory, GenCos in LM contracts are obliged to regulate their power output to follow DisCos' contracted load changes, and DisCos are to monitor their load continuously to avoid contract violations [55, 56]. The entire contract data are used to build the DPM which is available to the TSO for supervision, and also for supplementary control purposes when uncontracted load changes occur [29]. The nomenclature used in this section is defined in Table 5.1.

5.3.1 DisCo participation matrix

The DPM of an interconnected power system with n GenCos (DPM rows) and m DisCos (DPM columns) is

$$\text{DPM} = \begin{bmatrix} \eta_{1,1} & \eta_{1,2} & \cdots & \eta_{1,m} \\ \eta_{2,1} & \eta_{2,2} & \cdots & \eta_{2,m} \\ \vdots & \vdots & \vdots & \vdots \\ \eta_{(n-1),1} & \eta_{(n-1),2} & \cdots & \eta_{(n-1),m} \\ \eta_{n,1} & \eta_{n,2} & \cdots & \eta_{n,m} \end{bmatrix}; \quad \sum_{k=1}^{n} \eta_{k,l} = 1 \qquad (5.1)$$

where η is a contract participation factor; $\eta_{k,l}$ represents the fraction of the lth DisCo's total LM requirements contracted to the kth GenCo; $\eta_{k,l} = 0$ if there is no LM contract between GenCo k and DisCo l , or GenCo k and DisCo l belong to a different CA with no tie line

Table 5.1: Nomenclature

$\mathcal{A}$	Index set of the CAs in the network $\{1, 2, \cdots, \mathrm{N}\}$
$\mathcal{A}_d$	Index set of CAs with independent tie line flows, $\mathcal{A}_d \subseteq \mathcal{A}$
$\mathcal{A}_i^{\mathrm{Ne}}$	Index set of CAs connected to the ith CA, $\mathcal{A}_i^{\mathrm{Ne}} \subseteq \mathcal{A}$
$\mathcal{G}$	Index set of GenCos in the network, $\{1, 2, \cdots, n\}$
$\mathcal{G}_i$	Index of GenCos in the ith CA, $\mathcal{G}_i \subseteq \mathcal{G}$
$\mathcal{D}$	Index set of DisCos in the network, $\{1, 2, \cdots, m\}$
$\mathcal{D}_i$	Index set of DisCos in the ith CA, $\mathcal{D}_i \subseteq \mathcal{D}$
$\mathcal{G}_i^{\mathrm{Ne}}$	Index set of GenCos in the CA(s) connected to the ith CA
Δf_i	Deviation in frequency in the ith CA [Hz]
$\Delta P_i^{\mathrm{tie}}$	Deviation in net interchange power in the ith CA [pu]
ΔP_i^{L}	Total contracted load change of DisCos in the ith CA [pu]
ΔP_i^{U}	Total uncontracted load change in the ith CA [pu]
H_i	Equivalent inertia constant in the ith CA [pu s]
D_i	Equivalent damping coefficient in the ith CA [pu/Hz]
$\Delta P_i^{\mathrm{tie,sh}}$	Net scheduled incremental tie-line flow in the ith CA
ACE_i	Area control error in the ith CA
β_i	Frequency bias setting in the ith CA
ΔP_i^{M}	Total change in power output in the ith CA [pu]
$\Delta P_{i,\mathrm{k}}^{\mathrm{M}}$	change in power output of GenCo k in the ith CA [pu]
$\Delta P_{i,l}^{\mathrm{L}}$	Contracted load change of DisCo l in the ith CA
$T_{\mathrm{T}_{i,\mathrm{k}}}$	Turbine time constant ofGenCo k in the ith CA [s]
$T_{\mathrm{G}_{i,\mathrm{k}}}$	Governor time constant of GenCo k in the ith CA [s]
$\Delta P_{i,\mathrm{k}}^{\mathrm{V}}$	Change in governor output, of GenCo k in the ith CA [pu]
$R_{i,\mathrm{k}}$	Droop characteristic of GenCo k in the ith CA [Hz/pu]
$S_{i,\mathrm{k}}$	Contracted demands of GenCo k in the ith CA
$\gamma_{i,\mathrm{k}}$	Area participating factor of GenCo k in the ith CA
P_{r_i}	Rated capacity of the ith CA

connections. Also, each contract participation must satisfy the condition $0 \leq \eta_{\mathrm{k},l} \leq 1$. The entries of the DPM are the contract information. The block diagram of the ith CA is shown in Figure 5.1.

5.3.2 Swing equation

For the ith CA, assuming small deviations from nominal, the linearised swing equation is:

$$\Delta \dot{f}_i \;\; = \frac{1}{H_i} \Big(\Delta P_i^{\mathrm{M}} - D_i \Delta f_i - \Delta P_i^{\mathrm{tie}} - \Delta P_i^{\mathrm{L}} - \Delta P_i^{\mathrm{U}} \Big) \;\;\; \forall i \in \mathcal{A} \tag{5.2}$$

where

$$\Delta P_i^{\mathrm{M}} = \sum_{\mathrm{k}\in\mathcal{G}_i}\Delta P_{i,\mathrm{k}}^{\mathrm{M}}; \quad \Delta P_i^{\mathrm{L}} = \sum_{l\in\mathcal{D}_i}\Delta P_{i,l}^{\mathrm{L}} \qquad (5.3)$$

Note that it is assumed that all generators in a CA form a coherent group, i.e., they all swing in unison when the CA is subjected to a small disturbance, hence, the reason to define a single frequency Δf_i for the ith CA.

The tie line equations (5.4), (5.5a) and (5.5b) presented in the following section were extracted from Section (2.1.3.4) and the only additions are the index sets $\mathcal{A}$ and $\mathcal{A}_d$ appended to (5.4) for the generalised case; the expressions (5.5a) and (5.5b) and descriptions are included for readability.

5.3.3 Net tie line flow deviation

The net tie line deviation $\Delta P_i^{\mathrm{tie}}$ in the ith CA, based on DC power flow equation, is

$$
\begin{aligned}
\Delta P_i^{\mathrm{tie}} &= \sum_{j\in\mathcal{A}_i^{\mathrm{Ne}}}\Delta P_{ij}^{\mathrm{tie}} \quad \forall i\in\mathcal{A} \\
\Delta \dot{P}_i^{\mathrm{tie}} &= \sum_{j\in\mathcal{A}_i^{\mathrm{Ne}}}\Delta \dot{P}_{ij}^{\mathrm{tie}} \quad \forall i\in\mathcal{A}_d
\end{aligned}
\qquad (5.4)
$$

where

$$\Delta P_{ij}^{\mathrm{tie}} = Y_{ij}\Big(\Delta\delta_i - \Delta\delta_j\Big); \quad \Delta\dot{P}_{ij}^{\mathrm{tie}} = T_{ij}\Big(\Delta f_i - \Delta f_j\Big) \qquad (5.5\mathrm{a})$$

$$\Delta P_{ji}^{\mathrm{tie}} = -\frac{P_{r_i}}{P_{r_j}}\Delta P_{ij}^{\mathrm{tie}} = -\alpha_{ij}\Delta P_{ij}^{\mathrm{tie}} \qquad (5.5\mathrm{b})$$

Here, $T_{ij} = 2\pi Y_{ij}$; δ_i rad is the equivalent rotor swing angle of the ith CA (assuming coherency within a CA); $\Delta P_{ij}^{\mathrm{tie}}$ pu, T_{ij} pu/Hz, Y_{ij} pu/rad and α_{ij} are the deviation in tie line flow, tie line synchronizing coefficient, line admittance and rated capacity ratio between the ith and jth CAs respectively; $\alpha_{ij} = 1$ if the rated capacities of the ith and jth CAs are equal . Note that in reality, no two CAs are equal in rated capacity, and this is considered in this new formulation. In network analysis, a convention for the direction of power flow between two connected nodes (CAs) is usually chosen. Hence, (5.5b) is used to adjust the direction of tie line flow between two connected areas to reflect the convention chosen in the interconnected CAs.

For an N-area system, there would be N net tie line power flows $\{\Delta P_1^{\mathrm{tie}}, \Delta P_2^{\mathrm{tie}}, \cdots, P_{\mathrm{N}}^{\mathrm{tie}}\}$, and only $\mathrm{N}-1$ net tie line flows can be independently controlled. Hence only $\mathrm{N}-1$ independent net tie line deviations are considered as system states, and the Nth dependent tie line flow is

automatically controlled once the $N-1$ independent net flows are regulated to their scheduled (contracted) value. An uncontrollability problem may arise if one attempts to regulate the N net tie line flows to their respective contracted values. The dependence property can be verified by evaluating the rank of the network admittance matrix, which depends on the network topology [223]. The N net tie line deviations can be collectively expressed as:

$$
\begin{bmatrix} \Delta P_1^{\text{tie}} \\ \Delta P_2^{\text{tie}} \\ \vdots \\ \Delta P_N^{\text{tie}} \end{bmatrix} = \underbrace{\begin{bmatrix} \sum_{j \in \mathcal{A}_1^{\text{Ne}}} Y_{1j} & -Y_{12} & \cdots & -Y_{1N} \\ -Y_{21} & \sum_{j \in \mathcal{A}_2^{\text{Ne}}} Y_{2j} & \cdots & -Y_{2N} \\ \vdots & \vdots & \ddots & \vdots \\ -Y_{N1} & -Y_{N2} & \cdots & \sum_{j \in \mathcal{A}_N^{\text{Ne}}} Y_{Nj} \end{bmatrix}}_{Y} \begin{bmatrix} \Delta \delta_1 \\ \Delta \delta_2 \\ \vdots \\ \Delta \delta_N \end{bmatrix} \tag{5.6}
$$

where $Y \in \mathbb{R}^{N \times N}$ is the network admittance matrix, entry $Y_{ij} = 0$ if there is no connection between area i and j. The rank of the admittance matrix indicates the number of net tie line flows that can be controlled independently, and it is usually $N-1$.

5.3.4 Turbine dynamics

The turbine equation (5.7) in this section has the same form as the one presented in (4.9). However, (5.7) has the index sets $\mathcal{A}$ and $\mathcal{G}_i$ written alongside to have the generalised case. For small deviations around nominal settings, the turbine dynamics of the kth GenCo in the ith CA is:

$$
\Delta \dot{P}_{i,\text{k}}^{\text{M}} = \text{sat}_{\Delta \dot{P}_{i,\text{k}}^{\text{M}}}^{i} \left(\left(\frac{1}{T_{\text{T}_{i,\text{k}}}} (\Delta P_{i,\text{k}}^{\text{V}} - \Delta P_{i,\text{k}}^{\text{M}}) \right) \right) \quad \forall i \in \mathcal{A}, \forall \text{k} \in \mathcal{G}_i \tag{5.7}
$$

5.3.5 Governor dynamics

The governor equation (5.8) in this section has the same form as the one presented in (4.6). However, (5.8) has the index sets $\mathcal{A}$ and $\mathcal{G}_i$ written alongside to have the generalised case. The description provided immediately after (5.8) is to aid readability. The governor dynamics of the kth GenCo in the ith CA is

$$
\Delta \dot{P}_{i,\text{k}}^{\text{V}} = \frac{1}{T_{\text{G}_{i,\text{k}}}} \left(\gamma_{i,\text{k}} \Delta P_i^{\text{C}} - \Delta P_{i,\text{k}}^{\text{V}} - \frac{1}{R_{i,\text{k}}} \Delta f_i + S_{i,\text{k}} \right) \quad \forall i \in \mathcal{A}, \forall \text{k} \in \mathcal{G}_i \tag{5.8}
$$

Note that in the deregulated environment, TSOs secure LFC commitments in advance from GenCos to cater for uncontracted load variations in their CA, and each participating GenCo

would provide information on how much they can contribute in compensating for the total uncontracted variations that may occur in their CA; the magnitude of $\gamma_{i,\mathrm{k}}$ determines how much each GenCo participating in a TSO's supplementary control is ready to contribute. For the ith CA, a vector of the area particpating factors, $\boldsymbol{\gamma}_i$, is:

$$\boldsymbol{\gamma}_i = \begin{bmatrix} \gamma_{i,1} & \gamma_{i,2} & \cdots & \gamma_{i,n_i} \end{bmatrix}^{\mathrm{T}}; \quad \sum_{\mathrm{k}=1}^{n_i} \gamma_{i,\mathrm{k}} = 1; \quad 0 \leq \gamma_{i,k} \leq 1 \tag{5.9}$$

Here, for clarity, it is assumed that GenCos the ith CA are indexed from 1 to n_i, that is, $\mathcal{G}_i = \{1, 2, \cdots, n_i\}$, and n_i is the total number of GenCos in the ith CA. Note that a different indexing (not necessarily serial) can be used and the concept here remains unchanged. In (5.9), the area participation factor of a GenCo not participating in TSO's supplementary control is set to zero.

5.3.6 Contracted signal

The contracted signal, $S_{i,\mathrm{k}}$, in the generalised form, accounting for the difference in rated capacities of CAs is

$$S_{i,\mathrm{k}} = \sum_{l \in \mathcal{D}_i} \eta_{\mathrm{k},l} \Delta P_{i,l}^{\mathrm{L}} + \sum_{j \in \mathcal{A}_i^{\mathrm{Ne}}} \left\{ \sum_{l \in \mathcal{D}_j} \eta_{\mathrm{k},l} \alpha_{ji} \Delta P_{j,l}^{\mathrm{L}} \right\} \quad \forall i \in \mathcal{A}, \forall \mathrm{k} \in \mathcal{G}_i \tag{5.10}$$

The signal, $S_{i,\mathrm{k}}$, consist of the lumped LM requirements of DisCos in the ith CA and DisCos in CAs connected to area i (neighbouring CAs). $S_{i,\mathrm{k}}$ is zero if GenCo k in area i is not committed to a LM contract. The desired output of a GenCo k in area i participating in both a LM contract and TSO's supplementary control $\Delta P_{i,\mathrm{k}}^{\mathrm{M}}(\mathrm{desired})$ can be calculated using

$$\begin{aligned} \Delta P_{i,\mathrm{k}}^{\mathrm{M}}(\mathrm{desired}) &= S_{i,\mathrm{k}} + \gamma_{i,\mathrm{k}} \Delta P_i^{\mathrm{U}} \\ \Delta P_i^{\mathrm{M}}(\mathrm{desired}) &= \sum_{\mathrm{k} \in \mathcal{G}_i} \Delta P_{i,\mathrm{k}}^{\mathrm{M}}(\mathrm{desired}) \end{aligned} \tag{5.11}$$

If a GenCo k in area i subscribed to LM contract only, $\gamma_{i,\mathrm{k}}$ in (5.11) is zero; if the GenCo subscribed to TSO's supplementary control only (to handle uncontracted load changes), $S_{i,\mathrm{k}}$ is set to zero. Note that (5.11) is not part of the system model, but can serve as a reference to check that a GenCo is fulfilling its LFC obligations.

The expression (5.12) in the following section is exactly the same as (4.11) but included for readability.
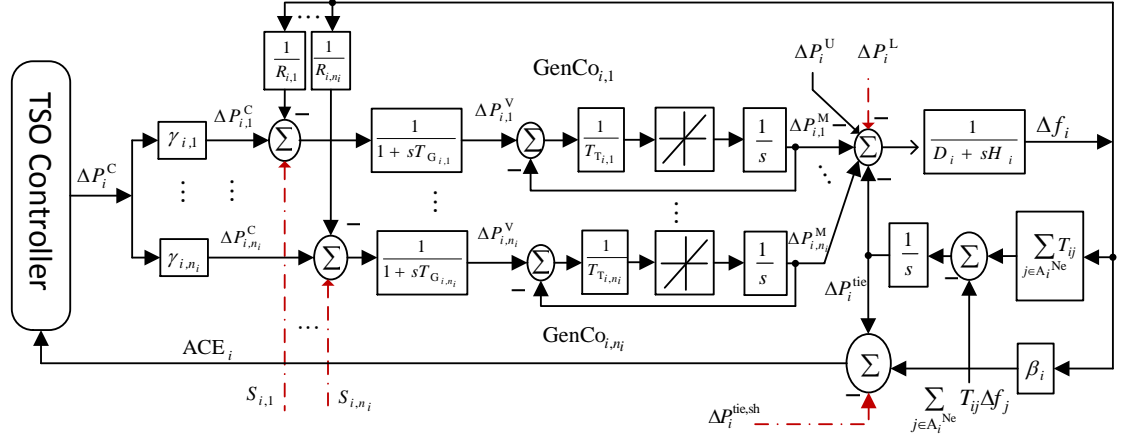
Figure 5.1: Block diagram of ith CA in the deregulated framework. Diagram assumes GenCos in the ith CA are indexed $\{1, 2, \cdots n_i\}$, and n_i is the total number of GenCos in the ith CA. The red dash-dot lines indicates contractual information, and this is absent in the VIU framework.

5.3.7 Scheduled net incremental tie line flow

The scheduled (contracted) net incremental tie line flow of the ith CA $\Delta P_i^{\text{tie,sch}}$ is

$$
\Delta P_i^{\text{tie,sh}} = \left\{ \begin{array}{c} \text{contracted incremental demands of DisCos} \\ \text{in other areas from GenCos in area } i \end{array} \right\}
$$
$$
- \left\{ \begin{array}{c} \text{contracted incremental demands of DisCos} \\ \text{in area } i \text{ from GenCos in other areas} \end{array} \right\} \tag{5.12}
$$

A generalised form of the scheduled net incremental tie line flow, accounting for the difference in rated capacities of CAs is

$$
\Delta P_i^{\text{tie,sh}} = \sum_{j \in \mathcal{A}_i^{\text{Ne}}} \sum_{g \in \mathcal{G}_i} \sum_{l \in \mathcal{D}_j} \eta_{g,l} \alpha_{ji} \Delta P_{j,l}^{\text{L}} - \sum_{g \in \mathcal{G}_i^{\text{Ne}}} \sum_{l \in \mathcal{D}_i} \eta_{g,l} \Delta P_{i,l}^{\text{L}} \quad \forall i \in \mathcal{A} \tag{5.13}
$$

Note that ΔP_i^{tie} should be equal to $\Delta P_i^{\text{tie,sh}}$ at steady state, even when uncontracted load changes are present. Also, because DisCos can purchase LFC in the form of LM contracts within and across their CA boundaries, ΔP_i^{tie} could be nonzero at steady state. The non-zero ΔP_i^{tie} means that contract data/information and measurements must be incorporated in the traditional area control error calculation. This is a departure from the VIU framework where one of the control objectives is to regulate ΔP_i^{tie} to zero. Note that (5.10) and (5.13) are the new information in the deregulated environment, and they have been expressed as a function

of α_{ji} to account for the different CA ratings, which has been largely ignored in the previous works.

The area control error (5.14) presented in the following section is exactly the same as (4.13) except for the index set $\mathcal{A}$ that was included in (5.14) to have the generalised form.

5.3.8 Area control error

The area control error (ACE) of the ith CA in the new framework is

$$\text{ACE}_i = \beta_i \Delta f_i + \Delta P_i^{\text{tie,err}}; \quad \Delta P_i^{\text{tie,err}} = \Delta P_i^{\text{tie}} - \Delta P_i^{\text{tie,sh}} \quad \forall i \in \mathcal{A} \tag{5.14}$$

With the modification of the ACE to include $\Delta P_i^{\text{tie,err}}$ instead of using the net tie line deviation ΔP_i^{tie} used in the traditional LFC formulation (see (2.17)) , the primary objective of regulating ACE to zero is retained in the deregulated scenario.

5.3.9 Summary

A generalised power system model for LFC studies in a deregulated power system has been developed based on the DPM concept. This formulation can handle interconnected CAs with equal and unequal ratings, making it more versatile than the previous formulations. The key equations needed to develop a deregulated LFC model are (5.1), (5.2), (5.4), (5.7), (5.8), (5.10), (5.13) and (5.14).

5.4 7-area LFC deregulated model

This section presents one of the contributions of this chapter, which is to develop a 7-area deregulated benchmark system; the benchmark system is required to show the significance and effectiveness of the generalised formulation. The 7-area model is also needed to demonstrate the efficacy of the predictive control schemes proposed in Chapters 6 and 7. As stated earlier, the 7-area network is a modification/extension of the 7-machine CIGRE test network; the CIGRE network consists of 7 generators and 3 load buses/nodes. Most LFC studies in the literature limit their formulations to a maximum of 4-area, where equal area rated capacities are often assumed. A single line diagram of the partitioned 7-machine CIGRE network and the resulting 7-area deregulated network is shown in Figure 5.2 and Figure 5.3 respectively.

In this work, the extended 7 CAs network contains a total of 33 GenCos and 46 DisCos which are distributed as shown in Table 5.2; the network also has a CA that is connected to 5 other CAs, and another CA linked to 4 other CAs, and with the majority of the CAs connected
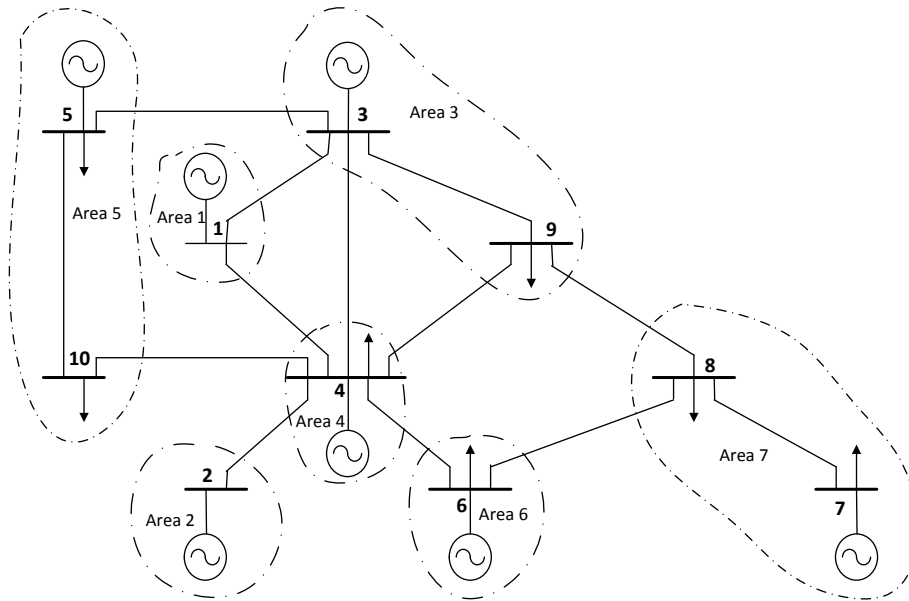
Figure 5.2: 7-machine CIGRE network partitioned into 7-areas
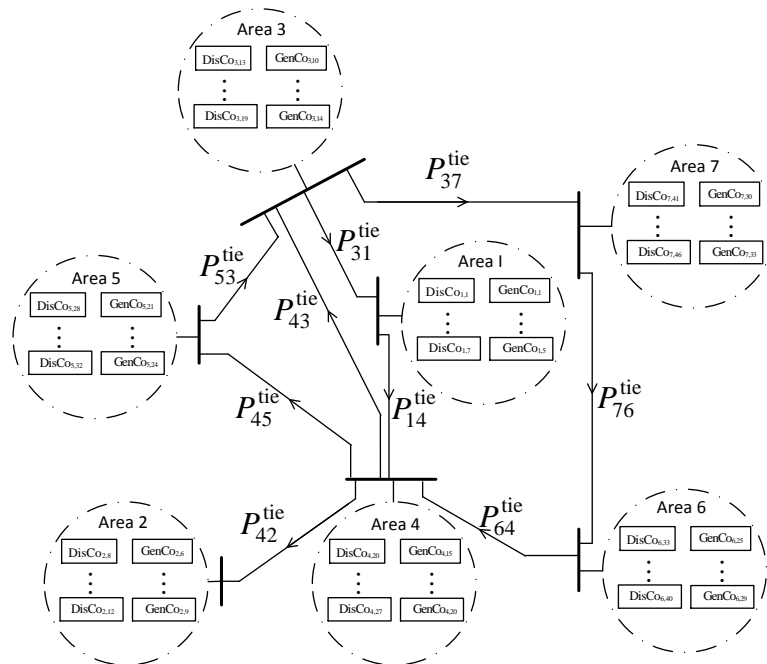
Figure 5.3: 7-area deregulated system having GenCos and DisCos in each area

Table 5.2: GenCos and DisCos distribution within CAs for the 7-area network

CA index	No. of GenCo & index $(\mathcal{G}_i)$	No. of DisCo & index $(\mathcal{D}_i)$
1	5 & $\{1, \cdots, 5\}$	7 & $\{1, \cdots, 7\}$
2	4 & $\{6, \cdots, 9\}$	5 & $\{8, \cdots, 12\}$
3	5 & $\{10, \cdots, 14\}$	7 & $\{13, \cdots, 19\}$
4	6 & $\{15, \cdots, 20\}$	8 & $\{20, \cdots, 27\}$
5	4 & $\{21, \cdots, 24\}$	5 & $\{28, \cdots, 32\}$
6	5 & $\{25, \cdots, 29\}$	8 & $\{33, \cdots, 40\}$
7	4 & $\{30, \cdots, 33\}$	6 & $\{41, \cdots, 46\}$

to two neighbours. Such level of complexity has never been considered in the deregulated environment. Also shown in the table, are the indexes of the GenCos and DisCos, and they are numbered serially from area 1 through 7; though they can also be indexed randomly and would still fit into the new generalised formulation.

To develop the benchmark model, the index sets defined alongside the equations in Section 5.3 must be stated. Once these sets are specified, it can be applied appropriately in the generalised formulation to model the 7-area interconnected system. From Table 5.2 and Figure 5.3, the relevant index sets can be defined, and they are presented in Table 5.3; these sets are used throughout this section.

5.4.1 Swing equation : 7-area system

For the 7-area system, the swing equations for each area can be written by applying the index sets $\mathcal{A}$, $\mathcal{G}_i$, $\mathcal{D}_i$ defined in Table 5.3 on (5.2) and (5.3):

$$
\Delta \dot{f}_1 = \frac{1}{H_1}\Big(\{\triangle P_{1,1}^{\mathrm{M}} + \cdots + \triangle P_{1,5}^{\mathrm{M}}\} - \Delta P_1^{\mathrm{tie}} - D_1 \Delta f_1
$$
$$
- \{\triangle P_{1,1}^{\mathrm{L}} + \cdots + \triangle P_{1,7}^{\mathrm{L}}\} - \Delta P_1^{\mathrm{U}} \Big) \tag{5.15a}
$$

$$
\vdots
$$

$$
\Delta \dot{f}_7 \quad \frac{1}{H_7}\Big(\{\triangle P_{7,30}^{\mathrm{M}} + \cdots + \triangle P_{7,33}^{\mathrm{M}}\} - \Delta P_7^{\mathrm{tie}} - D_7 \Delta f_7
$$
$$
- \{\triangle P_{7,41}^{\mathrm{L}} + \cdots + \triangle P_{7,46}^{\mathrm{L}}\} - \Delta P_7^{\mathrm{U}} \Big) \tag{5.15b}
$$

Table 5.3: Index sets of 7-area benchmark system

$\mathcal{G}_1 = \{1, \cdots, 5\}$, $\mathcal{G}_2 = \{6, \cdots, 9\}$, $\mathcal{G}_3 = \{10, \cdots, 14\}$, $\mathcal{G}_4 = \{15, \cdots, 20\}$ $\mathcal{G}_5 = \{21, \cdots, 24\}$, $\mathcal{G}_6 = \{25, \cdots, 29\}$, $\mathcal{G}_7 = \{30, \cdots, 33\}$
$\mathcal{D}_1 = \{1, \cdots, 7\}$, $\mathcal{D}_2 = \{8, \cdots, 12\}$, $\mathcal{D}_3 = \{13, \cdots, 19\}$, $\mathcal{D}_4 = \{20, \cdots, 27\}$ $\mathcal{D}_5 = \{28, \cdots, 32\}$, $\mathcal{D}_6 = \{33, \cdots, 40\}$, $\mathcal{D}_7 = \{41, \cdots, 46\}$
$\mathcal{A}_1^{\text{Ne}} = \{3, 4\}$, $\mathcal{A}_2^{\text{Ne}} = \{4\}$, $\mathcal{A}_3^{\text{Ne}} = \{1, 4, 5, 7\}$, $\mathcal{A}_4^{\text{Ne}} = \{1, 2, 3, 5, 6\}$ $\mathcal{A}_5^{\text{Ne}} = \{3, 4\}$, $\mathcal{A}_6^{\text{Ne}} = \{4, 7\}$, $\mathcal{A}_7^{\text{Ne}} = \{3, 6\}$,
$\mathcal{A} = \{1, 2, 3, 4, 5, 6, 7\}$, $\mathcal{A}_d = \{1, 3, 4, 5, 6, 7\}$
$\mathcal{G}_1^{\text{Ne}} = \mathcal{G}_3 \cup \mathcal{G}_4$, $\mathcal{G}_2^{\text{Ne}} = \mathcal{G}_4$, $\mathcal{G}_3^{\text{Ne}} = \mathcal{G}_1 \cup \mathcal{G}_4 \cup \mathcal{G}_5 \cup \mathcal{G}_7$, $\mathcal{G}_7^{\text{Ne}} = \mathcal{G}_3 \cup \mathcal{G}_6$ $\mathcal{G}_4^{\text{Ne}} = \mathcal{G}_1 \cup \mathcal{G}_2 \cup \mathcal{G}_3 \cup \mathcal{G}_5 \cup \mathcal{G}_6$, $\mathcal{G}_5^{\text{Ne}} = \mathcal{G}_3 \cup \mathcal{G}_4$, $\mathcal{G}_6^{\text{Ne}} = \mathcal{G}_4 \cup \mathcal{G}_7$

5.4.2   Net tie line flow deviation : 7-area system

The net tie line flows for the 7-areas based on the flow convention (direction of arrows on tie lines) adopted in Figure 5.3, with $\mathcal{A}$ and $\mathcal{A}_d$ defined in Table 5.3, are:

$$\Delta P_1^{\text{tie}} = \Delta P_{14}^{\text{tie}} - \alpha_{31}\Delta P_{31}^{\text{tie}} \tag{5.16a}$$

$$\Delta P_2^{\text{tie}} = -\alpha_{42}\Delta P_{42}^{\text{tie}} \tag{5.16b}$$

$$\Delta P_3^{\text{tie}} = \Delta P_{37}^{\text{tie}} + \Delta P_{31}^{\text{tie}} - \alpha_{43}\Delta P_{43}^{\text{tie}} - \alpha_{53}\Delta P_{53}^{\text{tie}} \tag{5.16c}$$

$$\Delta P_4^{\text{tie}} = \Delta P_{45}^{\text{tie}} + \Delta P_{43}^{\text{tie}} - \alpha_{14}\Delta P_{14}^{\text{tie}} - \alpha_{64}\Delta P_{64}^{\text{tie}} + \Delta P_{42}^{\text{tie}} \tag{5.16d}$$

$$\Delta P_5^{\text{tie}} = \Delta P_{53}^{\text{tie}} - \alpha_{45}\Delta P_{45}^{\text{tie}} \tag{5.16e}$$

$$\Delta P_6^{\text{tie}} = \Delta P_{64}^{\text{tie}} - \alpha_{76}\Delta P_{76}^{\text{tie}} \tag{5.16f}$$

$$\Delta P_7^{\text{tie}} = \Delta P_{76}^{\text{tie}} - \alpha_{37}\Delta P_{37}^{\text{tie}} \tag{5.16g}$$

An admittance matrix $Y \in \mathbb{R}^{7\times7}$ can be constructed for the 7-area network by substituting $\Delta P_{ij}^{\text{tie}}$ of (5.5a) into (5.16a)-(5.16g), and this is presented in (A.6). For any value of Y_{ij} assumed, the admittance matrix Y of (A.6) always has a rank of 6, and therefore one of the 7 net tie line flows must be eliminated[1]. Here, ΔP_2^{tie} is eliminated (any other choice of ΔP_i^{tie} is also convenient) and expressed as:

$$
\begin{aligned}
\Delta P_2^{\text{tie}} \quad = \quad & -(\alpha_{42}\alpha_{14}\Delta P_1^{\text{tie}} + \frac{\alpha_{42}}{\alpha_{43}}\Delta P_3^{\text{tie}} + \alpha_{42}\Delta P_4^{\text{tie}} + \frac{\alpha_{42}}{\alpha_{45}}\Delta P_5^{\text{tie}} \\
& +\alpha_{42}\alpha_{64}\Delta P_6^{\text{tie}} + \alpha_{42}\alpha_{64}\alpha_{76}\Delta P_7^{\text{tie}})
\end{aligned}
\tag{5.17}
$$

---

[1]To check that Y is always singular, replace Y_{ij} in (A.6) with any value, assume equal area capacities $\alpha_{ij} = 1$ and then compute the determinant of Y. This is also true when $\alpha_{ij} \neq 1$.

Consequently, the dynamics of the net tie line deviations adopted as part of system states are:

$$\Delta \dot{P}_1^{\text{tie}} = (T_{14} + \alpha_{31}T_{31})\Delta f_1 - \alpha_{31}T_{31}\Delta f_3 - T_{14}\Delta f_4 \tag{5.18a}$$

$$\begin{aligned} \Delta \dot{P}_3^{\text{tie}} &= (T_{31} + \alpha_{53}T_{53} + \alpha_{43}T_{43} + T_{37})\Delta f_3 - T_{31}\Delta f_1 - \alpha_{43}T_{43}\Delta f_4 \\ &\quad -\alpha_{53}\Delta f_5 - T_{37}\Delta f_7 \end{aligned} \tag{5.18b}$$

$$\begin{aligned} \Delta \dot{P}_4^{\text{tie}} &= (T_{42} + T_{45} + \alpha_{14}T_{14} + T_{43} + \alpha_{64}T_{64})\Delta f_4 - \alpha_{14}T_{14}\Delta f_1 - T_{42}\Delta f_2 \\ &\quad -T_{43}\Delta f_3 - T_{45}\Delta f_5 - \alpha_{64}T_{64}\Delta f_6 \end{aligned} \tag{5.18c}$$

$$\Delta \dot{P}_5^{\text{tie}} = (T_{53} + \alpha_{45}T_{45})\Delta f_5 - T_{53}\Delta f_3 - \alpha_{45}T_{45}\Delta f_4 \tag{5.18d}$$

$$\Delta \dot{P}_6^{\text{tie}} = (T_{64} + \alpha_{76}T_{76})\Delta f_6 - T_{64}\Delta f_4 - \alpha_{76}T_{76}\Delta f_7 \tag{5.18e}$$

$$\Delta \dot{P}_7^{\text{tie}} = (T_{76} + \alpha_{37}T_{37})\Delta f_7 - \alpha_{37}T_{37}\Delta f_3 - T_{76}\Delta f_6 \tag{5.18f}$$

5.4.3 Turbine dynamics : 7-area system

The turbine dynamics of the 7-area system can be written by applying the sets $\mathcal{A}$ and $\mathcal{G}_i$ defined in Table 5.3 on (5.7):

$$\Delta \dot{P}_{1,1}^{\text{M}} = \frac{1}{T_{\text{T}_{1,1}}}\left(\Delta P_{1,1}^{\text{V}} - \Delta P_{1,1}^{\text{M}}\right), \cdots, \Delta \dot{P}_{1,5}^{\text{M}} = \frac{1}{T_{\text{T}_{1,5}}}\left(\Delta P_{1,5}^{\text{V}} - \Delta P_{1,5}^{\text{M}}\right) \tag{5.19a}$$

$$\vdots$$

$$\Delta \dot{P}_{7,30}^{\text{M}} = \frac{1}{T_{\text{T}_{7,30}}}\left(\Delta P_{7,30}^{\text{V}} - \Delta P_{7,30}^{\text{M}}\right), \cdots, \Delta \dot{P}_{7,33}^{\text{M}} = \frac{1}{T_{\text{T}_{7,33}}}\left(\Delta P_{7,33}^{\text{V}} - \Delta P_{7,33}^{\text{M}}\right) \tag{5.19b}$$

The saturation in (5.7), representing generation rate constraint, has been omitted for convenience. It will be considered in the design of model predictive controllers in Chapters 6 and 7.

5.4.4 Governor dynamics : 7-area system

The governor dynamics of the 7-area system can be written by applying the sets $\mathcal{A}$ and $\mathcal{G}_i$ defined in Table 5.3 on (5.8):

$$
\begin{aligned}
\Delta \dot{P}_{1,1}^{\mathrm{V}} &= \frac{1}{T_{\mathrm{G}_{1,1}}}\left(\gamma_{1,1}\Delta P_1^{\mathrm{C}} - \Delta P_{1,1}^{\mathrm{V}} - \frac{\Delta f_1}{R_{1,1}} + S_{1,1}\right), \cdots, \Delta \dot{P}_{1,5}^{\mathrm{V}} = \frac{1}{T_{\mathrm{G}_{1,5}}}\left(\gamma_{1,5}\Delta P_1^{\mathrm{C}} - \Delta P_{1,5}^{\mathrm{V}} \right. \\
&\qquad \left. -\frac{\Delta f_1}{R_{1,5}} + S_{1,5}\right)
\end{aligned}
\tag{5.20a}
$$

$$
\vdots
$$

$$
\begin{aligned}
\Delta \dot{P}_{7,30}^{\mathrm{V}} &\quad \frac{1}{T_{\mathrm{G}_{7,30}}}\left(\gamma_{7,30}\Delta P_7^{\mathrm{C}} - \Delta P_{7,30}^{\mathrm{V}} - \frac{\Delta f_7}{R_{7,30}} + S_{7,30}\right), \cdots, \Delta \dot{P}_{7,33}^{\mathrm{V}} = \frac{1}{T_{\mathrm{G}_{7,33}}}\left(\gamma_{7,33}\Delta P_7^{\mathrm{C}} \right. \\
&\qquad \left. -\Delta P_{7,33}^{\mathrm{V}} - \frac{\Delta f_7}{R_{7,33}} + S_{7,33}\right)
\end{aligned}
\tag{5.20b}
$$

5.4.5 Contracted signal : 7-area system

For the 7-area network, the contracted signal $S_{i,\mathrm{k}}$ of each the 33 GenCos is derived using (5.10) and the defined sets $\mathcal{A}$, $\mathcal{G}_i$, $\mathcal{D}_i$ and $\mathcal{A}_i^{\mathrm{Ne}}$, and they are substituted in the governor dynamics of Section 5.4.4. For GenCo 1 in area 1, the contracted signal $S_{1,1}$ is

$$
\begin{aligned}
S_{1,1} &= \sum_{l \in \mathcal{D}_1} \eta_{1,l}\Delta P_{1,l}^{\mathrm{L}} + \sum_{j \in \mathcal{A}_1^{\mathrm{Ne}}}\left\{\sum_{l \in \mathcal{D}_j} \eta_{1,l}\alpha_{j1}\Delta P_{j,l}^{\mathrm{L}}\right\} \\
&= \left(\eta_{1,1}\Delta P_{1,1}^{\mathrm{L}} + \cdots + \eta_{1,7}\Delta P_{1,7}^{\mathrm{L}}\right) + \sum_{l \in \mathcal{D}_3} \eta_{1,l}\alpha_{31}\Delta P_{3,l}^{\mathrm{L}} + \sum_{l \in \mathcal{D}_4} \eta_{1,l}\alpha_{41}\Delta P_{4,l}^{\mathrm{L}} \\
&= \eta_{1,\mathcal{D}_1}\boldsymbol{\Delta P}_1^{\mathrm{L}} + \alpha_{31}\eta_{1,\mathcal{D}_3}\boldsymbol{\Delta P}_3^{\mathrm{L}} + \frac{1}{\alpha_{14}}\eta_{1,\mathcal{D}_4}\boldsymbol{\Delta P}_4^{\mathrm{L}}
\end{aligned}
\tag{5.21}
$$

$$
\Delta \boldsymbol{P}_1^{\mathrm{L}} = \begin{bmatrix} \Delta P_{1,1}^{\mathrm{L}} \\ \vdots \\ \Delta P_{1,7}^{\mathrm{L}} \end{bmatrix}, \Delta \boldsymbol{P}_3^{\mathrm{L}} = \begin{bmatrix} \Delta P_{3,13}^{\mathrm{L}} \\ \vdots \\ \Delta P_{3,19}^{\mathrm{L}} \end{bmatrix}, \Delta \boldsymbol{P}_4^{\mathrm{L}} = \begin{bmatrix} \Delta P_{4,20}^{\mathrm{L}} \\ \vdots \\ \Delta P_{4,27}^{\mathrm{L}} \end{bmatrix}
$$

$$
\eta_{1,\mathcal{D}_1} = \begin{bmatrix} \eta_{1,1} \\ \vdots \\ \eta_{1,7} \end{bmatrix}; \eta_{1,\mathcal{D}_3} = \begin{bmatrix} \eta_{1,13} \\ \vdots \\ \eta_{1,19} \end{bmatrix}; \eta_{1,\mathcal{D}_4} = \begin{bmatrix} \eta_{1,20} \\ \vdots \\ \eta_{1,27} \end{bmatrix}
$$

where $\Delta \boldsymbol{P}_i^{\mathrm{L}}$ and $\eta_{\mathrm{k},\mathcal{D}_i}$ are a column vector of contracted load changes of DisCos in the ith CA and row vector of the contract particpation factors of DisCos in the ith CA having contract with GenCo k respectively. A more compact form of (5.10) can be written:

$$S_{i,\text{k}} = \eta_{\text{k},\mathcal{D}_i}\boldsymbol{\Delta P}^{\text{L}}_i + \sum_{j\in\mathcal{A}^{\text{Ne}}_i} \eta_{\text{k},\mathcal{D}_j}\alpha_{ji}\boldsymbol{\Delta P}^{\text{L}}_j \qquad (5.22)$$

For example, for GenCo 33 in area 7, the contracted signal $S_{7,33}$ using the compact from (5.22) is:

$$S_{7,33} = \eta_{33,\mathcal{D}_7}\boldsymbol{\Delta P}^{\text{L}}_7 + \eta_{33,\mathcal{D}_3}\alpha_{37}\boldsymbol{\Delta P}^{\text{L}}_3 + \eta_{33,\mathcal{D}_6}\alpha_{67}\boldsymbol{\Delta P}^{\text{L}}_6 \qquad (5.23)$$

$$\boldsymbol{\Delta P}^{\text{L}}_6 = \begin{bmatrix} \Delta P^{\text{L}}_{6,33} \\ \vdots \\ \Delta P^{\text{L}}_{6,40} \end{bmatrix} ; \boldsymbol{\Delta P}^{\text{L}}_7 = \begin{bmatrix} \Delta P^{\text{L}}_{7,41} \\ \vdots \\ \Delta P^{\text{L}}_{7,46} \end{bmatrix}$$

$$\eta_{33,\mathcal{D}_7} = \begin{bmatrix} \eta_{33,41} \\ \vdots \\ \eta_{33,46} \end{bmatrix} ; \eta_{33,\mathcal{D}_3} = \begin{bmatrix} \eta_{33,13} \\ \vdots \\ \eta_{33,19} \end{bmatrix} ; \eta_{33,\mathcal{D}_6} = \begin{bmatrix} \eta_{33,33} \\ \vdots \\ \eta_{33,40} \end{bmatrix}$$

Note that (5.23) can also be obtained using (5.10). The $S_{i,\text{k}}$ for the other GenCos can be derived using (5.23) and the derivations are omitted.

5.4.6 Scheduled net incremental tie line flow : 7-area system

The scheduled net incremental tie line flows for the 7-area system can be derived using (5.13) and the following defined sets $\mathcal{A}$, $\mathcal{A}^{\text{Ne}}_i$, $\mathcal{G}_i$, $\mathcal{G}^{\text{Ne}}_i$ and $\mathcal{D}_i$ in Table 5.3:

$$
\begin{aligned}
\Delta P_1^{\text{tie,sh}} &= \sum_{j \in \mathcal{A}_1^{\text{Ne}}} \left\{ \sum_{g \in \mathcal{G}_1} \left\{ \sum_{l \in \mathcal{D}_j} \eta_{g,l} \alpha_{j1} \Delta P_{j,l}^{\text{L}} \right\} \right\} - \sum_{g \in \mathcal{G}_1^{\text{Ne}}} \left\{ \sum_{l \in \mathcal{D}_1} \eta_{g,l} \Delta P_{1,l}^{\text{L}} \right\} \\
&= \sum_{g \in \mathcal{G}_1} \left\{ \sum_{l \in \mathcal{D}_3} \eta_{g,l} \alpha_{31} \Delta P_{3,l}^{\text{L}} \right\} + \sum_{g \in \mathcal{G}_1} \left\{ \sum_{l \in \mathcal{D}_4} \eta_{g,l} \alpha_{41} \Delta P_{4,l}^{\text{L}} \right\} - \sum_{g \in \mathcal{G}_1^{\text{Ne}}} \left\{ \sum_{l \in \mathcal{D}_1} \eta_{g,l} \Delta P_{1,l}^{\text{L}} \right\} \\
&= \sum_{l \in \mathcal{D}_3} \eta_{1,l} \alpha_{31} \Delta P_{3,l}^{\text{L}} + \sum_{l \in \mathcal{D}_3} \eta_{2,l} \alpha_{31} \Delta P_{3,l}^{\text{L}} + \sum_{l \in \mathcal{D}_3} \eta_{3,l} \alpha_{31} \Delta P_{3,l}^{\text{L}} + \sum_{l \in \mathcal{D}_3} \eta_{4,l} \alpha_{31} \Delta P_{3,l}^{\text{L}} \\
&\quad + \sum_{l \in \mathcal{D}_3} \eta_{5,l} \alpha_{31} \Delta P_{3,l}^{\text{L}} + \sum_{l \in \mathcal{D}_4} \eta_{1,l} \alpha_{41} \Delta P_{4,l}^{\text{L}} + \sum_{l \in \mathcal{D}_4} \eta_{2,l} \alpha_{41} \Delta P_{4,l}^{\text{L}} + \sum_{l \in \mathcal{D}_4} \eta_{3,l} \alpha_{41} \Delta P_{4,l}^{\text{L}} \\
&\quad + \sum_{l \in \mathcal{D}_4} \eta_{4,l} \alpha_{41} \Delta P_{4,l}^{\text{L}} + \sum_{l \in \mathcal{D}_4} \eta_{5,l} \alpha_{41} \Delta P_{4,l}^{\text{L}} - \sum_{l \in \mathcal{D}_1} \eta_{10,l} \Delta P_{1,l}^{\text{L}} - \sum_{l \in \mathcal{D}_1} \eta_{11,l} \Delta P_{1,l}^{\text{L}} \\
&\quad - \sum_{l \in \mathcal{D}_1} \eta_{12,l} \Delta P_{1,l}^{\text{L}} - \sum_{l \in \mathcal{D}_1} \eta_{13,l} \Delta P_{1,l}^{\text{L}} - \sum_{l \in \mathcal{D}_1} \eta_{14,l} \Delta P_{1,l}^{\text{L}} - \sum_{l \in \mathcal{D}_1} \eta_{15,l} \Delta P_{1,l}^{\text{L}} \\
&\quad - \sum_{l \in \mathcal{D}_1} \eta_{16,l} \Delta P_{1,l}^{\text{L}} - \sum_{l \in \mathcal{D}_1} \eta_{17,l} \Delta P_{1,l}^{\text{L}} - \sum_{l \in \mathcal{D}_1} \eta_{18,l} \Delta P_{1,l}^{\text{L}} - \sum_{l \in \mathcal{D}_1} \eta_{19,l} \Delta P_{1,l}^{\text{L}} \\
&\quad - \sum_{l \in \mathcal{D}_1} \eta_{20,l} \Delta P_{1,l}^{\text{L}} \\
&= \alpha_{31} \Big(\eta_{1,\mathcal{D}_3} + \eta_{2,\mathcal{D}_3} + \eta_{3,\mathcal{D}_3} + \eta_{4,\mathcal{D}_3} + \eta_{5,\mathcal{D}_3} \Big) \boldsymbol{\Delta P}_3^{\text{L}} + \frac{1}{\alpha_{14}} \Big(\eta_{1,\mathcal{D}_4} + \eta_{2,\mathcal{D}_4} + \eta_{3,\mathcal{D}_4} \\
&\quad + \eta_{4,\mathcal{D}_4} + \eta_{5,\mathcal{D}_4} \Big) \boldsymbol{\Delta P}_4^{\text{L}} - \Big(\eta_{10,\mathcal{D}_1} + \eta_{11,\mathcal{D}_1} + \eta_{12,\mathcal{D}_1} + \eta_{13,\mathcal{D}_1} + \eta_{14,\mathcal{D}_1} + \eta_{15,\mathcal{D}_1} \\
&\quad + \eta_{16,\mathcal{D}_1} + \eta_{17,\mathcal{D}_1} + \eta_{18,\mathcal{D}_1} + \eta_{19,\mathcal{D}_1} + \eta_{20,\mathcal{D}_1} \Big) \boldsymbol{\Delta P}_1^{\text{L}} \quad (5.24)
\end{aligned}
$$

A more compact form of (5.13) can be written:

$$
\Delta P_i^{\text{tie,sch}} = \sum_{j \in \mathcal{A}_i^{\text{Ne}}} \left\{ \sum_{r \in \mathcal{G}_i} \eta_{r,\mathcal{D}_j} \alpha_{ji} \boldsymbol{\Delta P}_j^{\text{L}} \right\} - \sum_{r \in \mathcal{G}_i^{\text{Ne}}} \eta_{r,\mathcal{D}_i} \boldsymbol{\Delta P}_i^{\text{L}} \quad (5.25)
$$

$$
\begin{aligned}
\Delta P_7^{\text{tie,sh}} &= \sum_{r \in \mathcal{G}_7} \left\{ \eta_{r,\mathcal{D}_3} \alpha_{37} \boldsymbol{\Delta P}_3^{\text{L}} + \eta_{r,\mathcal{D}_6} \alpha_{67} \boldsymbol{\Delta P}_6^{\text{L}} \right\} - \left\{ \sum_{r \in \mathcal{G}_3} \eta_{r,\mathcal{D}_7} + \sum_{r \in \mathcal{G}_6} \eta_{r,\mathcal{D}_7} \right\} \boldsymbol{\Delta P}_7^{\text{L}} \\
&= \alpha_{37} \Big(\eta_{30,\mathcal{D}_3} + \eta_{31,\mathcal{D}_3} + \eta_{32,\mathcal{D}_3} + \eta_{33,\mathcal{D}_3} \Big) \boldsymbol{\Delta P}_3^{\text{L}} + \frac{1}{\alpha_{76}} \Big(\eta_{30,\mathcal{D}_6} + \eta_{31,\mathcal{D}_6} + \eta_{32,\mathcal{D}_6} \\
&\quad + \eta_{33,\mathcal{D}_6} \Big) \boldsymbol{\Delta P}_6^{\text{L}} - \Big(\eta_{10,\mathcal{D}_7} + \eta_{11,\mathcal{D}_7} + \eta_{12,\mathcal{D}_7} + \eta_{13,\mathcal{D}_7} + \eta_{14,\mathcal{D}_7} + \eta_{25,\mathcal{D}_7} + \eta_{26,\mathcal{D}_7} \\
&\quad + \eta_{27,\mathcal{D}_7} + \eta_{28,\mathcal{D}_7} + \eta_{29,\mathcal{D}_7} \Big) \boldsymbol{\Delta P}_7^{\text{L}} \quad (5.26)
\end{aligned}
$$

Similar to how $\Delta P_1^{\text{tie,sh}}$ and $\Delta P_7^{\text{tie,sh}}$ are derived, $\Delta P_2^{\text{tie,sh}}$, $\Delta P_3^{\text{tie,sh}}$, $\Delta P_4^{\text{tie,sh}}$, $\Delta P_5^{\text{tie,sh}}$ and $\Delta P_6^{\text{tie,sh}}$ can be derived using either (5.13) or (5.25); the details are omitted.

5.4.7 The Area Control Error : 7-area system

The area control error (5.14) can be written for each area, given the set $\mathcal{A}$ and the expressions $\Delta P_i^{\text{tie,sh}}$:

$$
\begin{align}
\text{ACE}_1 &= \beta_1 \Delta f_1 + \Delta P_1^{\text{tie}} - \Delta P_1^{\text{tie,sh}} \tag{5.27} \\
\text{ACE}_2 &\quad \beta_2 \Delta f_2 + \Delta P_2^{\text{tie}} - \Delta P_2^{\text{tie,sh}} \tag{5.28} \\
&\qquad \vdots \\
\text{ACE}_7 &= \beta_7 \Delta f_7 + \Delta P_7^{\text{tie}} - \Delta P_7^{\text{tie,sh}} \tag{5.29}
\end{align}
$$

Note that ΔP_2^{tie} in (5.28) is replaced by (5.17) since ΔP_2^{tie} is eliminated in the development of the 7-area deregulated model.

5.4.8 State-space representation

Collecting the expressions in Sections 5.4.1 - 5.4.7 (as well as the expressions omitted), a continuous time (CT) state space representation of the 7-area system can be expressed in a compact form as:

$$
\dot{x} = A^c x + B^c u + B^{dc} d + B^{bc} b; \quad y = C^c x + D^c d \tag{5.30}
$$

where

$$
x = \begin{bmatrix} x_1 \\ \Delta P_1^{\text{tie}} \\ \hline x_2 \\ \hline x_3 \\ \Delta P_3^{\text{tie}} \\ \hline \vdots \\ \hline x_7 \\ \Delta P_7^{\text{tie}} \end{bmatrix}
; d = \begin{bmatrix} \boldsymbol{\Delta P_1^{\text{L}}} \\ \boldsymbol{\Delta P_2^{\text{L}}} \\ \hline \vdots \\ \boldsymbol{\Delta P_7^{\text{L}}} \end{bmatrix}
; u = \begin{bmatrix} \Delta P_1^{\text{C}} \\ \Delta P_2^{\text{C}} \\ \hline \vdots \\ \Delta P_7^{\text{C}} \end{bmatrix}
; b = \begin{bmatrix} \Delta P_1^{\text{U}} \\ \Delta P_2^{\text{U}} \\ \hline \vdots \\ \Delta P_7^{\text{U}} \end{bmatrix}
; y = \begin{bmatrix} \text{ACE}_1 \\ \text{ACE}_2 \\ \hline \vdots \\ \text{ACE}_7 \end{bmatrix}
$$

$$
x_1 = \begin{bmatrix} \Delta f_1 \\ \Delta P_{1,1}^{\text{M}} \\ \Delta P_{1,1}^{\text{V}} \\ \vdots \\ \Delta P_{1,5}^{\text{M}} \\ \Delta P_{1,5}^{\text{V}} \end{bmatrix}
; x_2 = \begin{bmatrix} \Delta f_2 \\ \Delta P_{2,6}^{\text{M}} \\ \Delta P_{2,6}^{\text{V}} \\ \vdots \\ \Delta P_{2,9}^{\text{M}} \\ \Delta P_{2,9}^{\text{V}} \end{bmatrix}
; \cdots , x_7 = \begin{bmatrix} \Delta f_7 \\ \Delta P_{7,30}^{\text{M}} \\ \Delta P_{7,30}^{\text{V}} \\ \vdots \\ \Delta P_{7,33}^{\text{M}} \\ \Delta P_{7,33}^{\text{V}} \end{bmatrix}
$$

Table 5.4: Contracted load changes $\Delta P_{i,j}^{\mathrm{L}}$ of each DisCo

$\Delta P_{1,1}^{\mathrm{L}}$	$\Delta P_{1,2}^{\mathrm{L}}$	$\Delta P_{1,3}^{\mathrm{L}}$	$\Delta P_{1,4}^{\mathrm{L}}$	$\Delta P_{1,5}^{\mathrm{L}}$	$\Delta P_{1,6}^{\mathrm{L}}$	$\Delta P_{1,7}^{\mathrm{L}}$
0	0	0	0.04	0	0.04	0

$\Delta P_{2,8}^{\mathrm{L}}$	$\Delta P_{2,9}^{\mathrm{L}}$	$\Delta P_{2,10}^{\mathrm{L}}$	$\Delta P_{2,11}^{\mathrm{L}}$	$\Delta P_{2,12}^{\mathrm{L}}$
0.04	0	0.02	0.02	0.02

$\Delta P_{3,13}^{\mathrm{L}}$	$\Delta P_{3,14}^{\mathrm{L}}$	$\Delta P_{3,15}^{\mathrm{L}}$	$\Delta P_{3,16}^{\mathrm{L}}$	$\Delta P_{3,17}^{\mathrm{L}}$	$\Delta P_{3,18}^{\mathrm{L}}$	$\Delta P_{3,19}^{\mathrm{L}}$
0.04	0.04	0.02	0.02	0.02	0	0.04

$\Delta P_{4,20}^{\mathrm{L}}$	$\Delta P_{4,21}^{\mathrm{L}}$	$\Delta P_{4,22}^{\mathrm{L}}$	$\Delta P_{4,23}^{\mathrm{L}}$	$\Delta P_{4,24}^{\mathrm{L}}$	$\Delta P_{4,25}^{\mathrm{L}}$	$\Delta P_{4,26}^{\mathrm{L}}$	$\Delta P_{4,27}^{\mathrm{L}}$
0.02	0	0.02	0	0	0.02	0	0.02

$\Delta P_{5,28}^{\mathrm{L}}$	$\Delta P_{5,29}^{\mathrm{L}}$	$\Delta P_{5,30}^{\mathrm{L}}$	$\Delta P_{5,31}^{\mathrm{L}}$	$\Delta P_{5,32}^{\mathrm{L}}$
0.02	0.04	0	0.02	0

$\Delta P_{6,33}^{\mathrm{L}}$	$\Delta P_{6,34}^{\mathrm{L}}$	$\Delta P_{6,35}^{\mathrm{L}}$	$\Delta P_{6,36}^{\mathrm{L}}$	$\Delta P_{6,37}^{\mathrm{L}}$	$\Delta P_{6,38}^{\mathrm{L}}$	$\Delta P_{6,39}^{\mathrm{L}}$	$\Delta P_{6,40}^{\mathrm{L}}$
0.04	0	0.04	0.02	0	0.04	0.02	0

$\Delta P_{7,41}^{\mathrm{L}}$	$\Delta P_{7,42}^{\mathrm{L}}$	$\Delta P_{7,43}^{\mathrm{L}}$	$\Delta P_{7,44}^{\mathrm{L}}$	$\Delta P_{7,45}^{\mathrm{L}}$	$\Delta P_{7,46}^{\mathrm{L}}$
0	0	0	0.02	0	0.02

$$\Delta \boldsymbol{P}_1^{\mathrm{L}} = \begin{bmatrix} \Delta P_{1,1}^{\mathrm{L}} \\ \Delta P_{1,2}^{\mathrm{L}} \\ \vdots \\ \Delta P_{1,7}^{\mathrm{L}} \end{bmatrix}, \boldsymbol{\Delta P}_2^{\mathrm{L}} = \begin{bmatrix} \Delta P_{2,8}^{\mathrm{L}} \\ \Delta P_{2,9}^{\mathrm{L}} \\ \vdots \\ \Delta P_{2,12}^{\mathrm{L}} \end{bmatrix}, \cdots, \boldsymbol{\Delta P}_7^{\mathrm{L}} = \begin{bmatrix} \Delta P_{7,41}^{\mathrm{L}} \\ \Delta P_{7,42}^{\mathrm{L}} \\ \vdots \\ \Delta P_{7,46}^{\mathrm{L}} \end{bmatrix}$$

and $\mathrm{A^c} \in \mathbb{R}^{79 \times 79}$, $\mathrm{B^c} \in \mathbb{R}^{79 \times 7}$, $\mathrm{B^{dc}} \in \mathbb{R}^{79 \times 46}$, $\mathrm{B^{bc}} \in \mathbb{R}^{79 \times 7}$, $\mathrm{C^c} \in \mathbb{R}^{7 \times 79}$, $\mathrm{D^c} \in \mathbb{R}^{7 \times 46}$. Note that the state-space form of (5.30) is exactly the same as the one stated in Chapter 4; however the definition of the various system matrices and the vector of states, input and load changes are different.

In summary, a state space model in CT has been developed for a 7-area deregulated power system, and this benchmark system is needed to demonstrate significance and effectiveness of the proposed generalised formulation. The test system is a modification of the 7-machine CIGRE network, where the network was partitioned into 7-areas, and each area was populated with a number of GenCos and DisCos.

5.5 Simulation and discussion

In this section, three case studies are presented to establish the significance and effectiveness of the proposed generalised modelling framework for deregulated LFC studies. As stated in Section 5.2, the difference in capacity ratings of the control areas can only create an imbalance
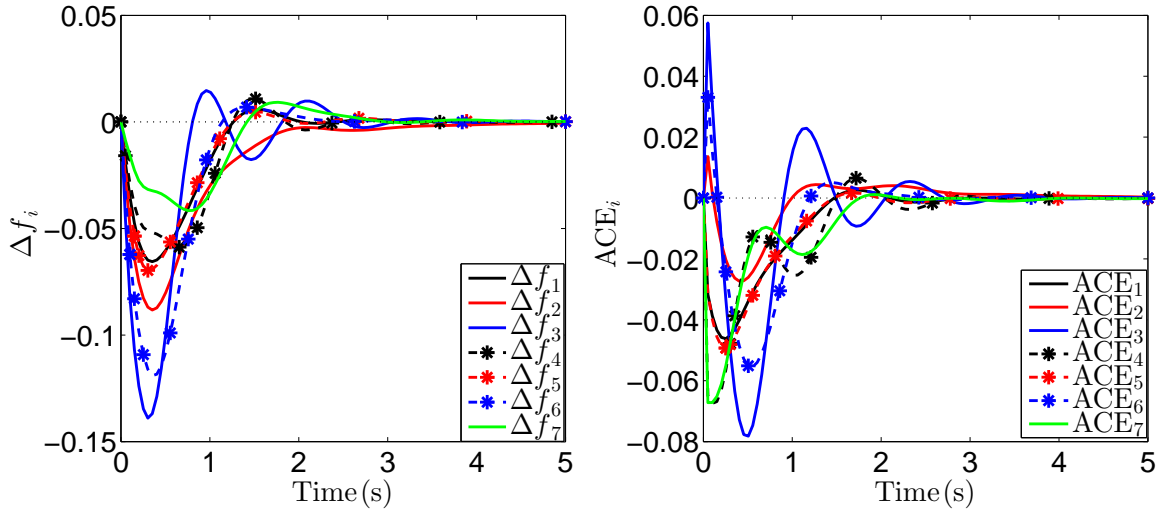
Figure 5.4: Frequency deviations (left) and area control error (right) in each CA (case-1).

when inter-area bilateral power transaction exists. Thus, in this chapter, it is assumed that LFC is procured via bilateral LM transactions only, where inter-area transaction is possible and no uncontracted load variations.

Moreover, the key message in this chapter is not to argue the superiority of a control design technique for LFC, but to show that the generalised framework proposed can be utilised for LFC studies. Thus, an unconstrained centralised model predictive control is used to coordinate the transient behaviour of the 7-area benchmark model and its details are omitted. The parameters of the 7-area system are shown in Tables A.1, A.2 and A.3. The DPM $\in \mathbb{R}^{33 \times 46}$ considered is given in (A.7). Also, the CT state space representation (5.30) is discretised with a sampling time $t_s = 0.05$ s to obtain a discrete time equivalent.

5.5.1   Case-1: Equal rated capacities

This section presents the scenario where interconnected control areas are assumed to have equal rated capacities, that is, in Section 5.4.2 the net tie line deviations, Section 5.4.5 contracted signal to each GenCo, Section 5.4.6 scheduled net incremental tie line flows, $\alpha_{ij} = 1$. This is the common assumption in the LFC literature and this section is to show that the proposed generalised formulation can accommodate such an assumption. Also, uncontracted load variations are not considered, that is, $\Delta P_i^{\mathrm{U}} = 0$.

The assumed contracted load change of each DisCo is presented in Table 5.4. Figure 5.4 shows the frequency deviations Δf_i and area control error ACE_i in each area. As expected, both Δf_i and ACE_i converged to zero since it is assumed that load changes in the network are completely supplied via LM contracts and no uncontracted load variations. The net tie line flow deviation in each area $\Delta P_i^{\mathrm{tie}}$ is shown in Figure 5.5, where the black dotted lines are the

scheduled net incremental tie line flows $\Delta P_i^{\text{tie,sh}}$ calculated using the expressions in Section 5.4.6; ΔP_5^{tie} is skipped. From Figure 5.5, it can be seen that each ΔP_i^{tie} tracks the scheduled (contracted) value. Note that a negative ΔP_i^{tie} indicates that an area is importing power. Note that although ΔP_2^{tie} was eliminated from system states, it automatically tracked its scheduled value.

Also, Figure 5.6 shows the total change in power output ΔP_i^{M} in each area, with areas 2, 4 and 6 omitted; the dotted lines in the figure are the total desired change in power output in each area. The total change in power output in each area was obtained by summing the individual changes in power output $\Delta P_{i,\text{k}}^{\text{M}}$ of the GenCos in each area using the first expression in (5.3), while the total desired output change is calculated using (5.11). It can be seen from Figure 5.6
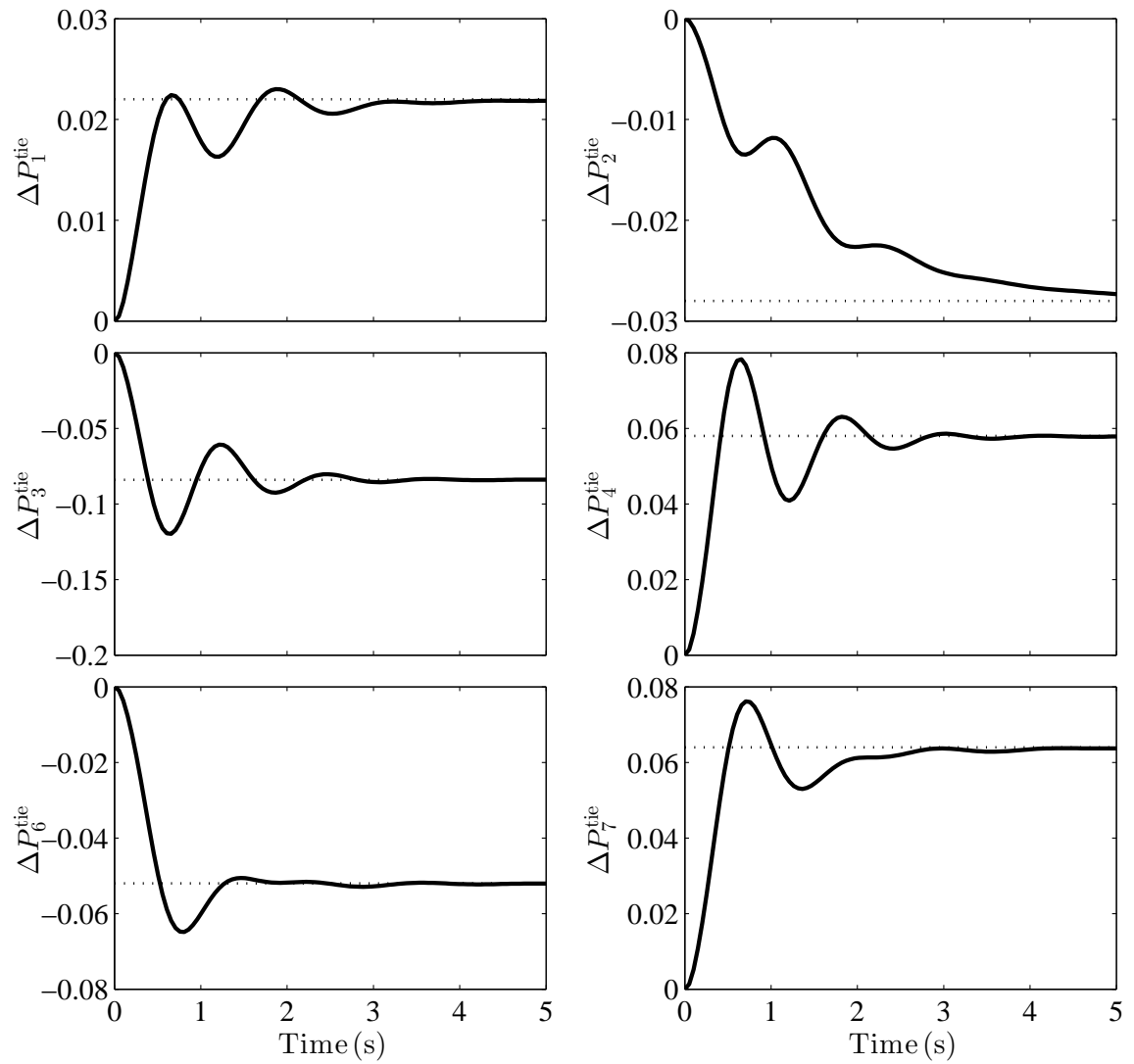
Figure 5.5: The net tie line deviation in each CA (case-1). The back dotted lines indicate the scheduled (contracted) net incremental tie line flows $\Delta P_i^{\text{tie,sh}}$ of each area. ΔP_5^{tie} is omitted as it behaviour is similar to the others.
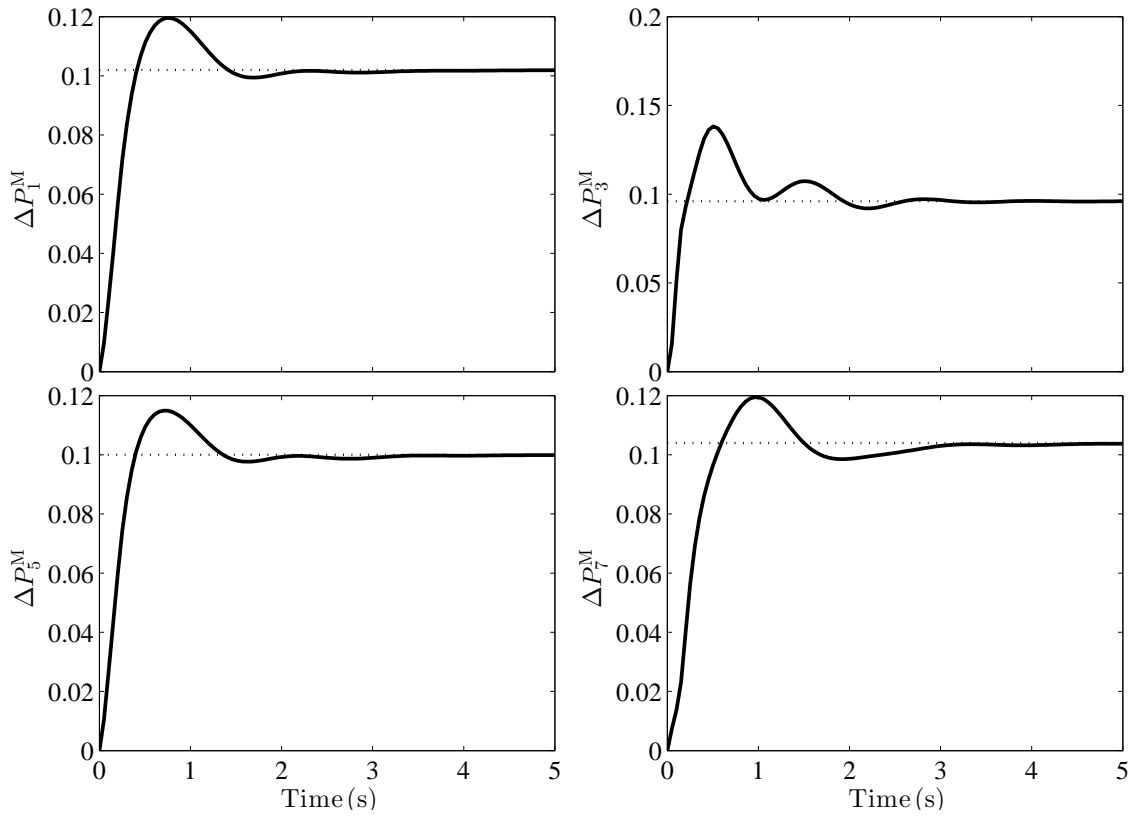
Figure 5.6: Total change in power output ΔP_i^{M} in each CA (case-1). The black dotted lines indicate the desired value in each CA. ΔP_i^{M} in area 2, 4 and 6 are not shown as their behaviour is similar to the ones presented.
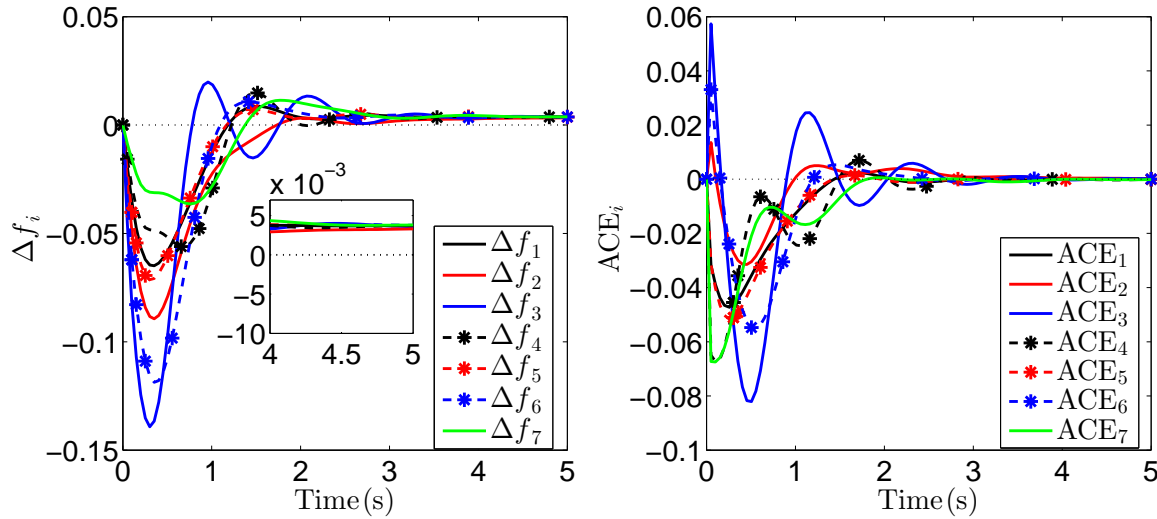
Figure 5.7: Frequency deviations (left) and area control error (right) in each CA (case-2).

that the total power output of each area tracks its desired values, and this is the reason why Δf_i and ACE_i converged to zero and $\Delta P_i^{\mathrm{tie}}$ settles at its scheduled value.
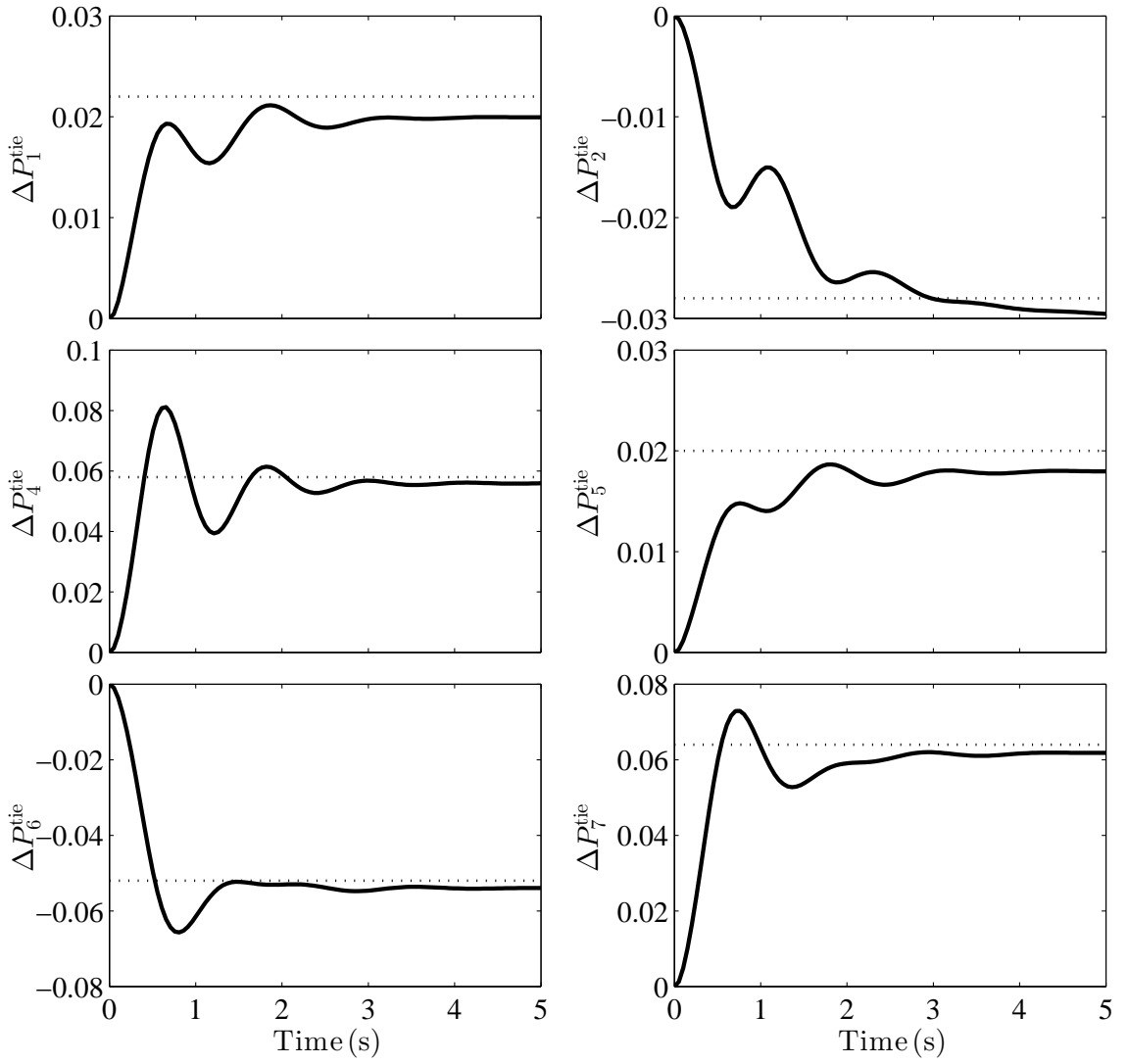
Figure 5.8: The net tie line deviation in each CA (case-2). The back dotted lines indicate the scheduled (contracted) net incremental tie line flows $\Delta P_i^{\text{tie,sh}}$ of each area assuming equal area capacities as in case-1. ΔP_3^{tie} is omitted as it behaviour is similar to the others.

5.5.2 Case-2: Unequal rated capacities but neglected in the contract (or new) information

This section considers the scenario where each control area has different rated capacities, that is, $\alpha_{ij} \neq 1$ in the net tie line expressions of Section 5.4.2. The following area rated capacities are assumed for each area: $\{P_{r_1}, P_{r_2}, \cdots, P_{r_7}\} = \{5500, 4800, 5000, 6200, 4500, 5800, 5600\}$. Also, the $\Delta P_i^{\text{U}} = 0$ scenario is considered. To demonstrate the effect of not incorporating the difference in rated capacities of the CAs in the contract information, the different α_{ij} in Section 5.4.5 contracted signals and Section 5.4.6 contracted/scheduled net incremental flows are set to unity.
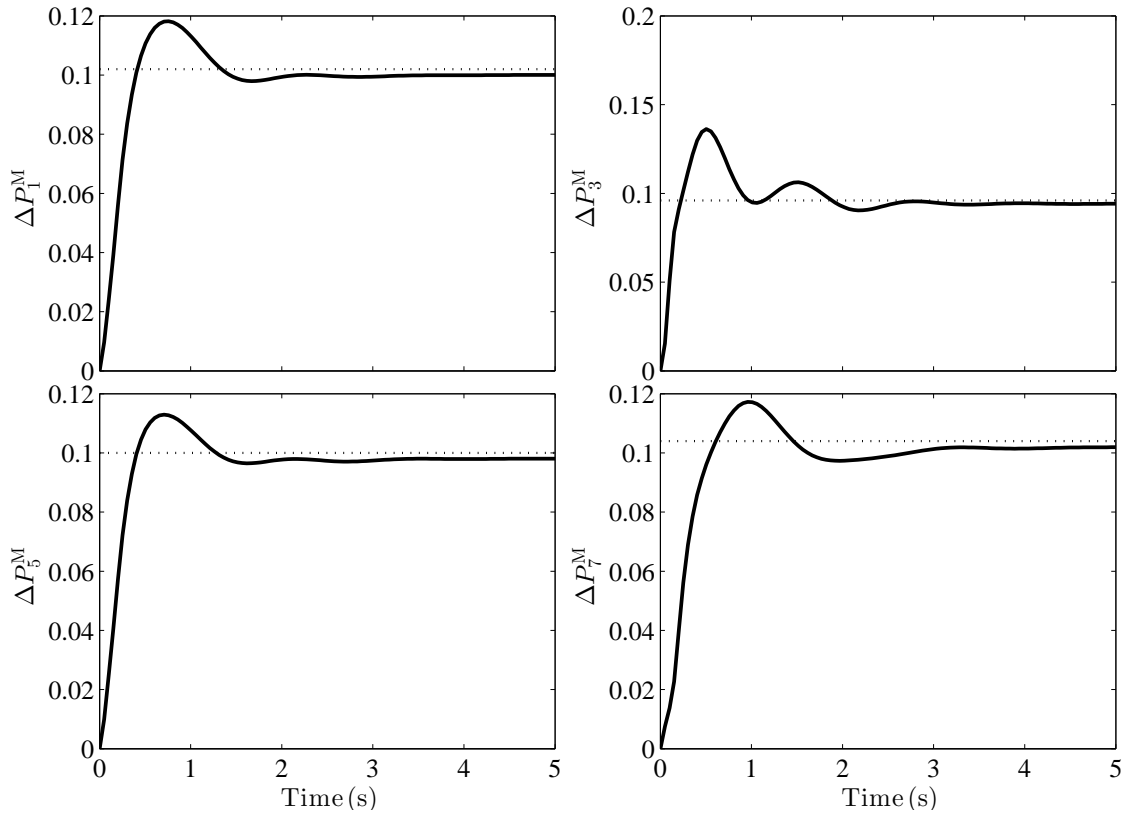
Figure 5.9: Total change in power output ΔP_i^{M} in each CA (case-2). The black dotted lines indicate the desired value in each CA assuming equal area capacities as in case-1. ΔP_i^{M} in area 2, 4 and 6 are not shown as their behaviour is similar to the ones presented.
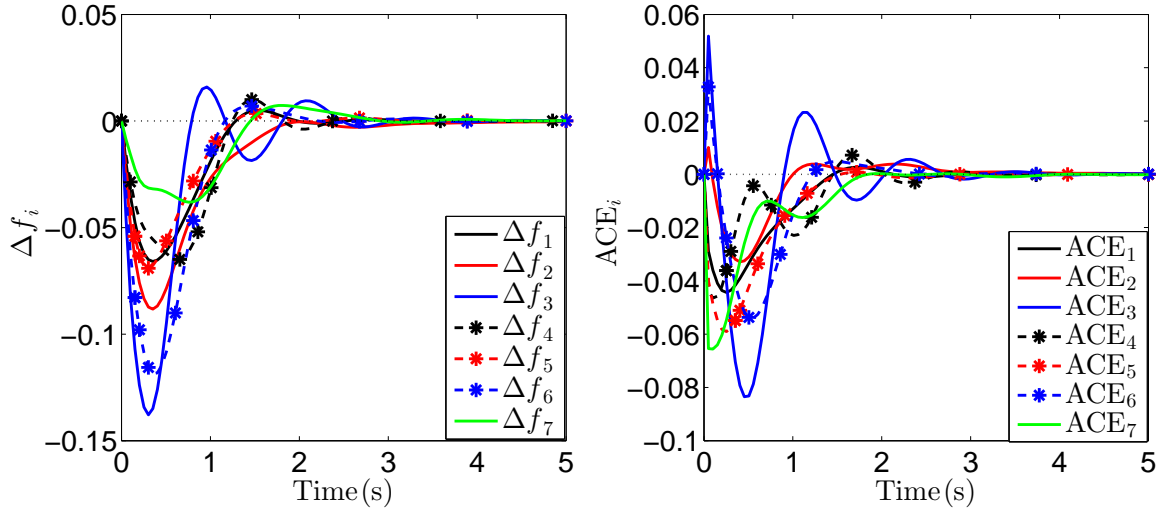
Figure 5.10: Frequency deviations (left) and area control error (right) in each CA (case-3)

Assume the same contracted load changes of each DisCo as in case-1. Figure 5.7 shows frequency deviations Δf_i (left) and area control error ACE_i (right) in each area. The ACE of each area converged to zero, similar to case-1. However, the frequency deviation of each area experienced some offset. The fact that each ACE converged to zero could be misleading as an
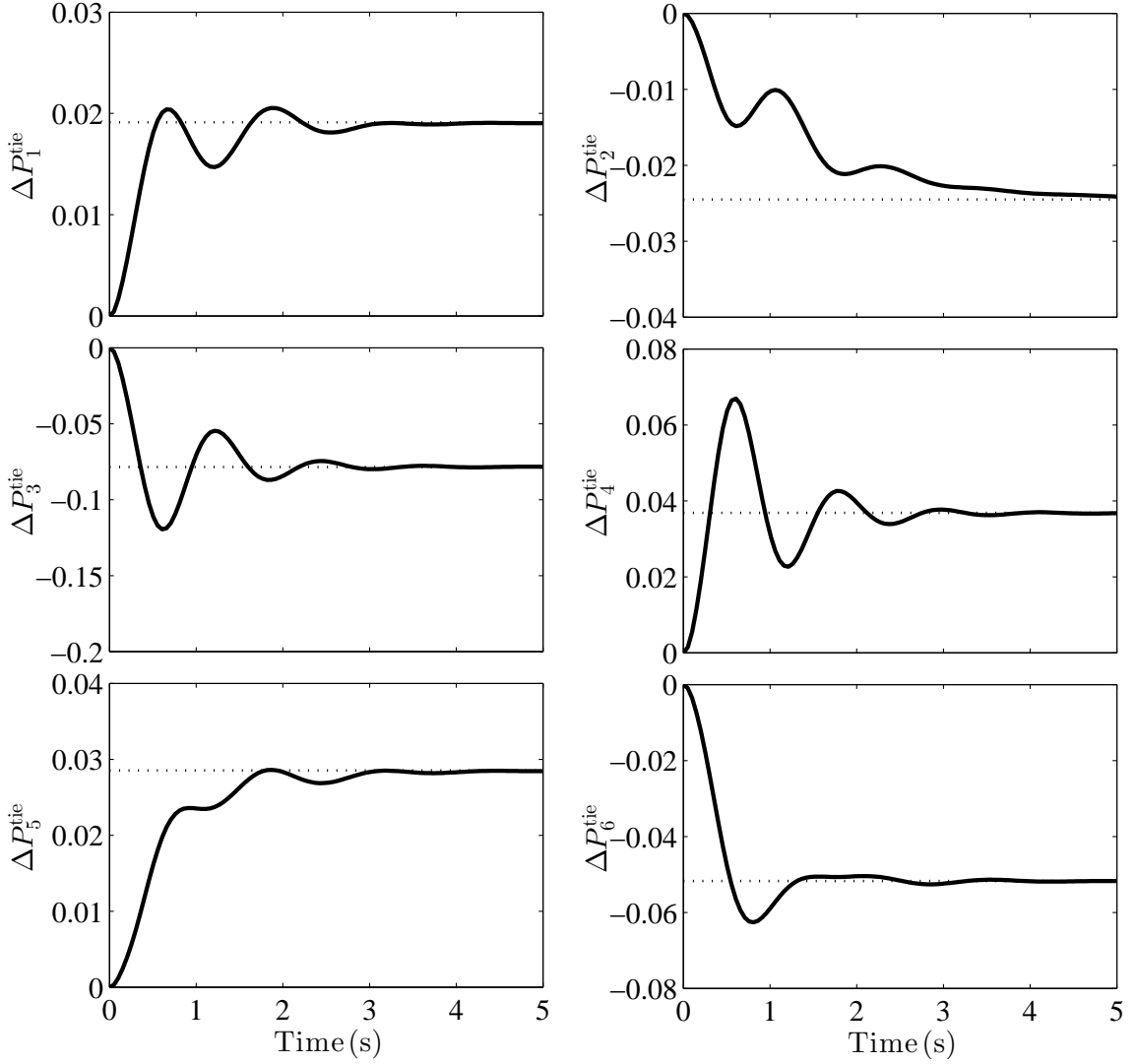
Figure 5.11: The net tie line deviation in each CA (case-3). The back dotted lines indicate the scheduled (contracted) net incremental tie line flows $\Delta P_i^{\text{tie,sh}}$ of each area assuming unequal area capacities. ΔP_7^{tie} is omitted as it behaviour is similar to the others.

operator monitoring the ACE of its local area may assume that the LFC objective has been met. Nonetheless, according to (5.14), zeroing the ACE of each area can be accomplished in two ways [2]: (i) It can be achieved when $\Delta P_i^{\text{tie}} = \Delta P_i^{\text{tie,sch}}$ and $\Delta f_i = 0$. This is the situation in case-1 and it represents a more appropriate outcome. (ii) It can also be achieved when $\beta_i \Delta f_i = \Delta P_i^{\text{tie,sch}} - \Delta P_i^{\text{tie}}$, that is, when a compromise exists between the frequency error and tie line error. This is the situation in case-2.

Furthermore, the net tie line flow deviation in each area ΔP_i^{tie} (ΔP_3^{tie} is omitted) and total change in power output in each area ΔP_i^{M} (areas 2, 4 and 6 omitted) are shown in Figures 5.8 and 5.9 respectively. The unconstrained MPC, whose objective is to zero each ACE, regulates the total generation change in each area, see Figure 5.9, as well as the net tie line flow deviation in each area, see Figure 5.8, to achieve a $\beta_i \Delta f_i = \Delta P_i^{\text{tie,sch}} - \Delta P_i^{\text{tie}}$, and thus eliminate the
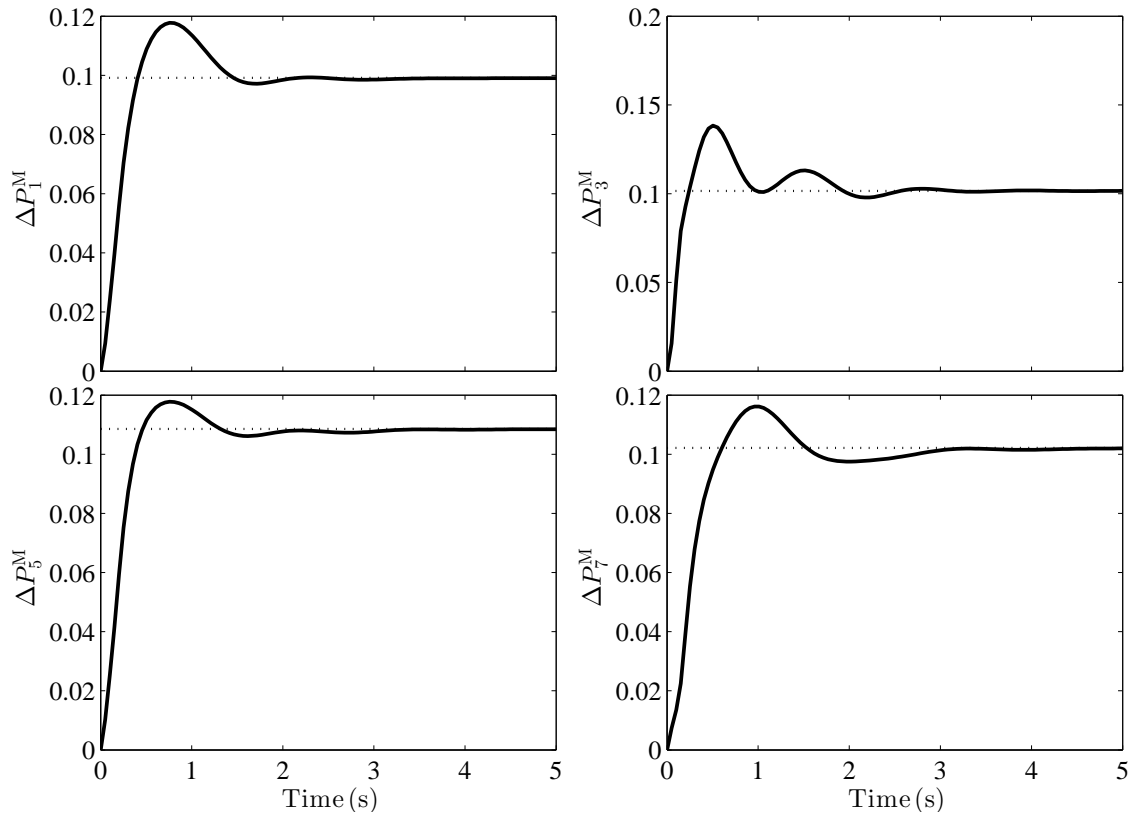
Figure 5.12: Total change in power output ΔP_i^M in each CA (case-3). The black dotted lines indicate the desired value in each CA assuming unequal area capacities. ΔP_i^M in area 2, 4 and 6 are not shown as their behaviour is similar to the ones presented.
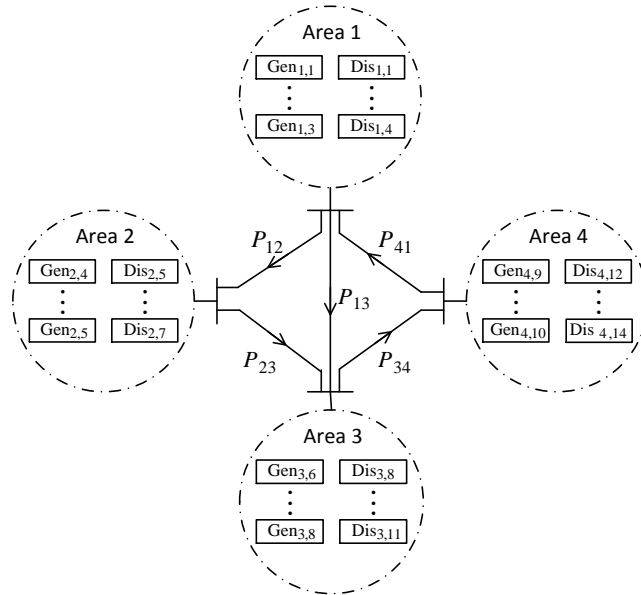
Figure 5.13: Single line diagram of a four-area network

ACE in each area, see Figure 5.7 (right). However, in addition to frequency deviation offsets, each ΔP_i^M and ΔP_i^{tie} ends without tracking the desired values (indicated by black dotted

lines). This is because, the difference in rated capacities was not considered in the contract information.

5.5.3 Case-3: Unequal rated capacities and included in contract information

This section presents the scenario where the rated capacities of the CAs are different, i.e. $\alpha_{ij} \neq 1$, and this fact is also considered in the contract information. The rated capacities assumed in case-2 are used here. Also, the $\Delta P_i^{\mathrm{U}} = 0$ scenario is considered. The contracted load changes assumed in case-1 are used here.

Figure 5.10 shows the frequency deviations Δf_i (left) and area control error ACE_i (right) in each area. Both Δf_i and ACE_i converged to zero indicating that the difference in rated capacities of each area was correctly incoroporated in the contract information (Section 5.4.5 contracted signals and Section 5.4.6 contracted/scheduled net incremental flows) .

Moreover, Figures 5.11 and 5.12 show the net tie line flow deviations ($\Delta P_7^{\mathrm{tie}}$ is omitted) and total change in power output (areas 2, 4 and 6 omitted) in each area respectively. It can be seen that each ΔP_i^{M} tracks the desired value (black dotted lines) and each $\Delta P_i^{\mathrm{tie}}$ settles at the scheduled value (black dotted lines). It is vital to note that each ΔP_i^{M} and $\Delta P_i^{\mathrm{tie}}$ settles at values different from what was obtained in case-1, even though both cases use the same contracted load changes (hence the total contracted load changes in the 7-area network are the same in case-1, case-2 and case-3) and DPM. This happens because the different α_{ij} incorporated in the new information redistribute the LM commitment of each GenCo.

5.6 Four-area deregulated state space model

This section presents one of the contributions of this chapter, which is to develop a deregulated benchmark model for a 4-area power network. This is important to give the reader more insight into how to build deregulated LFC models from the generalised formulation proposed in Section 5.3, and to further show the benefits of the generalised framework. The 4-area model is used in Chapter 7, in addition to the 7-area model, to provide more evidence on the benefits of a distributed MPC scheme. Figure 5.13 shows the single line diagram to the benchmark network. The next thing that is required is to state the elements of the various index sets associated with the generalised framework as it will differ from one network to another.

Table 5.5 shows the distribution of GenCos and DisCos within each CA for the 4-area network; the index sets $\mathcal{G}_i$ and $\mathcal{D}_i$ with their entries are also provided in the table . From Table 5.5, the index set of the CAs in the network is: $\mathcal{A} = \{1, 2, 3, 4\}$; this indicates that the network has

Table 5.5: GenCos and DisCos distribution within CAs for the 4-area network

CA index	No. of GenCos & index $(\mathcal{G}_i)$	No. of DisCos & index $(\mathcal{D}_i)$
1	3 & $\{1,2,3\}$	4 & $\{1,2,3,4\}$
2	2 & $\{4,5\}$	3 & $\{5,6,7\}$
3	3 & $\{6,7,8\}$	4 & $\{8,9,10,11\}$
4	2 & $\{9,10\}$	3 & $\{12,13,14\}$

4 areas. Moreover, the index sets of CAs connected to the ith area $\mathcal{A}_i^{\text{Ne}}$, as seen from Figure 5.13, are: $\mathcal{A}_1^{\text{Ne}} = \{2,3,4\}$, $\mathcal{A}_2^{\text{Ne}} = \{1,3\}$, $\mathcal{A}_3^{\text{Ne}} = \{1,2,4\}$, $\mathcal{A}_4^{\text{Ne}} = \{1,3\}$. Also, the index set of GenCos in the CAs connected to the ith area $\mathcal{G}_i^{\text{Ne}}$ are: $\mathcal{G}_1^{\text{Ne}} = \mathcal{G}_2 \cup \mathcal{G}_3 \cup \mathcal{G}_4$, $\mathcal{G}_2^{\text{Ne}} = \mathcal{G}_1 \cup \mathcal{G}_3$, $\mathcal{G}_3^{\text{Ne}} = \mathcal{G}_1 \cup \mathcal{G}_2 \cup \mathcal{G}_4$, $\mathcal{G}_4^{\text{Ne}} = \mathcal{G}_1 \cup \mathcal{G}_3$. With the elements of the necessary index sets being defined, the swing equations in Section 5.4.1, dynamics of turbines in Section 5.4.3, dynamics of governors in Section 5.4.4 and area control errors in Section 5.4.7, which were presented for the 7-area network, can be easily written for the 4-area system; the details are not repeated here.

The net tie line flows dynamics in Section 5.4.2, contracted signals in Section 5.4.5 scheduled net incremental tie line flows in Section 5.4.6, derived for the 7-area network, are dependent on the topology and size of the power interconnection; hence they need to be derived specifically for the 4-area network. Their derivations are briefly described in the following sections.

5.6.1 Net tie line flow deviation : 4-area system

For a 4-area network, there would be four net tie line power flows $\{\Delta P_1^{\text{tie}}, \Delta P_2^{\text{tie}}, \Delta P_3^{\text{tie}}, P_4^{\text{tie}}\}$ and only three out of the four net flows can be controlled independently, and one of the net flows must be eliminated from system's states and expressed as a linear combination of the others. In this study, the deviation in net tie line flow in area 3 ΔP_3^{tie} is eliminated and the index set of independent net flows is: $\mathcal{A}_d = \{1,2,4\}$. Therfore, from Figure 5.13, ΔP_i^{tie} of the different areas, given the sets $\mathcal{A}_i^{\text{Ne}}$, $\mathcal{A}$ and $\mathcal{A}_d$ and using the generalised form (5.4), are:

$$\Delta P_1^{\text{tie}} = \Delta P_{12} + \Delta P_{13} - \alpha_{41}\Delta P_{41} \tag{5.31a}$$

$$\Delta P_2^{\text{tie}} = \Delta P_{23} - \alpha_{12}\Delta P_{12} \tag{5.31b}$$

$$\Delta P_3^{\text{tie}} = \Delta P_{34} - \alpha_{23}\Delta P_{23} - \alpha_{13}\Delta P_{13} \tag{5.31c}$$

$$\Delta P_4^{\text{tie}} = \Delta P_{41} - \alpha_{34}\Delta P_{34} \tag{5.31d}$$

Expressing ΔP_3^{tie} as a linear combination of the other net tie line flows gives:

$$\Delta P_3^{\text{tie}} = -(\alpha_{13}\Delta P_1^{\text{tie}} + \alpha_{23}\Delta P_2^{\text{tie}} + \frac{1}{\alpha_{34}}\Delta P_4^{\text{tie}}) \tag{5.32}$$

and the dynamic equations of the independent net flows are:

$$\Delta \dot{P}_1^{\text{tie}} = \left(T_{12} + T_{13} + \alpha_{41}T_{41}\right)\Delta f_1 - T_{12}\Delta f_2 - T_{13}\Delta f_3 - \alpha_{41}T_{41}\Delta f_4 \tag{5.33a}$$

$$\Delta \dot{P}_2^{\text{tie}} = \left(T_{23} + \alpha_{12}T_{12}\right)\Delta f_2 - \alpha_{12}T_{12}\Delta f_1 - T_{23}\Delta f_3 \tag{5.33b}$$

$$\Delta \dot{P}_4^{\text{tie}} = \left(T_{41} + \alpha_{34}T_{34}\right)\Delta f_4 - T_{14}\Delta f_1 - \alpha_{34}T_{34}\Delta f_3 \tag{5.33c}$$

5.6.2 Contracted signal : 4-area system

The contracted signals, ten in number, required in the 4-area benchmark system are: S_{11}, S_{12}, S_{13} (area 1), $S_{2,4}, S_{2,5}$ (area 2), $S_{3,6}, S_{3,7}, S_{3,8}$ (area 3) and $S_{4,9}, S_{4,10}$ (area 4). However, two out of the ten will be described here. From the compact generalised representation of the contracted signal (5.22),

$$S_{2,4} = \eta_{4,\mathcal{D}_2}\boldsymbol{\Delta P}_2^{\text{L}} + \sum_{j\in\mathcal{A}_2^{\text{Ne}}} \eta_{4,\mathcal{D}_j}\alpha_{j2}\boldsymbol{\Delta P}_j^{\text{L}} \tag{5.34}$$

Substituting $\mathcal{A}_2^{\text{Ne}} = \{1,3\}$ into (5.34) gives:

$$S_{2,4} = \eta_{4,\mathcal{D}_2}\boldsymbol{\Delta P}_2^{\text{L}} + \eta_{4,\mathcal{D}_1}\alpha_{12}\boldsymbol{\Delta P}_1^{\text{L}} + \eta_{4,\mathcal{D}_3}\alpha_{32}\boldsymbol{\Delta P}_3^{\text{L}} \tag{5.35}$$

$$S_{3,6} = \eta_{6,\mathcal{D}_3}\boldsymbol{\Delta P}_3^{\text{L}} + \sum_{j\in\mathcal{A}_3^{\text{Ne}}} \eta_{6,\mathcal{D}_j}\alpha_{j3}\boldsymbol{\Delta P}_j^{\text{L}} \tag{5.36}$$

Substituting $\mathcal{A}_3^{\text{Ne}} = \{1,2,4\}$ into (5.36) gives:

$$S_{3,6} = \eta_{6,\mathcal{D}_3}\boldsymbol{\Delta P}_3^{\text{L}} + \eta_{6,\mathcal{D}_1}\alpha_{13}\boldsymbol{\Delta P}_1^{\text{L}} + \eta_{6,\mathcal{D}_2}\alpha_{23}\boldsymbol{\Delta P}_2^{\text{L}} + \eta_{6,\mathcal{D}_4}\alpha_{43}\boldsymbol{\Delta P}_4^{\text{L}} \tag{5.37}$$

See Section 5.4.5 for the definition of $\boldsymbol{\Delta P}_i^{\text{L}}$ and $\eta_{\text{k},\mathcal{D}_i}$

5.6.3 Scheduled net incremental tie line flow : 4-area system

There are four scheduled net incremental tie line flows $\left\{\Delta P_1^{\text{tie,sh}}, \Delta P_2^{\text{tie,sh}}, \Delta P_3^{\text{tie,sh}}, P_4^{\text{tie,sh}}\right\}$; here the expression for only one will be derived. From the compact generalised representation of $\Delta P_i^{\text{tie,sh}}$ (5.25),

$$\Delta P_1^{\text{tie,sch}} = \sum_{j \in \mathcal{A}_1^{\text{Ne}}} \left\{ \sum_{r \in \mathcal{G}_1} \eta_{r,\mathcal{D}_j} \alpha_{j1} \boldsymbol{\Delta P}_j^{\text{L}} \right\} - \sum_{r \in \mathcal{G}_1^{\text{Ne}}} \eta_{r,\mathcal{D}_1} \boldsymbol{\Delta P}_1^{\text{L}} \tag{5.38}$$

Substituting $\mathcal{A}_1^{\text{Ne}}$, $\mathcal{G}_1$ and $\mathcal{G}_1^{\text{Ne}} = \{4,5,6,7,8,9,10\}$ into (5.38) gives:

$$
\begin{aligned}
\Delta P_1^{\text{tie,sch}} &= \sum_{r \in \mathcal{G}_1} \eta_{r,\mathcal{D}_2} \alpha_{21} \boldsymbol{\Delta P}_2^{\text{L}} + \sum_{r \in \mathcal{G}_1} \eta_{r,\mathcal{D}_3} \alpha_{31} \boldsymbol{\Delta P}_3^{\text{L}} + \sum_{r \in \mathcal{G}_1} \eta_{r,\mathcal{D}_4} \alpha_{41} \boldsymbol{\Delta P}_4^{\text{L}} - \Big(\eta_{4,\mathcal{D}_1} + \eta_{5,\mathcal{D}_1} \\
&\quad + \cdots + \eta_{10,\mathcal{D}_1} \Big) \boldsymbol{\Delta P}_1^{\text{L}} \\
&= \Big(\eta_{1,\mathcal{D}_2} + \eta_{2,\mathcal{D}_2} + \eta_{3,\mathcal{D}_2} \Big) \alpha_{21} \boldsymbol{\Delta P}_2^{\text{L}} + \Big(\eta_{1,\mathcal{D}_3} + \eta_{2,\mathcal{D}_3} + \eta_{3,\mathcal{D}_3} \Big) \alpha_{31} \boldsymbol{\Delta P}_3^{\text{L}} \\
&\quad - \Big(\eta_{4,\mathcal{D}_1} + \eta_{5,\mathcal{D}_1} + \cdots + \eta_{10,\mathcal{D}_1} \Big) \boldsymbol{\Delta P}_1^{\text{L}}
\end{aligned}
\tag{5.39}
$$

The other scheduled net tie line flows $\Delta P_2^{\text{tie,sh}}, \Delta P_3^{\text{tie,sh}}, P_4^{\text{tie,sh}}$ can be derived in the same way as $\Delta P_1^{\text{tie,sch}}$. Thus, similar to the 7-area benchmark, a continuous time (CT) state space representation of the 4-area system is:

$$\dot{\text{x}} = \text{A}^{\text{c}}\text{x} + \text{B}^{\text{c}}\text{u} + \text{B}^{\text{dc}}\text{d} + \text{B}^{\text{bc}}\text{b}; \quad \text{y} = \text{C}^{\text{c}}\text{x} + \text{D}^{\text{c}}\text{d} \tag{5.40}$$

The form (5.40) is exactly the same as the ones stated in (5.30); however key difference comes in the definition of the various system matrices, vector of states, input, and load changes.

$$
\text{x} = \begin{bmatrix} \text{x}_1 \\ \Delta P_1^{\text{tie}} \\ \hline \text{x}_2 \\ \Delta P_2^{\text{tie}} \\ \hline \text{x}_3 \\ \hline \text{x}_4 \\ \Delta P_4^{\text{tie}} \end{bmatrix} \in \mathbb{R}^{27}; \ \text{x}_1 = \begin{bmatrix} \Delta f_1 \\ \Delta P_{1,1}^{\text{M}} \\ \Delta P_{1,1}^{\text{V}} \\ \Delta P_{1,2}^{\text{M}} \\ \Delta P_{1,2}^{\text{V}} \\ \Delta P_{1,3}^{\text{M}} \\ \Delta P_{1,3}^{\text{V}} \end{bmatrix}; \ \text{x}_2 = \begin{bmatrix} \Delta f_2 \\ \Delta P_{2,4}^{\text{M}} \\ \Delta P_{2,4}^{\text{V}} \\ \Delta P_{2,5}^{\text{M}} \\ \Delta P_{2,5}^{\text{V}} \end{bmatrix}; \ \text{x}_3 = \begin{bmatrix} \Delta f_3 \\ \Delta P_{3,6}^{\text{M}} \\ \Delta P_{3,6}^{\text{V}} \\ \Delta P_{3,7}^{\text{M}} \\ \Delta P_{3,7}^{\text{V}} \\ \Delta P_{3,8}^{\text{M}} \\ \Delta P_{3,8}^{\text{V}} \end{bmatrix}; \ \text{x}_4 = \begin{bmatrix} \Delta f_4 \\ \Delta P_{4,9}^{\text{M}} \\ \Delta P_{4,9}^{\text{V}} \\ \Delta P_{4,10}^{\text{M}} \\ \Delta P_{4,10}^{\text{V}} \end{bmatrix}
$$

$$
\text{u} = \begin{bmatrix} \Delta P_1^{\text{C}} \\ \Delta P_2^{\text{C}} \\ \Delta P_3^{\text{C}} \\ \Delta P_4^{\text{C}} \end{bmatrix} \in \mathbb{R}^4; \ \text{d} = \begin{bmatrix} \boldsymbol{\Delta P}_1^{\text{L}} \\ \boldsymbol{\Delta P}_2^{\text{L}} \\ \boldsymbol{\Delta P}_3^{\text{L}} \\ \boldsymbol{\Delta P}_4^{\text{L}} \end{bmatrix} \in \mathbb{R}^{14}; \ \text{b} = \begin{bmatrix} \Delta P_1^{\text{U}} \\ \Delta P_2^{\text{U}} \\ \Delta P_3^{\text{U}} \\ \Delta P_4^{\text{U}} \end{bmatrix} \in \mathbb{R}^4; \ \text{y} = \begin{bmatrix} \text{ACE}_1 \\ \text{ACE}_2 \\ \text{ACE}_3 \\ \text{ACE}_4 \end{bmatrix} \in \mathbb{R}^4
$$

Note that the dashed lines partitioned the centralised system (5.40) into four subsystem models (the LFC model of each control area in the multi-area system) and system decomposition will be carried out along the dashed lines to obtain subsystem models needed for distributed MPC designs in Chapter 7. This is applicable to the 7-area system developed in Section 5.4. In summary, this section developed the 4-area deregulated benchmark model which will be used

as one of the case study models to test decentralised and distributed MPC algorithms proposed in Chapter 7.

5.7 Conclusion

Most modern day large-scale deregulated interconnections comprise of numerous control areas, and a great number of intra-area and inter-area bilateral power transactions/contracts exist between the various GenCos and DisCos; currently, an increasing amount of new contracts are being entered by these entities. Hence, with regards to developing benchmark models for large-scale LFC studies, the size of the DisCo participation matrix (DPM) is expected to be large, and incorporating the entries of the DPM into the traditional LFC framework may be an arduous task and prone to errors.

The generalised framework proposed in this chapter provides a relatively straightforward and systematic approach to developing any large-scale LFC model in the deregulated environment and represents a more efficient method of handling a large-sized DPM encountered when studying LFC in large scale multi-area systems with numerous GenCos and DisCos making LM contracts. The framework is also effective irrespective of the topology of the interconnection and number of links to a given control area.

Furthermore, by incorporating CA rated capacity ratios in the generalised framework, the proposed framework offers the flexiblity to study LFC in large interconnections with equal CAs ratings or the more realistic unequal CAs ratings. A 7-area benchmark model was developed to illustrate how one could utilise the generalised formulation, and was also used in simulation studies, where it was shown that neglecting the difference in rated capacities of interconnected control areas in the contract information, where in reality the areas have unequal rated capacities, can result in the frequency deviation not converging to zero, even in the presence of an adequate supplementary LFC scheme. This chapter also developed a deregulated benchmark model for a 4-area network to demonstrates the versatility of the generalised framework.

Chapter 6

A 7-area deregulated LFC based on centralised MPC

6.1 Introduction

In the 2-area centralised model predictive control (CMPC) based load frequency control (LFC) scheme proposed in Chapter 4, the primary drive was to provide a lucid description of the procedure involved in developing deregulated LFC models, and also to show, via simulation, the constraints handling capability of MPC stated in Chapter 3. However, the proposal in Chapter 4 fall short of some key ingredients in most realistic power system interconnections; these drawbacks are stated below:

- Realistic systems may consist of more than 2-areas, where each area would normally have different rated capacities. Also, the number of GenCos and DisCos within an area may be higher than that considered in Chapter 4, and some GenCos may choose not to participate in the supplementary control service offered by a transmission system operator (TSO). Note that the CMPC scheme represents the LFC controller that would normally run on a TSO's computer in practice.

- Also in Chapter 4, a single (lumped) supplementary control signal ΔP_i^{C} was generated for each control area (CA), and the lumped signal is distributed to the GenCos within that area in proportion to their individual area participation factors $\gamma_{i,\mathrm{k}}$ (see Figure 4.2). Deregulated LFC schemes in the literature [79–87] also adopted this approach. Thus, the CMPC scheme proposed in Chapter 4 considered the constraints on lumped inputs ΔP_1^{C} and ΔP_2^{C} rather than the constraints on the input to the individual generating units[1] in area 1 ($\Delta P_{1,1}^{\mathrm{C}}$, $\Delta P_{1,2}^{\mathrm{C}}$) and area 2 ($\Delta P_{2,3}^{\mathrm{C}}$, $\Delta P_{2,4}^{\mathrm{C}}$). The key point here is that

---

[1]A single generating unit represents a GenCo in this thesis.

imposing constraints on the lumped inputs may not translate to constraint satisfaction on the individual inputs of the GenCos.

• Finally, the control scheme proposed in Chapter 4 is centralised and this architecture may be unrealistic for large scale interconnections where CAs have large geographical separations and each CA belonging to a different organisation. Other drawbacks of a CMPC for large scale interconnectiions are stated in Table 3.1.

In respect of the first item above, the previous chapter presented a new generalised multi-area LFC modelling framework where unequal area capacities and an arbitrary number of CAs, GenCos and DisCos can be accommodated. A 7-area deregulated benchmark model was also developed. The third item is addressed in Chapter 7.

This chapter, therefore, extends the work in Chapter 4 by proposing a more general CMPC based LFC scheme for a multi-area deregulated power system interconnection. It is assumed that the deregulated system is subjected to measured (contracted) and unmeasured (uncontracted) load changes (disturbances), and the CMPC scheme is designed to reject uncontracted disturbances and coordinate the transient behaviour of the system when contracted load changes are acting. The generation rate constraints of each GenCo is incorporated in the CMPC design. Furthermore, the scheme takes into account the individual constraints on the inputs of the generating units rather than the lumped input for each area by incorporating the area participation factors of the GenCos explicitly in its cost function; including the area participation factors in the CMPC cost ensures that input constraints are satisfied during transient. Moreover, the CMPC scheme uses an output feedback, where a discrete time Luenberger observer is used to estimate uncontracted load changes and system states. The proposed CMPC scheme is tested on the 7-area benchmark model developed in Chapter 5 and compared with an infinite horizon linear quadratic regulator (LQR) to demostrate its efficacy.

This chapter is based on the work in [36] and its a key **contribution** in this thesis. The organisation of the chapter is as follows: Section 6.2 summarises the main contributions of this chapter; Section 6.3 briefly re-introduced the 7-area deregulated model and state some slight modification made to it; Section 6.4 presents the key parts of the proposed CMPC scheme; Section 6.5 shows simulation results and discussions; Section 6.6 gives some concluding remarks.

6.2 Summary of main contributions

This chapter extends the contributions itemised in Section 4.2 by making the following additions summarised below:

- Proposes a CMPC scheme for a deregulated LFC problem where CAs have unequal rated capacities, large scale network with a more complex topology considered (network houses 33 GenCos and 46 DisCos), some GenCos do not participate in serving uncontracted load changes in their area, and not all DisCos purchase a load matching (LM) contract (zero contracted demands). This represents a more appropriate power system setting.

- Incorporates the area participation factor of each GenCo in the CMPC cost function to ensure that the individual input constraints of each GenCo is satisfied during transients.

6.3 7-area benchmark model

The 7-area deregulated benchmark model used in this chapter has been developed in Chapter 5 and this is presented in Section 5.4; hence, the details of the model are not repeated here. However, in order to be able to account for the input constraints of each generating unit, a modification is made to the general form of the governor dynamics (5.8) and this is described in Section 6.3.1

6.3.1 Modified governor dynamics : 7-area system

The modified dynamics of the governor is:

$$\Delta \dot{P}_{i,k}^{V} = \frac{1}{T_{G_{i,k}}} \left(\Delta P_{i,k}^{C} - \Delta P_{i,k}^{V} - \frac{1}{R_{i,k}} \Delta f_i + S_{i,k} \right) \quad \forall i \in \mathcal{A}, \forall k \in \mathcal{G}_i \tag{6.1}$$

Observe that the term $\gamma_{i,k} \Delta P_i^{C}$ in (5.8) has been replaced by the input to the individual generating unit $\Delta P_{i,k}^{C}$ in (6.1); $\Delta P_{i,k}^{C}$ is the LFC or supplementary control input to the kth GenCo in the ith CA. Thus, the governor dynamics of each GenCo Section 5.4.4, and can be rewritten as:

$$
\begin{aligned}
\Delta \dot{P}_{1,1}^{V} &= \frac{1}{T_{G_{1,1}}}\Big(\Delta P_{1,1}^{C} - \Delta P_{1,1}^{V} - \frac{\Delta f_1}{R_{1,1}} + S_{1,1}\Big), \cdots, \Delta \dot{P}_{1,5}^{V} = \frac{1}{T_{G_{1,5}}}\Big(\Delta P_{1,5}^{C} - \Delta P_{1,5}^{V} \\
&\quad - \frac{\Delta f_1}{R_{1,5}} + S_{1,5}\Big) \tag{6.2a}\\
\Delta \dot{P}_{2,6}^{V} &= \frac{1}{T_{G_{2,6}}}\Big(\Delta P_{2,6}^{C} - \Delta P_{2,6}^{V} - \frac{\Delta f_2}{R_{2,6}} + S_{2,6}\Big), \cdots, \Delta \dot{P}_{2,9}^{V} = \frac{1}{T_{G_{2,9}}}\Big(\Delta P_{2,9}^{C} - \Delta P_{2,9}^{V} \\
&\quad - \frac{\Delta f_2}{R_{2,9}} + S_{2,9}\Big) \tag{6.2b}
\end{aligned}
$$

$$\vdots$$

$$
\begin{aligned}
\Delta \dot{P}_{7,30}^{V} &\quad \frac{1}{T_{G_{7,30}}}\Big(\Delta P_{7,30}^{C} - \Delta P_{7,30}^{V} - \frac{\Delta f_7}{R_{7,30}} + S_{7,30}\Big), \cdots, \Delta \dot{P}_{7,33}^{V} = \frac{1}{T_{G_{7,33}}}\Big(\Delta P_{7,33}^{C} \\
&\quad - \Delta P_{7,33}^{V} - \frac{\Delta f_7}{R_{7,33}} + S_{7,33}\Big) \tag{6.2c}
\end{aligned}
$$

6.3.2 State-space model

The continuous time (CT) state space representation of the 7-area deregulated benchmark model is:

$$
\dot{x} = A^{c}x + B^{c}u + B^{dc}d + B^{bc}b; \quad y = C^{c}x + D^{c}d \tag{6.3}
$$

where the dimension of the matrix A^{c}, B^{dc}, B^{bc}, C^{c} and D^{c} are the same as presented in Section 5.4.8. However, in this chapter, $B^{c} \in \mathbb{R}^{79 \times 33}$ as opposed to $B^{c} \in \mathbb{R}^{79 \times 7}$ in Section 5.4.8. Furthermore, the definition of the input vector u is different from that presented in Section 5.4.8, and this is given as:

$$
u = \begin{bmatrix} \Delta P_1^{C} \\ \Delta P_2^{C} \\ \vdots \\ \Delta P_7^{C} \end{bmatrix} \in \mathbb{R}^{33 \times 1}, \text{ and } \Delta P_1^{C} = \begin{bmatrix} \Delta P_{1,1}^{C} \\ \Delta P_{1,2}^{C} \\ \vdots \\ \Delta P_{1,5}^{C} \end{bmatrix}, \Delta P_2^{C} = \begin{bmatrix} \Delta P_{2,6}^{C} \\ \Delta P_{2,7}^{C} \\ \vdots \\ \Delta P_{2,9}^{C} \end{bmatrix}, \cdots, \Delta P_7^{C} = \begin{bmatrix} \Delta P_{7,30}^{C} \\ \Delta P_{7,31}^{C} \\ \vdots \\ \Delta P_{7,33}^{C} \end{bmatrix}
$$

Using area 1 for illustration, the often assumed structure of the control input, where a lumped control is computed for each area, is shown in Figure 6.1. The structure considered in this chapter is shown in Figure 6.2.
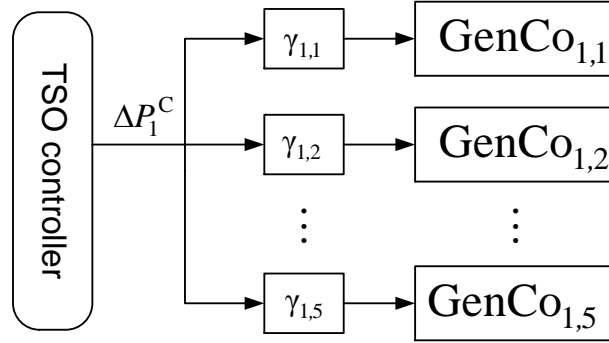
Figure 6.1: Description of lumped control to GenCos in area 1
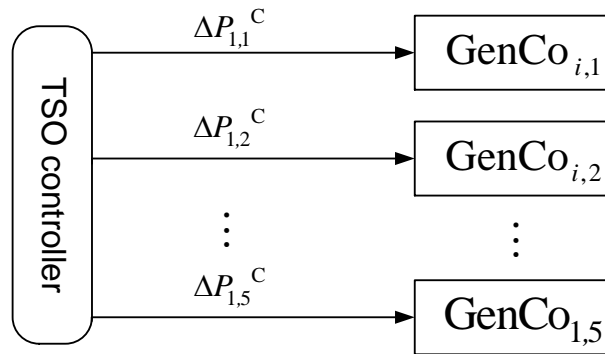
Figure 6.2: Description of separate control to each GenCo in area 1

6.4 Design of the CMPC based LFC scheme

In this section, the key parts of the CMPC scheme proposed for the deregulated LFC problem is summarised. In most instances, a reference will be made to some sections in Chapters 3 and 4 to avoid repetitions, though few expressions will be restated to aid reading. Identical to Chapter 4, the focus here is to design an LFC controller that would reject uncontracted load changes (unmeasurable), coordinate the transient behaviour of the system when contracted load changes (measurable) are acting, while accounting for GRC and control input limits/constraints of each GenCo.

6.4.1 Model prediction

This section is similar to Section 4.4.1 but included for readability. The discrete time (DT) form of (6.3) in terms of deviation variables and the corresponding $n_c - $ step state prediction are:

$$\bar{x}_{k+1} = A\bar{x}_k + B\bar{u}_k; \quad \bar{y}_k = C\bar{x}_k \tag{6.4}$$

$$\underset{\rightarrow k}{\bar{x}} = P_x\bar{x}_k + H_u \underset{\rightarrow k-1}{\bar{u}} \tag{6.5}$$

Here, $\bar{x}_k = x_k - x_{ss}$; $\bar{u}_k = u_k - u_{ss}$; $\bar{y}_k = y_k - y_{ss}$. Refer to Section 4.4.1 for further details.

6.4.2 Design of observer and steady state target calculator

Similar to the proposal in Chapter 4, the proposed scheme here is output feedback. The details of the observer design is skipped here as it is similar to what was presented in Section 4.4.4. For the steady state target pair (x_{ss}, u_{ss}) calculation, like (4.30), the consistency expression is given as:

$$\underbrace{\begin{bmatrix} I - A & -B \\ C & \mathbf{0} \end{bmatrix}}_{M_C} \begin{bmatrix} x_{ss} \\ u_{ss} \end{bmatrix} = \begin{bmatrix} B^d d_{ss} + B^b b_{ss} \\ y_{ss} - D d_{ss} \end{bmatrix} \tag{6.6}$$

The matrix M_C, as presented in (6.6) is nonsquare since $\bar{y}_k \in \mathbb{R}^{7 \times 1}$ and $\bar{u}_k \in \mathbb{R}^{33 \times 1}$. However, M_C can be reduced to a square matrix by performing the following algebra[2]:

---

[2]Recall that the area participation factors of the GenCos in any control area sum up to 1; see (5.9).

$$
\left[\begin{array}{c|cccc|cc|c|ccc}
I - A & -b^c_{1,1} & \cdots & -b^c_{1,5} & -b^c_{2,6} & \cdots & -b^c_{2,9} & \cdots & -b^c_{7,30} & \cdots & -b^c_{7,33} \\
\hline
C & 0 & \cdots & 0 & 0 & \cdots & 0 & \cdots & 0 & \cdots & 0
\end{array} \right]
\begin{bmatrix}
x_{ss} \\ \hline
\gamma_{1,1} u^1_{ss} \\ \vdots \\ \gamma_{1,5} u^1_{ss} \\ \hline
\gamma_{2,6} u^2_{ss} \\ \vdots \\ \gamma_{2,9} u^2_{ss} \\ \hline \vdots \\ \hline
\gamma_{7,30} u^7_{ss} \\ \vdots \\ \gamma_{7,33} u^7_{ss}
\end{bmatrix}
=
\begin{bmatrix}
B^d d_{ss} + B^b b_{ss} \\
y_{ss} - D d_{ss}
\end{bmatrix}
$$

$$(6.7)$$

where each $b^c_{i,k}$ represents a column of the matrix B which has 33 columns. The term u^i_{ss} is the lumped steady state input target of the ith CA. The expression (6.7) can be further expressed as:

$$
\underbrace{\left[\begin{array}{c|c|c|c|c}
I - A & \sum\limits_{k \in \mathcal{G}_1} \gamma_{1,k} b^c_{1,k} & \sum\limits_{k \in \mathcal{G}_2} \gamma_{2,k} b^c_{2,k} & \cdots & \sum\limits_{k \in \mathcal{G}_7} \gamma_{7,k} b^c_{7,k} \\
\hline
C & 0 & 0 & \cdots & 0
\end{array} \right]}_{M_S}
\begin{bmatrix}
x_{ss} \\ \hline u^1_{ss} \\ \hline u^2_{ss} \\ \hline \vdots \\ \hline u^7_{ss}
\end{bmatrix}
=
\begin{bmatrix}
B^d d_{ss} + B^b b_{ss} \\
y_{ss} - D d_{ss}
\end{bmatrix}
\quad (6.8)
$$

$$
b_{ss} = \widehat{b}_k, \quad d_{ss} = d_k, \quad y_{ss} = 0
$$

The matrix M_S of (6.8) is a square matrix, hence the state targets x_{ss} and the lumped input targets $u^1_{ss}, u^2_{ss}, u^3_{ss}, \cdots, u^7_{ss}$ can be computed repeatedly as an estimate of an uncontracted load change (provided by the observer) becomes available. Finally, the vector of steady state input targets of each GenCo can be obtained using:

$$
\mathrm{u_{ss}} =
\begin{bmatrix}
\gamma_{1,1} & 0 & \cdots & 0 \\
\vdots & \vdots & \vdots & \vdots \\
\gamma_{1,5} & 0 & \cdots & 0 \\
0 & \gamma_{2,6} & \cdots & 0 \\
\vdots & \vdots & \vdots & \vdots \\
0 & \gamma_{2,9} & \cdots & 0 \\
\vdots & \vdots & \ddots & \vdots \\
0 & 0 & \cdots & \gamma_{7,30} \\
\vdots & \vdots & \vdots & \vdots \\
0 & 0 & \cdots & \gamma_{7,33}
\end{bmatrix}
\begin{bmatrix}
\mathrm{u_{ss}^1} \\
\mathrm{u_{ss}^2} \\
\vdots \\
\mathrm{u_{ss}^7}
\end{bmatrix}
$$

6.4.3 Cost function

The CMPC cost, incorporating the area participation factor of each GenCo can be expressed as:

$$
J = \sum_{t=k}^{\infty} \frac{1}{2}\left\{ \overline{\mathrm{x}}_{t+1}^T Q\, \overline{\mathrm{x}}_{t+1} + \sum_{i \in \mathcal{A}} \left\{ \sum_{\mathrm{k} \in \mathcal{G}_i} \left(\mathrm{u}_t^{i,\mathrm{k}} - \gamma_{i,\mathrm{k}} \mathrm{u}_{ss}^i \right)^2 \right\} \right\}
\tag{6.9}
$$

where the definition of the index sets $\mathcal{A}$ and $\mathcal{G}_i$ can be found in Table 5.1. Note the difference between k (sampling instant) and k (GenCo index). $\mathrm{u}_t^{i,\mathrm{k}}$ is the control input of a GenCo k in area i at a given sampling instant t, and it is the DT equivalent of $\Delta P_{i,\mathrm{k}}^C = \mathrm{u}^{i,\mathrm{k}}$. Utilising the elements of $\mathcal{A}$ for the 7-area network stated in Table 5.3, the cost function (6.9) can be further expressed as:

$$
\begin{aligned}
J \;=\; & \sum_{t=k}^{\infty} \frac{1}{2}\left\{ \overline{\mathrm{x}}_{t+1}^T Q\, \overline{\mathrm{x}}_{t+1} + \sum_{\mathrm{k} \in \mathcal{G}_1} \left(\mathrm{u}_t^{1,\mathrm{k}} - \gamma_{1,\mathrm{k}} \mathrm{u}_{ss}^1 \right)^2 + \sum_{\mathrm{k} \in \mathcal{G}_2} \left(\mathrm{u}_t^{2,\mathrm{k}} - \gamma_{2,\mathrm{k}} \mathrm{u}_{ss}^2 \right)^2 + \cdots \right. \\
& \left. + \sum_{\mathrm{k} \in \mathcal{G}_7} \left(\mathrm{u}_t^{7,\mathrm{k}} - \gamma_{7,\mathrm{k}} \mathrm{u}_{ss}^7 \right)^2 \right\}
\end{aligned}
\tag{6.10}
$$

Let $\overline{\mathrm{u}_t^{i,\mathrm{k}}} = \mathrm{u}_t^{i,\mathrm{k}} - \gamma_{i,\mathrm{k}} \mathrm{u}_{ss}^i$ represent the deviation from the steady state input target of a GenCo k in area i at a given sampling instant t. Thus, (6.10) becomes:

$$J = \sum_{t=k}^{\infty} \frac{1}{2} \left\{ \overline{x}_{t+1}^T Q\, \overline{x}_{t+1} + \sum_{k\,\in\,\mathcal{G}_1} \left(\overline{u_t^{1,k}}\right)^2 + \sum_{k\,\in\,\mathcal{G}_2} \left(\overline{u_t^{2,k}}\right)^2 + \cdots \right.$$
$$\left. + \sum_{k\,\in\,\mathcal{G}_7} \left(\overline{u_t^{7,k}}\right)^2 \right\} \tag{6.11}$$

Furthermore, with the elements of the index sets $\mathcal{G}_1$, $\mathcal{G}_2$, $\cdots$, $\mathcal{G}_7$ known (see Table 5.3), the expression (6.11) can be written as:

$$J = \sum_{t=k}^{\infty} \frac{1}{2} \left\{ \overline{x}_{t+1}^T Q\, \overline{x}_{t+1} + \left\{ \left(\overline{u_t^{1,1}}\right)^2 + \cdots + \left(\overline{u_t^{1,5}}\right)^2 \right\} + \left\{ \left(\overline{u_t^{2,6}}\right)^2 + \cdots + \left(\overline{u_t^{2,9}}\right)^2 \right\} \right.$$
$$\left. + \cdots + \left\{ \left(\overline{u_t^{7,30}}\right)^2 + \cdots + \left(\overline{u_t^{7,33}}\right)^2 \right\} \right\} \tag{6.12}$$

The cost function (6.12) can be written compactly as:

$$J = \sum_{t=k}^{\infty} \frac{1}{2} \left\{ \overline{x}_{t+1}^T Q\, \overline{x}_{t+1} + u_t^T \overline{u}_t \right\} \tag{6.13}$$

where

$$\overline{u}_t = \left[\overline{u_t^{1,1}} \cdots \overline{u_t^{1,5}} \; \overline{u_t^{2,6}} \cdots \overline{u_t^{2,9}} \; \overline{u_t^{3,10}} \cdots \overline{u_t^{3,14}} \cdots \overline{u_t^{7,30}} \cdots \overline{u_t^{7,33}} \right]^T \in \mathbb{R}^{33\times1}$$

The cost function (6.13) is in the form presented in (3.8) with R taken as an identity matrix; hence the standard quadratic form (4.20) is valid here.

6.4.4 Generation rate and input constraints.

The GRC and input limit in CT for the kth GenCo in the ith CA are respectively:

$$\Delta P_{i,k}^{\dot{M},min} \leq \Delta \dot{P}_{i,k}^{M} \leq \Delta P_{i,k}^{\dot{M},max} \tag{6.14a}$$

$$\Delta P_{i,k}^{C,min} \leq \Delta P_{i,k}^{C} \leq \Delta P_{i,k}^{C,max} \tag{6.14b}$$

For notational convenience, let $\Delta \dot{P}_{i,k}^{M} = g^{i,k}$ and $\Delta P_{i,k}^{C} = q^{i,k}$. The DT time representation of the GRC and input limits $\forall t = \{k, k+1, \cdots, k+n_c-1\}$, $k \geq 0$ are respectively:

$$t_s \Delta P_{i,k}^{\dot{M},\min} \leq g_{t+1/k}^{i,k} - g_{t/k}^{i,k} \leq t_s \Delta P_{i,k}^{\dot{M},\max} \quad \forall i \in \mathcal{A}, \forall k \in \mathcal{G}_i^C \tag{6.15a}$$

$$\Delta are P_{i,k}^{C,\min} \leq q_{t/k}^{i,k} \leq \Delta P_{i,k}^{C,\max} \quad \forall i \in \mathcal{A}, \forall k \in \mathcal{G}_i^C \tag{6.15b}$$

where t_s is the sampling time. Note that in these studies, GRC and input constraints are considered for GenCos participating (GenCos with a nonzero area participation factors) in supplementary control, that is, GenCos in each area that have made commitments to compensate for uncontracted load changes. Hence $\mathcal{G}_i^C \subseteq \mathcal{G}_i$ is the index set of GenCos with a nonzero area participation factor in the ith CA. Identical to what was presented in Section 4.4.3, the generation rate constraints (6.15a) and input limits (6.15b) can be collected into a single compact matrix inequality:

$$G_c \bar{x}_k + F_c \bar{u}_k \leq h_c \tag{6.16}$$

and the corresponding matrix inequality obtained by advancing (6.16), n_y steps into the future, is:

$$\boldsymbol{F_c} \, \underset{\rightarrow k-1}{\bar{\mathrm{u}}} \leq \boldsymbol{h_c} \tag{6.17}$$

Note that (6.16) and (6.17) are exactly the same as (4.27) and (4.28); however, the dimensions of matrices G_c, F_c, and h_c, and thus $\boldsymbol{F_c}$ and $\boldsymbol{h_c}$, are different from that in (4.27) and (4.28). Section (4.4.3) contains more details.

6.4.5 The CMPC problem

The statement of the CMPC problem is exactly that presented in Section 4.4.5 and can be skipped by a reader. However, it is duplicated here for readability:

$$\mathrm{P_{CMPC}}: \qquad \min_{\underset{\rightarrow k-1}{\bar{\mathrm{u}}}} \left\{ \frac{1}{2} \underset{\rightarrow k-1}{\bar{\mathrm{u}}^T} S_f \underset{\rightarrow k-1}{\bar{\mathrm{u}}} + H_f^T \underset{\rightarrow k-1}{\bar{\mathrm{u}}} \right\} \tag{6.18}$$

Subject to

$$\boldsymbol{F_c} \, \underset{\rightarrow k-1}{\bar{\mathrm{u}}} \leq \boldsymbol{h_c}$$

Table 6.1: DisCos' contracted load changes $\Delta P_{i,j}^{\mathrm{L}}$.

$\Delta P_{1,1}^{\mathrm{L}}$	$\Delta P_{1,2}^{\mathrm{L}}$	$\Delta P_{1,3}^{\mathrm{L}}$	$\Delta P_{1,4}^{\mathrm{L}}$	$\Delta P_{1,5}^{\mathrm{L}}$	$\Delta P_{1,6}^{\mathrm{L}}$	$\Delta P_{1,7}^{\mathrm{L}}$
0	0	0	0.005	0	0.005	0

$\Delta P_{2,8}^{\mathrm{L}}$	$\Delta P_{2,9}^{\mathrm{L}}$	$\Delta P_{2,10}^{\mathrm{L}}$	$\Delta P_{2,11}^{\mathrm{L}}$	$\Delta P_{2,12}^{\mathrm{L}}$
0.01	0	0.005	0.005	0.005

$\Delta P_{3,13}^{\mathrm{L}}$	$\Delta P_{3,14}^{\mathrm{L}}$	$\Delta P_{3,15}^{\mathrm{L}}$	$\Delta P_{3,16}^{\mathrm{L}}$	$\Delta P_{3,17}^{\mathrm{L}}$	$\Delta P_{3,18}^{\mathrm{L}}$	$\Delta P_{3,19}^{\mathrm{L}}$
0.01	0.01	0.005	0.005	0.005	0	0.01

$\Delta P_{4,20}^{\mathrm{L}}$	$\Delta P_{4,21}^{\mathrm{L}}$	$\Delta P_{4,22}^{\mathrm{L}}$	$\Delta P_{4,23}^{\mathrm{L}}$	$\Delta P_{4,24}^{\mathrm{L}}$	$\Delta P_{4,25}^{\mathrm{L}}$	$\Delta P_{4,26}^{\mathrm{L}}$	$\Delta P_{4,27}^{\mathrm{L}}$
0.005	0	0.005	0	0	0.005	0	0.005

$\Delta P_{5,28}^{\mathrm{L}}$	$\Delta P_{5,29}^{\mathrm{L}}$	$\Delta P_{5,30}^{\mathrm{L}}$	$\Delta P_{5,31}^{\mathrm{L}}$	$\Delta P_{5,32}^{\mathrm{L}}$
0.01	0.01	0	0.01	0

$\Delta P_{6,33}^{\mathrm{L}}$	$\Delta P_{6,34}^{\mathrm{L}}$	$\Delta P_{6,35}^{\mathrm{L}}$	$\Delta P_{6,36}^{\mathrm{L}}$	$\Delta P_{6,37}^{\mathrm{L}}$	$\Delta P_{6,38}^{\mathrm{L}}$	$\Delta P_{6,39}^{\mathrm{L}}$	$\Delta P_{6,40}^{\mathrm{L}}$
0.01	0	0.01	0.005	0	0.01	0.005	0

$\Delta P_{7,41}^{\mathrm{L}}$	$\Delta P_{7,42}^{\mathrm{L}}$	$\Delta P_{7,43}^{\mathrm{L}}$	$\Delta P_{7,44}^{\mathrm{L}}$	$\Delta P_{7,45}^{\mathrm{L}}$	$\Delta P_{7,46}^{\mathrm{L}}$
0	0	0	0.005	0	0.005

6.4.6 Summary

Section 6.4 provided a description of the key components in the proposed CMPC design for the LFC of the 7-area deregulated network. Some expressions in this section were drawn directly from Section 4.4.

6.5 Simulation and discussion

In this section, simulation results obtained from utilising the proposed CMPC scheme as the LFC controller of the 7-area deregulated benchmark model are presented; discussions of the results are also provided. The system parameters considered in Chapter 5 are also used here, and they are presented in Tables A.1, A.2 and A.3. Also, the same DPM employed in Chapter 5 is used and this is given in (A.7). The capacity ratings considered for each control area here are the same as that used in case-2 and case-3 in Chapter 5. A sampling time $t_s = 0.1$ s is used. Note that the model utilised in the CMPC design is also used to represent the 7-area system.

In the CMPC, the input weighting $R = 0.01\mathrm{I_u}$, where $\mathrm{I_u}$ is an indentity matrix of dimension 33 (total number of GenCos). The state weighting $Q \in \mathbb{R}^{79 \times 79}$ is a postive semi-definite matrix that penalises each Δf_i, $\Delta P_i^{\mathrm{tie}}$ and $\Delta P_{i,\mathrm{k}}^{\mathrm{M}}$ of GenCos participating in supplementary control; these GenCos are the ones with a nonzero $\gamma_{i,\mathrm{k}}$ in Table A.1. The number of degrees of freedom

in control used, $n_c = 30$, and the constraints are checked $n_y = 5n_c$ steps into the future; the reason behind the choice of n_y is is stated in Section 4.5. Similar to the results in Chapter 4, an infinite horizon LQR is also simulated here, with the same Q , R, and initial states as the CMPC, and the results presented alongside.
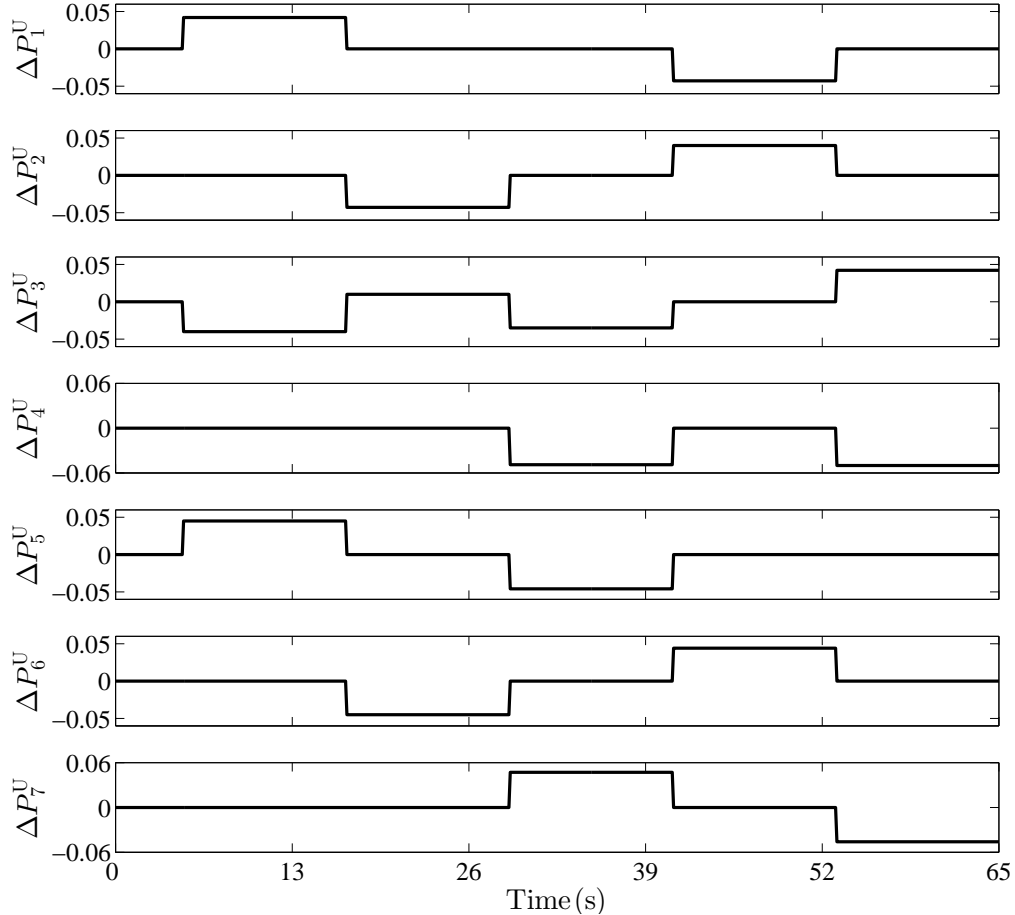
Figure 6.3: Uncontracted load changes in each area

The case-1 in Section 4.5 focused on the scenario where DisCos self-provide LFC via intra-area and inter-area bilateral LM contracts (only contracted load changes) with no uncontracted load changes present, that is $\Delta P_i^{\mathrm{U}} = 0$. This is similar to what was considered in Section 5.5 and thus the strictly-bilateral-LM contracts scenario is not considered here. Similar to case-2 Section 4.5, the simulation here focuses on the scenario where both contracted load changes (mostly procured, in practice, by DisCos via bilateral LM contract) and uncontracted load changes (commonly procured by a TSO from GenCos that submitted incremental power/energy bids in the poolco market) are acting.

The contracted load change of each DisCo is assumed to be fixed over the simulation time considered (65 s) and it is presented in Table 6.1. Some DisCos have a zero contracted demand and they represent DisCos that have not purchased an LM contract; it is assumed here that
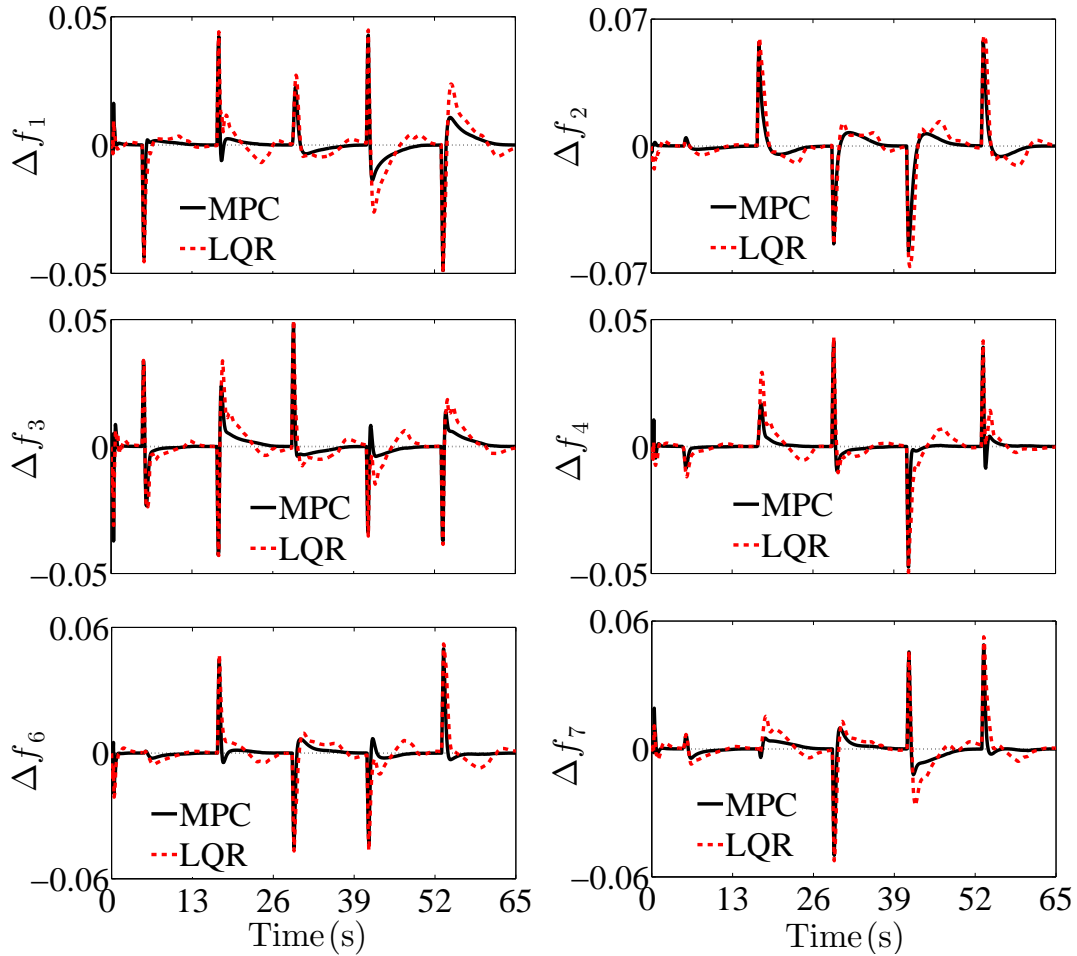
Figure 6.4: Frequency deviation Δf_i Hz in each control area; Δf_5 is omitted as its trend is similar to the frequency deviations shown. The frequency deviations are expected to converge to zero (black dotted lines) at steady state when the load disturbances have been completely rejected.

load changes from such DisCos form part of the uncontracted load changes. The uncontracted load change in each area is shown in Figure 6.3.

The values of the GRC and limits on the input of GenCos under supplementary control have been plotted as upper and lower bounds (black dotted lines) alongside the generation rates $\Delta \dot{P}_{i,k}^{M}$ in Figure 6.8 and control inputs $\Delta P_{i,k}^{C}$ in Figures 6.9 and 6.10 signals of the GenCos. In each area contracted load changes only occur in the first 5 s ($\Delta P_{i}^{U} = 0$ in the first 5 s in areas 1-7) before uncontracted changes set in; this is done to show that the net tie line flow deviation $\Delta P_{i}^{\text{tie}}$ in each area returns to its scheduled (contracted) value in the presence of uncontracted load variations (which is supplied locally).

Figures 6.4, 6.5 and 6.6, respectively, show the frequency deviations (Δf_5 is omitted), net tie line flow deviations (ΔP_6^{tie} is omitted) and area control errors (ACE$_5$ omitted) of each area. As expected, Δf_i and ACE$_i$ settle to a zero value at steady state after a load disturbance; this
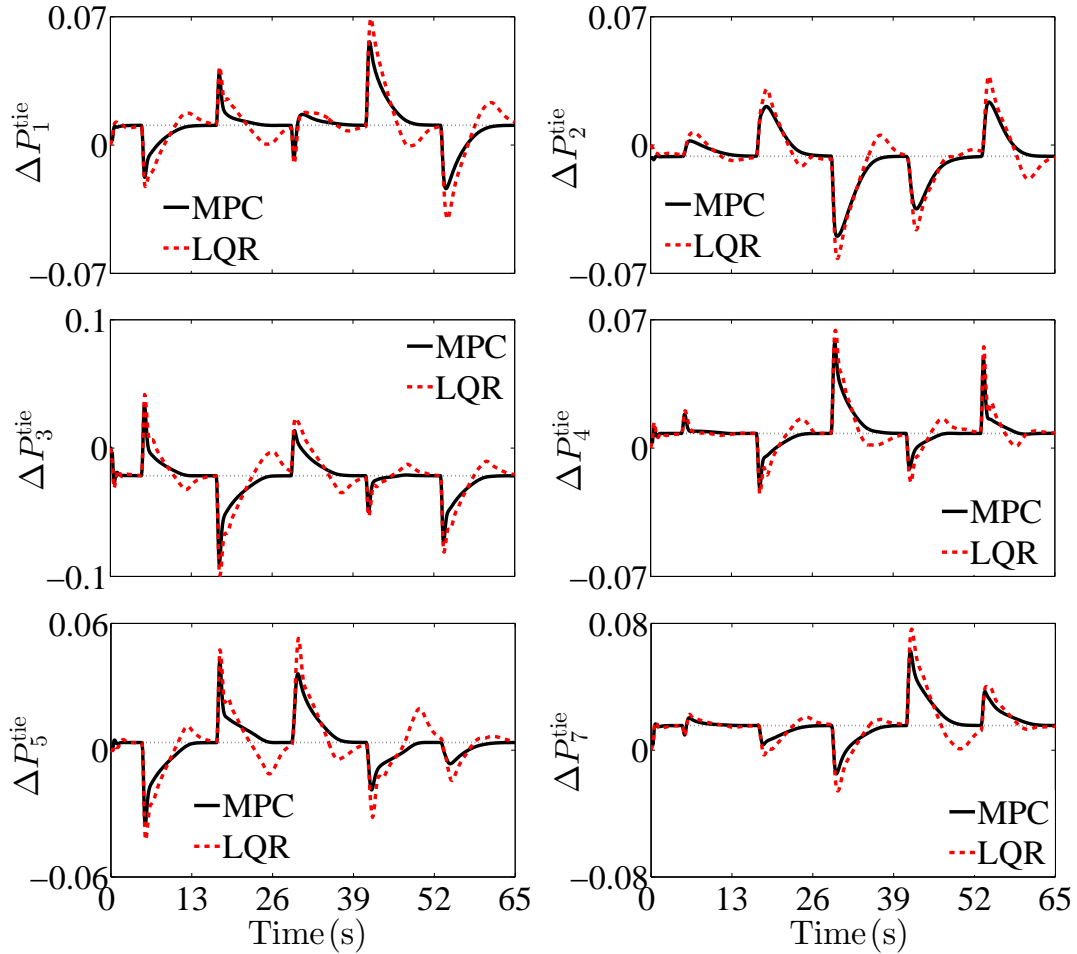
Figure 6.5: The net tie line flow deviation ΔP_i^{tie} pu in each control area. The black dotted lines denote the scheduled or contracted net incremental tie line flow $\Delta P_i^{\text{tie,sch}}$ in each area. It is expected that each ΔP_i^{tie} settles at $\Delta P_i^{\text{tie,sch}}$ since the value of $\Delta P_i^{\text{tie,sch}}$ is set by contracted inter-area contracts (fixed), and any uncontracted load change in an area is supplied locally. ΔP_6^{tie} is omitted.

indicates that the disturbance has been rejected and the balance between active power supply and system load has been restored. Also, it can be seen that each ΔP_i^{tie}, at steady, converges to its scheduled value (black dotted lines) even in the presence of uncontracted variations; this shows that the uncontracted load changes in each area are supplied by GenCos in the area where the load changes had occurred.

The change in power output of each GenCo is shown in Figure 6.7, where the ouputs of only three GenCos are displayed for each area. The desired outputs of the GenCos have been plotted alongside and they are shown as the black dotted lines; these are calculated using the first expression in (5.11). The GenCos, from Figure 6.7, with a fixed desired outputs are on bilateral LM contracts only (supplies contracted demands only) while the other GenCos supply both contracted and uncontracted load changes. It can be observed that each GenCo tracks the desired reference.
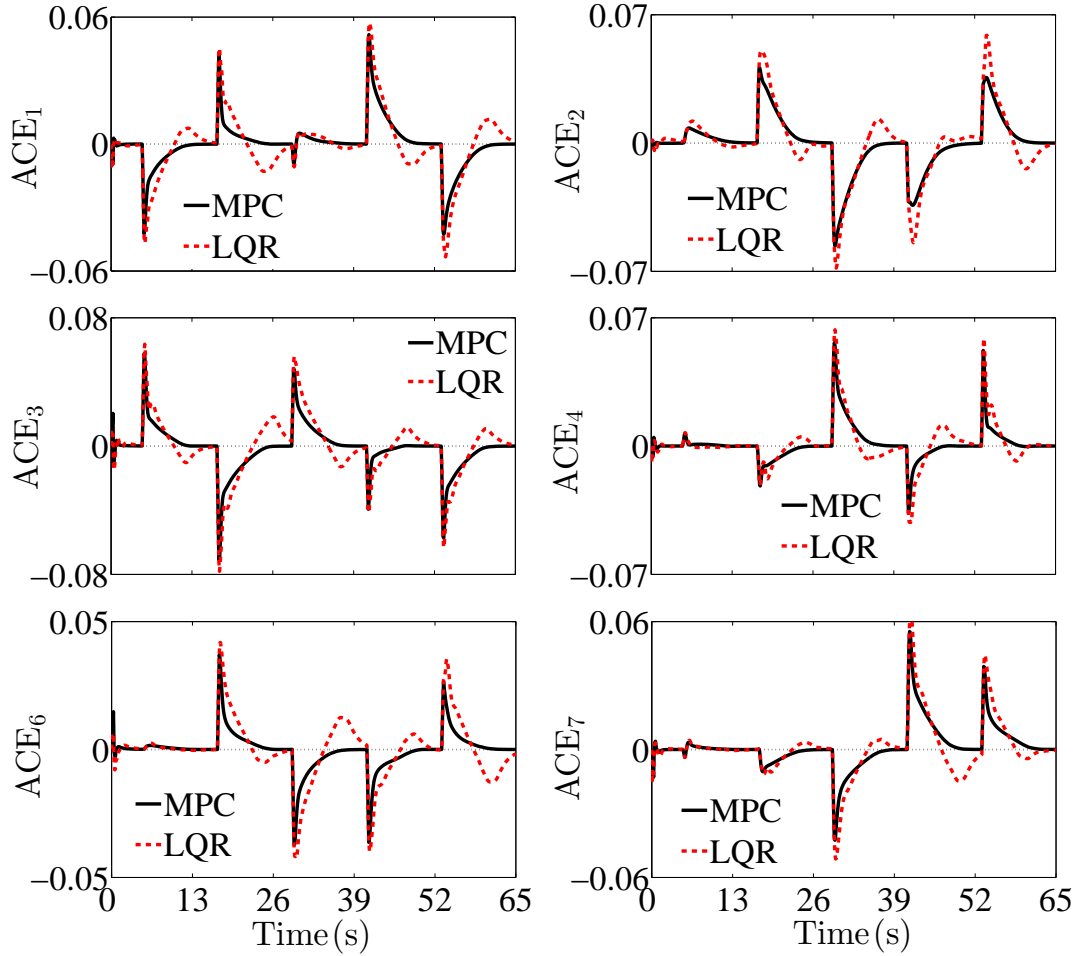
Figure 6.6: Area control error (ACE) in each area. It is expected that each ACE converges to zero (black dotted lines) at steady state when load changes have been completely rejected. ACE_5 also converged to zero but omitted.

The generation rate of the GenCos (one generation rate shown for each area) and the control signals to the GenCos (two inputs shown for each area) are shown in Figure 6.8 and Figure 6.9 - 6.10 respectively. From the $\Delta \dot{P}_{i,k}^{M}$ and $\Delta P_{i,k}^{C}$ signals, it is seen that the CMPC handles the constraints more effectively because it has an explicit knowledge of it while the LQR based scheme results in more saturation of the generation rate and control input. The effect of this can be seen in the frequency deviations (see Figures 6.4), net tie line deviations (see Figure 6.5), area control error (see Figure 6.6) and change in power outputs (see Figure 6.7) were the magnitudes of undershoots and overshoots are larger with the LQR controller. It can also be seen from Figures 6.9 - 6.10 that the input constraints of the indvidual units on supplementary control are handled effectively by the CMPC scheme.
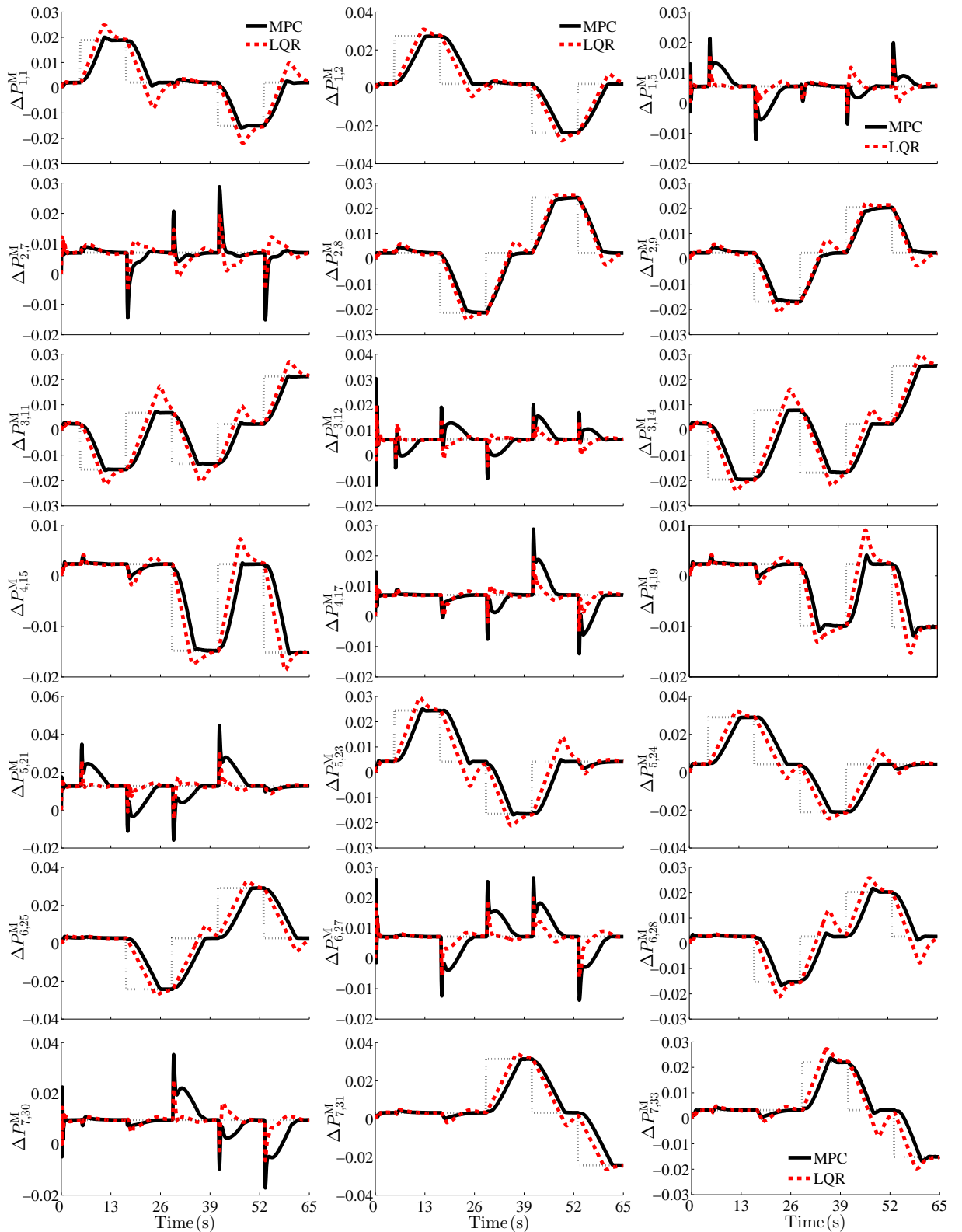
Figure 6.7: The change in the output power $\Delta P_{i,k}^{\mathrm{M}}$ pu of each GenCos in the 7-area system. The outputs of only three GenCos in an area are displayed. Black dotted lines are the desired generation of the GenCos whose outputs are displayed.
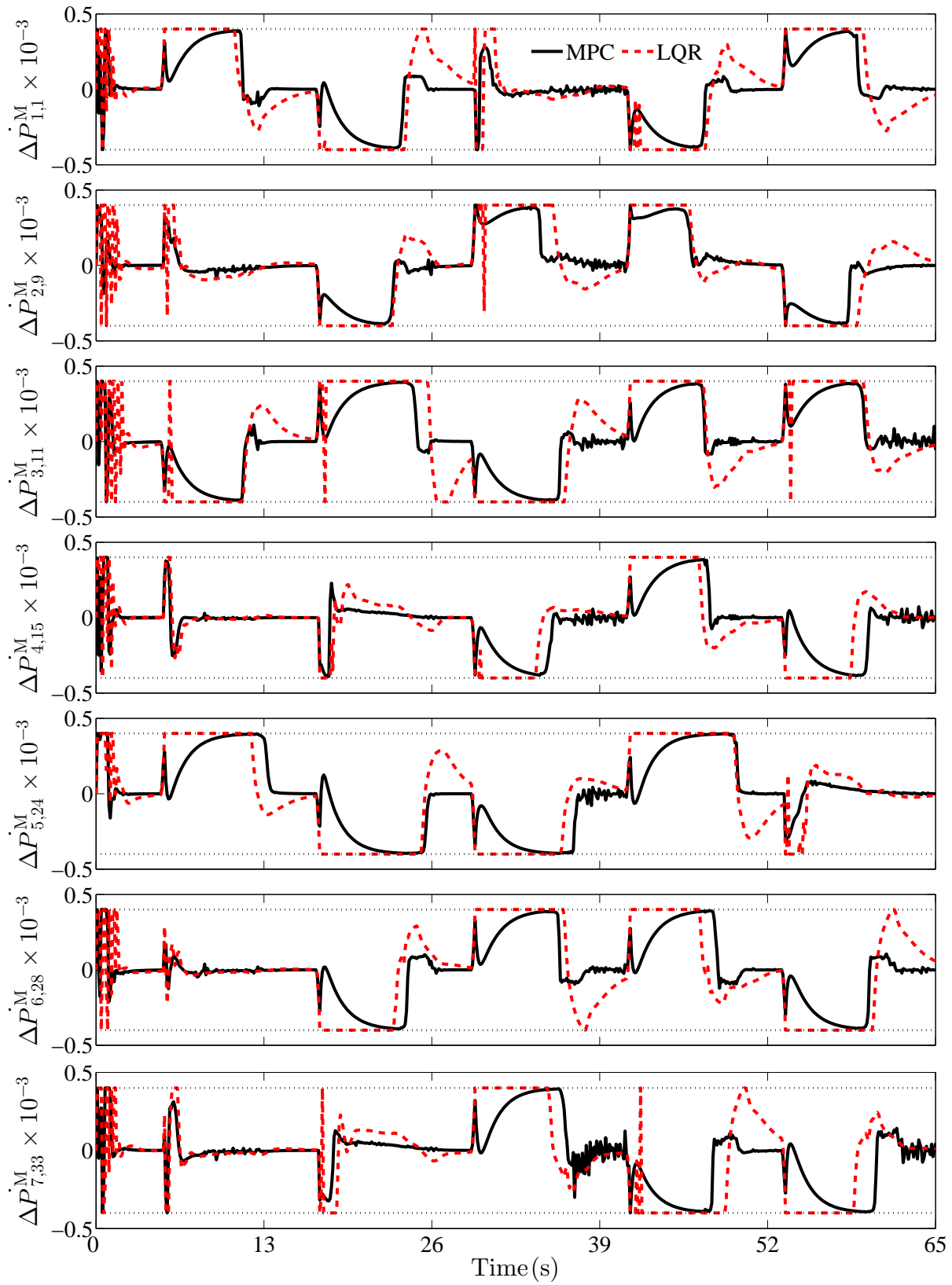
Figure 6.8: Generation rate of GenCos $\Delta \dot{P}_{i,k}^{M}$ pu/s. The black dotted lines are the constraint bounds. A single $\Delta \dot{P}_{i,k}^{M}$ per control area is displayed as the others behaved in a similar manner.
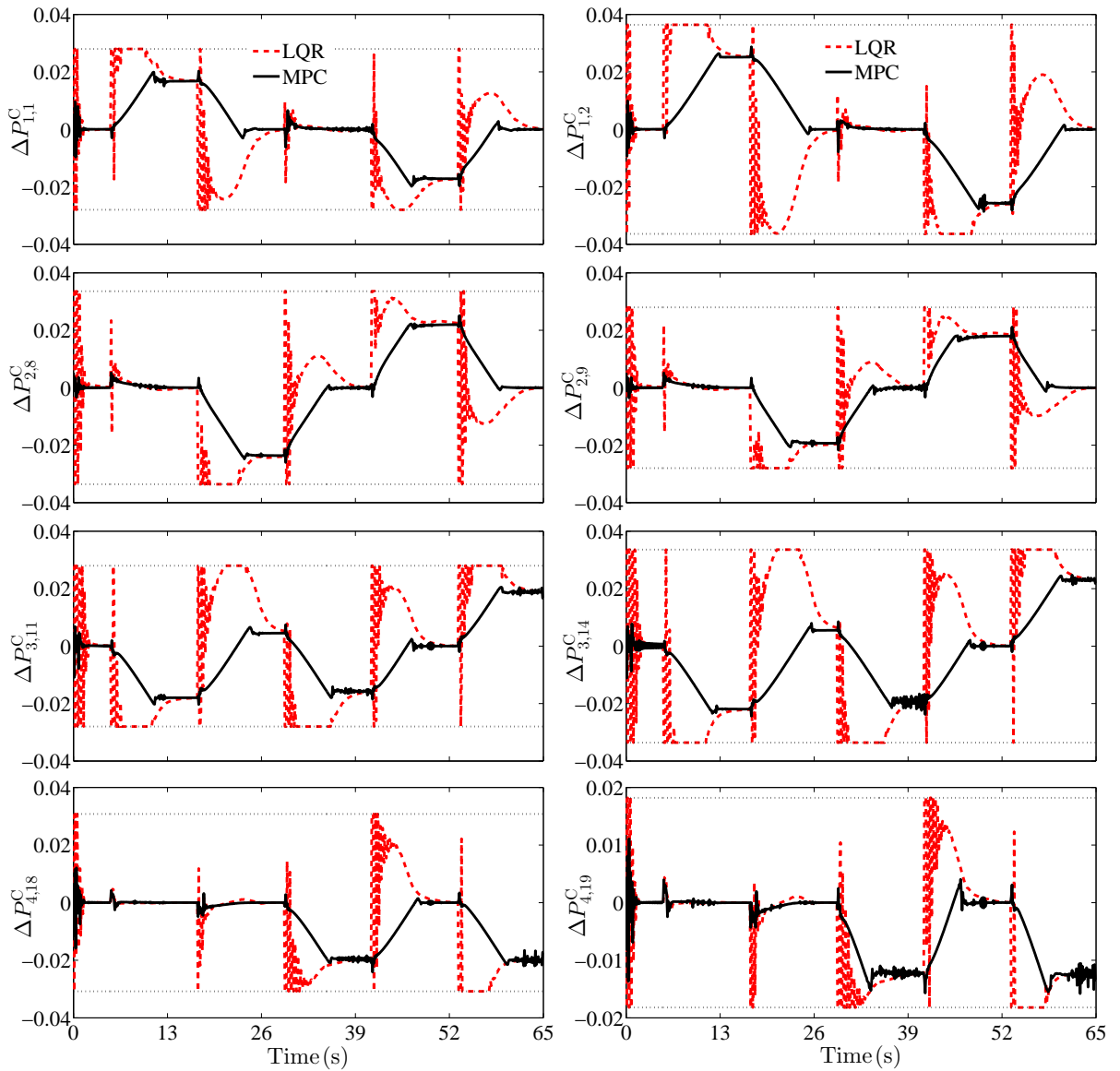
Figure 6.9: The control input to each GenCo, with the input limits shown in the black dot-ted lines. GenCos in areas 1-4 are considered here, and two inputs in each control area are displayed.

6.6   Conclusion

In this chapter, the utilisation of a centralised MPC scheme is proposed for the accomplishment of load frequency control in a deregulated (new) power system environment, where a more proper setting in terms of the number of interconnected control areas, rated capacities of CAs and the structure of control inputs to GenCos was considered. The proposed scheme, applied to a 7-area system developed in Chapter 5, is effective with respect to the main objectives of LFC; it works by coordinating the dynamic behaviour of the system when contracted load changes are acting and rejects uncontracted load disturbances.
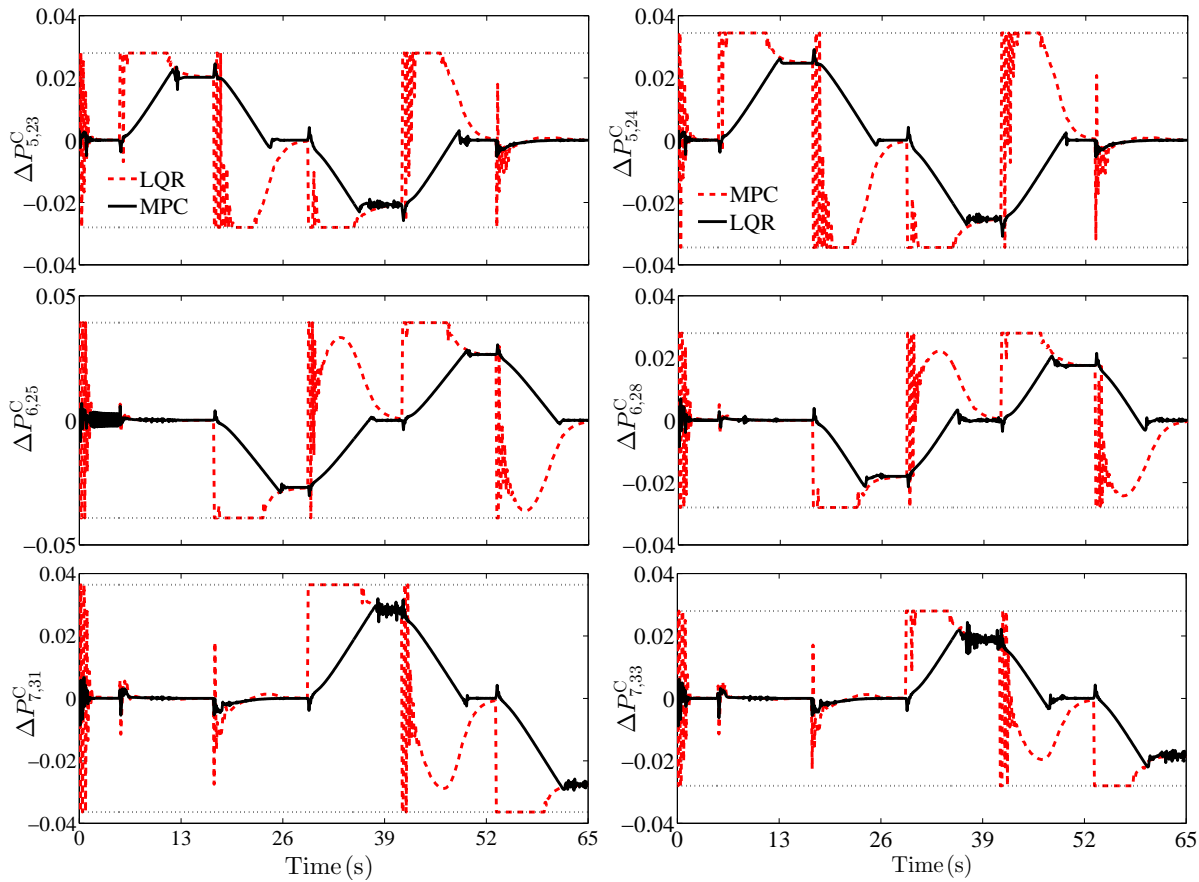
Figure 6.10: The control input to each GenCo, with the input limits shown in the black dotted lines. GenCos in areas 5-7 are considered here, and two inputs in each control area are displayed.

Furthermore, it was shown that by explicitly incorporating the area participation factors of each generating unit (GenCo) in the MPC cost, separate control inputs, satisfying constraints, can be computed for each generating unit in an area. Hence, this addresses the limitation of previous works where a single control input is computed for an area.

However, the scheme might not be realistic for large scale systems where CAs have large geographical separation. Hence, the next chapter will investigate a distributed MPC architecture for deregulated LFC and the centralised scheme proposed here will serve as a benchmark to ascertain the performance of the distributed scheme.

Chapter 7

Distributed model predictive load frequency control of a deregulated power system

7.1 Introduction

Chapter 6 extended the CMPC proposed in Chapter 4 by applying it to the relatively large scale system (7-area deregulated benchmark model). Also, some modifications were made to the governor model which allowed the input constraints of each generating unit (GenCo) in an area to be handled. However, the predictive control schemes proposed in Chapters 4 and 6 are purely centralised and may not be practicable for the increasingly large scale power networks, where CAs are geographically far apart and operated by different organisations.

Consequently, this chapter proposes a distributed model predictive control strategy for tracking incremental load changes, suitable to any finite number of control areas (subsystems), and thus, represents a more pragmatic LFC framework for large scale interconnected networks. The proposed DMPC is non-cooperative and developed to operate using output feedback, where distributed observers using local measurements (area control error) are designed and utilised to estimate each subsystem's states and unmeasured disturbances (uncontracted load changes). The 4-area and the 7-area deregulated benchmark models developed in Chapter 5 are utilised as case studies models to demonstrate the efficacy of the proposed controller; the two models are vital to demonstrate the scalability of the proposed DMPC and provide more evidence of its efficacy. The control scheme accounts for the generation rate constraints and input limits of each GenCo participating in supplementary control, and unlike other non-cooperative schemes, is simple and devoid of extensive offline parameter tuning. Some comparisons and discussions are provided between the proposed DMPC and alternative model predictive control schemes.

7.2 A brief summary of algorithms that will be proposed and compared

In this chapter, three different non-centralised MPC algorithms will be proposed and compared against a centralised MPC alogorithm serving as a benchmark. In order words, four different MPC algorithms, which consider state and input constraints, will be compared. The centralised MPC (CMPC) algorithm is exactly the one that was proposed in Chapter 6 and tested on the 7-area deregulated benchmark model; the CMPC algorithm can easily be adapted to the 4-area deregulated LFC problem and thus the details will not be repeated in this chapter. Note that in the CMPC scheme, a single model predictive controller performs the frequency regulation task in the entire multi-area network.

For the non-centralised MPC algorithms, firstly, a DMPC algorithm is proposed where a local MPC handle LFC tasks in each subsystem (control area), and the subsystem communicates its previous state predictions, previous optimal input sequence, contracted load changes (measured at every sampling instant), and uncontracted load changes (estimated at every sampling instant) to other subsystems (CAs), which are used by their local MPC schemes. Thus, we have a fully connected DMPC algorithm and it is called dense DMPC (dDMPC) in this thesis; the reason behind the term "dense" is described in Section 7.5. Moreover, each local subsystem communicates once within a sampling instant and its MPC minimises a local cost function, hence, the dDMPC belongs to the non-cooperative, non-iterative category. In addition, a local Luenberger observer is designed to estimate local system states and uncontracted load changes in each CA using a local area control error (ACE) measurements, and therefore the dDMPC algorithm operates using output feedback. Each local Luenberger observer uses current states' information, inputs and contracted load changes from all of the other CAs; thus fully connected distributed observers operates with the dDMPC.

Next, a partially connected DMPC algorithm is proposed where each CA, with a local MPC handling LFC tasks, communicates with their direct neighbours only, that is, each CA communicates with the CAs that it shares a tie line with only. Besides, only previous state predictions and contracted load changes are exchanged between subsystems. This is called sparse DMPC (sDMPC) in this thesis and the reason for the term "sparse" is described in Section 7.5. The sDMPC algorithm is developed from the dDMPC by simply "cutting off" exchanges of previous optimal input sequences and uncontracted load changes between subsystems, and limiting the exchange of state predictions and contracted load changes to direct neighbours. The only exception is the subsystem or CA whose net tie line power was eliminated from the states considered in the benchmark models, where it was expressed as a linear combination of the net tie line flows in the other CAs; see Sections 5.3.3, 5.4.2 and 5.6.1; the CA receives previous state predictions and contracted load change information from all of the other CAs and it is

named "dependent CA" in here. Furthermore, the sDMPC operates with partially connected distributed observers, each estimating subsystem's states and uncontracted load changes within its CA using local ACE measurements. The local observers only use current state and contracted load change information from direct neighbours. An exception to this is the dependent CA where its local observer uses the current state information from all of the other CAs. The sDMPC algorithm belongs to the non-cooperative, non-iterative category.

The third of the non-centralised MPC paradigm is a decentralised MPC (DeMPC) algorithm. Here, local MPCs handles LFC tasks within their CAs independently without an exchange of information between CAs or subsystems. Moreover, the local observers also operate in a completely decentralised fashion. The DeMPC algorithm is obtained from the dDMPC scheme by disconnecting all forms of communication between CAs/subsystems.

This chapter has been drawn from [37, 38] and its a key **contribution** in this thesis. The remaining parts of this chapter is organised as follows: Section 7.3 summarises the main contributions of this chapter; Section 7.4 provides some information about the benchmark models; Section 7.5 clarifies the concept of sparse and dense; Section 7.6 describes the main assumptions considered in the DMPC and distributed observer designs; Section 7.7 presents the key parts of the proposed DMPC algorithms; Section 7.8 shows simulation results from testing the proposed DMPC on the 4-area and 7-area benchmark models, and also provides discussions; Section 7.9 gives some concluding remarks.

7.3 A summary of the main contributions

This chapter makes the following contributions:

- Proposes DMPC (sDMPC and dDMPC) algorithms for LFC problems, and demonstrates its efficacy on a 4-area and a 7-area benchmark systems with unequal CA ratings. It is shown how decentralised LFC in a deregulated power network may be performed by a simple distributed MPC scheme, without reliance on excessive offline tuning of controller parameters and prohibitively complex invariant sets (please see [218]); the price is the lack of feasibility and stability guarantees, but the approach is shown to work effectively, with good closed-loop performance on the representative 4-area and 7-area power systems.

- Designs and utilises distributed observers to estimate uncontracted load disturbances and local subsystem states from area control error measurements, thus the proposed DMPC is output feedback.

- Generation rate constraints and input limits of each of the GenCos participating in a TSO's supplementary control are considered individually in the DMPC design and simulations.

- The consideration of discretisation scheme on both performance and on system dynamics and information sharing requirements. Note that this is an issue that is overlooked in both the DMPC literature, and the LFC literature where the control design is model based. The practical implications, especially in terms of what information needs to be shared, are highly significant. This contribution relates to how discrete time subsystem models used by local MPCs are obtained and it is clarified in Section 7.5.

- Lastly, a performance and cost comparison of centralised MPC (benchmark), decentralised MPC (DeMPC), sparse DMPC (sDMPC) and dense DMPC (dDMPC) is made (the concept of sparse and dense are clarified in Section 7.5).

7.4 Description of benchmark models

As emphasised earlier, two different deregulated LFC models will be used to test the MPC algorithms in this chapter; these are the 4-area and the 7-area deregulated LFC models. These models were developed in Chapter 5, hence their modelling details are skipped. In Chapter 6, a modification was made to the general form of the governor dynamics presented in (5.8) so as to account for the input constraints of each GenCo[1]; see Section 6.3. The 7-area benchmark model considered here is the one with the modified governor dynamics used in Chapter 6. The 4-area model is considered for the first time in this chapter and its governor dynamics are also modified; thus the input constraints of each GenCo in the 4-area deregulated network will be accounted for separately in the MPC algorithms. The modified governor dynamics of the 4-area system have exactly the same form as the one presented in Section 6.3 for the 7-area system; however, they are described in the following subsection for convenience.

7.4.1 Modified governor dynamics : 4-area system

The modified dynamics of the governors in the 4-area deregulated network, based on the general form in (6.1) and the index set information in Section 5.6 and Table 5.5 are:

---

[1]A GenCo is represented by a single generating unit whose model consists of a governor and a turbine model.

$$
\begin{aligned}
\Delta \dot{P}_{1,1}^{\mathrm{V}} &= \frac{1}{T_{\mathrm{G}_{1,1}}}\Big(\Delta P_{1,1}^{\mathrm{C}} - \Delta P_{1,1}^{\mathrm{V}} - \frac{\Delta f_1}{R_{1,1}} + S_{1,1}\Big), \cdots, \Delta \dot{P}_{1,3}^{\mathrm{V}} = \frac{1}{T_{\mathrm{G}_{1,3}}}\Big(\Delta P_{1,3}^{\mathrm{C}} - \Delta P_{1,3}^{\mathrm{V}} \\
&\quad - \frac{\Delta f_1}{R_{1,3}} + S_{1,3}\Big) \tag{7.1a}
\end{aligned}
$$

$$
\begin{aligned}
\Delta \dot{P}_{2,4}^{\mathrm{V}} &= \frac{1}{T_{\mathrm{G}_{2,4}}}\Big(\Delta P_{2,4}^{\mathrm{C}} - \Delta P_{2,4}^{\mathrm{V}} - \frac{\Delta f_2}{R_{2,4}} + S_{2,4}\Big), \ \Delta \dot{P}_{2,5}^{\mathrm{V}} = \frac{1}{T_{\mathrm{G}_{2,5}}}\Big(\Delta P_{2,5}^{\mathrm{C}} - \Delta P_{2,5}^{\mathrm{V}} \\
&\quad - \frac{\Delta f_2}{R_{2,5}} + S_{2,5}\Big) \tag{7.1b}
\end{aligned}
$$

$$
\vdots
$$

$$
\begin{aligned}
\Delta \dot{P}_{4,9}^{\mathrm{V}} \quad & \frac{1}{T_{\mathrm{G}_{4,9}}}\Big(\Delta P_{4,9}^{\mathrm{C}} - \Delta P_{4,9}^{\mathrm{V}} - \frac{\Delta f_4}{R_{4,9}} + S_{4,9}\Big), \ \Delta \dot{P}_{4,10}^{\mathrm{V}} = \frac{1}{T_{\mathrm{G}_{4,10}}}\Big(\Delta P_{4,10}^{\mathrm{C}} \\
&\quad - \Delta P_{4,10}^{\mathrm{V}} - \frac{\Delta f_4}{R_{4,10}} + S_{4,10}\Big) \tag{7.1c}
\end{aligned}
$$

7.4.2 State space representation

A generic continuous time (CT) state space equation can be written as:

$$
\dot{x} = A^{\mathrm{c}}x + B^{\mathrm{c}}u + B^{\mathrm{dc}}d + B^{\mathrm{bc}}b; \quad y = C^{\mathrm{c}}x + D^{\mathrm{c}}d \tag{7.2}
$$

The state space form in (7.2) is exactly the same as the ones presented in previous chapters; it is restated for completeness. It also covers for the 4-area and 7-area benchmark models. Due to the modification made to governor dynamics of the 4-area model, the dimension of its input vector is changed, and the new vector of inputs is:

$$
u = \begin{bmatrix} \Delta P_1^{\mathrm{C}} \\ \Delta P_2^{\mathrm{C}} \\ \Delta P_3^{\mathrm{C}} \\ \Delta P_4^{\mathrm{C}} \end{bmatrix} \in \mathbb{R}^{10}; \Delta P_1^{\mathrm{C}} = \begin{bmatrix} \Delta P_{1,1}^{\mathrm{C}} \\ \Delta P_{1,2}^{\mathrm{C}} \\ \Delta P_{1,3}^{\mathrm{C}} \end{bmatrix}, \Delta P_2^{\mathrm{C}} = \begin{bmatrix} \Delta P_{2,4}^{\mathrm{C}} \\ \Delta P_{2,5}^{\mathrm{C}} \end{bmatrix}, \Delta P_3^{\mathrm{C}} = \begin{bmatrix} \Delta P_{3,6}^{\mathrm{C}} \\ \Delta P_{3,7}^{\mathrm{C}} \\ \Delta P_{3,8}^{\mathrm{C}} \end{bmatrix}, \Delta P_4^{\mathrm{C}} = \begin{bmatrix} \Delta P_{4,9}^{\mathrm{C}} \\ \Delta P_{4,10}^{\mathrm{C}} \end{bmatrix}
$$

Obserse that in Section 5.6, $u \in \mathbb{R}^4$ and for the modified governor case (4-area system), $u \in \mathbb{R}^{10}$. The dimensions of other vectors in (7.2) remain unchanged.

Remark 7.4.1. *The model of the LFC function in the multi-area system leads to state space models coupled via states in both the state equation and the output equation, and, hence, coupled control and coupled estimation problems.*

7.5 Clarification of the concept of sparse and dense

The discussion presented in this section is applicable to the 4-area and 7-area deregulated networks. To illustrate the concept of sparse and dense, consider a hypothetical system which is made up of of three subsystems, shown in Figure 7.1a. Assuming that the system is represented by a CT state space expression given as:

$$
\begin{bmatrix} \dot{\zeta}_1 \\ \dot{\zeta}_2 \\ \dot{\zeta}_3 \end{bmatrix} = \begin{bmatrix} -2 & 1 & -6 \\ -4 & -3 & 0 \\ 9 & 0 & -3 \end{bmatrix} \begin{bmatrix} \zeta_1 \\ \zeta_2 \\ \zeta_3 \end{bmatrix} + \begin{bmatrix} 4 & 0 & 0 \\ 0 & 6 & 0 \\ 0 & 0 & 2 \end{bmatrix} \begin{bmatrix} \omega_1 \\ \omega_2 \\ \omega_3 \end{bmatrix} \tag{7.3a}
$$

$$
\begin{bmatrix} \Upsilon_1 \\ \Upsilon_1 \\ \Upsilon_1 \end{bmatrix} = \begin{bmatrix} 1 & 0 & 0 \\ 0 & 1 & 0 \\ 0 & 0 & 1 \end{bmatrix} \begin{bmatrix} \zeta_1 \\ \zeta_2 \\ \zeta_3 \end{bmatrix} \tag{7.3b}
$$

where ζ_i, ω_i and Υ_i are the state, input and output of the ith subsystem respectively. Clearly it can be seen from Figure 7.1a and the system model in (7.3a) and (7.3b) that the input signals to the system are decoupled, that is, there are no input interactions between each subsystem. Furthermore, it can be seen that there are no interactions between the states of subsystems 2 and 3. We refer to this system as a sparse one. Assuming the CT system, (7.3a) and (7.3b), is decomposed to obtain three CT subsystem models given as:

$$
\dot{\zeta}_1 = -2\zeta_1 + 4\omega_1 + \zeta_2 - 6\zeta_3; \ \Upsilon_1 = \zeta_1 \tag{7.4a}
$$

$$
\dot{\zeta}_2 = -3\zeta_2 + 6\omega_2 - 4\zeta_1; \ \Upsilon_2 = \zeta_2 \tag{7.4b}
$$

$$
\dot{\zeta}_3 = -3\zeta_3 + 2\omega_3 + 9\zeta_1; \ \Upsilon_3 = \zeta_3 \tag{7.4c}
$$

Applying zero-order hold method to discretise each of the subsystems, (7.4a), (7.4b), and (7.4c), separately using a sampling time of 1 s yields:

$$
\zeta_{1,k+1} = 0.135\zeta_{1,k} + 1.729\omega_{1,k} + 0.432\zeta_{2,k} - 2.594\zeta_{3,k} \tag{7.5a}
$$

$$
\zeta_{2,k+1} = 0.050\zeta_{2,k} + 1.900\omega_{2,k} - 1.267\zeta_{1,k} \tag{7.5b}
$$

$$
\zeta_{3,k+1} = 0.050\zeta_{3,k} + 0.634\omega_{3,k} + 2.851\zeta_{1,k} \tag{7.5c}
$$

It can be seen that the discrete time (DT) expressions, (7.5a), (7.5b) and (7.5c) preserved the sparsity of the CT system and this is shown in Figure 7.1b; hence they are called a DT sparse subsystem models. A DMPC algorithm developed where the subsystem model used by each local MPC is obtained by decomposition of the CT centralised system before discretisation is called sDMPC in this thesis. Now consider the case where the CT centralised system, (7.3a)

and (7.3b), is discretised directly by applying zero-order hold method and sampling time of 1 s. The resulting centralised DT state space expression is given as:

$$
\begin{bmatrix} \zeta_{1,k+1} \\ \zeta_{2,k+1} \\ \zeta_{3,k+1} \end{bmatrix} \begin{bmatrix} 0.023 & 0.011 & -0.063 \\ -0.042 & 0.047 & 0.014 \\ 0.094 & 0.005 & 0.018 \end{bmatrix} \begin{bmatrix} \zeta_{1,k} \\ \zeta_{2,k} \\ \zeta_{3,k} \end{bmatrix} + \begin{bmatrix} 0.221 & 0.089 & -0.179 \\ -0.238 & 1.786 & 0.229 \\ 0.536 & 0.257 & 0.119 \end{bmatrix} \begin{bmatrix} \omega_{1,k} \\ \omega_{2,k} \\ \omega_{3,k} \end{bmatrix}
$$
(7.6)

Now, assuming the DT system, (7.6) is decomposed into three subsystems; the resulting DT models for the subsystems are:

$$
\zeta_{1,k+1} = 0.023\zeta_{1,k} + 0.221\omega_{1,k} + 0.011\zeta_{2,k} - 0.063\zeta_{3,k} + 0.089\omega_{2,k} - 0.179\omega_{3,k}
$$
(7.7a)

$$
\zeta_{2,k+1} = 0.047\zeta_{2,k} + 1.786\omega_{2,k} - 0.042\zeta_{1,k} + 0.014\zeta_{3,k} - 0.238\omega_{1,k} + 0.229\omega_{3,k}
$$
(7.7b)

$$
\zeta_{3,k+1} = 0.018\zeta_{3,k} + 0.119\omega_{3,k} + 0.094\zeta_{1,k} + 0.005\zeta_{2,k} + 0.536\omega_{1,k} + 0.257\omega_{2,k}
$$
(7.7c)

From the DT subsystems, (7.7a), (7.7b) and (7.7c), it can be seen that the sparsity of the original CT centralised system is lost; see Figure 7.1c for the resulting system interconnections. A fully connected system has been obtained where each subsystem is coupled via states and input to all other subsystems. We call this new model a dense model. A DMPC algorithm developed were each subsystem model used by a local MPC is obtained by first discretising the centralised CT model before decomposition/partitioning is called a dDMPC in this thesis.

Clearly, dense subsystem models are more accurate than sparse subsystem models, and thus will provide more accurate predictions in the MPC scheme. However, the amount of information that each subsystem will communicate (also receive) in the dense DMPC algorithm would be higher as compared to the sDMPC scheme; this is a very important aspect of DMPC schemes and also LFC, where models are required for the control system design.

7.5.1 Linking the concept of spare and dense to the benchmark models

The CT benchmark models of the 4-area and the 7-area deregulated networks consist of matrices A^c and B^{dc} where A^c is made up of block submatrices A^c_{ii} (local system matrix) and A^c_{ij} (state interaction or coupling matrices) and B^{dc} is made up of B^{dc}_{ii} (local) and B^{dc}_{ij} (coupling). Because not all areas are connected (see Figures 5.3 and 5.13), some A^c_{ij} and B^{dc}_{ij} are zero block matrices (when area i is not connected to area j), and therefore, A^c and B^{dc} are sparse matrices. Furthermore, B^c and B^{bc} are block diagonal matrices, that is, only

(a) CT system (sparse) (b) DT system (sparse) (c) DT system (dense)
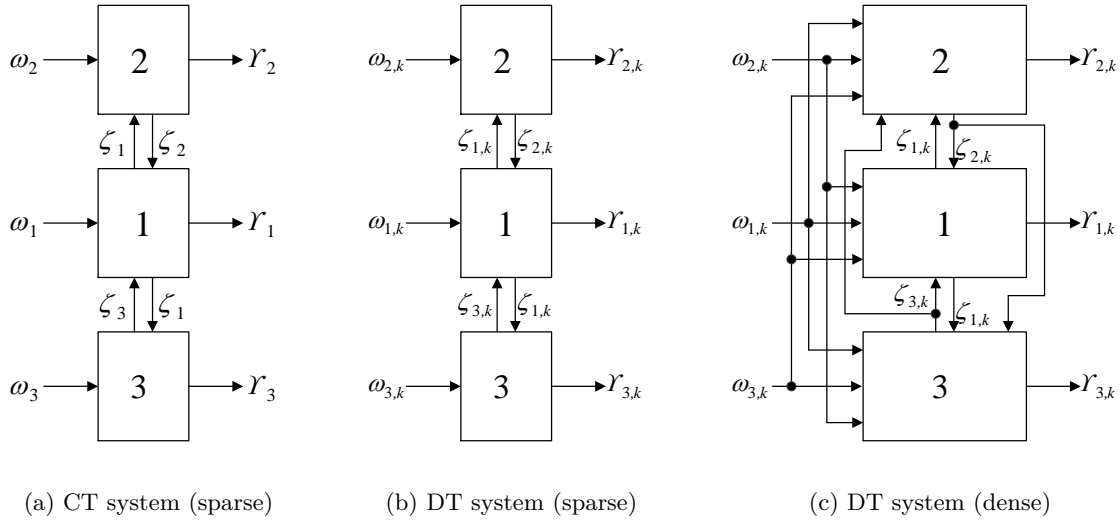
Figure 7.1: An illustration of the concept of sparse and dense

B^c_{ii} and B^{bc}_{ii} are present in CT. Hence the supplementary control signals and uncontracted load changes of each CA (subsystem), in the CT, are decoupled.

If the CT centralised model represented by the state space expression in (7.2) is decomposed to obtain subsystem models and each of the CT subsystem models is subsequently discretised separately; the sparsity of the CT system is preserved. In this thesis, a DMPC algorithm is developed with subsystem models that preserve the centralised system sparsity and as stated earlier, it is termed as a sDMPC algorithm. This approach also introduces a model mismatch with respect to the DT centralised system.

One the other hand, if the CT centralised model (7.2) is discretised before decomposition into subsystems, the sparsity in A^c, B^c, B^{dc}, and B^{bc} is lost and the resulting DT subsystems are fully connected (dense), that is, each subsystem model is coupled through state, input, contracted and uncontracted disturbances to other subsystem models; the original structure of the CT centralised models (and hence the topologies of the 4-area and 7-area networks) is not preserved. In this chapter, a DMPC algorithm will be developed using subsystem models obtained after the discretisation of the centralised systems (applicable to the 4-area and 7-area) and as stated earlier, is termed as a dDMPC algorithm. Moreover, the centralised model in discrete time is used as the plant (power system) and therefore, there are no mismatches between the dense subsystem models and the plant.

The following section will describe the requirements for the development of the DMPC scheme and the main assumptions that should hold; DeMPC scheme is not discussed as its algorithm, as stated in Section 7.2, can be obtained by disconnecting all forms of communication between local subsystems.

7.6 Requirements and key assumptions in DMPC design

From Section 7.3, it can be gathered that the complete DMPC scheme for LFC problems in the deregulated environment would require a local MPC in each CA performing the disturbance rejection tasks (regulating generating units on LFC to track uncontracted load changes based on their individual area participation factors), and a local observer that estimates the states and uncontracted load changes (unmeasured disturbances) associated with its subsystem and supply them to its local MPC; these tasks are performed online. Also, the local MPC and its observer will utilise some information received from other CAs. Consider the DT state space equivalent of (7.2), given as:

$$x_{k+1} = Ax_k + Bu_k + B^d d_k + B^b b_k, \quad y_k = Cx_k + Dd_k \qquad (7.8)$$

where $x_k \in \mathbb{R}^{n_x}$, $u_k \in \mathbb{R}^{n_u}$ and $y_k \in \mathbb{R}^{n_y}$. Assuming that (7.8) can be partitioned and expressed in the form presented in (3.36) and (3.37), then the ith subsystem model can be expressed as:

$$x_{k+1}^{[i]} = \underbrace{A_{ii}x_k^{[i]} + B_{ii}u_k^{[i]} + B_{ii}^d d_k^{[i]} + B_{ii}^b b_k^{[i]}}_{\text{Local subsystem}} + \underbrace{\sum_{\substack{j \in \mathcal{A} \\ i \neq j}} \{A_{ij}x_k^{[j]} + B_{ij}u_k^{[j]} + B_{ij}^d d_k^{[j]} + B_{ij}^b b_k^{[j]}\}}_{\text{coupling}} \qquad (7.9a)$$

$$y_k^{[i]} = C_{ii}x_k^{[i]} + D_{ii}d_k^{[i]} + \underbrace{\sum_{\substack{j \in \mathcal{A} \\ i \neq j}} C_{ij}x_k^{[j]}}_{\text{coupling}} \qquad (7.9b)$$

where $x_k^{[i]} \in \mathbb{R}^{n_x^i}$, $u_k^{[i]} \in \mathbb{R}^{n_u^i}$, $b_k^{[i]} \in \mathbb{R}^{n_b^i}$ and $y_k^{[i]} \in \mathbb{R}^{n_y^i}$. Note that, with respect to the 4-area and 7-area benchmark models, B_{ij} and B_{ij}^b are zero matrices for the sparse subsystem model form. Some of the block matrices A_{ij} and B_{ij}^d are also zero for the sparse case (CAs not linked by tie lines). For the decentralised paradigm, the form of the ith subsystem model is such that coupling terms in (7.9a) and (7.9b) do not exist. Thus, (7.9a) represents a more general ith subsystem and the development of the DMPC schemes will be based on this generic representation. Moreover, there is a C_{ij} term in (7.9b) because ΔP_3^{tie} in (5.32) is a linear combination of the deviation in net tie line powers in other areas (areas 1,2, and 4) and this goes into the ACE calculation in area 3. This is also applicable to the 7-area system where ΔP_2^{tie} in (5.17) is expressed as a linear combination of the deviation in net tie line powers in other areas (areas 1,3,4,5,6 and 7). Hence, for the 4-area scenario, only the third row of C_{ij} is nonzero and for the 7-area case, only the second row of C_{ij} is nonzero. Thus, state couplings exist in the output equation, resulting in a coupled estimation problem. Expressing the triple $(x_k^{[i]}, y_k^{[i]}, u_k^{[i]})$ in (7.9a) and (7.9b) as a deviation from steady state targets $(x_{ss}^{[i]}, y_{ss}^{[i]}, u_{ss}^{[i]})$:

$$\overline{\mathrm{x}}_{k+1}^{[i]} = \mathrm{A}_{ii}\overline{\mathrm{x}}_k^{[i]} + \mathrm{B}_{ii}\overline{\mathrm{u}}_k^{[i]} + \sum_{\substack{j\in\mathcal{A} \\ i\neq j}}\{\mathrm{A}_{ij}\overline{\mathrm{x}}_k^{[j]} + \mathrm{B}_{ij}\overline{\mathrm{u}}_k^{[j]}\} \tag{7.10a}$$

$$\overline{\mathrm{y}}_k^{[i]} = \mathrm{C}_{ii}\overline{\mathrm{x}}_k^{[i]} + \sum_{\substack{j\in\mathcal{A} \\ i\neq j}}\mathrm{C}_{ij}\overline{\mathrm{x}}_k^{[j]} \tag{7.10b}$$

$$\overline{\mathrm{x}}_k^{[i]} = \mathrm{x}_k^{[i]} - \mathrm{x}_{\mathrm{ss}}^{[i]}; \overline{\mathrm{u}}_k^{[i]} = \mathrm{u}_k^{[i]} - \mathrm{u}_{\mathrm{ss}}^{[i]}; \overline{\mathrm{y}}_k^{[i]} = \mathrm{y}_k^{[i]} - \mathrm{y}_{\mathrm{ss}}^{[i]} \tag{7.10c}$$

where the triple $(\mathrm{x}_{\mathrm{ss}}^{[i]}, \mathrm{y}_{\mathrm{ss}}^{[i]}, \mathrm{u}_{\mathrm{ss}}^{[i]})$ is introduced to achieve offset free tracking of uncontracted load changes; $\overline{\mathrm{x}}_k^{[i]}$, $\overline{\mathrm{u}}_k^{[i]}$ and $\overline{\mathrm{y}}_k^{[i]}$ represents a deviation of the variables from a steady state value; this is commonplace in the MPC literature and it is a strategy to introduce integral action in MPC problems [132]; $\mathcal{A}$ is the index set of the CAs (subsystems) in the network (global system) and it is expressed as $\mathcal{A} = \{1, 2, \cdots, \mathrm{N}\}$; $\mathrm{N} = 4$ for the 4-area network and $\mathrm{N} = 7$ for the 7-area network. Note that the centralised DT model (7.8) in terms of deviation variables can be obtained from (7.10a) and (7.10b) by aggregation; it takes the same form as (4.17) and its given as:

$$\overline{\mathrm{x}}_{k+1} = \mathrm{A}\overline{\mathrm{x}}_k + \mathrm{B}\overline{\mathrm{u}}_k; \quad \overline{\mathrm{y}}_k = \mathrm{C}\overline{\mathrm{x}}_k \tag{7.11}$$

To successfully design an output feedback DMPC scheme (local MPC and observer) for frequency regulation, it is required that the benchmark models (representing the power systems) fulfil two key assumptions:

- One dwells on the existence of local fixed state feedback gains K_{ii}, each of which stabilises the subsystem given in (7.10a) assuming the coupling term $\sum_{\substack{j\in\mathcal{A} \\ i\neq j}}\{\mathrm{A}_{ij}\overline{\mathrm{x}}_k^{[j]} + \mathrm{B}_{ij}\overline{\mathrm{u}}_k^{[j]}\}$ is absent, and when these feedback gains are aggregated into a block diagonal gain matrix K (decentralised stabilsing control for a coupled system), it should stabilise the global (centralised) system given in (7.11) which embeds the couplings in A and B matrices.

- The other is the dual of the decentralised control and it dwells on the existence of local stabilising observer gains L_{ii} whose aggregation into a block diagonal observer gain matrix L stabilises a centralised observer (decentralised stabilising observer gain for a coupled system).

These gains (K_{ii} and L_{ii}) are determined via offline calculations. In addition, each local MPC would require a terminal weight $P_{fii} = P_{fii}^T \succeq 0$ which when aggregated gives $P_f = P_f{}^T \succeq 0$, where $P_f = \mathrm{blkdiag}(P_{f11}, \cdots, P_{f\mathrm{NN}})$ is the CMPC terminal weight; see Section 3.3.2. These assumptions are considered formally in the following subsections.

7.6.1 Stabilising local feedback gains K_{ii} and terminal weight $P_{f_{ii}}$ (offline)

The following assumption on decentralised stabilisation of the centralised system (7.11) is based on the work in [218] and it is key requirement for the design of DMPC algorithms proposed in this thesis. Before the assumption is stated, it is important to point out that that the local feedback gain K_{ii} is a key component of the control signal $\bar{u}_k^{[i]}$ computed for the ith subsystem/CA; see the ith control law in (7.24).

Assumption 7.1. *There exists a fixed block diagonal gain matrix* $K = \text{blkdiag}(K_{11}, \cdots, K_{NN})$, $N = |\mathcal{A}|$ *and* $K_{ii} \in \mathbb{R}^{n_u^i \times n_x^i}$, $\forall i \in \mathcal{A}$ *such that: (i)* $\rho(A + BK) < 1$, *(ii)* $\rho(A_{ii} + B_{ii}K_{ii}) < 1$ $\forall i \in \mathcal{A}$.

In Assumption 7.1, $|\bullet|$ denotes set cardinality and $\rho(\bullet)$ denotes the spectral radius of a square matrix. If the different subsystems/CAs in the power network are decoupled, that is A_{ij} and B_{ij} are zero matrices, then it is easy to fulfil Assumption 7.1, that is, each K_{ii} can easily be obtained by using the standard LQR or pole placement methods. However, since A_{ij} and B_{ij} are nonzero (A and/or B are/is not block diagonal), then K_{ii} obtained using LQR or pole placement methods may not stabilise the centralised system. To overcome this challenge, the task of obtaining a stabilising decentralised control gain can be transformed into a linear matrix inequality (LMI) optimisation problem [218]. To develop the LMI problem, the Schur complement expression is required:

Lemma 7.1. *A symmetric matrix* Θ *partitioned into low dimensional matrix blocks given as:*

$$\Theta = \begin{bmatrix} \Theta_a & \Theta_b \\ \Theta_b^T & \Theta_c \end{bmatrix} \succ 0, \ \Theta_a = \Theta_a^T \succ 0, \ \Theta_c \succ 0 \tag{7.12a}$$

can be represented as:

$$\Theta_c - \Theta_b^T \Theta_a^{-1} \Theta_b \succ 0, \ \Theta_a \succ 0 \tag{7.12b}$$

Theorem 7.1. *Let the Assumption 7.1 holds. Then the required local feedback gains matrices* K_{ii}, $\forall i \in \mathcal{A}$ *whose aggregate actions can stabilise the system (7.11), and terminal weights* $P_{f_{ii}}$, $\forall i \in \mathcal{A}$ *are given by:*

$$P_{f_{ii}} = S_{ii}^{-1}, \quad K_{ii} = Y_{ii}S_{ii}^{-1} \quad \forall i \in \mathcal{A} \tag{7.13}$$

and S_{ii} *and* Y_{ii} *are the solutions to the following LMIs:*

$$\begin{bmatrix} S_{ii} & A_{ii}S_{ii} + B_{ii}Y_{ii} \\ (A_{ii}S_{ii} + B_{ii}Y_{ii})^T & S_{ii} \end{bmatrix} \succ 0, \ S_{ii} = S_{ii}^T \succ 0 \quad \forall i \in \mathcal{A} \tag{7.14a}$$

$$\begin{bmatrix} S & AS + BY \\ (AS + BY)^T & S \end{bmatrix} \succ 0, \ S = S^T \succ 0 \tag{7.14b}$$

where $Y = \text{blkdiag}(Y_{11}, \cdots, Y_{NN})$, $S = \text{blkdiag}(S_{11}, \cdots, S_{NN})$; $Y_{ii} \in \mathbb{R}^{n_u^i \times n_x^i}$, $S_{ii} \in \mathbb{R}^{n_x^i \times n_x^i}$.

Proof of Theorem 7.1

Let $K = \text{blkdiag}(K_{11}, \cdots, K_{NN})$ be the stabilising decentralised state feedback gain for the global system given in (7.11), the global system in closed-loop is:

$$\bar{x}_{k+1} = (A + BK)\bar{x}_k \tag{7.15a}$$

Employing the Lyapunov criteria for stability to system (7.15a) gives:

$$\bar{x}_k^T (A + BK)^T P_f (A + BK)\bar{x}_k - \bar{x}_k^T P_f \bar{x}_k < 0 \tag{7.15b}$$

where as stated before, $P_f = \text{blkdiag}(P_{f11}, \cdots, P_{fNN})$. The inequality (7.15b) holds for $\bar{x}_k \neq 0$ on condition that:

$$(A + BK)^T P_f (A + BK) - P_f \prec 0 \tag{7.15c}$$

Let $P_f = S^{-1}$ and $K = YS^{-1}$, where $Y = \text{blkdiag}(Y_{11}, \cdots, Y_{NN})$ and $S = \text{blkdiag}(S_{11}, \cdots, S_{NN})$. By substituting these relationships into (7.15c), multiply through by -1, pre-multiplying by S and post-multiply by S gives:

$$S - (AS + BY)^T S^{-1} (AS + BY) \succ 0 \tag{7.15d}$$

Applying Lemma 7.1 to (7.15d) gives:

$$\begin{bmatrix} S & AS + BY \\ (AS + BY)^T & S \end{bmatrix} \succ 0, \ S = S^T \succ 0 \qquad \blacksquare$$

The same procedure is followed to derive the LMI expression for the ith subsystem (7.14a). The LMI problem to compute the local gains K_{ii} and terminal weights $P_{f_{ii}}$ is summarised in Algorithm 7.1

Algorithm 7.1 Computation of local gains K_{ii} and terminal weights $P_{f_{ii}}$ (OFFLINE)

---

1. Given the subsystem matrices A_{ii} and B_{ii} and the global system matrices A and B, and that Assumption 7.1 holds. Define the following unknown local matrices $\mathrm{Y}_{ii} \in \mathbb{R}^{n_u^i \times n_x^i}$, $\mathrm{S}_{ii} \in \mathbb{R}^{n_x^i \times n_x^i}$, $\forall i \in \mathcal{A}$, where $\mathrm{S}_{ii} = \mathrm{S}_{ii}^T \succ 0$, and construct the following block diagonal matrices $\mathrm{S} = \mathrm{blkdiag}(\mathrm{S}_{11}, \cdots, \mathrm{S}_{NN})$, $\mathrm{Y} = \mathrm{blkdiag}(\mathrm{Y}_{11}, \cdots, \mathrm{Y}_{NN})$.

2. Solve the following linear matrix inequalities (LMIs) to obtain the pair $(\mathrm{S}_{ii}, \mathrm{Y}_{ii})$, $\forall i \in \mathcal{A}$:

$$
\begin{bmatrix} \mathrm{S} & \mathrm{AS} + \mathrm{BY} \\ (\mathrm{AS} + \mathrm{BY})^T & \mathrm{S} \end{bmatrix} \succ 0
$$

$$
\begin{bmatrix} \mathrm{S}_{ii} & \mathrm{A}_{ii}\mathrm{S}_{ii} + \mathrm{B}_{ii}\mathrm{Y}_{ii} \\ (\mathrm{A}_{ii}\mathrm{S}_{ii} + \mathrm{B}_{ii}\mathrm{Y}_{ii})^T & \mathrm{S}_{ii} \end{bmatrix} \succ 0 \quad \forall i \in \mathcal{A}
$$

with the added constraints:

$$
\mathrm{S}_{ii} \succ 0 \quad \forall i \in \mathcal{A}, \qquad S \succ 0
$$

The LMIs can be solved using the CVX package, which is compatible with matlab [224].

3. Finally, compute the local gains K_{ii} and terminal weights $P_{f_{ii}}$ using the relationships:

$$
P_{f_{ii}} = \mathrm{S}_{ii}^{-1}, \quad \mathrm{K}_{ii} = \mathrm{Y}_{ii}\mathrm{S}_{ii}^{-1} \quad \forall i \in \mathcal{A}
$$

The ith terminal weight $P_{f_{ii}}$ is a key component of the local cost of the ith subsystem MPC, while the local gain K_{ii} is a component of the control law computed for the ith subsystem.

It is important to emphasise that the results presented in this section is based on the work in [218] but adapted to the deregulated LFC problem investigated in this chapter.

7.6.2 Stabilising local observer gains L_{ii} and distributed observer design

Before stating, explicitly, the assumption required to design each local observer, and describe how the stabilising local observer gains L_{ii} $\forall i \in \mathcal{A}$, can be computed, let us first consider the dynamics of the ith observer. In this current work, let the state variables and uncontracted load changes estimates in the ith subsystem (control area) be $\hat{\mathrm{x}}_k^{[i]}$ and $\hat{\mathrm{b}}_k^{[i]}$ respectively. Also, let us assume that measurements of the ACE in the ith control area $\mathrm{y}_k^{[i]}$ (a local quantity) is available at every sampling instant. The dynamics of the ith observer are given as:

$$
\begin{aligned}
\xi_{k+1}^{\widehat{[i]}} = {} & \mathrm{A}_{ii}^{\mathrm{o}}\xi_k^{\widehat{[i]}} + \mathrm{B}_{ii}^{\mathrm{o}}\mathrm{u}_k^{[i]} + \mathrm{B}_{ii}^{\mathrm{do}}\mathrm{d}_k^{[i]} + \sum_{\substack{j \in \mathcal{A} \\ i \neq j}} \{ \mathrm{A}_{ij}^{\mathrm{o}}\xi_k^{\widehat{[j]}} + \mathrm{B}_{ij}^{\mathrm{o}}\mathrm{u}_k^{[j]} \\
& + \mathrm{B}_{ij}^{\mathrm{do}}\mathrm{d}_k^{[j]} \} - \mathrm{L}_{ii}(\mathrm{y}_k^{[i]} - \mathrm{C}_{ii}^{\mathrm{o}}\xi_k^{\widehat{[i]}} - \mathrm{D}_{ii}\mathrm{d}_k - \sum_{\substack{j \in \mathcal{A} \\ i \neq j}} \mathrm{C}_{ij}^{\mathrm{o}}\xi_k^{\widehat{[j]}})
\end{aligned} \tag{7.16}
$$

$$
\mathrm{A}_{ii}^{\mathrm{o}} = \begin{bmatrix} \mathrm{A}_{ii} & \mathrm{B}_{ii}^{\mathrm{b}} \\ \mathbf{0} & 1 \end{bmatrix}; \ \mathrm{A}_{ij}^{\mathrm{o}} = \begin{bmatrix} \mathrm{A}_{ij} & \mathrm{B}_{ij}^{\mathrm{b}} \\ \mathbf{0} & 0 \end{bmatrix}; \ \mathrm{B}_{ii}^{\mathrm{o}} = \begin{bmatrix} \mathrm{B}_{ii} \\ \mathbf{0} \end{bmatrix}; \ \mathrm{B}_{ij}^{\mathrm{o}} = \begin{bmatrix} \mathrm{B}_{ij} \\ \mathbf{0} \end{bmatrix}
$$

$$\mathrm{B}_{ii}^{do} = \begin{bmatrix} \mathrm{B}_{ii}^{d} \\ \mathbf{0} \end{bmatrix}; \ \mathrm{B}_{ij}^{do} = \begin{bmatrix} \mathrm{B}_{ij}^{d} \\ \mathbf{0} \end{bmatrix}; \ \mathrm{C}_{ii}^{o} = \begin{bmatrix} \mathrm{C}_{ii} & 0 \end{bmatrix}; \ \mathrm{C}_{ij}^{o} = \begin{bmatrix} \mathrm{C}_{ij} & 0 \end{bmatrix}$$

where $\xi_k^{\hat{[i]}} = \begin{bmatrix} \hat{\mathrm{x}}_k^{[i]T} & \hat{\mathrm{b}}_k^{[i]T} \end{bmatrix}^T$. The stability and convergence properties of the ith observer depends mainly on the local observer gain matrix L_{ii}. Consider the dynamics of the global observer obtained by the aggregation of (7.16) for all subsystems:

$$\hat{\xi_{k+1}} = \mathrm{A}_o\hat{\xi}_k + \mathrm{B}_o u_k + \mathrm{B}_o^d d_k - \mathrm{L}(y_k - \mathrm{C}_o\hat{\xi}_k - \mathrm{D}d_k) \tag{7.17}$$

where $\hat{\xi}_k = \begin{bmatrix} \xi_k^{\hat{[1]}^T} & \cdots & \xi_k^{\hat{[i-1]}^T} & \xi_k^{\hat{[i]}^T} & \xi_k^{\hat{[i+1]}^T} & \cdots & \xi_k^{\hat{[N]}^T} \end{bmatrix}^T$

$$\mathrm{A}^o = \begin{bmatrix} \mathrm{A}_{11}^o & \mathrm{A}_{12}^o & \cdots & \mathrm{A}_{1i}^o & \cdots & \mathrm{A}_{1N}^o \\ \mathrm{A}_{21}^o & \mathrm{A}_{22}^o & \cdots & \mathrm{A}_{2i}^o & \cdots & \mathrm{A}_{2N}^o \\ \vdots & \vdots & \ddots & \vdots & \vdots & \vdots \\ \mathrm{A}_{i1}^o & \mathrm{A}_{i2}^o & \cdots & \mathrm{A}_{ii}^o & \cdots & \mathrm{A}_{iN}^o \\ \vdots & \vdots & \vdots & \vdots & \ddots & \vdots \\ \mathrm{A}_{N1}^o & \mathrm{A}_{N2}^o & \cdots & \mathrm{A}_{Ni}^o & \cdots & \mathrm{A}_{NN}^o \end{bmatrix}; \ \mathrm{C}^o = \begin{bmatrix} \mathrm{C}_{11}^o & \mathrm{C}_{12}^o & \cdots & \mathrm{C}_{1i}^o & \cdots & \mathrm{C}_{1N}^o \\ \mathrm{C}_{21}^o & \mathrm{C}_{22}^o & \cdots & \mathrm{C}_{2i}^o & \cdots & \mathrm{C}_{2N}^o \\ \vdots & \vdots & \ddots & \vdots & \vdots & \vdots \\ \mathrm{C}_{i1}^o & \mathrm{C}_{i2}^o & \cdots & \mathrm{C}_{ii}^o & \cdots & \mathrm{C}_{iN}^o \\ \vdots & \vdots & \vdots & \vdots & \ddots & \vdots \\ \mathrm{C}_{N1}^o & \mathrm{C}_{N2}^o & \cdots & \mathrm{C}_{Ni}^o & \cdots & \mathrm{C}_{NN}^o \end{bmatrix}$$

Now, we focus on the assumption required to design a distributed observer in this thesis. Since observability is the dual of controllability, we extend the idea in [218] to design the distributed observer and the required assumption for a successful design is stated next:

Assumption 7.2. *There exists a fixed block diagonal observer gain matrix* $\mathrm{L} = \mathrm{blkdiag}(\mathrm{L}_{11}, \cdots, \mathrm{L}_{NN})$, $\mathrm{N} = |\mathcal{A}|$ *and* $\mathrm{L}_{ii} \in \mathbb{R}^{n_x^i + n_b^i \times n_y^i}$, $\forall i \in \mathcal{A}$ *such that: (i)* $\rho(\mathrm{A}^o + \mathrm{LC}^o) < 1$, *(ii)* $\rho(\mathrm{A}_{ii}^o + \mathrm{L}_{ii}\mathrm{C}_{ii}^o) < 1$ $\forall i \in \mathcal{A}$.

Similar to challenge inherent in determining local decentralised controller gains K_{ii} using standard methods, L_{ii} computed using the standard methods may not lead to a stabilising global observer, that is, $\mathrm{L} = \mathrm{blkdiag}(\mathrm{L}_{11}, \cdots, \mathrm{L}_{NN})$, where each L_{ii} is computed by appying pole placement or LQR methods (in the dual sense) on local subsystem matrices (A_{ii}^o and C_{ii}^o) may lead to an unstable global observer. Note that if the collective actions of the local observers do not translate to a stable global behaviour, then the estimates of system states and uncontracted load changes will not converge to their true values and could diverge. Hence, we resort to an LMI optimisation approach to compute observer gains that fulfil the Assumption 7.2

Theorem 7.2. *Let the Assumption 7.2 holds. Then the required local observer gains* L_{ii}, $\forall i \in \mathcal{A}$ *whose collective actions translate to a global stable observer is given as:*

$$\mathrm{L}_{ii} = (\mathrm{S}_{ii}^o)^{-1}\mathrm{Z}_{ii} \quad \forall i \in \mathcal{A} \tag{7.18}$$

and S_{ii}^{o} *and* Z_{ii} *are the solutions to the following LMIs:*

$$\begin{bmatrix} S_{ii}^{o} & S_{ii}^{o}A_{ii}^{o} + Z_{ii}C_{ii}^{o} \\ (S_{ii}^{o}A_{ii}^{o} + Z_{ii}C_{ii}^{o})^{T} & S_{ii}^{o} \end{bmatrix} \succ 0 \ S_{ii}^{o} = (S_{ii}^{o})^{T} \succ 0 \quad \forall i \in \mathcal{A} \tag{7.19a}$$

$$\begin{bmatrix} S^{o} & S^{o}A^{o} + ZC^{o} \\ (S^{o}A^{o} + ZC^{o})^{T} & S^{o} \end{bmatrix} \succ 0, \ S^{o} = (S^{o})^{T} \succ 0 \tag{7.19b}$$

where $S^{o} = \text{blkdiag}(S_{11}^{o}, \cdots, S_{NN}^{o}) \succ 0$, $Z = \text{blkdiag}(Z_{11}, \cdots, Z_{NN})$; $S_{ii}^{o} \in \mathbb{R}^{n_x^i + n_b^i \times n_x^i + n_b^i}$, $Z_{ii} \in \mathbb{R}^{n_x^i + n_b^i \times n_y^i}$.

Proof of Theorem 7.2

From the global observer in (7.17), the augmented system without the observer gain can be written as:

$$\xi_{k+1} = A_{o}\xi_{k} + B_{o}u_{k} + B_{o}^{d}d_{k} \tag{7.20a}$$

where $\xi_{k} = \begin{bmatrix} \xi_{k}^{[1]T} & \cdots & \xi_{k}^{[i-1]T} & \xi_{k}^{[i]T} & \xi_{k}^{[i+1]T} & \cdots & \xi_{k}^{[N]T} \end{bmatrix}^{T}$ and $\xi_{k}^{[i]} = \begin{bmatrix} x_{k}^{[i]T} & b_{k}^{[i]T} \end{bmatrix}^{T}$. Let the observer error $e_{k} = \xi_{k} - \hat{\xi}_{k}$; substracting (7.17) from (7.20a) gives:

$$e_{k+1} = (A_{o} + LC_{o})e_{k} \tag{7.20b}$$

where $L = \text{blkdiag}(L_{11}, \cdots, L_{NN})$. Employing the Lyapunov criteria for the convergence of the error dynamics (7.20b) gives:

$$e_{k}^{T}(A_{o} + LC_{o})^{T}S^{o}(A_{o} + LC_{o})e_{k} - e_{k}^{T}S^{o}e_{k} < 0 \tag{7.20c}$$

Here, $S^{o} = (S^{o})^{T} = \text{blkdiag}(S_{11}^{o}, \cdots, S_{NN}^{o}) \succ 0$. For $e_{k} \neq 0$, the inequality (7.20c) holds on condition that:

$$(A^{o} + LC^{o})^{T}S^{o}(A^{o} + LC^{o}) - S^{o} \prec 0 \tag{7.20d}$$

Let $L = (S^{o})^{-1}Z$, where $Z = \text{blkdiag}(Z_{11}, \cdots, Z_{NN})$; substituting into (7.20d) gives:

$$(A^{o} + (S^{o})^{-1}ZC^{o})^{T}S^{o}(A^{o} + (S^{o})^{-1}ZC^{o}) - S^{o} \prec 0 \tag{7.20e}$$

$$S^{o} - (S^{o}A^{o} + ZC^{o})^{T}(S^{o})^{-1}(S^{o}A^{o} + ZC^{o}) \succ 0 \tag{7.20f}$$

Applying Lemma 7.1 to (7.20f) gives:

Algorithm 7.2 Computation of local observer gains L_{ii} (OFFLINE)

1. Given the augmented matrices A_{ii}^{o} and C_{ii}^{o} for the ith observer (see (7.16)) and the corresponding global matrices A^{o} and C^{o}(see (7.17)), and that Assumption 7.2 holds. Define the following unknown local matrices $S_{ii}^{o} \in \mathbb{R}^{n_x^i + n_b^i \times n_x^i + n_b^i}$, $Z_{ii} \in \mathbb{R}^{n_x^i + n_b^i \times n_y^i}$, $\forall i \in \mathcal{A}$, where $S_{ii}^{o} = (S_{ii}^{o})^T \succ 0$, and construct the following block diagonal matrices $S^{o} = \text{blkdiag}(S_{11}^{o}, \cdots, S_{NN}^{o})$, $Z = \text{blkdiag}(Z_{11}, \cdots, Z_{NN})$

2. Solve the following linear matrix inequalities (LMIs) to obtain the pair (S_{ii}^{o}, Z_{ii}), $\forall i \in \mathcal{A}$:

$$\begin{bmatrix} S^{o} & S^{o}A^{o} + ZC^{o} \\ (S^{o}A^{o} + ZC^{o})^T & S^{o} \end{bmatrix} \succ 0$$

$$\begin{bmatrix} S_{ii}^{o} & S_{ii}^{o}A_{ii}^{o} + Z_{ii}C_{ii}^{o} \\ (S_{ii}^{o}A_{ii}^{o} + Z_{ii}C_{ii}^{o})^T & S_{ii}^{o} \end{bmatrix} \succ 0 \quad \forall i \in \mathcal{A}$$

with the added constraints:

$$S_{ii}^{o} \succ 0 \quad \forall i \in \mathcal{A}, \quad S^{o} \succ 0$$

The LMIs can be solved using the CVX package compatible with matlab [224]

3. Finally, compute the local observer gains L_{ii} using the relationship:

$$L_{ii} = (S_{ii}^{o})^{-1}Z_{ii} \quad \forall i \in \mathcal{A}$$

$$\begin{bmatrix} S^{o} & S^{o}A^{o} + ZC^{o} \\ (S^{o}A^{o} + ZC^{o})^T & S^{o} \end{bmatrix} \succ 0, \ S^{o} = (S^{o})^T \succ 0 \qquad \blacksquare$$

The same procedure is followed to derive the LMI expression (7.19a). The LMI problem to compute the local gains L_{ii} is summarised in Algorithm 7.2. In the interim, let us summarise what has been presented in this section so far:

In section 7.6.1, it was noted that the existence of a decentralised stable control for a centralised system (which has coupled dynamics) is a precondition to design the DMPC algorithm in this thesis; see Assumption 7.1. Moreover, Algorithm 7.1 was provided to compute the local gains $K_{ii} \ \forall i \in \mathcal{A}$ (block diagonal components of the stable decentralised control gain matrix for the centralised system) that satisfy Assumption 7.1. It was noted that K_{ii} is a key component of the control law of the ith subsystem; see the ith control law in (7.24). Also, the terminal weights of local MPCs $P_{f_{ii}} \ \forall i \in \mathcal{A}$ naturally emerge from Algorithm 7.1.

In section 7.6.2, it was emphasised that the existence of a decentralised stable observer for a coupled centralised dynamical system is a precondition for the design of a distributed observer scheme; see Assumption 7.2. Algorithm 7.2 was provided to compute the local observer gains L_{ii}, $\forall i \in \mathcal{A}$ which constitute the diagonal block elements of the stabilising decentralised observer gain matrix of a centralised observer.

An important part of the DMPC scheme in this thesis is the determination of steady state targets for each local MPC. This is discussed in the following subsection.

7.6.3 Determination of steady state targets

The steady state targets are used to transform the states, inputs and ouputs variables of the dynamical system, in state space form, to deviation variables; see the systems (7.10a), (7.10b) and (7.10c). These targets include the input target $u_{ss}^{[i]}$, the state target $x_{ss}^{[i]}$ and the output target $y_{ss}^{[i]}$. The output target is usually known and the target calculation problem is to determine $u_{ss}^{[i]}$ and $x_{ss}^{[i]}$ that are consistent, given a $y_{ss}^{[i]}$. As noted previously, deviation variables are introduced to embed an integral action in the MPC calculations to achieve offset free tracking.

In the context of the LFC problem, the $y_{ss}^{[i]}$ represents the desired ACE value of the ith area which is zero. Moreover, the $u_{ss}^{[i]}$ represents the total desired incremental/decremental control in the ith area, in response to an uncontracted load change in the area, to achieve the LFC objective in the area, that is, to eliminate frequency deviations and restore the area's net tie line power to its scheduled/contracted value. The state target vector $x_{ss}^{[i]}$ contains key targets information such as the generation change desired by each GenCo on LFC and the net contracted tie line power in the ith area. Hence the local MPC-based LFC problem considered by an area's transmission system operator (TSO) in the context of this work translates to regulating $\bar{u}_k^{[i]}$ to $u_{ss}^{[i]}$ and $\bar{x}_k^{[i]}$ to $x_{ss}^{[i]}$ while satisfying system constraints. Thus, the accuracy $u_{ss}^{[i]}$ and $x_{ss}^{[i]}$ is key to meeting the LFC objective in the deregulated paradigm considered in this thesis. Since the networks considered in this work translates to benchmark models with coupled dynamics, calculating $u_{ss}^{[i]}$ and $x_{ss}^{[i]}$ in a decentralised or distributed fashion could give inaccurate results, as each local target calculator would require steady state target information from dynamic neighbours, which these neighbours are yet to calculate. Hence, the distributed MPC algorithms and the DeMPC proposed here use a centralised approach to steady state target determination. The approach for a centralised target calculation, described in Section 6.4.2, is used here and the main results are duplicated here for convenience:

$$\underbrace{\begin{bmatrix} I-A & \sum\limits_{k\in\mathcal{G}_1} \gamma_{1,k} b_{1,k}^c & \sum\limits_{k\in\mathcal{G}_2} \gamma_{2,k} b_{2,k}^c & \cdots & \sum\limits_{k\in\mathcal{G}_7} \gamma_{7,k} b_{7,k}^c \\ C & 0 & 0 & \cdots & 0 \end{bmatrix}}_{M_S} \begin{bmatrix} x_{ss} \\ u_{ss}^1 \\ u_{ss}^2 \\ \vdots \\ u_{ss}^7 \end{bmatrix} = \begin{bmatrix} B^d d_{ss} + B^b b_{ss} \\ y_{ss} - D d_{ss} \end{bmatrix} \quad (7.21a)$$

$$b_{ss} = \widehat{b}_k, \quad d_{ss} = d_k, \quad y_{ss} = 0$$

$$
u_{ss} =
\begin{bmatrix}
\gamma_{1,1} & 0 & \cdots & 0 \\
\vdots & \vdots & \vdots & \vdots \\
\gamma_{1,5} & 0 & \cdots & 0 \\
0 & \gamma_{2,6} & \cdots & 0 \\
\vdots & \vdots & \vdots & \vdots \\
0 & \gamma_{2,9} & \cdots & 0 \\
\vdots & \vdots & \ddots & \vdots \\
0 & 0 & \cdots & \gamma_{7,30} \\
\vdots & \vdots & \vdots & \vdots \\
0 & 0 & \cdots & \gamma_{7,33}
\end{bmatrix}
\begin{bmatrix}
u_{ss}^1 \\
u_{ss}^2 \\
\vdots \\
u_{ss}^7
\end{bmatrix}
\tag{7.21b}
$$

where $b_{i,k}^c$ represents a column of the matrix B. The expressions (7.21a) and (7.21b) were stated for the 7-area network; it can be easily adapted (scaled down) to fit into the 4-area problem.

In summary, this section has described the important assumptions and developed some of the key components that are required for a complete design of the DMPC algorithms in this thesis. In particular, Section 7.6.1 introduced the Assumption 7.1 on a decentralised stabilisation of the centralised coupled system, as a prerequisite for DMPC designs and provided an algorithm to compute local gains $K_{ii} \; \forall i \in \mathcal{A}$ that constitute the decentralised stabilising controller; see Algorithm 7.1. Terminal weights of each subsystem MPCs $P_{f_{ii}} \; \forall i \in \mathcal{A}$ also emerge from Algorithm 7.1. The gains $K_{ii} \; \forall i \in \mathcal{A}$ are key components of each local MPC control law and the terminal weights $P_{f_{ii}} \; \forall i \in \mathcal{A}$ are key components of a local MPC cost; these parameters are computed offline.

Moreover, Section 7.6.2 introduced the Assumption 7.2 on a decentralised stabilising observer for a coupled system, as a prerequisite for the design of a distributed observer scheme. An algorithm was provided to compute (offline) the local observer gains $L_{ii}, \forall i \in \mathcal{A}$, Algorithm 7.2, which are the diagonal block elements of the stabilising decentralised observer gain matrix for the global system. Furthermore, the dynamics of the ith local observer were provided, see the system in (7.16). Section 7.6.3 concludes the section by describing the reason why a centralised approach to steady state target determination is adopted in this work. Note that the target calculator uses the estimates of uncontracted load changes $\hat{b}_k^{[i]}$ from the local observers; See Figure 4.3 and Section 7.6.3.

The next section develops the main DMPC algorithm for LFC which will utilise the pair (K_{ii}, $P_{f_{ii}}$) in its local controllers; each local MPC would receive steady state target information ($u_{ss}^{[i]}$ and $x_{ss}^{[i]}$) from the target calculator and also state estimates $\hat{x}_k^{[i]}$ from its local observer.

7.7 DMPC scheme for LFC

In this section, we propose a DMPC scheme suitable for LFC problems, and this is a vital contribution in this chapter. The design presented in this section is summarised in Algorithm 7.3. System constraints such as GRC, and input limits are incorporated into the design and are taken as hard constraints. The DMPC would operate alongside a distributed observer to estimate the states of each local subsystem and uncontracted load variations and a centralised target calculator; see Sections 7.6.2 and 7.6.3. Here, the problem for the dDMPC, which is applicable to a fully connected system, is considered; the sDMPC algorithm can easily be obtained from the dDMPC by disconnecting some communication links between subsystems (described in Algorithm 7.4), while the DeMPC can be obtained by disconnecting all communication links (described in Algorithm 7.5). In order to design the DMPC, supposing at a given time, k, where $k \geq 0$, the ith subsystem communicates to its dynamic neighbours, its previous optimal open loop control sequence $\bar{v}_t^{[i]} \quad \forall t \in \{k, \cdots, k+n_c - 1\}$ and corresponding state sequence $\bar{z}_t^{[i]} \quad \forall t \in \{k, \cdots, k+n_c - 1\}$, respectively, where n_c is the number of degrees of freedom (d.o.f) in the control and also taken as the MPC prediction horizon, then (7.10a) can be expressed as:

$$\bar{x}_{k+1}^{[i]} = A_{ii}\bar{x}_k^{[i]} + B_{ii}\bar{u}_k^{[i]} + \sum_{\substack{j \in \mathcal{A} \\ i \neq j}}\{A_{ij}\bar{z}_k^{[j]} + B_{ij}\bar{v}_k^{[j]}\} + w_k^{[i]} \tag{7.22a}$$

where

$$w_k^{[i]} = \sum_{\substack{j \in \mathcal{A} \\ i \neq j}}\{A(\bar{x}_k^{[j]} - \bar{z}_k^{[j]}) + B_{ij}(\bar{u}_k^{[j]} - \bar{v}_k^{[j]})\} \tag{7.22b}$$

Note that the summation term in (7.22a) represents a planned interaction, while (7.22b) represents an unplanned interaction. Define the nominal ith subsystem model associated with (7.22a) as:

$$z_{k+1}^{[i]} = A_{ii}z_k^{[i]} + B_{ii}v_k^{[i]} + \sum_{\substack{j \in \mathcal{A} \\ i \neq j}}\{A_{ij}\bar{z}_k^{[j]} + B_{ij}\bar{v}_k^{[j]}\} \tag{7.23}$$

The control law for the ith subsystem at $k \geq 0$ is

$$u_k^{[i]} = v_{k/k}^{[i]} + u_{ss}^{[i]} + K_{ii}(\hat{x}_k^{[i]} - x_{ss}^{[i]} - z_k^{[i]}) \tag{7.24}$$

Observe that the control law (7.24) includes the local gain K_{ii} which can be determined offline using Algorithm 7.1, the ith subsystem state estimates $\hat{x}_k^{[i]}$ supplied by the ith observer described in Section 7.6.2 and the target pair $(x_{ss}^{[i]}, u_{ss}^{[i]})$ supplied by a target calculator. $v_{k/k}^{[i]}$ is the first control action in the optimal control sequence $v_{t/k}^{[i]}, \forall t \in \{k, \cdots, k+n_c - 1\}$, obtained from the ith linear DMPC problems, $\overline{P_i(z_k^{[i]})}, \ k = 0$ and $P_i(z_k^{[i]}), \ k > 0$, which are formally described:

$$k = 0: \quad z^{[i]}_{0/0} = x^{[i]}_0$$

$$\overline{\mathrm{P}_i(z^{[i]}_k)} \quad : \quad \min_{\{v^{[i]}_{k/k}, \cdots, v^{[i]}_{k+n_c-1/k}\}} J_i(z^{[i]}_k, v^{[i]}_{t/k}) \tag{7.25a}$$

Subject to $\forall t \in \{k, \cdots, k + n_c - 1\}$:

$$z^{[i]}_{t+1/k} = \mathrm{A}_{ii} z^{[i]}_{t/k} + \mathrm{B}_{ii} v^{[i]}_{t/k} \tag{7.25b}$$

$$x^{[i],\min} \leq \frac{z^{[i]}_{t+1/k}}{\sigma^{[i]}_x} + x^{[i]}_{ss} \leq x^{[i],\max}; \quad \sigma^{[i]}_x \in (0,1] \tag{7.25c}$$

$$u^{[i],\min} \leq \frac{v^{[i]}_{t/k}}{\sigma^{[i]}_u} + u^{[i]}_{ss} \leq u^{[i],\max}; \quad \sigma^{[i]}_u \in (0,1] \tag{7.25d}$$

$k > 0:$

$$\mathrm{P}_i(z^{[i]}_k) \quad : \quad \min_{\{v^{[i]}_{k/k}, \cdots, v^{[i]}_{k+n_c-1/k}\}} J_i(z^{[i]}_k, v^{[i]}_{t/k}) \tag{7.26a}$$

Subject to $\forall t \in \{k, \cdots, k + n_c - 1\}$:

$$z^{[i]}_{t+1/k} = \mathrm{A}_{ii} z^{[i]}_{t/k} + \mathrm{B}_{ii} v^{[i]}_{t/k} + \sum_{\substack{j \in \mathcal{A} \\ i \neq j}} \{\mathrm{A}_{ij} \bar{z}^{[j]}_{t/k} + \mathrm{B}_{ij} \bar{v}^{[j]}_{t/k}\} \tag{7.26b}$$

$$\bar{z}^{[j]}_{t/k} = z^{[j]}_{t/k-1}; \quad \bar{v}^{[j]}_{t/k} = v^{[j]}_{t/k-1} \tag{7.26c}$$

$$x^{[i],\min} \leq \frac{z^{[i]}_{t+1/k}}{\sigma^{[i]}_x} + x^{[i]}_{ss} \leq x^{[i],\max}, \quad \sigma^{[i]}_x \in (0,1] \tag{7.26d}$$

$$u^{[i],\min} \leq \frac{v^{[i]}_{t/k}}{\sigma^{[i]}_u} + u^{[i]}_{ss} \leq u^{[i],\max}, \quad \sigma^{[i]}_u \in (0,1] \tag{7.26e}$$

In the both DMPC problems, the local cost $J_i(z^{[i]}_k, v^{[i]}_{t/k})$ is defined as:

$$J_i(z^{[i]}_k, v^{[i]}_{t/k}) = \sum_{t=k}^{k+n_c-1} \frac{1}{2} \{z^T_{t+1} Q_{ii} z_{t+1} + v^T_t R_{ii} v_t\} + z^T_{k+n_c} P_{f_{ii}} z_{k+n_c} \tag{7.27}$$

Note here that the local terminal weight $P_{f_{ii}} \succeq 0$ is determined offline using Algorithm 7.1. The expression (7.25c) (the same as (7.26d)) represents the state constraints, while (7.25d)

(the same as (7.26e)) represents the input constraints; $\sigma_{\mathrm{x}}^{[i]}$ and $\sigma_{\mathrm{u}}^{[i]}$ are tunable constraints tightening factors [204] selected to ensure that the constraints on the actual system (7.9a) are not violated; $Q_{ii} \succeq 0$ and $R_{ii} \succ 0$ in (7.27) represent weightings on the local states and input variables in the ith subsystem respectively. The solution to $\overline{\mathrm{P}_i\big(\mathrm{z}_k^{[i]}\big)}$ and $\mathrm{P}_i\big(\mathrm{z}_k^{[i]}\big)$ require the online computation of the pair $(\mathrm{x}_{\mathrm{ss}}^{[i]}, \mathrm{u}_{\mathrm{ss}}^{[i]})$ at every sampling instant. With $\mathrm{y}_{\mathrm{ss}}^{[i]}$ (known) and $\hat{\mathrm{b}}_k^{[i]}$ (online estimate of $\mathrm{b}_k^{[i]}$) available, the target pair $(\mathrm{x}_{\mathrm{ss}}^{[i]}, \mathrm{u}_{\mathrm{ss}}^{[i]})$, can be computed.

We now summarise the ith DMPC problem solved online under Algorithm 7.3 which is based on the dDMPC design (fully connected):

Algorithm 7.3 Description of the dense DMPC for the ith subsystem (ONLINE)

1. **Parameters designed offline:** Given K_{ii} and $P_{f_{ii}}$ computed using Algorithm 7.1 and L_{ii} computed using Algorithm 7.2.

2. **Initialisation:** Set $k = 0$; set the following: $\hat{\mathrm{x}}_{t/k}^{[i]} = \mathrm{x}_0^{[i]}$, $z_t^{[i]} = \mathrm{x}_0^{[i]}$ and $\hat{\mathrm{b}}_{t/k}^{[i]} = \mathrm{b}_0^{[i]}$ $\forall t \in [k, k+1)$; set the following coupling matrices in (7.9a) and (7.9b) to zero matrices: A_{ij}, B_{ij}, $\mathrm{B}_{ij}^{\mathrm{b}}$, $\mathrm{B}_{ij}^{\mathrm{d}}$ and C_{ij}. Hence, initialisation is decentralised as each subsystem does not have any information to communicate at the start. Note that k is a non-negative integer.

3. **Centralised steady state target calculation:** Solve the consistency expressions (7.21a) and (7.21b) and extract the target pair $(\mathrm{x}_{\mathrm{ss}}^{[i]}, \mathrm{u}_{\mathrm{ss}}^{[i]})$. This is a centralised calculation; see Section 7.6.3 for the reason.

4. **Decentralised control problem:** Solve the optimisation problem $\overline{\mathrm{P}_i(z_k^{[i]})}$ to obtain the optimal control sequence $\mathrm{v}_{t/k}^{[i]}$ $\forall t \in [k, \cdots, k + n_c - 1]$.

5. **Prediction calculations (decoupled subsystem):** Compute the nominal n_c- step state prediction sequence $z_{t+1/k}^{[i]}$ $\forall t \in [k, \cdots, k + n_c - 1]$ by using the decoupled nominal subsystem model (7.25b).

6. **Control input to subsystem:** Calculate the control input $\mathrm{u}_t^{[i]} = \mathrm{v}_{t/k}^{[i]} + \mathrm{u}_{\mathrm{ss}}^{[i]} + \mathrm{K}_{ii}(\hat{\mathrm{x}}_{t/k}^{[i]} - \mathrm{x}_{\mathrm{ss}}^{[i]} - z_t^{[i]})$ $\forall t \in [k, k+1)$ and apply to the ith subsystem (7.9a). Evaluate the local output $\overline{\mathrm{y}}_k^{[i]}$ using (7.9b).

7. **Estimation:** Determine, using the ith observer, (7.16), the following estimates from the local measurement $\overline{\mathrm{y}}_k^{[i]}$: $\hat{\mathrm{x}}_{t+1/k}^{[i]}$ and $\hat{\mathrm{b}}_{t+1/k}^{[i]}$ $\forall t \in [k, k+1)$.

8. **Communication:** Communicate the pair $(\mathrm{v}_{t/k}^{[i]}, z_{t+1/k}^{[i]})$ $\forall t \in [k, \cdots, k + n_c - 1]$ to all of the other subsystems j and receive the pair $(\mathrm{v}_{t/k}^{[j]}, z_{t+1/k}^{[j]})$ $\forall t \in [k, \cdots, k + n_c - 1]$ from them. Also, communicate the following $(\hat{\mathrm{x}}_{t+1/k}^{[i]}, \hat{\mathrm{b}}_{t+1/k}^{[i]}, \mathrm{d}_{t+1/k}^{[i]})$ $\forall t \in [k, k+1)$ to all of the other subsystems j and receive $(\hat{\mathrm{x}}_{t+1/k}^{[j]}, \hat{\mathrm{b}}_{t+1/k}^{[j]}, \mathrm{d}_{t+1/k}^{[j]})$ $\forall t \in [k, k+1)$ from them.

9. **Restore subsystem model to default:** Restore the couplings matrices to their default values (nonzero matrices): A_{ij}, B_{ij}, $\mathrm{B}_{ij}^{\mathrm{b}}$, $\mathrm{B}_{ij}^{\mathrm{d}}$ and C_{ij}. This is because each subsystem now has an information it can communicate.

10. **System increment:** Set $k = k + 1$; set $\overline{z}_{t/k}^{[j]} = z_{t/k-1}^{[j]}$, $\overline{\mathrm{v}}_{t/k}^{[j]} = \mathrm{v}_{t/k-1}^{[j]}$ $\forall t \in [k, \cdots, k + n_c - 1]$; set $\hat{\mathrm{x}}_{t/k}^{[j]} = \hat{\mathrm{x}}_{t/k-1}^{[j]}$, $\hat{\mathrm{b}}_{t/k}^{[j]} = \hat{\mathrm{b}}_{t/k-1}^{[i]}$, $\mathrm{d}_{t/k}^{[j]} = \mathrm{d}_{t/k-1}^{[j]}$ $\forall t \in [k, k+1)$.

11. **New steady state target:** Repeat step 3 to obtain new a target pair $(\mathrm{x}_{\mathrm{ss}}^{[i]}, \mathrm{u}_{\mathrm{ss}}^{[i]})$.

12. **Distributed control problem:** Solve the optimisation problem $\mathrm{P}_i(z_k^{[i]})$ to obtain the optimal control sequence $\mathrm{v}_{t/k}^{[i]}$ $\forall t \in [k, \cdots, k + n_c - 1]$.

13. **Prediction calculations (coupled subsystem):** Compute the nominal n_c-step state predictions $z_{t+1/k}^{[i]}$ $\forall t \in [k, \cdots, k + n_c - 1]$ using (7.26b) and repeat steps $6, 7, 8, 10, 11, 12, 13$.

7.7.1 Comments on sparse DMPC

As noted earlier, the sDMPC is based on DT subsystem models that retain the sparsity of the CT global system. For the sparse case, the subsystems' state equations can be expressed as:

$$\mathrm{x}_{k+1}^{[i]} = \underbrace{\mathrm{A}_{ii}\mathrm{x}_k^{[i]} + \mathrm{B}_{ii}\mathrm{u}_k^{[i]} + \mathrm{B}_{ii}^{\mathrm{d}}\mathrm{d}_k^{[i]} + \mathrm{B}_{ii}^{\mathrm{b}}\mathrm{b}_k^{[i]}}_{\text{Local subsystem}} + \underbrace{\sum_{\substack{j\in\mathcal{A}_i^{\mathrm{Ne}}\\i\neq j}} \{\mathrm{A}_{ij}\mathrm{x}_k^{[j]} + \mathrm{B}_{ij}^{\mathrm{d}}\mathrm{d}_k^{[j]}\}}_{\text{coupling}} \quad \forall i\in\mathcal{A}_d \qquad (7.28\mathrm{a})$$

$$\mathrm{x}_{k+1}^{[i]} = \underbrace{\mathrm{A}_{ii}\mathrm{x}_k^{[i]} + \mathrm{B}_{ii}\mathrm{u}_k^{[i]} + \mathrm{B}_{ii}^{\mathrm{d}}\mathrm{d}_k^{[i]} + \mathrm{B}_{ii}^{\mathrm{b}}\mathrm{b}_k^{[i]}}_{\text{Local subsystem}} + \underbrace{\sum_{\substack{j\in\mathcal{A}\\i\neq j}}\mathrm{A}_{ij}\mathrm{x}_k^{[j]}}_{\text{coupling}} + \underbrace{\sum_{\substack{j\in\mathcal{A}_i^{\mathrm{Ne}}\\i\neq j}}\mathrm{B}_{ij}^{\mathrm{d}}\mathrm{d}_k^{[j]}}_{\text{coupling}} \quad \forall i\in\mathcal{A}\setminus\mathcal{A}_d \quad (7.28\mathrm{b})$$

where $\mathcal{A}_d$ is the index set of CAs with independent net tie line flows; $\mathcal{A}_i^{\mathrm{Ne}}$ is the index set of CAs connected to the ith CA, $\mathcal{A}_i^{\mathrm{Ne}} \subseteq \mathcal{A}$. The expression (7.28a) represents subsystem models of CAs with independent net tie line flows and they retain the structure of the interconnected power system. Observe that (7.28a) is different from its dense counterpart (7.9a) as subsystems are coupled via states and contracted load changes to direct neighbours only, and therefore communications are restricted to the exchange of state predictions and contracted load changes between neighbouring CAs. The only exception is the dependent CA whose net tie line flow is eliminated and expressed as a linear combination of the independent net tie line flows; the subsystem model of such an area is given in (7.28b) and it receives state predictions from all of the other subsystems. Hence, Algorithm 7.3 can be modified slightly to obtain the sDMPC algorithm; the modified one is presented as Algorithm 7.4 for clarity. Changes were only made to steps 2, 8, 9 and 10 in Algorithm 7.3 (dDMPC) to obtain Algorithm 7.4 (sDMPC). See step 8 in Algorithms 7.3 (dDMPC) and Algorithm 7.4 (sDMPC) to see what information is shared between subsystems in both schemes.

7.7.2 Comments on decentralised MPC

The DeMPC algorithm ignores the couplings between subsystems, that is, it treats the interconnected network as though each CA is isolated. The ith subsystem model used is given as:

$$\mathrm{x}_{k+1}^{[i]} = \mathrm{A}_{ii}\mathrm{x}_k^{[i]} + \mathrm{B}_{ii}\mathrm{u}_k^{[i]} + \mathrm{B}_{ii}^{\mathrm{d}}\mathrm{d}_k^{[i]} + \mathrm{B}_{ii}^{\mathrm{b}}\mathrm{b}_k^{[i]} \qquad (7.29\mathrm{a})$$

$$\mathrm{y}_k^{[i]} = \mathrm{C}_{ii}\mathrm{x}_k^{[i]} + \mathrm{D}_{ii}\mathrm{d}_k^{[i]} \qquad (7.29\mathrm{b})$$

Algorithm 7.4 Description of the sparse DMPC for the ith subsystem (ONLINE)

1. **Parameters designed offline:** Given K_{ii} and $P_{f_{ii}}$ computed using Algorithm 7.1 and L_{ii} computed using Algorithm 7.2.

2. **Initialisation:** Set $k = 0$; set the following: $\hat{\mathrm{x}}_{t/k}^{[i]} = \mathrm{x}_0^{[i]}$, $\mathrm{z}_t^{[i]} = \mathrm{x}_0^{[i]}$ and $\hat{\mathrm{b}}_{t/k}^{[i]} = \mathrm{b}_0^{[i]}$ $\forall t \in [k, k+1)$; set the following coupling matrices in (7.28a) and (7.28b) to zero matrices: A_{ij}, $\mathrm{B}_{ij}^{\mathrm{d}}$ and C_{ij}. Hence, initialisation is decentralised as each subsystem does not have any information to communicate at the start. Note that k is a non-negative integer.

3. **Centralised steady state target calculation:** Solve the consistency expressions (7.21a) and (7.21b) and extract the target pair $(\mathrm{x}_{\mathrm{ss}}^{[i]}, \mathrm{u}_{\mathrm{ss}}^{[i]})$. This is a centralised calculation; see Section 7.6.3 for the reason.

4. **Decentralised control problem:** Solve the optimisation problem $\overline{\mathrm{P}_i(\mathrm{z}_k^{[i]})}$ to obtain the optimal control sequence $\mathrm{v}_{t/k}^{[i]}$ $\forall t \in [k, \cdots, k + n_c - 1]$.

5. **Prediction calculations (decoupled subsystem):** Compute the nominal n_c- step state prediction sequence $z_{t+1/k}^{[i]}$ $\forall t \in [k, \cdots, k + n_c - 1]$ by using the decoupled nominal subsystem model (7.25b).

6. **Control input to subsystem:** Calculate the control input $\mathrm{u}_t^{[i]} = \mathrm{v}_{t/k}^{[i]} + \mathrm{u}_{\mathrm{ss}}^{[i]} + \mathrm{K}_{ii}(\hat{\mathrm{x}}_{t/k}^{[i]} - \mathrm{x}_{\mathrm{ss}}^{[i]} - \mathrm{z}_t^{[i]})$ $\forall t \in [k, k+1)$ and apply to the ith subsystem (7.9a). Evaluate the local output $\overline{\mathrm{y}}_k^{[i]}$ using (7.9b).

7. **Estimation:** Determine, using the ith observer, (7.16), the following estimates from the local measurement $\overline{\mathrm{y}}_k^{[i]}$: $\hat{\mathrm{x}}_{t+1/k}^{[i]}$ and $\hat{\mathrm{b}}_{t+1/k}^{[i]}$ $\forall t \in [k, k+1)$.

8. **Communication:** Communicate $z_{t+1/k}^{[i]}$ $\forall t \in [k, \cdots, k + n_c - 1]$ to direct neighbours $j \in \mathcal{A}_i^{\mathrm{Ne}}$ and also to the dependent CA, $\mathcal{A} \setminus \mathcal{A}_d$ (if it is not a direct neighbour) and receive $z_{t+1/k}^{[j]}$ $\forall t \in [k, \cdots, k + n_c - 1]$ from them. Also, communicate $(\hat{\mathrm{x}}_{t+1/k}^{[i]}, \mathrm{d}_{t+1/k}^{[i]})$ $\forall t \in [k, k+1)$ to direct neighbours $j \in \mathcal{A}_i^{\mathrm{Ne}}$, and also $(\hat{\mathrm{x}}_{t+1/k}^{[i]})$ $\forall t \in [k, k+1)$ to the dependent CA, $\mathcal{A} \setminus \mathcal{A}_d$ (if it is not a direct neighbour) and receive $(\hat{\mathrm{x}}_{t+1/k}^{[j]}, \mathrm{d}_{t+1/k}^{[j]})$ $\forall t \in [k, k+1)$ from them.

9. **Restore subsystem model to default:** Restore the couplings matrices to their default values (nonzero matrices): A_{ij}, $\mathrm{B}_{ij}^{\mathrm{d}}$ and C_{ij}. This is because each subsystem now has an information it can communicate.

10. **System increment:** Set $k = k + 1$; set $\overline{\mathrm{z}}_{t/k}^{[j]} = z_{t/k-1}^{[j]}$ $\forall t \in [k, \cdots, k + n_c - 1]$; set $\hat{\mathrm{x}}_{t/k}^{[j]} = \hat{\mathrm{x}}_{t/k-1}^{[j]}$ $\forall t \in [k, k+1)$.

11. **New steady state target:** Repeat step 3 to obtain new a target pair $(\mathrm{x}_{\mathrm{ss}}^{[i]}, \mathrm{u}_{\mathrm{ss}}^{[i]})$.

12. **Distributed control problem:** Solve the optimisation problem $\mathrm{P}_i(\mathrm{z}_k^{[i]})$ to obtain the optimal control sequence $\mathrm{v}_{t/k}^{[i]}$ $\forall t \in [k, \cdots, k + n_c - 1]$, replacing B_{ij} in (7.26b) with a zero matrix.

13. **Prediction calculations (coupled subsystem):** Compute the nominal n_c-step state predictions $z_{t+1/k}^{[i]}$ $\forall t \in [k, \cdots, k + n_c - 1]$ using (7.26b) with B_{ij} taken as a zero matrix, and repeat steps $6, 7, 8, 10, 11, 12, 13$.

Algorithm 7.5 Description of the decentralised MPC for the ith subsystem (ONLINE)

1. **Parameters designed offline:** Given K_{ii} and $P_{f_{ii}}$ computed using Algorithm 7.1 and L_{ii} computed using Algorithm 7.2.

2. **Initialisation:** Set $k = 0$; set the following: $\hat{\mathrm{x}}^{[i]}_{t/k} = \mathrm{x}^{[i]}_0$, $\mathrm{z}^{[i]}_t = \mathrm{x}^{[i]}_0$ and $\hat{\mathrm{b}}^{[i]}_{t/k} = \mathrm{b}^{[i]}_0$ $\forall t \in [k, k+1)$. Note that k is a non-negative integer.

3. **Centralised steady state target calculation:** Solve the consistency expressions (7.21a) and (7.21b) and extract the target pair $(\mathrm{x}^{[i]}_{ss}, \mathrm{u}^{[i]}_{ss})$. This is a centralised calculation; see Section 7.6.3 for the reason.

4. **Decentralised control problem:** Solve the optimisation problem $\overline{\mathrm{P}_i\big(\mathrm{z}^{[i]}_k\big)}$ to obtain the optimal control sequence $\mathrm{v}^{[i]}_{t/k}$ $\forall t \in [k, \cdots, k+n_c-1]$.

5. **Prediction calculations (decoupled subsystem):** Compute the nominal n_c- step state prediction sequence $z^{[i]}_{t+1/k}$ $\forall t \in [k, \cdots, k+n_c-1]$ by using the decoupled nominal subsystem model (7.25b).

6. **Control input to subsystem:** Calculate the control input
$\mathrm{u}^{[i]}_t = \mathrm{v}^{[i]}_{t/k} + \mathrm{u}^{[i]}_{ss} + \mathrm{K}_{ii}(\hat{\mathrm{x}}^{[i]}_{t/k} - \mathrm{x}^{[i]}_{ss} - \mathrm{z}^{[i]}_t)$ $\forall t \in [k, k+1)$ and apply to the ith subsystem (7.9a). Evaluate the local output $\overline{\mathrm{y}}^{[i]}_k$ using (7.9b).

7. **Estimation:** Determine, using the ith observer, (7.16), the following estimates from the local measurement $\overline{\mathrm{y}}^{[i]}_k$: $\hat{\mathrm{x}}^{[i]}_{t+1/k}$ and $\hat{\mathrm{b}}^{[i]}_{t+1/k}$ $\forall t \in [k, k+1)$.

8. **System increment:** Set $k = k+1$ and repeat steps 3,4,5,6,7,8.

In the ith DeMPC problem, no information exchange is carried out between subsystems; it is synonymous with solving a centralised MPC problem within a CA. Algorithm 7.5 summarises the DeMPC steps.

Remark 7.7.1. *The DMPC algorithms here was adapted from the centralised tube-based MPC in [204], and theoretical results on stability and recursive feasibility were not considered. With proper offline selection of tuning paramaters such as gain matrices, weighting matrices and invariant sets, apriori stability and recursive feasibility can be guaranteed [225]. However, this current work considered a simple DMPC scheme which can easily be applied to practical systems.*

7.7.3 Generation rate and input constraints.

The DMPC proposed here considers the GRC and input limits of each GenCo participating in a supplementary control, that is, GenCos whose area participation factors are nonzero. The description of the GRC and input limits expressions can be found in Section 6.4.4.

In summary, this section presented three different non-centralised MPC algorithms for multi-area deregulated LFC problems, namely dDMPC, sDMPC and DeMPC. These three algorithms

Table 7.1: Contracted load changes (case-1).

$\Delta P_{1,1}^{\mathrm{L}}$	$\Delta P_{1,2}^{\mathrm{L}}$	$\Delta P_{1,3}^{\mathrm{L}}$	$\Delta P_{1,4}^{\mathrm{L}}$	$\Delta P_{2,5}^{\mathrm{L}}$	$\Delta P_{2,6}^{\mathrm{L}}$	$\Delta P_{2,7}^{\mathrm{L}}$
0.0065	0.0065	0.0065	0	0.0065	0.0065	0

$\Delta P_{3,8}^{\mathrm{L}}$	$\Delta P_{3,9}^{\mathrm{L}}$	$\Delta P_{3,10}^{\mathrm{L}}$	$\Delta P_{3,11}^{\mathrm{L}}$	$\Delta P_{4,12}^{\mathrm{L}}$	$\Delta P_{4,13}^{\mathrm{L}}$	$\Delta P_{4,14}^{\mathrm{L}}$
0.0065	0.0065	0.0065	0	0.0065	0.0065	0

differ in respect of the amount of information that is shared between subsystems. In dDMPC, each subsystem communicates its previous state and input sequences, contracted and uncontracted load changes to all other subsystems. In sDMPC, only direct neighbours (control areas with a tie line link) communicate with each other and they only exchange state predictions and contracted load changes. In the DeMPC, subsystems do not exchange any information.

7.8 Simulation and Discussion

This section presents and discusses the simulation results obtained by implementing the proposed DMPC (sparse and dense) based LFC schemes on two different multi-area deregulated benchmark models. Firstly, the 4-area benchmark model developed in Chapter 5 is considered and the results are presented under case-1 Section 7.8.1. Furthermore, the efficacy of the DMPC schemes are also demonstrated on the 7-area benchmark model developed in Chapter 5; the 7-area problem is presented under case-2 Section 7.8.2. In both case studies, a centralised MPC (benchmark control scheme) and the DeMPC scheme described in this chapter (interactions ignored in the ith DMPC problem) are implemented alongside the sDMPC and dDMPC.

7.8.1 Case-1: 4-area deregulated power system

In this section, the efficacy and applicability of the DMPC is illustrated on a 4-area network. The parameters of the 4-area model are shown in Table A.4 and A.5. The GenCos with a nonzero area participation factor are on supplementary control (to cater for uncontracted load changes) while the entire GenCos are assumed to have bilateral contracts with DisCos (for contracted load changes) within and outside their control areas. The DisCo participation matrix (DPM) that contains the contract data is given in (A.8). The rated capacities of the different control areas are $\{P_{r_1}, \cdots, P_{r_4}\} = \{5500, 4800, 5000, 6200\}$. The contracted load change of each DisCo and uncontracted load changes in each area is shown in Table 7.1 and 7.2 respectively.

In the ith DMPC, the number of d.o.f in control $n_c = 20$ and this is used as the prediction horizon n_y; a sampling time $t_s = 0.1$ s is used throughout the simulation. Also, the constraint
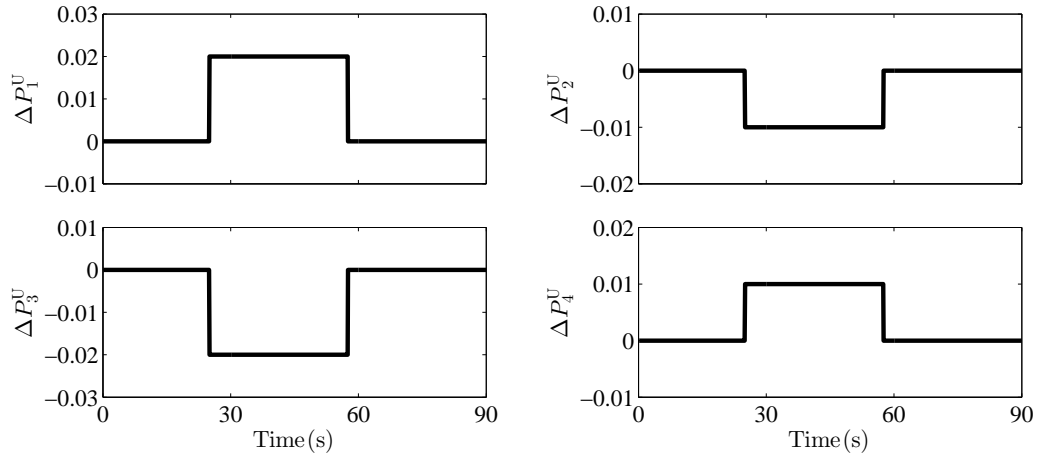
Figure 7.2: Uncontracted load changes (case-1).
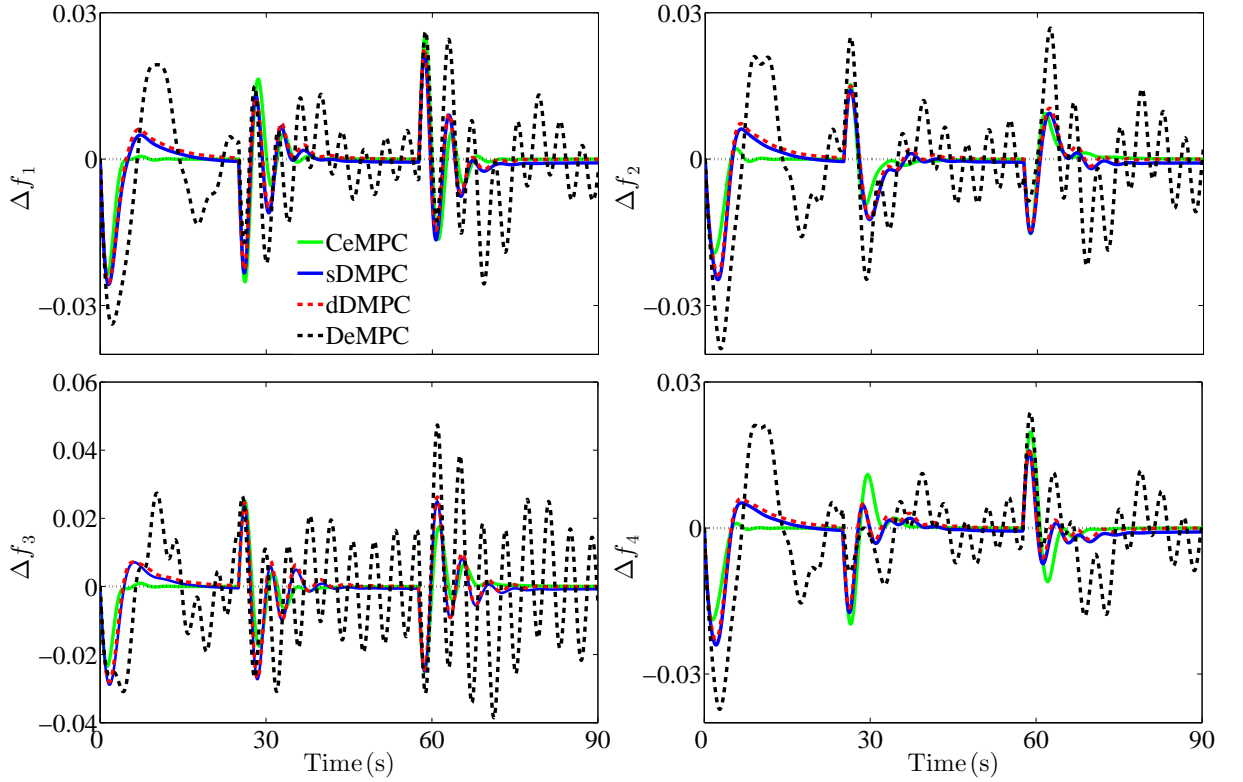
Figure 7.3: Frequency deviation in each control area (case-1). Note that the frequency deviations at steady state should be zero.

tightening factors are used in the three non-centralised schemes are $\sigma_{\text{x}}^{[i]} = 0.9$ and $\sigma_{\text{u}}^{[i]} = 0.95$; these values were chosen by trial and error to ensure that feasibility is achieved for sDMPC, dDMPC and DeMPC. The benchmark model developed is used as the plant. The weighting used in the ith DMPC are $Q_{ii} = 10I_{\text{x}}^{[i]}$ and $R_{ii} = I_{\text{u}}^{[i]}$, where $I_{\text{x}}^{[i]}$ and $I_{\text{u}}^{[i]}$ are identity matrices of appropriate sizes. The input constraints and GRC of GenCos on supplementary control are plotted as black dotted lines (upper and lower bounds) alongside their generation rates and inputs signals.
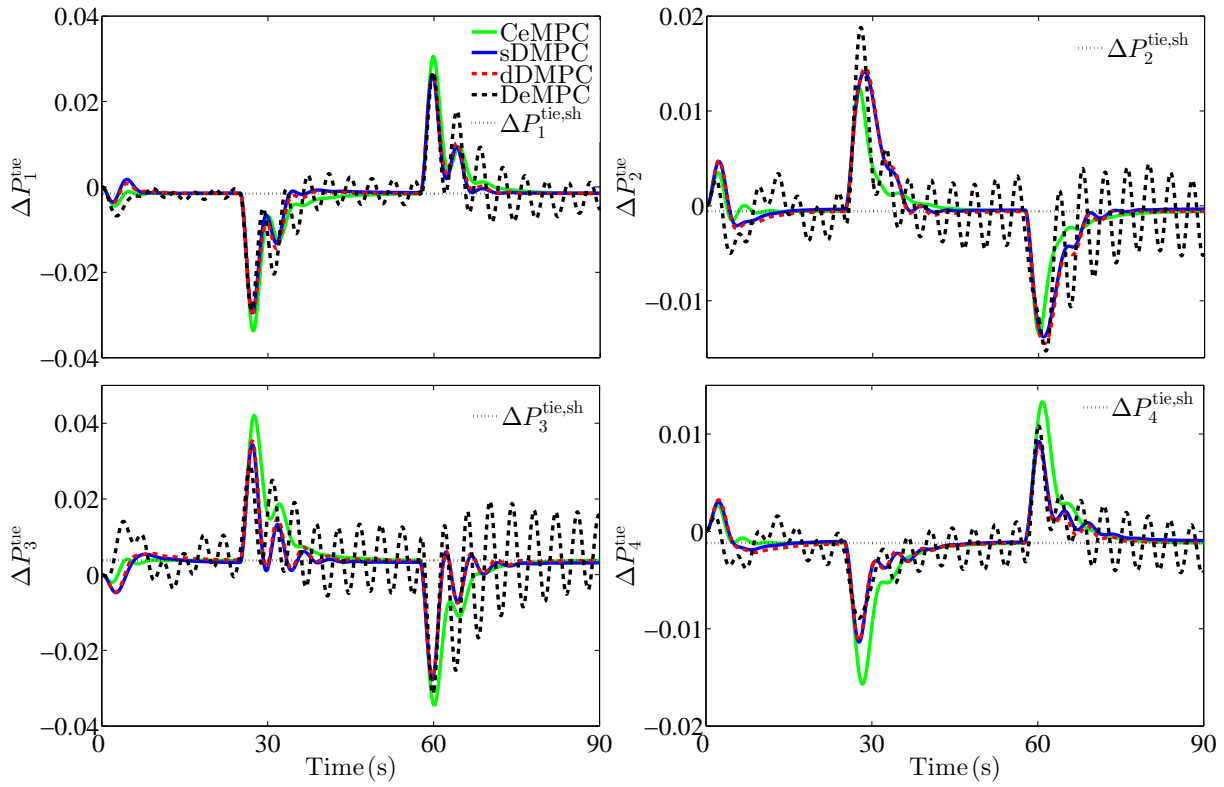
Figure 7.4: Deviation in net tie-line outflow in CA (case-1)
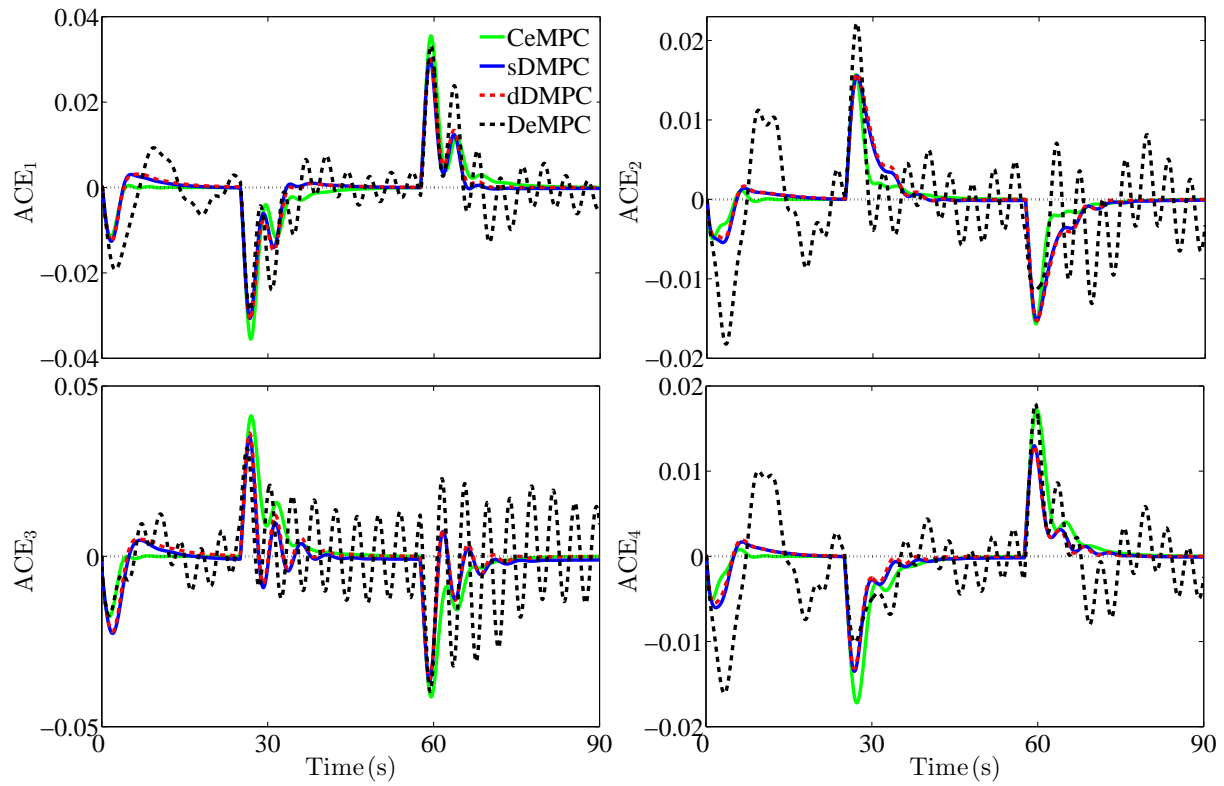
Figure 7.5: Area control error (4-area case)
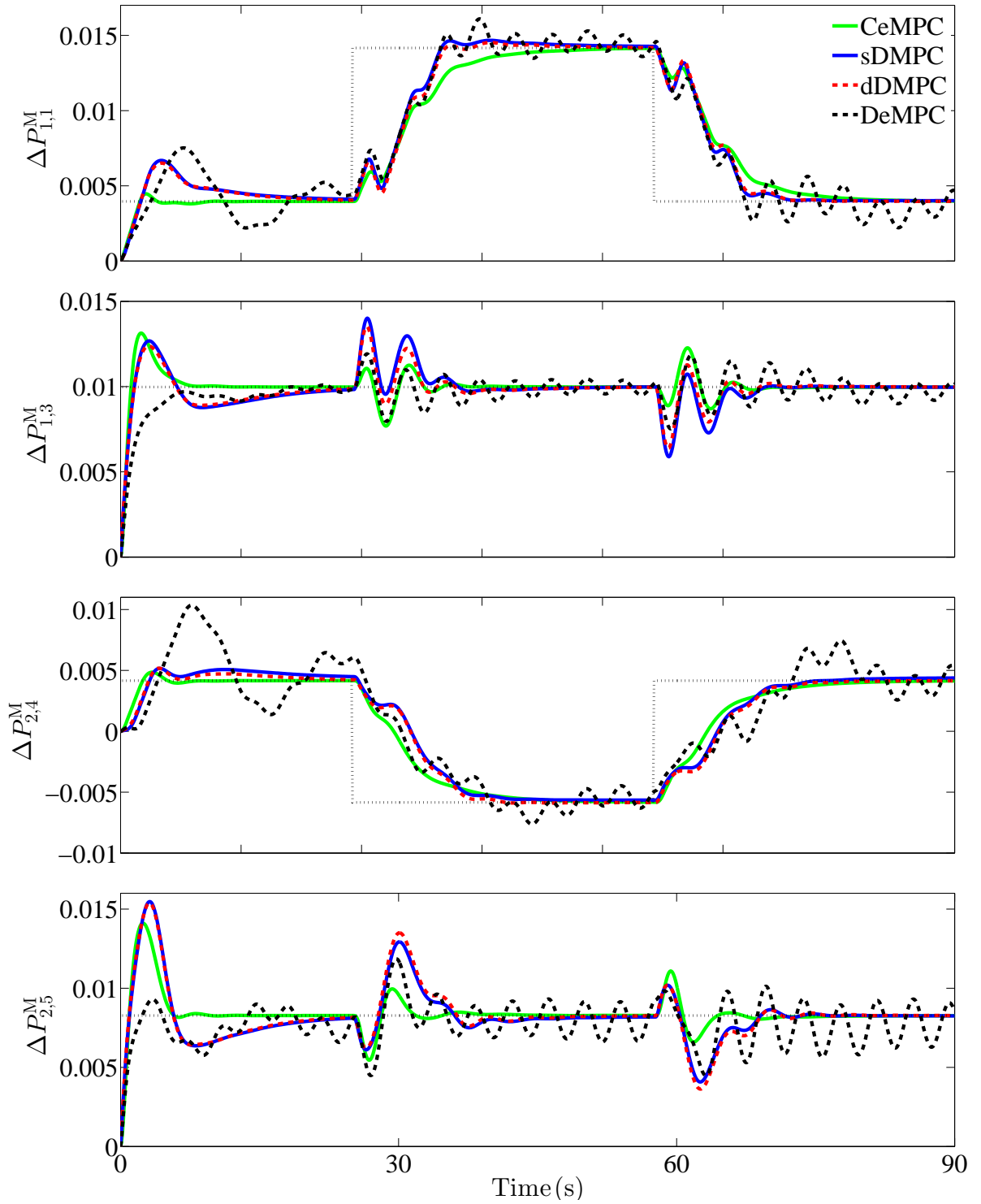
Figure 7.6: Change in power output of GenCos in area 1 and 2 $\Delta P_{i,k}^{\mathrm{M}}$ pu (case-1).

Table 7.2: Total cost of regulation (case-1).

Algorithm	CMPC	dDMPC	sDMPC	DeMPC
Regulation cost	5.9638	6.7483	6.8840	14.8356
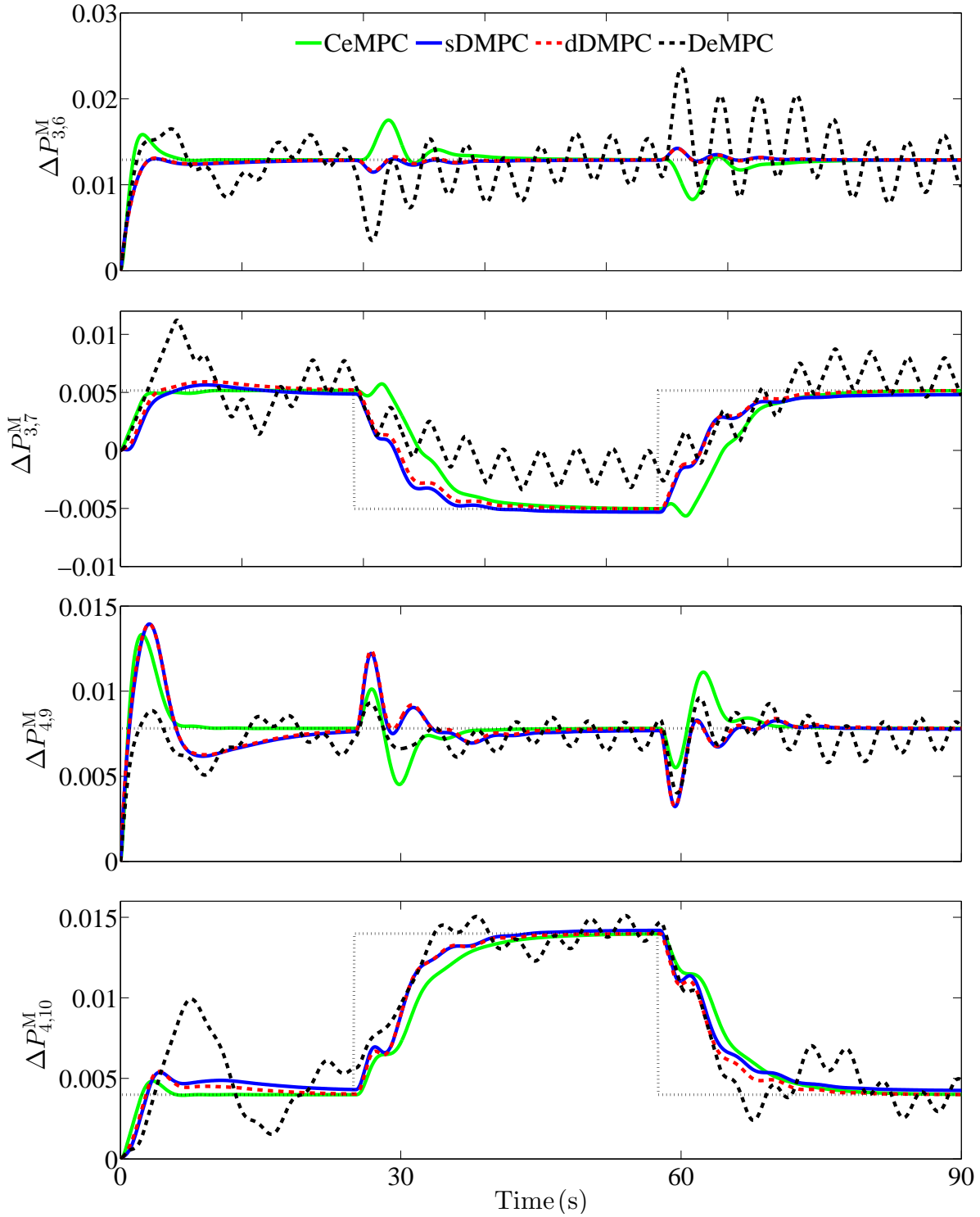
Figure 7.7: Change in power output of GenCos in area 3 and 4 $\Delta P_{i,k}^{\mathrm{M}}$ pu (case-1).
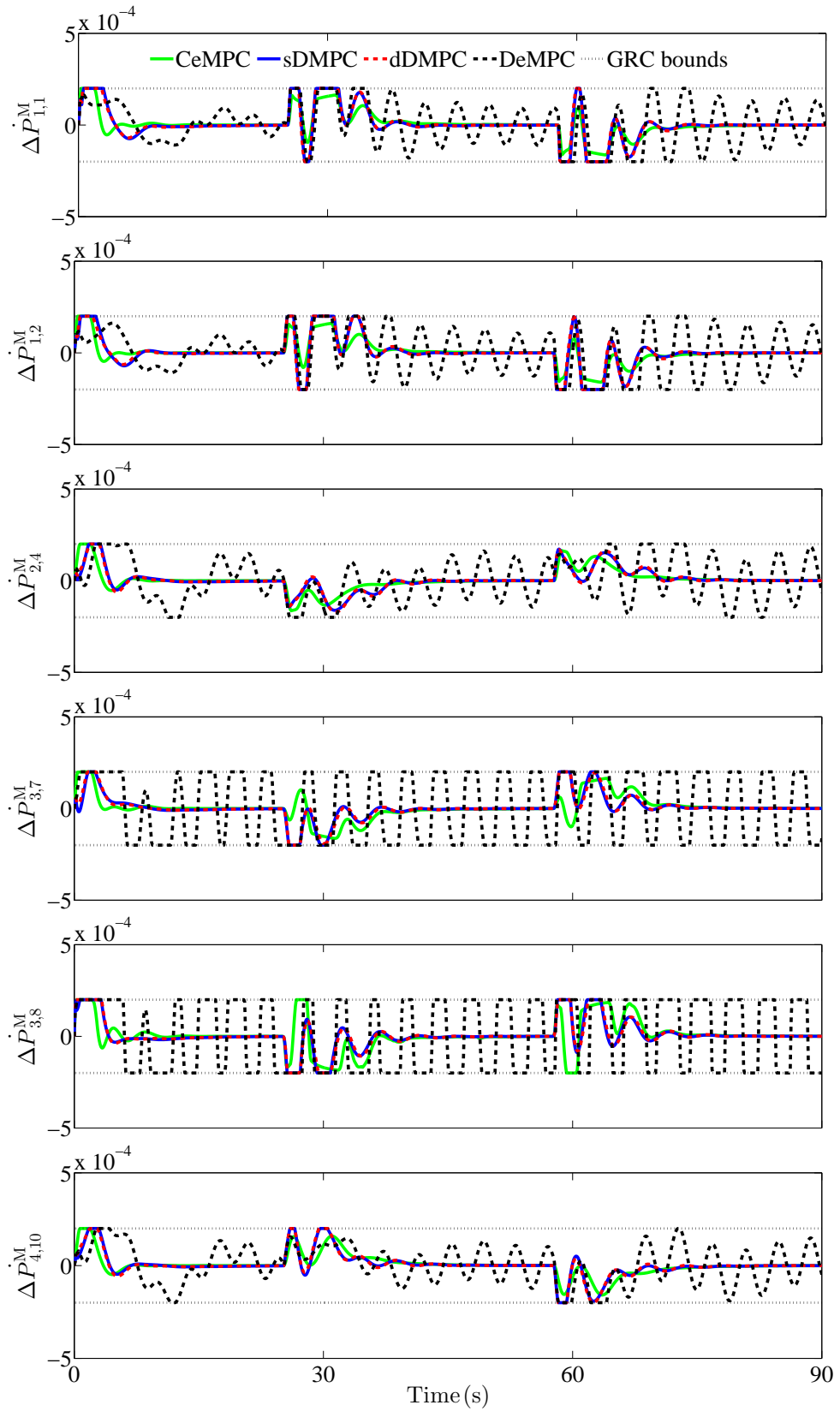
Figure 7.8: Generation rate of GenCos (case-1). Only GRC of GenCos with nonzero area participation factors (on supplementary control) are shown as they are the only ones constrained.
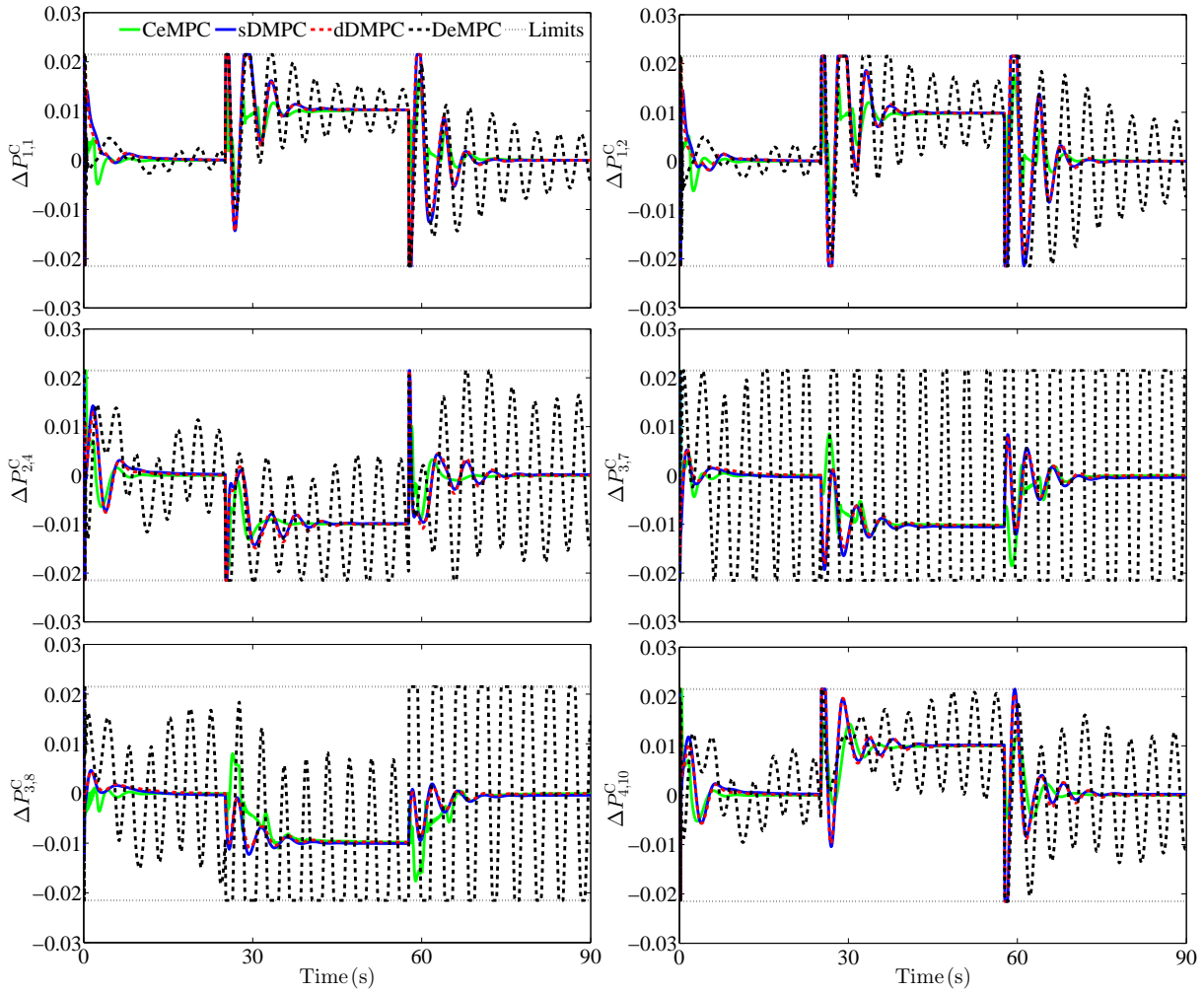
Figure 7.9: Control input of each GenCo (case-1). Only the input signals of GenCos on supplementary control are shown.

The frequency deviations, the deviations in net tie line power and the area control error in each area are shown in Figure 7.3, 7.4 and 7.5 respectively, for the four different control architectures. It is seen that the DeMPC has the the worst performance. This is because, each ith DeMPC scheme neglects the coupling effects from neigbouring subsystems. This also justifies what was stated in Section 2.3 that one of the causes of high frequency fluctuations recently [113] is due to the completely decentralised frequency control framework in operation in most interconnected power networks.

Moreover, it can be seen from Figure 7.3, 7.4 and 7.5 that the performance of CMPC, sDMPC and dDMPC are comparable, with CMPC, in some instances, giving a better performance. This is because, the CMPC has full knowledge of available system information. However, as stated earlier, CMPC may not be realistic for large scale multi-area system, where control areas have large geographical separations.

For this 4-area case, the performance between sDMPC and dDMPC are almost indistinguishable; however, the total regulation cost incured by applying each scheme has been calculated and presented in Table 7.2. The expression (7.30a) was utilised to calculate the total cost incured for the sDMPC,dDMPC and DeMPC while (7.30b) was used to compute the total cost based on the centralised scheme.

$$J_c = \sum_{i \in \mathcal{A}} \left\{ \sum_{t=1}^{L_s} \left\{ (x_{t+1}^{[i]} - x_{ss}^{[i]})^T Q_{ii}(x_{t+1}^{[i]} - x_{ss}^{[i]}) + (u_t^{[i]} - u_{ss}^{[i]})^T R_{ii}(u_t^{[i]} - x_{ss}^{[i]}) \right\} \right\} \tag{7.30a}$$

$$J_d = \sum_{t=1}^{L_s} \left\{ (x_{t+1} - x_{ss})^T Q(x_{t+1} - x_{ss}) + (u_t - u_{ss})^T R(u_t - x_{ss}) \right\} \tag{7.30b}$$

where L_s is the simulation length.

The CeMPC has the lowest regulation cost as expected while DeMPC has the highest cost. The total regulation cost incurred by dDMPC is lower compared to sDMPC. This is because, each ith dDMPC uses a more accurate model than the sDMPC. However, each local dDMPC requires far more information than the sDMPC. The ith dDMPC requires the control $v_{t/k}^{[j]}$ and state $z_{t+1/k}^{[j]}$ sequence, contracted $d_k^{[j]}$ and uncontracted $b_k^{[j]}$ load changes from every CA, while the ith sDMPC requires the state sequence $z_{t+1/k}^{[j]}$ and contracted load changes $d_k^{[j]}$ of its neighbours in the CT representation.

Figures 7.6 and 7.7 show the change in the power output of each GenCo based on the four MPC architectures; only one GenCo on supplementary control in each area is presented as the others showed a similar pattern. The black dotted lines are the desired generation changes and are included as a reference. The GenCos whose desired generation changes are constant are the ones on bilateral LM contract only, while the ones with a piecewise constant (rectangular) generation reference are on bilateral LM contract and supplementary control. Similar to what was seen in Figure 7.3, 7.4 and 7.5, DeMPC results in the worst performance and CeMPC generally provided better regulation that the other MPC schemes.

The generation rate and control input signal of each GenCo on supplementary control is shown in Figure 7.8 and 7.9 respectively, with their bounds shown as black dotted lines. The figures clearly illustrate the importance of communication and exchange of information between the LFC controller in each area as DeMPC results in oscillations and more saturation in the generation rates and input signals. Feasible cooperation DMPC proposed in [102] was implemented, but not included in the plots as the optimisation gave infeasibility at some sampling instants; this is because of the state rate constraints (GRC) .

A summary of the key observations from case-1 is provided in Table 7.3 to help a reader.

Table 7.3: Summary of key observations from results obtained in case-1 (4-area network)

Figures	Key observations (CMPC, DeMPC, sDMPC and dDMPC)
Figure 7.3 shows frequency deviations Δf_i; Figure 7.4 shows deviation in net tie line power ΔP_i^{tie}; Figure 7.5 shows ACE signals.	Large fluctuations in Δf_i, ΔP_i^{tie} and ACE signals are observed with DeMPC algorithm; this is because, system couplings are neglected. CMPC, sDMPC and dDMPC give comparable performances in Δf_i, ΔP_i^{tie} and ACE signals, with CMPC offering a better performance in some instances. Also, CMPC leads to a greater undershoots and overshoots in some instances as compared to sDMPC and dDMPC, and CMPC deliberately allowed that (no constraints on frequency, ACE and tie line power) to meet system constraints requirements since it has more information about the system. dDMPC slightly outperforms sDMPC because it uses a more accurate subsystem model, but this comes at the expense of more information exchange. A regulation cost comparison between the schemes is provided in Table 7.2, where CMPC has the lowest and DeMPC has the highest regulation cost. dDMPC cost is lower than sDMPC cost.
Figures 7.6 and 7.7 show the change in power outputs of GenCos $\Delta P_{i,k}^{\text{M}}$	The DeMPC results in a poor tracking of the desired generation; this is also because system couplings are neglected. CMPC results in best tracking performance, with about the right rate of generation change. sDMPC and dDMPC algorithms gave almost similar performance, but dDMPC provides a slightly better tracking performance.
Figure 7.8 shows the generation rates $\Delta \dot{P}_{i,k}^{\text{M}}$ of GenCos	The DeMPC algorithm results in more saturations and generation rates oscillates without settles to zero. This contributed to the large fluctuations in Δf_i, ΔP_i^{tie} and ACE signals observed and also poor tracking of the desired generation $\Delta P_{i,k}^{\text{M}}$. CMPC, having a complete knowledge of the system, handled the GRC better than sDMPC and dDMPC. sDMPC and dDMPC gave almost identical performance with respect to GRC handling.
Figure 7.9 shows the control input signals to GenCos $\Delta P_{i,k}^{\text{C}}$.	Again, $\Delta P_{i,k}^{\text{C}}$ signals from the DeMPC algorithm saturates most of the time and oscillate continuously. sDMPC and dDMPC give almost indistinguishable behaviour in terms on input constraints handling. The CMPC algorithm provide the best input constraints handling.

Table 7.4: Contracted load change of each GenCo(case-2).

$\Delta P^{\mathrm{L}}_{1,1}$	$\Delta P^{\mathrm{L}}_{1,2}$	$\Delta P^{\mathrm{L}}_{1,3}$	$\Delta P^{\mathrm{L}}_{1,4}$	$\Delta P^{\mathrm{L}}_{1,5}$	$\Delta P^{\mathrm{L}}_{1,6}$	$\Delta P^{\mathrm{L}}_{1,7}$
0	0	0	0.007	0	0.007	0

$\Delta P^{\mathrm{L}}_{2,8}$	$\Delta P^{\mathrm{L}}_{2,9}$	$\Delta P^{\mathrm{L}}_{2,10}$	$\Delta P^{\mathrm{L}}_{2,11}$	$\Delta P^{\mathrm{L}}_{2,12}$
0.0105	0	0.0052	0.0052	0.0052

$\Delta P^{\mathrm{L}}_{3,13}$	$\Delta P^{\mathrm{L}}_{3,14}$	$\Delta P^{\mathrm{L}}_{3,15}$	$\Delta P^{\mathrm{L}}_{3,16}$	$\Delta P^{\mathrm{L}}_{3,17}$	$\Delta P^{\mathrm{L}}_{3,18}$	$\Delta P^{\mathrm{L}}_{3,19}$
0.0091	0.0091	0.0046	0.0046	0.0046	0	0.0091

$\Delta P^{\mathrm{L}}_{4,20}$	$\Delta P^{\mathrm{L}}_{4,21}$	$\Delta P^{\mathrm{L}}_{4,22}$	$\Delta P^{\mathrm{L}}_{4,23}$	$\Delta P^{\mathrm{L}}_{4,24}$	$\Delta P^{\mathrm{L}}_{4,25}$	$\Delta P^{\mathrm{L}}_{4,26}$	$\Delta P^{\mathrm{L}}_{4,27}$
0.007	0	0.007	0	0	0.007	0	0.007

$\Delta P^{\mathrm{L}}_{5,28}$	$\Delta P^{\mathrm{L}}_{5,29}$	$\Delta P^{\mathrm{L}}_{5,30}$	$\Delta P^{\mathrm{L}}_{5,31}$	$\Delta P^{\mathrm{L}}_{5,32}$
0.0091	0.0091	0	0.0091	0

$\Delta P^{\mathrm{L}}_{6,33}$	$\Delta P^{\mathrm{L}}_{6,34}$	$\Delta P^{\mathrm{L}}_{6,35}$	$\Delta P^{\mathrm{L}}_{6,36}$	$\Delta P^{\mathrm{L}}_{6,37}$	$\Delta P^{\mathrm{L}}_{6,38}$	$\Delta P^{\mathrm{L}}_{6,39}$	$\Delta P^{\mathrm{L}}_{6,40}$
0.0091	0	0.0091	0.0046	0	0.0091	0.0046	0

$\Delta P^{\mathrm{L}}_{7,41}$	$\Delta P^{\mathrm{L}}_{7,42}$	$\Delta P^{\mathrm{L}}_{7,43}$	$\Delta P^{\mathrm{L}}_{7,44}$	$\Delta P^{\mathrm{L}}_{7,45}$	$\Delta P^{\mathrm{L}}_{7,46}$
0	0	0	0.007	0	0.007

Table 7.5: Total cost of regulation (case-2).

Algorithm	CMPC	dDMPC	sDMPC	DeMPC
Regulation cost	2518	2568	2620	3081

7.8.2 Case-2: 7-area deregulated power system

This section presents the results obtained by implementing the proposed DMPC on a 7-area system to further demonstrate its effectiveness and suitability for LFC. The area participation factors of GenCos and the DPM used in Chapter 6 is also used here. Other parameters of the
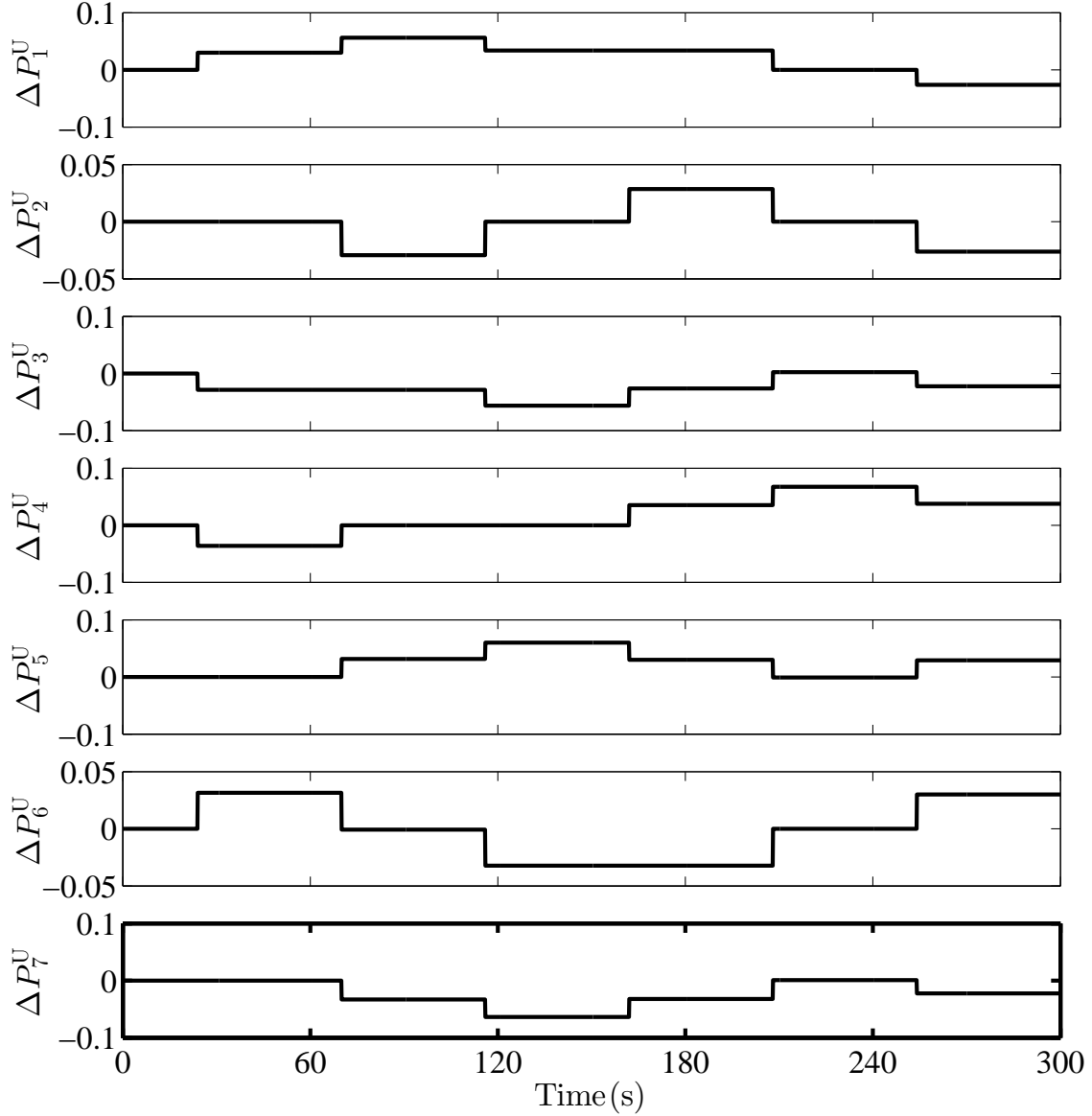
Figure 7.10: Uncontracted load changes in each area (case-2).

7-area system are provided in Tables A.6, A.7 and A.8. The rated capacities assumed for each area are $\{P_{r_1}, P_{r_2}, \cdots, P_{r_7}\} = \{5500, 6750, 5000, 6200, 4500, 5800, 5600\}$.

The ith DMPC uses the same number of d.o.f in control n_c and sampling time as in case-1 of Section 7.8.1. The constraints tightening factors used are $\sigma_{\mathrm{x}}^{[i]} = 0.95$ and $\sigma_{\mathrm{u}}^{[i]} = 0.95$. The state and input weighting used in Chapter 6 are partitioned according to the dimensions of each subsystem and used here. As the benchmark system used here is a much larger one (7-area with 33 GenCos and 46 DisCos), not all results are displayed. Nevertheless, the undisplayed results are similar in pattern to the ones shown in this section. Assuming the contracted load change of each DisCo is as shown in Table 7.4 and the uncontracted load variations that occurred in each area is as shown in Figure 7.10.

Figure 7.11: Frequency deviation and net tie line power deviation in area 1 (case-2).

The frequency deviation Δf_i and the deviation in net tie line power ΔP_i^{tie} in areas 1, 2, 4 and 7 are shown in Figures 7.11, 7.12, 7.13 and 7.14 respectively. The plots showing the area control error (ACE) signals in each area are not provided since from Section 5.4.7, ACE_i converges to zero when Δf_i converged to zero and ΔP_i^{tie} settles at the scheduled (contracted) value $\Delta P_i^{\text{tie,sh}}$; hence the signals Δf_i, ΔP_i^{tie} and $\Delta P_i^{\text{tie,sh}}$ are enough to conclude about the area control errors. Similar to what was seen in case-1, DeMPC results in more oscillations in Δf_i and ΔP_i^{tie} signals in each area and thus give the worst performance.

The change in power output of some GenCos (two selected from each control area, and power outputs of GenCos in area 5 and 6 are omitted) are presented in Figures 7.15, 7.16 and 7.17. A reduced performance is also observed for the DeMPC scheme. The generation rates of some GenCos are shown in Figure 7.18 with the bounds indicated as black dotted lines. The input signals to a few generating units are shown in Figures 7.19 and 7.20.

Furthermore, the overall regulation cost of each MPC scheme has been computed and is presented in Table 7.5. As expected, the DeMPC scheme incurred the highest cost of regulation while the CMPC (benchmark) resulted in the lowest cost. As obtained in case-1, sDMPC give

Figure 7.12: Frequency deviation and net tie line power deviation in area 2 (case-2).

rise to a higher regulation cost than the dDMPC scheme. These discussions are summarised in Table 7.6 to help a reader.

7.8.3 Summary

To summarise, this section illustrated the dynamic responses obtained by implementing DMPC algorithms proposed on a 4-area and 7-area deregulated benchmark models developed in Chapter 5. In particular, four MPC architectures namely, CMPC, dDMPC, sDMPC and DeMPC were simulated, in the presence of GRC, input constraints, and their performances were compared.

7.9 Conclusion

Achieving a tight control of frequency in modern deregulated power interconnections, as it were in the past, will require more efficient control strategies, as a result of the overlap of market transactions with control mechanisms and the physics of power grids, coupled with
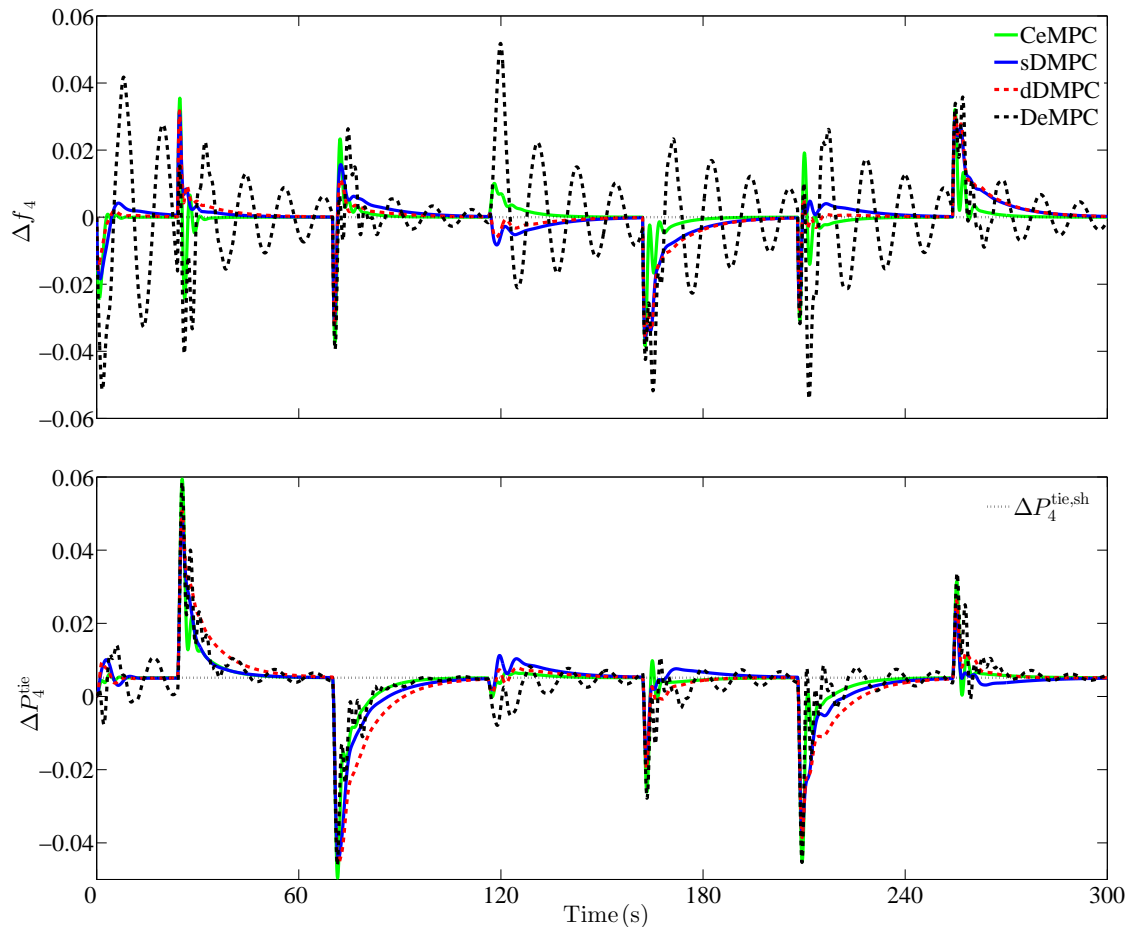
Figure 7.13: Frequency deviation and net tie line power deviation in area 4 (case-2).

high interactions between control areas in networks. Centralised MPC based LFC can bring some benefits in terms coordinating power transactions, cope with the interactions between CAs and honour physical system constraints. However CMPC is not realistic in general. Thus this chapter investigated the use of non-centralised MPC algorithms for LFC problems in a deregulated power system. In particular, three non-centralised MPC algorithms were developed, namely a dense DMPC (dDMPC), sparse DMPC (sDMPC) and a decentralised MPC (DeMPC). These algorithms differ in respect of the subsystem model used in a local MPC regulator design, which also dictated the amount of information shared between subsystems. The DeMPC utilised discrete time (DT) subsystem models which are completely decoupled.

Moreover, sDMPC and dDMPC utilised DT subsystem models obtained from the global system model via different discretisation approach: the sDMPC was developed to use subsystem models obtained by decomposing the global continuous time (CT) model into subsystems and then discretising each CT subsystem model separately, and this discretisation scheme preserved the sparsity of the CT global system; the dDMPC was based on subsystem models realised by first discretising the CT global model before decomposition, and thus the sparsity of the original CT global model is lost. As a consequence, subsystems do not communicate

195
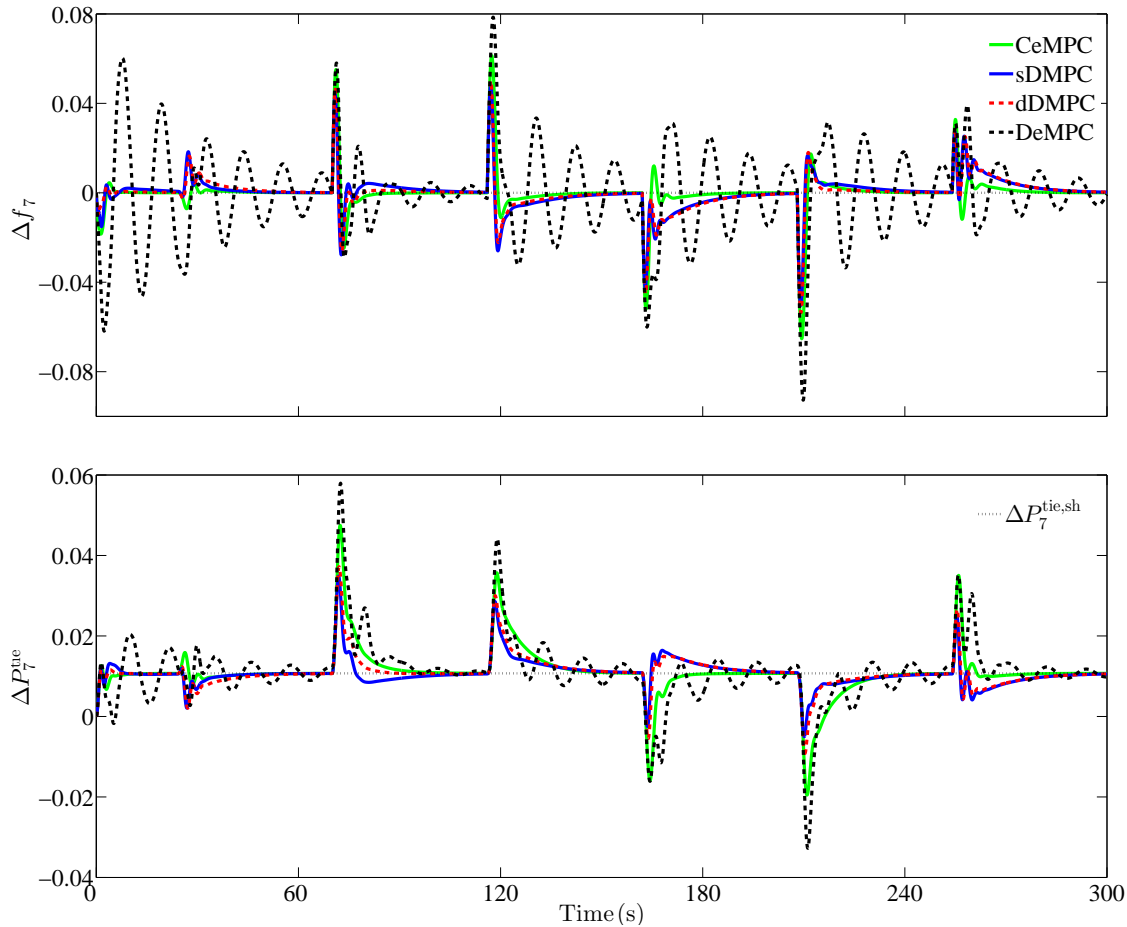
Figure 7.14: Frequency deviation and net tie line power deviation in area 7(case-2).

in the DeMPC scheme. Direct neighbours shared a limited amount of information between themselves in the sDMPC whereas in the dDMPC, all available information are shared between all subsystems.

Furthermore, local Luenberger observers were designed to estimate local system states and uncontracted load changes from local measurements and these estimates are used by local MPC regulators; hence the proposed schemes use output feedback. Each local observer uses a local stabilising gain designed by solving a set of linear matrix inequalities. Moreover, local observers do not communicate in the DeMPC case, shared a limited amount of information with direct neighbours in the sDMPC case, and shared all available information with the other local observers in the dDMPC case.

The proposed non-centralised MPC algorithms, developed for deregulated LFC problems, were tested on a 4-area and 7-area system, where control areas are unequally rated and compared with a CMPC benchmark. The results obtained, in the presence of GRC and input constraints, reveal the following:
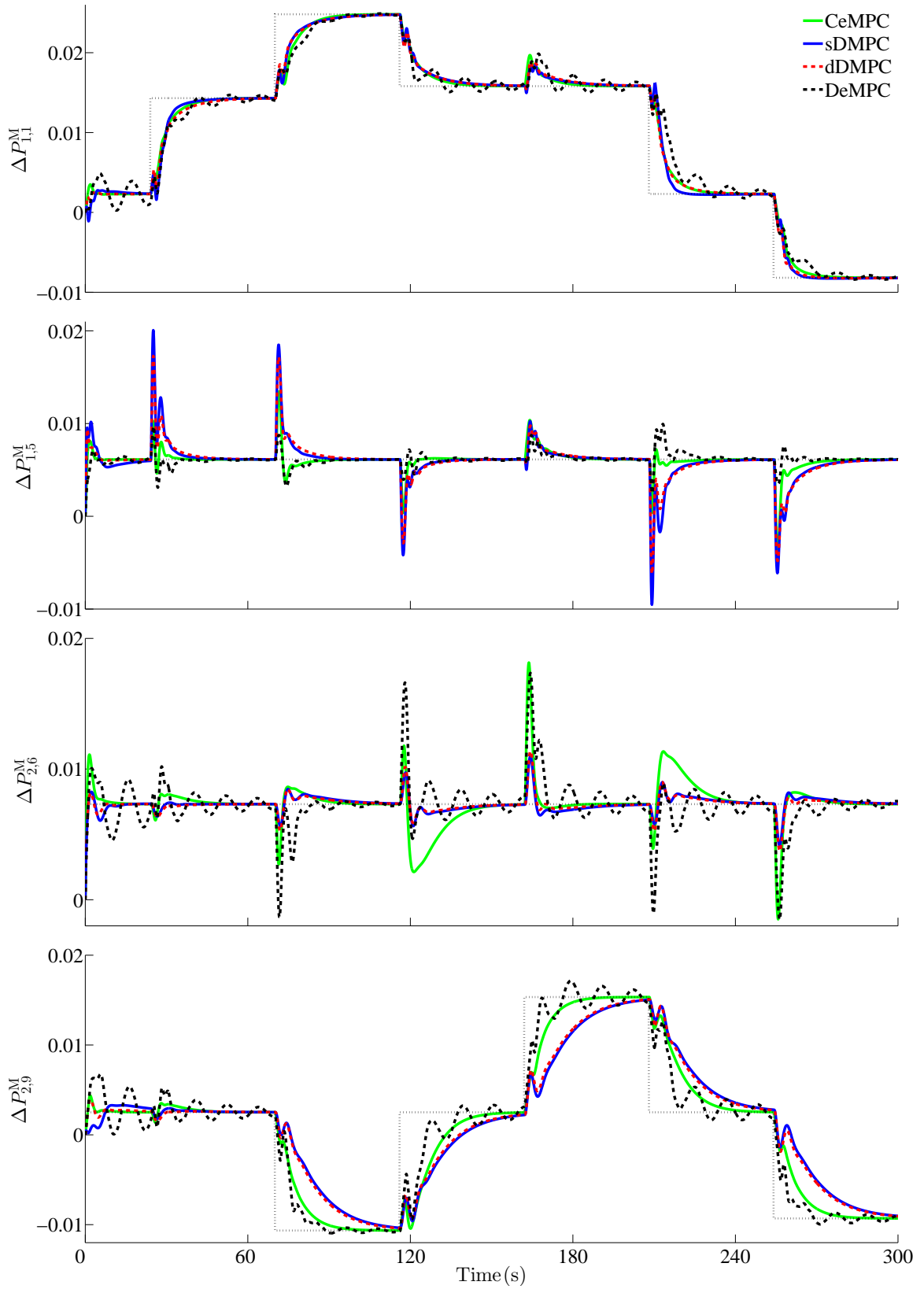
Figure 7.15: Change in power output of GenCos in area 1 and 2 (case-2).
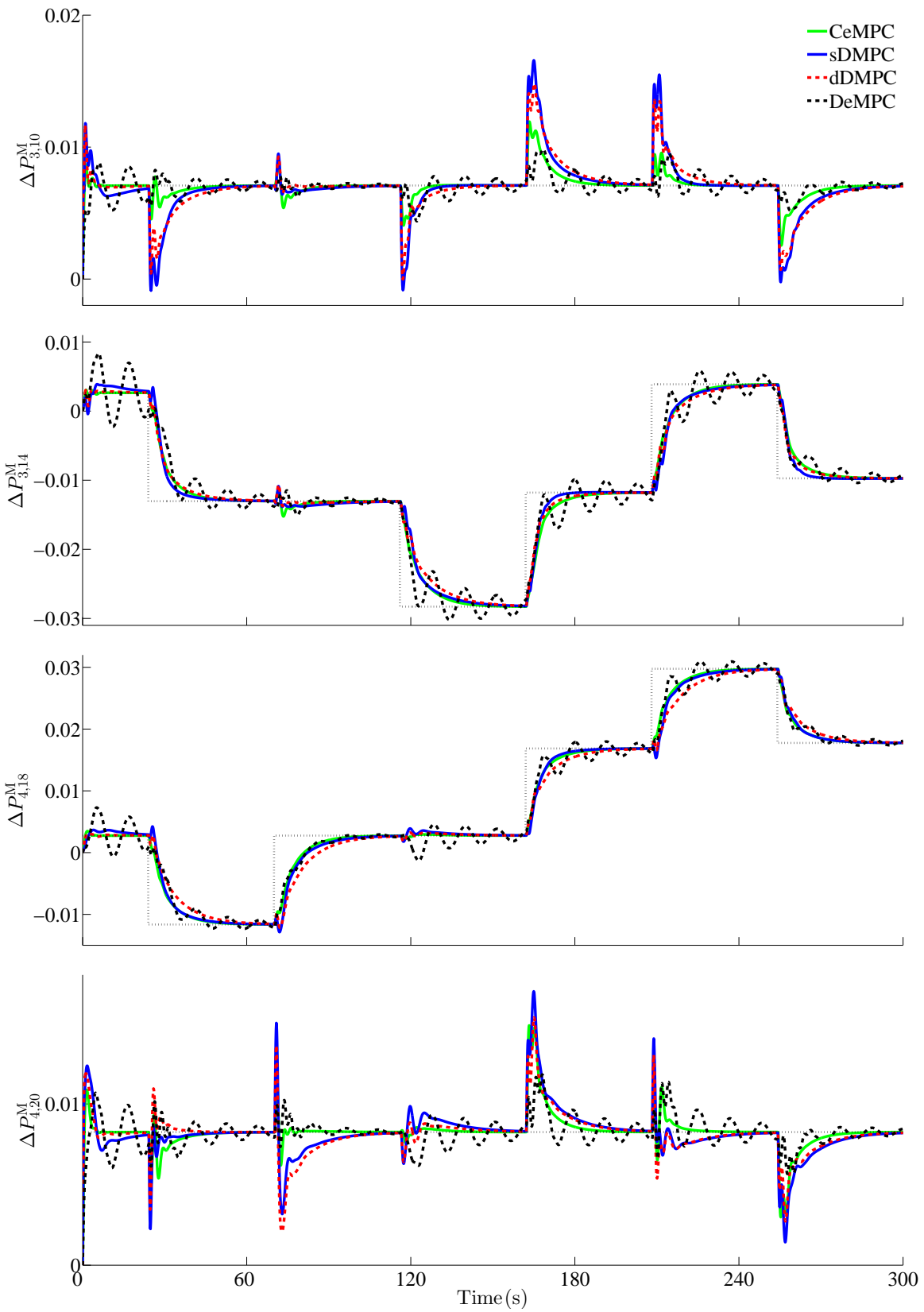
Figure 7.16: Change in power output of GenCos in area 3 and 4 (case-2)
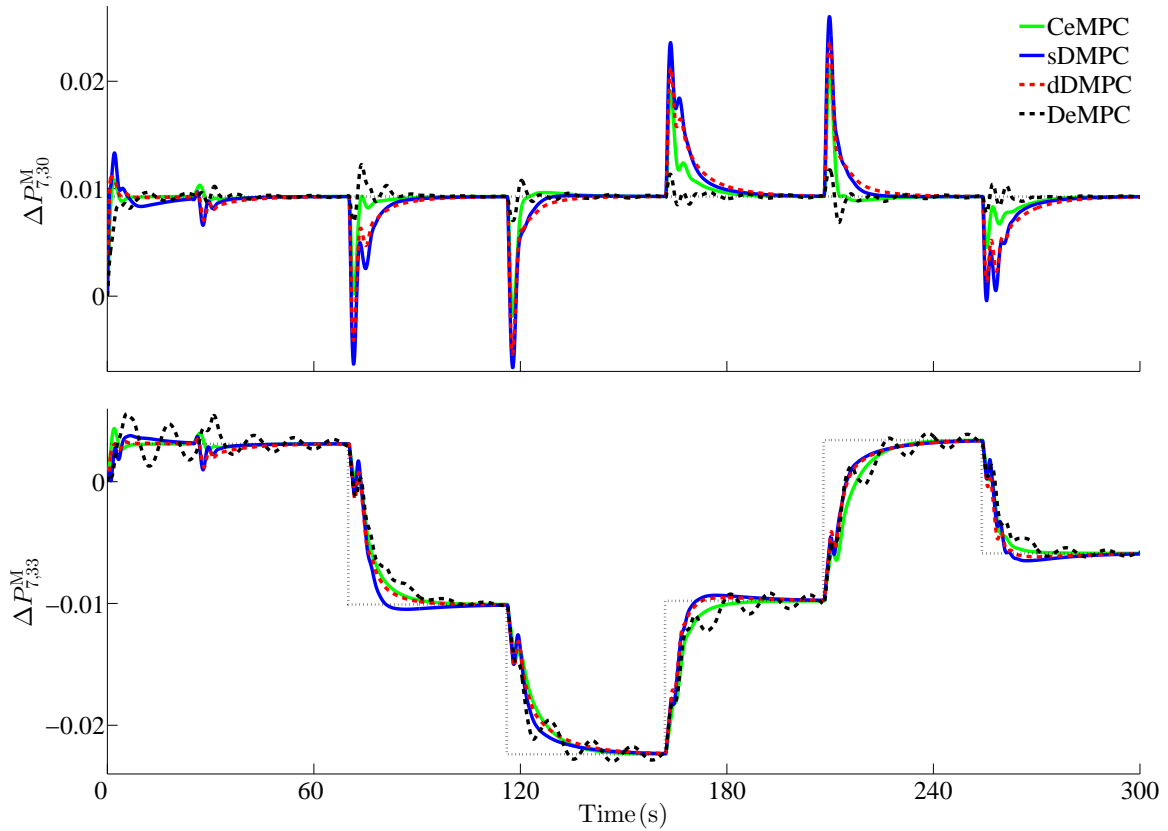
Figure 7.17: Change in power output of GenCos in area 7 (case-2)

- The amount of information shared between control areas (subsystems) in an interconnected power system can have an impact on overall system performance. Specifically, when the couplings between subsystems are neglected and therefore information are not shared between subsystems, poor system performance can result. This is seen from the large fluctuations in frequency, tie line power and ACE, and poor tracking of a desired generation, oscillatory generation rates and constraint saturations associated with the DeMPC algorithm. Furthermore, a better performance, comparable to a CMPC scheme, can be obtained if subsystems (CAs) share some information and coordinate themselves, as seen in the sDMPC and dDMPC schemes.

- It was also observed that the discretisation scheme employed in obtaining subsystem models (control area models) can effect the LFC performance. This is seen from the results and also from the total regulation cost where dDMPC give a slightly better performance when compared with the sDMPC algorithm.

Thus, the proposed DMPC algorithms could bring benefits in LFC in a practical deregulated power system environment.

Table 7.6: Summary of key observations from results obtained in case-2 (7-area network)

Figures	Key observations (CMPC, DeMPC, sDMPC and dDMPC)
Each of Figures 7.11, 7.12, 7.13 and 7.14 shows the frequency deviations Δf_i (top) and deviation in net tie line power ΔP_i^{tie} (bottom) in areas 1, 2, 4 and 7	Similar to the trends observed in case-1, the DeMPC algorithm leads to oscillations in Δf_i and ΔP_i^{tie} due to the coupling effects that were ignored. CeMPC, the benchmark, is observed to offer the best performance. A close observation of the results also shows that dDMPC performs slightly better than the sDMPC. The total cost of regulation for each of the schemes in presented in Table 7.5, where CMPC has the lowest and DeMPC has the highest. sDMPC incured a higher cost than dDMPC.
Figures 7.15, 7.16 and 7.17 show the change in power outputs $\Delta P_{i,\text{k}}^{\text{M}}$ of selected GenCos.	Again, DeMPC results in a poor tracking of desired generation changes. The benchmark algorithm (CMPC) achieved a better tracking as compared to sDMPC and dDMPC in some instances; some other times, their performances are almost indistinguishable.
Figure 7.18 shows the generation rates $\Delta \dot{P}_{i,\text{k}}^{\text{M}}$ of GenCos	The generate rate resulting from the DeMPC algorithm oscillates continuously and never converged to zero as desired. This contributed to the poor performance it displayed in Δf_i and ΔP_i^{tie} signals in Figures 7.11, 7.12, 7.13 and 7.14 and also poor tracking of the desired generation $\Delta P_{i,\text{k}}^{\text{M}}$. Moreover, a close observation will reveal that CMPC handled GRCs better than sDMPC and dDMPC and this is expected.
Figures 7.19 and 7.20 show the control input signals to GenCos $\Delta P_{i,\text{k}}^{\text{C}}$.	The $\Delta P_{i,\text{k}}^{\text{C}}$ signals from the DeMPC algorithm shows some oscillation. CeMPC, sDMPC and dDMPC displayed almost identical behaviour for the input signals.
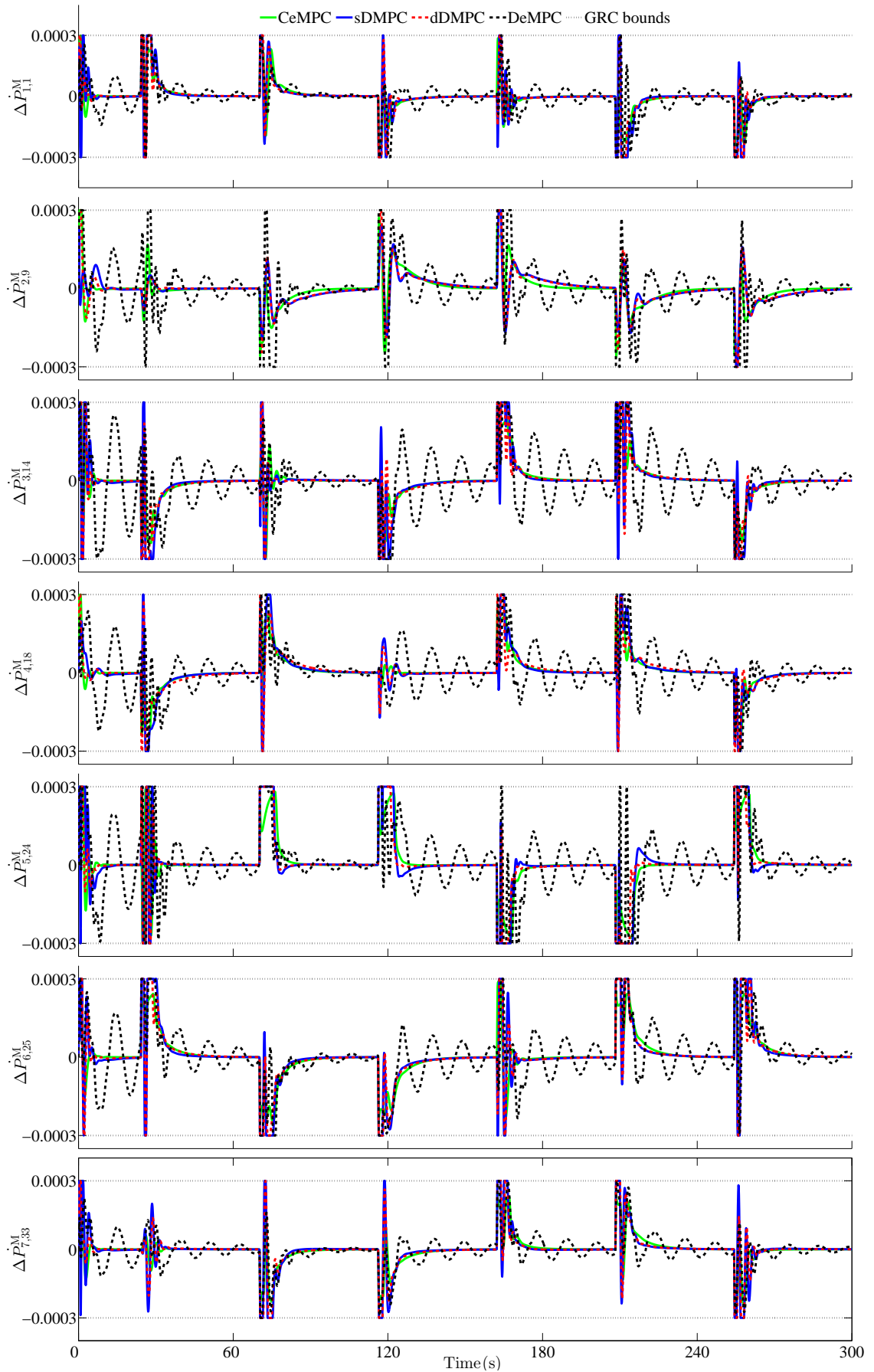
Figure 7.18: Generation rate of GenCos; one is selected from each control area and displayed (case-2).
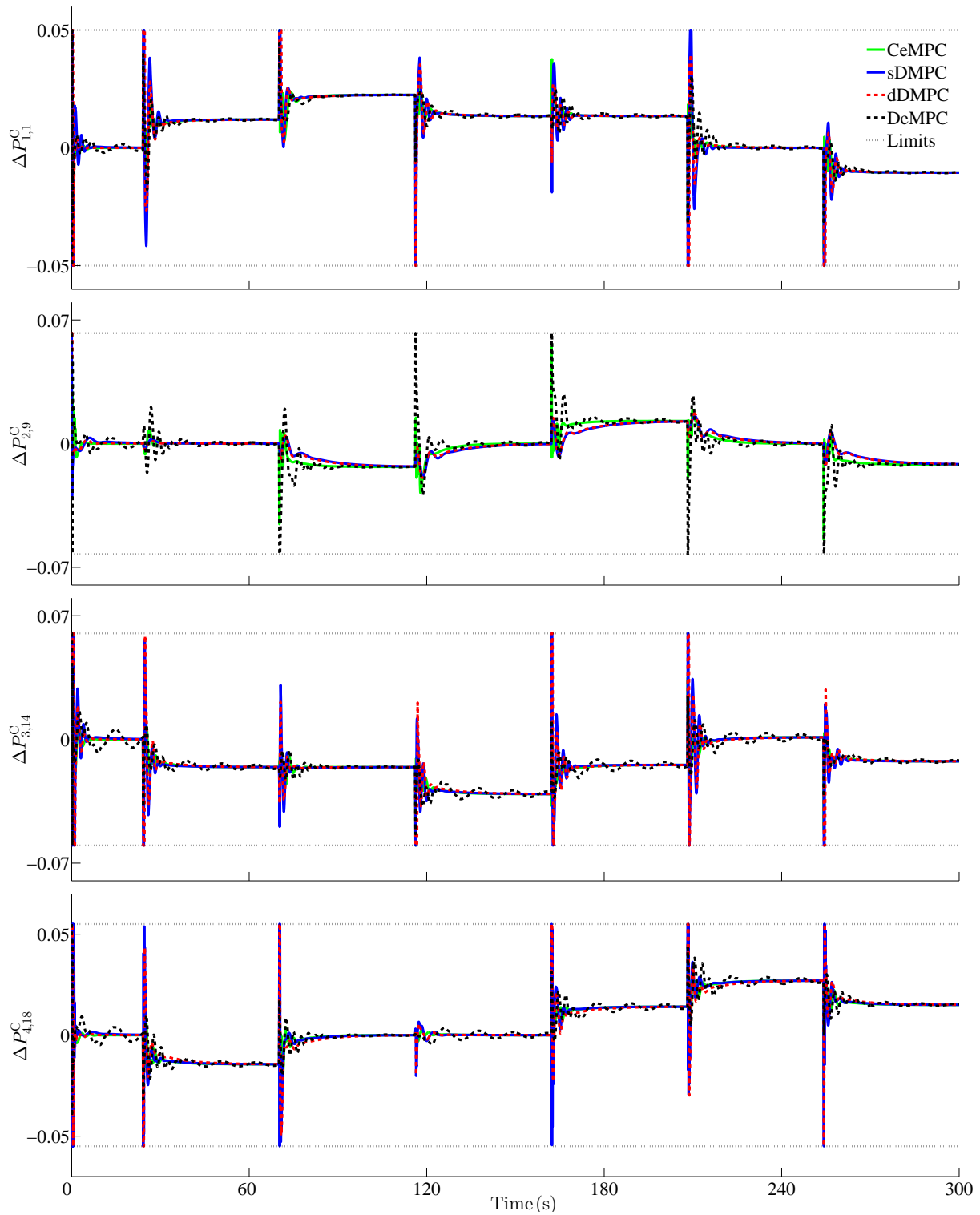
Figure 7.19: Control input of GenCos in areas 1-4 (case-2). One output per control area is shown.
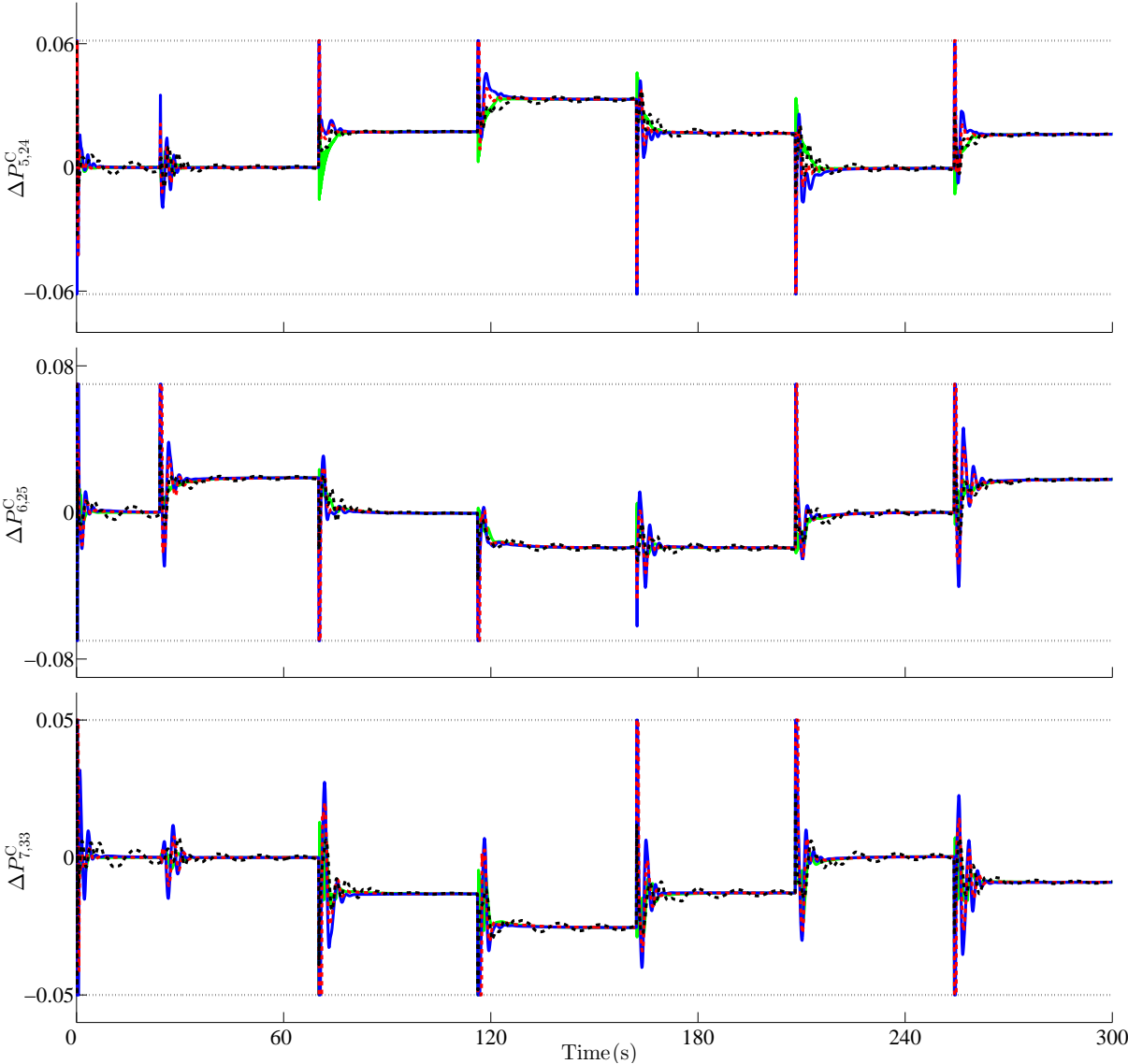
Figure 7.20: Control input of GenCos in areas 5-7 (case-2). One output per control area is shown.

Chapter 8

Conclusions and Future work

This chapter concludes the thesis and consists of the following: Section 8.1 presents overall concluding remarks on the work in the thesis; Section 8.2 pools the main contributions in the relevant chapters for convenience; Section 8.3 discusses some possible future work.

8.1 Conclusions

The work presented in this document focused on some technical concerns inherent in load frequency control (LFC) in interconnected power systems, which have arisen because of the ongoing deregulation being experienced by electric industries around the world. Deregulation has led to the emergence of private entities such as generation companies (GenCos) and distributed companies (DisCos) which sell (GenCos) and purchase (DisCos) electricity competitively. A transmission system operator (TSO) is saddled with the responsibility of providing LFC in each control area (CA) and must procure incremental power from the competitive power market. Furthermore, transmission companies (TranCos) in large interconnections (one TranCo in each CA and the TranCos are also the TSOs in some jurisdictions) were compelled by the deregulation policy to grant external entities open and unbaised access to their transmission networks, as they would allow for entities within their CAs. Consequently, the number of independent cross-border power contracts (electricity trading) between GenCos and DisCos in most deregulated interconnections has increased dramatically. Unpredicted flows are now being experienced by TSOs in their local networks as traded electricity does not necessarily flow via contract paths, and this has resulted in recurrent large frequency deviations globally [19, 21]. Note that a DisCo can participate in LFC in the form of load matching contract by contracting independently with GenCos within or outside its CA. LFC has become complex because the procurement of incremental power must obey the market rules.

Some factors that have also contributed to frequency deteriorations after deregulation are [21, 226]: (i) introduction of smaller generating units (with less inertia) and renewable energy sources (with neglegible or absolutely no inertia) in most interconnections, leading to a reduction in the inertia per unit generation available; (ii) lack of relevant data (contract data) by the load frequency controller in each area; (iii) poor coordination and lack of real-time information sharing between local LFC schemes; (iv) reduced security margins and a corresponding increase in system stress as transacting entities are driven by profit and not optimal system operations; (v) significant coupling between the electric grid's physics and electricity trading which has been largely ignored in electric industries. Large frequency deviations resulting from active power imbalance can damage turbines, reduce performance of power plants auxiliaries and overload tie lines. Moreover, tight frequency control is important so that serious grid problems that could lead to blackouts, masking as a normal frequency deviation, can be detected early. As a result these issues which has hindered tight frequency control in the new environment, there was a need for the following:

- A new modelling framework that incorporates power transactions (contracted data), and this is important as it will enable TSOs to effectively study LFC in the market environment; this will in turn lead to a proper planning and operation of the grid.

- A more effective LFC strategy in each area which can handle large number of transactions, share information and coordinate with LFC schemes in neigbouring areas to achieve acceptable overall system performance.

This thesis addressed the needs itemised above by setting six key objectives, presented in Section 1.4, which broadly fall into (i) an extensive literature review to evaluate the research contributions available towards addressing LFC challenges in the new environment in terms of their strengths and weaknesses, and thus to reveal the key gaps; (ii) development of a novel and more practical generalised LFC modelling framework for studies in the deregulated environment; (iii) an effective LFC design based on model predictive control (MPC) strategy, where both centralised, decentralised and distributed MPC architectures are investigated. Specifically, Chapter 2, firstly, described the age-long mathematical model used in traditional LFC studies and provided a simulation example to illustrate the key concept of LFC; the traditional model was important as it formed the basis for which the deregulated models in this work were developed. Furthermore, a thorough survey of the LFC literature was carried out, where the strengths and weaknesses of different control techniques that have considered for LFC, based on some minimum specifications, were compared; see Table 2.9. The survey revealed that no single control technique meets the minimum specification. The comparison also revealed that MPC can bring some benefits such as simple/systematic design, effective and systematic handling of constraints such as generation rate constraints (GRC) and limits on control inputs, MIMO capabilities, calculation of economically optimal control signals and distributed

control. These benefits, thus, motivated the investigation of the MPC technique in deregulated LFC problems as its potentials have not been well exploited in the new environment. Moreover, to be able to develop an MPC based solution for deregulated LFC, there was a need to understand the mathematical fundamentals of MPC, and thus, Chapter 3 presented the basic concepts of MPC, where a mathematical description was provided for centralised MPC (CMPC), decentralised MPC (DeMPC) and distributed MPC (DMPC) architectures. The key attributes of the different architectures were discussed, where it was emphasised that CMPC can offer the best performance but is unrealistic for large interconnections, while DeMPC, while being much simpler, could give poor performance as the effects of coupling between subsystems are neglected; refer to Table 3.1. The key qualities of MPC strategies and how they match some vital requirements of a practical LFC were reiterated. The possibility of deriving benefits from MPC in a deregulated LFC problem was investigated in Chapter 4 using a small-scale deregulated benchmark network in state-space form.

In particular, Chapter 4 began by providing a clear and step-by-step description of the key modifications required in a traditional LFC model to incorporate bilateral load matching (LM) transactions between GenCos and DisCos in a 2-area deregulated network, where the ratio of the total LM requirement of a DisCo contracted to a GenCo was represented as the entries of a DisCo participation matrix (DPM). The 2-area deregulated LFC model described in Chapter 4 was initially developed in [29] where the concept of DPM was pioneered, but presented slightly differently here. It was assumed, in the model, that a deregulated network can be subjected to contracted (measured) load changes which have been procured by DisCos through bilateral LM contract, and uncontracted (unmeasured) load changes are handled by a TSO who is assumed to have secured incremental (and decremental) reserve from local GenCos bidding in a pool and can dispatch them in real time based on their area participation factors. Furthermore, a CMPC based LFC scheme using output feedback, where a discrete time Luenberger observer was used to estimate uncontracted load changes and system states, was proposed for the 2-area benchmark. Simulations were conducted under two cases - firstly the network subjected to contracted load changes only and next contracted and uncontracted load changes - in the presence of turbine GRC and input constraints. The results obtained, which were compared with infinite horizon LQR based LFC, revealed that the predictive control is a promising strategy for deregulated LFC as GRC and input constraints were handled more effectively, leading to a better frequency regulation regarding the magnitude of overshoots and undershoots and the time taken to eliminate frequency deviations. The CMPC algorithm also provided a better regulation of the ouput powers of the generators leading to a more efficient rejection of uncontracted load changes.

Some of the steps presented in Chapter 4 to developing a deregulated model, such as obtaining the expressions for contracted LM signal 4.3.2, net tie line flow deviations 4.3.5 and scheduled net incremental tie line flow 4.3.6 could be burdensome and prone to error for large deregulated

networks with a complex topology and a sizeable number of control areas, GenCos and Dis-Cos. Furthermore, the 2-area system assumed that each CA has the same rated capacity and that is unrealistic. Thus Chapter 5 proposed a novel generalised deregulated LFC modelling framework which can provide key benefits: (i) a relatively easy and systematic approach to developing deregulated LFC models irrespective of the number of CA, GenCos and DisCos and complexity of the network topology, and thus represents a more efficient method of handling the increasing number of local and cross-border transactions in modern day deregulated interconnections; (ii) incorporates the capacity ratios between neighbouring CAs and thus offers the flexiblity to study LFC in large interconnections wth equal CAs ratings or the more realistic unequal CAs ratings. A 7-area deregulated benchmark model with 33 GenCos and 46 DisCos was developed to clearly illustrate how the generalised formulation can be used, and also served as a simulation model to demonstrate the flexibility of the formulation in accommodating equal and unequal area studies. It was revealed using unity capacity ratios in unequal multi-area systems can result in frequency offsets. An additional 4-area deregulated model was developed to further demonstrate the usefulness of the generalised formulation, and to provide more insight into how the LFC model of any deregulated power network can be developed from the generalised formulation.

The 7-area benchmark developed was used in Chapter 6 to further examine the potentials of a predictive control solution to deregulated LFC problems. In particular, Chapter 6 extended the work in Chapter 4 by considering a more appropriate settings where CAs have unequal rated capacities and some GenCos do not participate in serving uncontracted load changes in their area. Previous work on deregulated LFC, and that presented in Chapter 4 proposed control schemes that generate lumped signals for each area which are then distributed to GenCos according to their area participation factors (refer to Figure 4.2, 5.1 and 6.1), and this approach may result in a violation of the input constraints of each GenCo. The proposed CMPC scheme in this chapter considers a separate control signal for each GenCo (refer to figure 6.2) by incorporating, explicitly, the area participation factors of each generating unit (GenCo) in the CMPC cost function, and therefore, accounted for the input constraints of GenCos serving uncontracted load changes in their area, in addition to their individual GRCs. This approach also permits greater flexibility and a more efficient use of a predictive control capability on multiple inputs coordination. Simulation results demonstrate that the proposed scheme, when compared with LQR based LFC, also gives a more acceptable frequency and tie line control, regulates generating units' output more efficiently and handles the input constraints and GRC of individual units more effectively.

The predictive control scheme proposed in Chapter 6 (and also in Chapter 4) is completely centralised and hence scheme might not be realistic for large scale systems where CAs have large geographical separation (refer to Section 3.2.5 and Table 3.1). Hence, the key aim of Chapter 7 was to investigate a distributed control solution for deregulated LFC problems. To

accomplish this, a DMPC scheme that can suitably be applied to an interconnection with a sizeable number of CAs was proposed. The DMPC algorithm was developed to use output feedback where local observers were designed to estimate uncontracted load changes in their areas and local subsystem states, and make these estimates available their local MPCs. The local observers use local measurements (area control error signals) and communicate to obtain better estimates, hence it is distributed. The DMPC was tested on the 4-area and 7-area systems developed earlier in the presence of GRC, input limits, contracted and uncontracted load changes, and compared with a CMPC (benchmark) and DeMPC scheme to evaluate its efficacy. Results revealed that communication between local MPCs (sDMPC and dDMPC) offers a performance comparable to CMPC whereas reduced communication between local MPCs (DeMPC) results in poor LFC performance.

As a closing remark, the novel generalised modelling framework proposed to study LFC in the deregulated environment, that incorporates area capacity information, is one of the key achievements in this thesis. The behaviour exhibited by the benchmark models developed from the generalised framework, when subjected to load disturbances, conform to what would be expected in practical systems. In light of these evidence, the generalised formulation represents a valuable framework for power system researchers to develop their own benchmark models and test their LFC proposals/study frequency phenomenon in the deregulated environment. Power networks, because of their interactive nature, represent a proper system for testing distributed control algorithms, and thus, the generalised framework, as well as the benchmark models, are beneficial in that respect. Furthermore, the generalised model could be used in deregulated power industries to develop simulation models, with parameters validated with actual measured data, to study frequency phenomenon. Another key achievement is the predictive control schemes proposed. The CMPC, though not suitable for multi-area networks, could be easily adapted and utilised for LFC studies in isolated power networks; the model of such networks would normally exclude tie line equations and utilise a single swing equation. More importantly, the evidence gathered from implementing the proposed DMPC revealed that it could deal with the increasing frequency oscillations that are being experienced globally in deregulated interconnections. The design approach of each local MPC is pretty close to that of the widely used industrial MPC and hence can be easily understood by power sytem operators.

8.2 Summary of key contributions

The main contributions in this thesis are pooled from the relevant chapters and presented here for convenience.

Chapter 2

- Presented a thorough review of the LFC literature to reveal opportunies for contributions. Note that previous reviews [50, 61, 62] ignored MPC based LFC proposals.

Chapter 4

- Proposes a CMPC scheme for the LFC problem of a 2-area deregulated power system with contracted (measured) and uncontracted (unmeasured) load pertubations. The uncontracted load pertubation of an area represents the net load pertubations from entities that have either violated the LM contract or did not purchase LM contracts.

- The work here employs an observer to estimate system states as well as uncontracted load variations (which is assumed to be unmeasured) from ACE measurements, hence the proposed CMPC is output feedback

- GRC and limits on governor setpoints are included in the MPC design and simulations.

Chapter 5

- Proposes a generalised formulation of a deregulated LFC model for an N control area network, which can accommodate studies where control areas either have unequal rated capacities or equal rated capacities.

- Develops a 7-area deregulated benchmark model by applying the proposed generalised model, and provides simulation evidence to demonstrate the importance of considering the difference in area rated capacities.

- A 4-area deregulated benchmark model is also developed to further demonstrate the usefulness of the generalised formulation, and to provide more insight into how the LFC model of any deregulated power network can be developed from the generalised formulation.

Chapter 6

- Proposes a CMPC scheme for a deregulated LFC problem where CAs have unequal rated capacities, large scale network with a more complex topology considered (network houses 33 GenCos and 46 DisCos) , some GenCos do not participate in serving uncontracted load changes in their area, and not all DisCos purchase a load matching (LM) contract (zero contracted demands). This represents a more appropriate power system setting.

209

- Incorporates the area participation factor of each GenCo in the CMPC cost function to ensure that the individual input constraints of each GenCo is satisfied during transients.

Chapter 7

- Proposes a DMPC (sDMPC and dDMPC) algorithms for LFC problems, and demonstrates its efficacy on a 4-area and a 7-area benchmark systems with unequal CA ratings. It is shown how decentralised LFC in a deregulated power network may be performed by a simple distributed MPC scheme, without reliance on excessive offline tuning of controller parameters and prohibitively complex invariant sets (please see [218]); the price is the lack of feasibility and stability guarantees, but the approach is shown to work effectively, with good closed-loop performance on the representative 4-area and 7-area power systems.

- Designs and utilises distributed observers to estimate uncontracted load disturbances and local subsystem states from area control error measurements, thus the proposed DMPC is output feedback.

- Generation rate constraints and input limits of each of the GenCos participating in a TSO's supplementary control are considered individually in the DMPC design and simulations.

- The consideration of discretisation scheme on both performance and on system dynamics and information sharing requirements. Note that this is an issue that is overlooked in both the DMPC literature, and the LFC literature where the control design is model based. The practical implications, especially in terms of what information needs to be shared, are highly significant. This contribution relates to how discrete time subsystem models used by local MPCs are obtained and it is clarified in Section 7.5.

- Lastly, a performance and cost comparison of centralised MPC (benchmark), decentralised MPC (DeMPC), sparse DMPC (sDMPC) and dense DMPC (dDMPC) is made (the concept of sparse and dense are clarified in Section 7.5).

8.3 Future work

A number extensions from this thesis are possible. However, for completeness a few obvious avenues are highlighted next.

8.3.1 DMPC designs for pluralistic and hierarchical networks

The modelling framework utilised in this thesis assumes that large synchronous interconnected networks are divided, strictly, into CAs. Each local MPC in the proposed distributed control scheme, solely performs the LFC in its own area, and thus, centralised with respect to that area; the Union for the Coordination of Transmission of Electricity (UCTE), an association consisting of TSOs (one TSO in a CA) in Continental Europe, defines this structure as centralised. Note that centralised here is with respect to each CA and not the whole interconnection. Other structures identified by UCTE within the Continental Europe interconnection is the pluralistic and hierarchical structures [227]. These two structures arise from the fact that the European synchronous grid consists of interconnected control blocks. A control block comprises of one or more interconnected CAs collaborating to meet predefined LFC obligations with reference to the adjoining control blocks. In the pluralistic structure, the TSO of a CA within a multi-area control block, called a block coordinator, performs the LFC task of the whole block with respect to neighbouring blocks by directly controlling generation resources in its CA, while the other TSOs in the control block separately performs LFC functions in their control areas. In the hierarchical structure, a block coordinator performs LFC by operating a block controller that sends corrective signals directly to the LFC scheme of all control areas within a control block. In order words, the block coordinator does not directly control any generation resource to perform LFC functions in its block with respect to adjoining control blocks, but computes the ACE of the whole block, generates a corrective signal and distributes the signal to the TSO LFC scheme in each CA within the block based on some participation factors. These schemes are currently decentralised. It would be an interesting future work to investigate a two-level DMPC solution for LFC, where local MPCs within a control block exchange information and each block coordinating LFC could be a number of MPCs communicating at the control block level. Depending on the tologogy of the synchronous interconnection, a control area may have tie connections with control areas outside its control block. Hence, communication between such CAs may be necessary or such interactions could be handled by block coordinators' MPCs.

8.3.2 Ecomomic MPC layer for updating area participation factors in deregulated LFC

The work presented in this thesis assumed that the area participation factors $\gamma_{i,\mathrm{k}}$ of GenCos serving uncontracted load changes with their area are fixed. Also, it was implicitly assumed that there are no constraints on the amount of incremental/decremental power reserves of each GenCo available to a TSO to respond to uncontracted load changes in its area. However, in practice, the reserve levels of GenCos vary throughout the day as they also sell power in other markets (e.g energy) and not strictly the LFC market. GenCos participating in LFC can also experience an unanticipated power plant failure, leading to a change in reserve level. Moreover,

there has been an increased variability in the balancing requirements of most power systems recently due to the increasing penetration of renewables. Hence it would be interesting to consider the scenario where the area participation factors of GenCos are updated in real time as reserve levels and/or balancing requirements change. An ecomomic MPC (eMPC) scheme is suggested to accomplish this; the eMPC in each area, operating on a slower timescale, will compute new $\gamma_{i,\mathrm{k}}$ as conditions change and pass it to the local MPC handling LFC.

The eMPC, using a linear cost, will minimise the overall cost of addressing a given power imbalance, where the decision variables will be the area participation factors. GenCos bidding to provide LFC (incremental/decremental bids) usually supply their price, reserve quantity and duration of provison. The price information can be used as the weightings on each $\gamma_{i,\mathrm{k}}$ to be determined in the eMPC cost function. The reserve quantity of each GenCo is represented by set of linear inequalities, the total balancing requirements and the dynamics of the GenCos will serve as constraints. As some generators might be low-priced and slow while others pricey and fast, the technical characteristics such as ramp rates of the GenCos can be incorporated into the eMPC formulation. The idea of incorporating generator technical characteristics in selecting GenCos for LFC has been recommended by experts [226] as selecting GenCos based on price only does not automatically promise optimal system response to disturbances.

Appendix A

Appendix

A.1   2-area deregulated system

$$
\mathrm{B^c} = \begin{bmatrix} 0 & 0 \\ 0 & 0 \\ \dfrac{\gamma_{1,1}}{T_{\mathrm{G}_{1,1}}} & 0 \\ 0 & 0 \\ \dfrac{\gamma_{1,2}}{T_{\mathrm{G}_{1,2}}} & 0 \\ 0 & 0 \\ 0 & 0 \\ 0 & 0 \\ 0 & \dfrac{\gamma_{2,3}}{T_{\mathrm{G}_{2,3}}} \\ 0 & 0 \\ 0 & \dfrac{\gamma_{2,4}}{T_{\mathrm{G}_{2,4}}} \end{bmatrix} ; \quad \mathrm{B^{dc}} = \begin{bmatrix} -\dfrac{1}{H_1} & -\dfrac{1}{H_1} & 0 & 0 \\ \dfrac{\eta_{1,1}}{T_{\mathrm{G}_{1,1}}} & \dfrac{\eta_{1,2}}{T_{\mathrm{G}_{1,1}}} & \dfrac{\eta_{1,3}}{T_{\mathrm{G}_{1,1}}} & \dfrac{\eta_{1,4}}{T_{\mathrm{G}_{1,1}}} \\ 0 & 0 & 0 & 0 \\ \dfrac{\eta_{2,1}}{T_{\mathrm{G}_{1,2}}} & \dfrac{\eta_{2,2}}{T_{\mathrm{G}_{1,2}}} & \dfrac{\eta_{2,3}}{T_{\mathrm{G}_{1,3}}} & \dfrac{\eta_{2,4}}{T_{\mathrm{G}_{1,4}}} \\ 0 & 0 & 0 & 0 \\ 0 & 0 & 0 & 0 \\ 0 & 0 & -\dfrac{1}{H_2} & -\dfrac{1}{H_2} \\ 0 & 0 & 0 & 0 \\ \dfrac{\eta_{3,1}}{T_{\mathrm{G}_{2,3}}} & \dfrac{\eta_{3,2}}{T_{\mathrm{G}_{2,3}}} & \dfrac{\eta_{3,3}}{T_{\mathrm{G}_{2,3}}} & \dfrac{\eta_{3,4}}{T_{\mathrm{G}_{2,3}}} \\ 0 & 0 & 0 & 0 \\ \dfrac{\eta_{4,1}}{T_{\mathrm{G}_{2,4}}} & \dfrac{\eta_{4,2}}{T_{\mathrm{G}_{2,4}}} & \dfrac{\eta_{4,3}}{T_{\mathrm{G}_{2,4}}} & \dfrac{\eta_{4,4}}{T_{\mathrm{G}_{2,4}}} \end{bmatrix} ; \quad \mathrm{B^{bc}} = \begin{bmatrix} -\dfrac{1}{H_1} & 0 \\ 0 & 0 \\ 0 & 0 \\ 0 & 0 \\ 0 & 0 \\ 0 & 0 \\ 0 & -\dfrac{1}{H_2} \\ 0 & 0 \\ 0 & 0 \\ 0 & 0 \\ 0 & 0 \end{bmatrix}
$$

$$\tag{A.1}$$

$$
\mathrm{C^c} = \begin{bmatrix} \beta_1 & 0 & 0 & 0 & 0 & 1 & 0 & 0 & 0 & 0 & 0 \\ 0 & 0 & 0 & 0 & 0 & -1 & \beta_2 & 0 & 0 & 0 & 0 \end{bmatrix} \tag{A.2}
$$

$$
\mathrm{D^c} = \begin{bmatrix} (\eta_{3,1} + \eta_{4,1}) & (\eta_{3,2} + \eta_{4,2}) & -(\eta_{1,3} + \eta_{2,3}) & -(\eta_{1,4} + \eta_{2,4}) \\[2mm] -(\eta_{3,1} + \eta_{4,1}) & -(\eta_{3,2} + \eta_{4,2}) & (\eta_{1,3} + \eta_{2,3}) & (\eta_{1,4} + \eta_{2,4}) \end{bmatrix}
\tag{A.3}
$$

$$
\mathrm{A^c} = \begin{bmatrix}
-\dfrac{D_1}{H_1} & \dfrac{1}{H_1} & 0 & \dfrac{1}{H_1} & 0 & -\dfrac{1}{H_1} & 0 & 0 & 0 & 0 & 0 \\[2mm]
0 & -\dfrac{1}{T_{\mathrm{T}_{1,1}}} & \dfrac{1}{T_{\mathrm{T}_{1,1}}} & 0 & 0 & 0 & 0 & 0 & 0 & 0 & 0 \\[2mm]
-\dfrac{1}{T_{\mathrm{G}_{1,1}}R_{1,1}} & 0 & -\dfrac{1}{T_{\mathrm{G}_{1,1}}} & 0 & 0 & 0 & 0 & 0 & 0 & 0 & 0 \\[2mm]
0 & 0 & 0 & -\dfrac{1}{T_{\mathrm{T}_{1,2}}} & \dfrac{1}{T_{\mathrm{T}_{1,2}}} & 0 & 0 & 0 & 0 & 0 & 0 \\[2mm]
-\dfrac{1}{T_{\mathrm{G}_{1,2}}R_{1,2}} & 0 & 0 & 0 & -\dfrac{1}{T_{\mathrm{G}_{1,2}}} & 0 & 0 & 0 & 0 & 0 & 0 \\[2mm]
T_{12} & 0 & 0 & 0 & 0 & -T_{12} & 0 & 0 & 0 & 0 & 0 \\[2mm]
0 & 0 & 0 & 0 & 0 & \dfrac{1}{H_2} & -\dfrac{D_2}{H_2} & \dfrac{1}{H_2} & 0 & \dfrac{1}{H_2} & 0 \\[2mm]
0 & 0 & 0 & 0 & 0 & 0 & 0 & -\dfrac{1}{T_{\mathrm{T}_{2,3}}} & \dfrac{1}{T_{\mathrm{T}_{2,3}}} & 0 & 0 \\[2mm]
0 & 0 & 0 & 0 & 0 & 0 & -\dfrac{1}{T_{\mathrm{G}_{2,3}}R_{2,3}} & 0 & -\dfrac{1}{T_{\mathrm{G}_{2,3}}} & 0 & 0 \\[2mm]
0 & 0 & 0 & 0 & 0 & 0 & 0 & 0 & 0 & -\dfrac{1}{T_{\mathrm{T}_{2,4}}} & \dfrac{1}{T_{\mathrm{T}_{2,4}}} \\[2mm]
0 & 0 & 0 & 0 & 0 & 0 & -\dfrac{1}{T_{\mathrm{G}_{2,4}}R_{2,4}} & 0 & 0 & 0 & -\dfrac{1}{T_{\mathrm{G}_{2,4}}}
\end{bmatrix}
\tag{A.4}
$$

$$
\Gamma^{\mathrm{g}} = \begin{bmatrix}
0 & 1 & 0 & 0 & 0 & 0 & 0 & 0 & 0 & 0 & 0 \\[2mm]
0 & 0 & 0 & 1 & 0 & 0 & 0 & 0 & 0 & 0 & 0 \\[2mm]
0 & 0 & 0 & 0 & 0 & 0 & 0 & 1 & 0 & 0 & 0 \\[2mm]
0 & 0 & 0 & 0 & 0 & 0 & 0 & 0 & 0 & 1 & 0
\end{bmatrix}
\tag{A.5}
$$

A.2   7-area deregulated system

$$
\begin{bmatrix} \Delta P_1^{\text{tie}} \\ \Delta P_2^{\text{tie}} \\ \Delta P_3^{\text{tie}} \\ \Delta P_4^{\text{tie}} \\ \Delta P_5^{\text{tie}} \\ \Delta P_6^{\text{tie}} \\ \Delta P_7^{\text{tie}} \end{bmatrix}
=
\underbrace{\begin{bmatrix}
Y_{14}+\alpha_{31}Y_{31} & 0 & -\alpha_{31}Y_{31} & -Y_{14} & 0 & 0 & 0 \\
0 & \alpha_{42}Y_{42} & 0 & -\alpha_{42}Y_{42} & 0 & 0 & 0 \\
-Y_{31} & 0 & Y_{37}+Y_{31}+\alpha_{43}Y_{43}+\alpha_{53}Y_{53} & -\alpha_{43}Y_{43} & -\alpha_{53}Y_{53} & 0 & -Y_{37} \\
-\alpha_{14}Y_{14} & -Y_{42} & -Y_{43} & \alpha_{14}Y_{14}+Y_{42}+Y_{43}+Y_{45}+\alpha_{64}Y_{64} & -Y_{45} & -\alpha_{64}Y_{64} & 0 \\
0 & 0 & -Y_{53} & -\alpha_{45}Y_{45} & Y_{53}+\alpha_{45}Y_{45} & 0 & 0 \\
0 & 0 & 0 & -Y_{64} & 0 & Y_{64}+\alpha_{76}Y_{76} & -\alpha_{76}Y_{76} \\
0 & 0 & -\alpha_{37}Y_{37} & 0 & 0 & -Y_{76} & Y_{64}+\alpha_{76}Y_{76}
\end{bmatrix}}_{Y}
\begin{bmatrix} \Delta\delta_1 \\ \Delta\delta_2 \\ \Delta\delta_3 \\ \Delta\delta_4 \\ \Delta\delta_5 \\ \Delta\delta_6 \\ \Delta\delta_7 \end{bmatrix}
\tag{A.6}
$$

$$
\text{DPM} = \begin{bmatrix}
\text{DPM}_1 & \text{DPM}_2 & \text{DPM}_3 \\
\text{DPM}_4 & \text{DPM}_5 & \text{DPM}_6 \\
\text{DPM}_7 & \text{DPM}_8 & \text{DPM}_9
\end{bmatrix}
\tag{A.7}
$$

where

$$
\mathrm{DPM}_1 =
\begin{bmatrix}
0.04 & 0.04 & 0.04 & 0.04 & 0.04 & 0.04 & 0.04 & 0 & 0 & 0 & 0 & 0 & 0.03 & 0.03 & 0.03 \\
0.04 & 0.04 & 0.04 & 0.04 & 0.04 & 0.04 & 0.04 & 0 & 0 & 0 & 0 & 0 & 0.03 & 0.03 & 0.03 \\
0.1 & 0.11 & 0.11 & 0.11 & 0.11 & 0.11 & 0.11 & 0 & 0 & 0 & 0 & 0 & 0.08 & 0.08 & 0.08 \\
0.11 & 0.11 & 0.11 & 0.11 & 0.11 & 0.11 & 0.11 & 0 & 0 & 0 & 0 & 0 & 0.08 & 0.08 & 0.08 \\
0.11 & 0.11 & 0.11 & 0.11 & 0.11 & 0.11 & 0.11 & 0 & 0 & 0 & 0 & 0 & 0.08 & 0.08 & 0.08 \\
0 & 0 & 0 & 0 & 0 & 0 & 0 & 0.23 & 0.22 & 0.22 & 0.22 & 0.22 & 0 & 0 & 0 \\
0 & 0 & 0 & 0 & 0 & 0 & 0 & 0.22 & 0.23 & 0.23 & 0.23 & 0.23 & 0 & 0 & 0 \\
0 & 0 & 0 & 0 & 0 & 0 & 0 & 0.07 & 0.07 & 0.07 & 0.08 & 0.07 & 0 & 0 & 0 \\
0 & 0 & 0 & 0 & 0 & 0 & 0 & 0.08 & 0.08 & 0.08 & 0.08 & 0.08 & 0 & 0 & 0 \\
0.08 & 0.08 & 0.08 & 0.08 & 0.08 & 0.08 & 0.08 & 0 & 0 & 0 & 0 & 0 & 0.05 & 0.05 & 0.05 \\
0.03 & 0.03 & 0.03 & 0.03 & 0.03 & 0.03 & 0.03 & 0 & 0 & 0 & 0 & 0 & 0.02 & 0.02 & 0.02
\end{bmatrix}
$$

$$
\mathrm{DPM}_2 =
\begin{bmatrix}
0.03 & 0.03 & 0.03 & 0.03 & 0.02 & 0.02 & 0.02 & 0.02 & 0.02 & 0.02 & 0.02 & 0.02 & 0 & 0 & 0 \\
0.03 & 0.03 & 0.03 & 0.03 & 0.02 & 0.02 & 0.02 & 0.02 & 0.02 & 0.02 & 0.02 & 0.02 & 0 & 0 & 0 \\
0.08 & 0.08 & 0.08 & 0.08 & 0.05 & 0.05 & 0.05 & 0.05 & 0.05 & 0.05 & 0.05 & 0.05 & 0 & 0 & 0 \\
0.08 & 0.08 & 0.08 & 0.08 & 0.05 & 0.05 & 0.05 & 0.05 & 0.05 & 0.05 & 0.05 & 0.05 & 0 & 0 & 0 \\
0.08 & 0.08 & 0.08 & 0.08 & 0.05 & 0.05 & 0.05 & 0.05 & 0.05 & 0.05 & 0.05 & 0.05 & 0 & 0 & 0 \\
0 & 0 & 0 & 0 & 0.06 & 0.06 & 0.06 & 0.06 & 0.06 & 0.06 & 0.06 & 0.06 & 0 & 0 & 0 \\
0 & 0 & 0 & 0 & 0.06 & 0.06 & 0.06 & 0.06 & 0.06 & 0.06 & 0.06 & 0.06 & 0 & 0 & 0 \\
0 & 0 & 0 & 0 & 0.02 & 0.02 & 0.02 & 0.02 & 0.02 & 0.02 & 0.02 & 0.02 & 0 & 0 & 0 \\
0 & 0 & 0 & 0 & 0.02 & 0.02 & 0.02 & 0.02 & 0.02 & 0.02 & 0.02 & 0.02 & 0 & 0 & 0 \\
0.05 & 0.05 & 0.05 & 0.05 & 0.04 & 0.04 & 0.04 & 0.04 & 0.04 & 0.04 & 0.04 & 0.04 & 0.04 & 0.04 & 0.04 \\
0.02 & 0.02 & 0.02 & 0.02 & 0.02 & 0.02 & 0.01 & 0.01 & 0.01 & 0.01 & 0.02 & 0.01 & 0.02 & 0.02 & 0.01
\end{bmatrix}
$$

$$
\mathrm{DPM}_3 =
\begin{bmatrix}
0 & 0 & 0 & 0 & 0 & 0 & 0 & 0 & 0 & 0 & 0 & 0 & 0 & 0 & 0 \\
0 & 0 & 0 & 0 & 0 & 0 & 0 & 0 & 0 & 0 & 0 & 0 & 0 & 0 & 0 \\
0 & 0 & 0 & 0 & 0 & 0 & 0 & 0 & 0 & 0 & 0 & 0 & 0 & 0 & 0 \\
0 & 0 & 0 & 0 & 0 & 0 & 0 & 0 & 0 & 0 & 0 & 0 & 0 & 0 & 0 \\
0 & 0 & 0 & 0 & 0 & 0 & 0 & 0 & 0 & 0 & 0 & 0 & 0 & 0 & 0 \\
0 & 0 & 0 & 0 & 0 & 0 & 0 & 0 & 0 & 0 & 0 & 0 & 0 & 0 & 0 \\
0 & 0 & 0 & 0 & 0 & 0 & 0 & 0 & 0 & 0 & 0 & 0 & 0 & 0 & 0 \\
0 & 0 & 0 & 0 & 0 & 0 & 0 & 0 & 0 & 0 & 0 & 0 & 0 & 0 & 0 \\
0 & 0 & 0 & 0 & 0 & 0 & 0 & 0 & 0 & 0 & 0 & 0 & 0 & 0 & 0 \\
0.04 & 0.04 & 0 & 0 & 0 & 0 & 0 & 0 & 0 & 0 & 0.08 & 0.08 & 0.08 & 0.08 & 0.08 & 0.08 \\
0.02 & 0.01 & 0 & 0 & 0 & 0 & 0 & 0 & 0 & 0 & 0.03 & 0.03 & 0.03 & 0.03 & 0.03 & 0.03
\end{bmatrix}
$$

$$
\mathrm{DPM_4} = \begin{bmatrix}
0.08 & 0.08 & 0.08 & 0.08 & 0.08 & 0.08 & 0.08 & 0 & 0 & 0 & 0 & 0 & 0.05 & 0.05 & 0.05 \\
0.08 & 0.08 & 0.08 & 0.08 & 0.08 & 0.08 & 0.08 & 0 & 0 & 0 & 0 & 0 & 0.05 & 0.05 & 0.05 \\
0.03 & 0.03 & 0.03 & 0.03 & 0.03 & 0.03 & 0.03 & 0 & 0 & 0 & 0 & 0 & 0.02 & 0.02 & 0.02 \\
0.02 & 0.02 & 0.02 & 0.02 & 0.02 & 0.03 & 0.02 & 0.03 & 0.03 & 0.03 & 0.03 & 0.03 & 0.01 & 0.01 & 0.01 \\
0.08 & 0.08 & 0.08 & 0.08 & 0.08 & 0.08 & 0.07 & 0.1 & 0.1 & 0.1 & 0.1 & 0.1 & 0.03 & 0.02 & 0.02 \\
0.07 & 0.07 & 0.07 & 0.07 & 0.07 & 0.07 & 0.08 & 0.1 & 0.1 & 0.1 & 0.1 & 0.1 & 0.02 & 0.03 & 0.03 \\
0.03 & 0.03 & 0.03 & 0.03 & 0.03 & 0.02 & 0.03 & 0.03 & 0.03 & 0.03 & 0.03 & 0.03 & 0.01 & 0.01 & 0.01 \\
0.03 & 0.03 & 0.03 & 0.03 & 0.03 & 0.02 & 0.03 & 0.03 & 0.03 & 0.03 & 0.03 & 0.03 & 0.01 & 0.01 & 0.01 \\
0.07 & 0.08 & 0.08 & 0.07 & 0.08 & 0.08 & 0.07 & 0.1 & 0.1 & 0.1 & 0.1 & 0.1 & 0.03 & 0.02 & 0.02 \\
0 & 0 & 0 & 0 & 0 & 0 & 0 & 0 & 0 & 0 & 0 & 0 & 0.08 & 0.07 & 0.08 \\
0 & 0 & 0 & 0 & 0 & 0 & 0 & 0 & 0 & 0 & 0 & 0 & 0.08 & 0.07 & 0.07
\end{bmatrix}
$$

$$
\mathrm{DPM_5} = \begin{bmatrix}
0.05 & 0.05 & 0.05 & 0.05 & 0.04 & 0.04 & 0.04 & 0.04 & 0.04 & 0.04 & 0.04 & 0.04 & 0.04 & 0.04 & 0.04 \\
0.05 & 0.05 & 0.05 & 0.05 & 0.04 & 0.04 & 0.04 & 0.04 & 0.04 & 0.04 & 0.04 & 0.04 & 0.04 & 0.04 & 0.04 \\
0.02 & 0.02 & 0.02 & 0.02 & 0.01 & 0.01 & 0.01 & 0.01 & 0.02 & 0.02 & 0.01 & 0.02 & 0.02 & 0.02 & 0.01 \\
0.01 & 0.01 & 0.01 & 0.01 & 0.02 & 0.02 & 0.02 & 0.02 & 0.02 & 0.02 & 0.02 & 0.02 & 0.02 & 0.02 & 0.02 \\
0.02 & 0.02 & 0.02 & 0.02 & 0.05 & 0.05 & 0.05 & 0.05 & 0.05 & 0.05 & 0.05 & 0.05 & 0.05 & 0.05 & 0.05 \\
0.03 & 0.02 & 0.03 & 0.03 & 0.05 & 0.05 & 0.05 & 0.05 & 0.05 & 0.05 & 0.05 & 0.05 & 0.05 & 0.05 & 0.05 \\
0.01 & 0.01 & 0.01 & 0.01 & 0.02 & 0.02 & 0.02 & 0.02 & 0.02 & 0.02 & 0.02 & 0.02 & 0.02 & 0.02 & 0.02 \\
0.01 & 0.01 & 0.01 & 0.01 & 0.02 & 0.02 & 0.02 & 0.02 & 0.02 & 0.02 & 0.02 & 0.02 & 0.02 & 0.02 & 0.02 \\
0.02 & 0.03 & 0.03 & 0.03 & 0.05 & 0.05 & 0.05 & 0.05 & 0.05 & 0.05 & 0.05 & 0.05 & 0.05 & 0.05 & 0.05 \\
0.07 & 0.08 & 0.08 & 0.08 & 0.06 & 0.06 & 0.06 & 0.06 & 0.06 & 0.06 & 0.06 & 0.06 & 0.25 & 0.25 & 0.24 \\
0.08 & 0.07 & 0.07 & 0.07 & 0.06 & 0.06 & 0.06 & 0.06 & 0.06 & 0.06 & 0.06 & 0.06 & 0.24 & 0.24 & 0.24
\end{bmatrix}
$$

$$
\mathrm{DPM_6} = \begin{bmatrix}
0.04 & 0.04 & 0 & 0 & 0 & 0 & 0 & 0 & 0 & 0 & 0.08 & 0.08 & 0.08 & 0.08 & 0.08 & 0.08 \\
0.04 & 0.04 & 0 & 0 & 0 & 0 & 0 & 0 & 0 & 0 & 0.08 & 0.08 & 0.08 & 0.08 & 0.08 & 0.08 \\
0.01 & 0.02 & 0 & 0 & 0 & 0 & 0 & 0 & 0 & 0 & 0.03 & 0.03 & 0.03 & 0.03 & 0.03 & 0.03 \\
0.02 & 0.02 & 0.01 & 0.01 & 0.01 & 0.01 & 0.01 & 0.01 & 0.01 & 0.01 & 0 & 0 & 0 & 0 & 0 & 0 \\
0.05 & 0.05 & 0.04 & 0.04 & 0.04 & 0.04 & 0.04 & 0.04 & 0.04 & 0.04 & 0 & 0 & 0 & 0 & 0 & 0 \\
0.05 & 0.05 & 0.04 & 0.04 & 0.04 & 0.04 & 0.04 & 0.04 & 0.04 & 0.04 & 0 & 0 & 0 & 0 & 0 & 0 \\
0.02 & 0.02 & 0.01 & 0.01 & 0.01 & 0.01 & 0.01 & 0.01 & 0.01 & 0.01 & 0 & 0 & 0 & 0 & 0 & 0 \\
0.02 & 0.02 & 0.01 & 0.01 & 0.01 & 0.01 & 0.01 & 0.01 & 0.01 & 0.01 & 0 & 0 & 0 & 0 & 0 & 0 \\
0.05 & 0.05 & 0.04 & 0.04 & 0.04 & 0.04 & 0.04 & 0.04 & 0.04 & 0.04 & 0 & 0 & 0 & 0 & 0 & 0 \\
0.25 & 0.24 & 0 & 0 & 0 & 0 & 0 & 0 & 0 & 0 & 0 & 0 & 0 & 0 & 0 & 0 \\
0.24 & 0.24 & 0 & 0 & 0 & 0 & 0 & 0 & 0 & 0 & 0 & 0 & 0 & 0 & 0 & 0
\end{bmatrix}
$$

217

$$\mathrm{DPM}_7 = \begin{bmatrix}
0 & 0 & 0 & 0 & 0 & 0 & 0 & 0 & 0 & 0 & 0 & 0 & 0.02 & 0.02 & 0.03 \\
0 & 0 & 0 & 0 & 0 & 0 & 0 & 0 & 0 & 0 & 0 & 0 & 0.02 & 0.03 & 0.02 \\
0 & 0 & 0 & 0 & 0 & 0 & 0 & 0 & 0 & 0 & 0 & 0 & 0 & 0 & 0 \\
0 & 0 & 0 & 0 & 0 & 0 & 0 & 0 & 0 & 0 & 0 & 0 & 0 & 0 & 0 \\
0 & 0 & 0 & 0 & 0 & 0 & 0 & 0 & 0 & 0 & 0 & 0 & 0 & 0 & 0 \\
0 & 0 & 0 & 0 & 0 & 0 & 0 & 0 & 0 & 0 & 0 & 0 & 0 & 0 & 0 \\
0 & 0 & 0 & 0 & 0 & 0 & 0 & 0 & 0 & 0 & 0 & 0 & 0 & 0 & 0 \\
0 & 0 & 0 & 0 & 0 & 0 & 0 & 0 & 0 & 0 & 0 & 0 & 0.08 & 0.07 & 0.07 \\
0 & 0 & 0 & 0 & 0 & 0 & 0 & 0 & 0 & 0 & 0 & 0 & 0.02 & 0.03 & 0.03 \\
0 & 0 & 0 & 0 & 0 & 0 & 0 & 0 & 0 & 0 & 0 & 0 & 0.07 & 0.08 & 0.08 \\
0 & 0 & 0 & 0 & 0 & 0 & 0 & 0 & 0 & 0 & 0 & 0 & 0.03 & 0.02 & 0.03
\end{bmatrix}$$

$$\mathrm{DPM}_8 = \begin{bmatrix}
0.02 & 0.03 & 0.03 & 0.02 & 0.02 & 0.02 & 0.02 & 0.02 & 0.02 & 0.02 & 0.02 & 0.02 & 0.08 & 0.08 & 0.08 \\
0.03 & 0.03 & 0.02 & 0.03 & 0.02 & 0.02 & 0.02 & 0.02 & 0.02 & 0.02 & 0.02 & 0.02 & 0.08 & 0.08 & 0.08 \\
0 & 0 & 0 & 0 & 0.02 & 0.02 & 0.02 & 0.02 & 0.01 & 0.02 & 0.02 & 0.01 & 0 & 0 & 0 \\
0 & 0 & 0 & 0 & 0.04 & 0.04 & 0.04 & 0.04 & 0.04 & 0.04 & 0.04 & 0.04 & 0 & 0 & 0 \\
0 & 0 & 0 & 0 & 0.04 & 0.04 & 0.04 & 0.04 & 0.04 & 0.04 & 0.04 & 0.04 & 0 & 0 & 0 \\
0 & 0 & 0 & 0 & 0.01 & 0.01 & 0.01 & 0.01 & 0.02 & 0.01 & 0.01 & 0.01 & 0 & 0 & 0 \\
0 & 0 & 0 & 0 & 0.04 & 0.04 & 0.04 & 0.04 & 0.04 & 0.04 & 0.04 & 0.04 & 0 & 0 & 0 \\
0.08 & 0.07 & 0.07 & 0.08 & 0 & 0 & 0 & 0 & 0 & 0 & 0 & 0 & 0 & 0 & 0 \\
0.03 & 0.03 & 0.03 & 0.02 & 0 & 0 & 0 & 0 & 0 & 0 & 0 & 0 & 0 & 0 & 0 \\
0.07 & 0.08 & 0.07 & 0.08 & 0 & 0 & 0 & 0 & 0 & 0 & 0 & 0 & 0 & 0 & 0 \\
0.02 & 0.03 & 0.02 & 0.03 & 0 & 0 & 0 & 0 & 0 & 0 & 0 & 0 & 0 & 0 & 0
\end{bmatrix}$$

$$\mathrm{DPM}_9 = \begin{bmatrix}
0.08 & 0.08 & 0 & 0 & 0 & 0 & 0 & 0 & 0 & 0 & 0 & 0 & 0 & 0 & 0 & 0 \\
0.08 & 0.08 & 0 & 0 & 0 & 0 & 0 & 0 & 0 & 0 & 0 & 0 & 0 & 0 & 0 & 0 \\
0 & 0 & 0.05 & 0.05 & 0.05 & 0.05 & 0.05 & 0.05 & 0.05 & 0.05 & 0.04 & 0.04 & 0.04 & 0.04 & 0.04 & 0.04 \\
0 & 0 & 0.13 & 0.13 & 0.13 & 0.14 & 0.13 & 0.13 & 0.14 & 0.13 & 0.11 & 0.11 & 0.11 & 0.1 & 0.11 & 0.11 \\
0 & 0 & 0.13 & 0.13 & 0.13 & 0.13 & 0.13 & 0.13 & 0.13 & 0.13 & 0.11 & 0.11 & 0.11 & 0.11 & 0.11 & 0.11 \\
0 & 0 & 0.05 & 0.05 & 0.05 & 0.05 & 0.05 & 0.05 & 0.05 & 0.05 & 0.04 & 0.04 & 0.04 & 0.04 & 0.04 & 0.04 \\
0 & 0 & 0.13 & 0.13 & 0.13 & 0.13 & 0.13 & 0.14 & 0.13 & 0.13 & 0.1 & 0.11 & 0.11 & 0.11 & 0.11 & 0.11 \\
0 & 0 & 0.13 & 0.13 & 0.13 & 0.13 & 0.13 & 0.13 & 0.13 & 0.13 & 0.11 & 0.11 & 0.11 & 0.11 & 0.11 & 0.11 \\
0 & 0 & 0.04 & 0.04 & 0.04 & 0.04 & 0.04 & 0.04 & 0.04 & 0.04 & 0.04 & 0.04 & 0.04 & 0.04 & 0.04 & 0.04 \\
0 & 0 & 0.13 & 0.13 & 0.13 & 0.13 & 0.13 & 0.13 & 0.13 & 0.13 & 0.11 & 0.11 & 0.11 & 0.11 & 0.11 & 0.11 \\
0 & 0 & 0.04 & 0.04 & 0.04 & 0.04 & 0.04 & 0.04 & 0.04 & 0.04 & 0.04 & 0.04 & 0.04 & 0.04 & 0.04 & 0.04
\end{bmatrix}$$

$$
\text{DPM} =
\begin{bmatrix}
0.07 & 0.07 & 0.07 & 0.07 & 0.08 & 0.08 & 0.08 & 0.05 & 0.06 & 0.06 & 0.06 & 0.05 & 0.06 & 0.05 \\
0.07 & 0.07 & 0.07 & 0.06 & 0.08 & 0.08 & 0.08 & 0.06 & 0.06 & 0.06 & 0.05 & 0.05 & 0.05 & 0.06 \\
0.16 & 0.16 & 0.17 & 0.17 & 0.19 & 0.2 & 0.19 & 0.14 & 0.14 & 0.14 & 0.14 & 0.14 & 0.14 & 0.14 \\
0.07 & 0.07 & 0.07 & 0.07 & 0.1 & 0.1 & 0.1 & 0.07 & 0.07 & 0.07 & 0.07 & 0 & 0 & 0 \\
0.13 & 0.13 & 0.13 & 0.13 & 0.2 & 0.2 & 0.2 & 0.13 & 0.13 & 0.13 & 0.13 & 0 & 0 & 0 \\
0.17 & 0.17 & 0.17 & 0.17 & 0.2 & 0.19 & 0.19 & 0.19 & 0.19 & 0.2 & 0.19 & 0.19 & 0.19 & 0.2 \\
0.07 & 0.07 & 0.07 & 0.07 & 0.08 & 0.08 & 0.08 & 0.08 & 0.08 & 0.08 & 0.08 & 0.08 & 0.08 & 0.08 \\
0.07 & 0.07 & 0.07 & 0.07 & 0.08 & 0.08 & 0.08 & 0.08 & 0.08 & 0.08 & 0.08 & 0.08 & 0.08 & 0.08 \\
0.13 & 0.13 & 0.13 & 0.13 & 0 & 0 & 0 & 0.13 & 0.13 & 0.13 & 0.13 & 0.26 & 0.27 & 0.27 \\
0.07 & 0.07 & 0.07 & 0.07 & 0 & 0 & 0 & 0.07 & 0.07 & 0.07 & 0.07 & 0.14 & 0.13 & 0.13
\end{bmatrix}
\tag{A.8}
$$

A.3 Parameters of the different models

Table A.1: Time constants of Turbines and Governors and Area participation factors.

	Gen1,1	Gen1,2	Gen1,3	Gen1,4	Gen1,5	Gen2,6	Gen2,7
$T_{\mathrm{G}_{i,k}}(\mathrm{sec})$	0.095	0.099	0.098	0.1	0.097	0.097	0.098
$T_{\mathrm{T}_{i,k}}(\mathrm{sec})$	0.59	0.58	0.51	0.55	0.5	0.55	0.5
$\gamma_{i,k}$	0.4	0.6	0	0	0	0	0
	Gen2,8	Gen2,9	Gen3,10	Gen3,11	Gen3,12	Gen3,13	Gen3,14
$T_{\mathrm{G}_{i,k}}(\mathrm{sec})$	0.1	0.099	0.096	0.098	0.1	0.095	0.099
$T_{\mathrm{T}_{i,k}}(\mathrm{sec})$	0.58	0.59	0.57	0.58	0.51	0.55	0.59
$\gamma_{i,k}$	0.55	0.45	0	0.45	0	0	0.55
	Gen4,15	Gen4,16	Gen4,17	Gen4,18	Gen4,19	Gen4,20	Gen5,21
$T_{\mathrm{G}_{i,k}}(\mathrm{sec})$	0.098	0.097	0.099	0.1	0.095	0.099	0.098
$T_{\mathrm{T}_{i,k}}(\mathrm{sec})$	0.57	0.55	0.5	0.57	0.53	0.59	0.57
$\gamma_{i,k}$	0.35	0	0	0.4	0.25	0	0
	Gen5,22	Gen5,23	Gen5,24	Gen6,25	Gen6,26	Gen6,27	Gen6,28
$T_{\mathrm{G}_{i,k}}(\mathrm{sec})$	0.097	0.099	0.1	0.1	0.098	0.099	0.099
$T_{\mathrm{T}_{i,k}}(\mathrm{sec})$	0.57	0.58	0.59	0.58	0.5	0.57	0.59
$\gamma_{i,k}$	0	0.45	0.55	0.6	0	0	0.4
	Gen6,29	Gen7,30	Gen7,31	Gen7,32	Gen7,33		
$T_{\mathrm{G}_{i,k}}(\mathrm{sec})$	0.095	0.097	0.099	0.098	0.1		
$T_{\mathrm{T}_{i,k}}(\mathrm{sec})$	0.56	0.57	0.58	0.53	0.59		
$\gamma_{i,k}$	0	0	0.6	0	0.4		

Table A.2: Equivalent inertia constants H_i pu s, droop $R_{i,k}$ Hz/pu (the same for all GenCos), frequency bias β_i pu/Hz (the same for each area) and equivalent damping D_i pu/Hz (the same for each area)

H_1	H_2	H_3	H_4	H_5	H_6	H_7	$R_{i,k}$	β_i	D_i
0.200	0.181	0.192	0.240	0.172	0.228	0.220	14	0.531	0.014

Table A.3: Tie line synchronising coefficients T_{ij} pu/Hz.

T_{14}	T_{31}	T_{53}	T_{43}	T_{37}	T_{42}	T_{45}	T_{64}	T_{76}
0.8645	0.8645	0.8625	0.8615	0.8635	0.8631	0.8605	0.8675	0.8625

Table A.4: Time constants of governors and turbines of each GenCos in the 4-area system and their area participation factors

	Gen1,1	Gen1,2	Gen1,3	Gen2,4	Gen 2,5	Gen 3,6	Gen 3,7
$T_{G_{i,k}}$(sec)	0.95	1.50	0.91	1.90	1.10	1.60	2.00
$T_{T_{i,k}}$(sec)	2.40	2.20	2.80	3.00	2.04	2.08	1.52
$\gamma_{i,k}$	0.51	0.49	0	1	0	0	0.51

	Gen 3,8	Gen 4,9	Gen 4,10
$T_{G_{i,k}}$(sec)	0.90	0.91	1.93
$T_{T_{i,k}}$(sec)	1.00	2.20	2.90
$\gamma_{i,k}$	0.49	0	1

Table A.5: Equivalent inertia constant H_i, damping D_i (equal for the 4 areas), droop $R_{i,k}$ (equal for each GenCo in area i) and frequency bias β_i (equal for the 4 areas).

H_1	H_2	H_3	H_4	D_i	$R_{1,k}$	$R_{2,k}$	$R_{3,k}$	$R_{4,k}$	β_i	T_{12}	T_{13}	T_{41}	T_{23}	T_{34}
0.56	0.51	0.56	0.46	0.04	13	14	12	15	0.423	0.23	0.21	0.22	0.24	0.22

Table A.6: Time constants of Turbines and Governors and Area participation factors (used for the DMPC scheme)

	Gen1,1	Gen1,2	Gen1,3	Gen1,4	Gen1,5	Gen2,6	Gen2,7
$T_{G_{i,k}}$(sec)	0.760	0.792	0.768	0.800	0.776	0.784	0.720
$T_{T_{i,k}}$(sec)	2.040	2.600	2.320	2.480	1.800	2.480	2.800
	Gen2,8	Gen2,9	Gen3,10	Gen3,11	Gen3,12	Gen3,13	Gen3,14
$T_{G_{i,k}}$(sec)	0.760	0.800	0.792	0.880	0.784	0.752	0.760
$T_{T_{i,k}}$(sec)	2.080	2.360	2.600	2.880	2.800	2.640	2.360
	Gen4,15	Gen4,16	Gen4,17	Gen4,18	Gen4,19	Gen4,20	Gen5,21
$T_{G_{i,k}}$(sec)	0.800	1.200	0.640	0.760	0.792	0.680	0.744
$T_{T_{i,k}}$(sec)	2.760	2.360	2.640	2.800	2.600	2.000	0.600
	Gen5,22	Gen5,23	Gen5,24	Gen6,25	Gen6,26	Gen6,27	Gen6,28
$T_{G_{i,k}}$(sec)	0.960	0.792	0.760	0.760	0.616	1.200	0.704
$T_{T_{i,k}}$(sec)	0.550	0.620	0.570	2.000	2.360	2.520	2.200
	Gen6,29	Gen7,30	Gen7,31	Gen7,32	Gen7,33		
$T_{G_{i,k}}$(sec)	0.680	0.760	0.640	0.704	0.800		

Table A.7: Equivalent inertia constants H_i pu s, droop $R_{i,\mathrm{k}}$ Hz/pu (the same for all GenCos) and frequency bias β_i pu/Hz (the same for each area). These parameters are used for the DMPC scheme

H_1	H_2	H_3	H_4	H_5	H_6	H_7	$R_{i,\mathrm{k}}$	β_i
0.39	0.36	0.38	0.45	0.42	0.46	0.42	15	0.531

Table A.8: Equivalent damping D_i pu/Hz an tie line synchronising coefficients T_{ij} pu/Hz (equal for all tie lines). These parameters are used for the DMPC scheme

D_1	D_2	D_3	D_4	D_5	D_6	D_7	T_{ij}
0.027	0.028	0.027	0.026	0.033	0.028	0.027	0.323

Bibliography

[1] F. Milano. *Power system modelling and scripting.* Springer Science & Business Media, 2010.

[2] J. Machowski, J.W. Bialek, and J.R. Bumby. *Power System Dynamics: Stability and Control.* John Wiley & Sons, Ltd, 2008.

[3] O. Elgerd. Control of electric power systems. *IEEE Control Systems Magazine*, 1(2):4–16, 1981.

[4] K.K. Sen and M.L. Sen. *Introduction to FACTS controllers: theory, modeling, and applications*, volume 54. John Wiley & Sons, 2009.

[5] Antonio Gómez-Expósito, Antonio J Conejo, and Claudio Cañizares. *Electric energy systems: analysis and operation.* CRC Press, 2016.

[6] P. Kundur. *Power System Stability and Control.* New York ; London : McGraw-Hill, 1994.

[7] O.I. Elgerd. Electric energy systems theory: An introduction. 1982.

[8] D.P. Kothari and I.J. Nagrath. *Modern power system analysis.* Tata McGraw-Hill Education, 2003.

[9] G. Andersson. Dynamics and control of electric power systems. pages 227–0528, 2012.

[10] P.W. Sauer. *Power system dynamics and stability.* Prentice Hall, 1998.

[11] L.L. Grigsby. *Power system stability and control*, volume 5. CRC press, 2012.

[12] N. Jaleeli, L. S. VanSlyck, D. N. Ewart, L.H . Fink, and A. G. Hoffmann. Understanding automatic generation control. *Power Systems, IEEE Transactions on*, 7(3):1106–1122, 1992.

[13] N. Bekhouche. Automatic generation control before and after deregulation. In *System Theory, 2002. Proceedings of the Thirty-Fourth Southeastern Symposium on*, pages 321–323, 2002.

[14] Consentec. Description of load-frequency control concept and market for control reserves, 2014.

[15] M. Prabavathi and R. Gnanadass. Energy bidding strategies for restructured electricity market. *International Journal of Electrical Power & Energy Systems*, 64:956–966, 2015.

[16] Reports by United Nation, Department of Economic and Social Affairs, New York. Multi Dimensional Issues in International Electric Power Grid Interconnections. `http://sustainabledevelopment.un.org/content/documents/interconnections.pdf`, 2006.

[17] J.W. Bialek. Blackouts in the us/canada and continental europe in 2003: Is liberalisation to blame? In *Power Tech, 2005 IEEE Russia*, pages 1–7, June 2005.

[18] B.J. Kirby, J. Dyer, C. Martinez, and et al. *Frequency control concerns in the North American electric power system*. United States. Department of Energy, 2003.

[19] EURELECTRIC ENTSO-E. Deterministic Frequency Deviations : Root Causes and Proposals for Potential Solutions. *Rep., Dec*, 2011.

[20] EURELECTRIC ENTSO-E. Deterministic Frequency Deviations : 2nd stage Impact Analysis. *Rep., Dec*, 2012.

[21] E.J. Lerner. What is wrong with the electric grid? *Gravitational, Electric, and Magnetic Forces: An Anthology of Current Thought*, page 41, 2005.

[22] H. Bevrani. *Robust power system frequency control*. Springer, 2008.

[23] G. Andersson, P. Donalek, R. Farmer, N. Hatziargyriou, I. Kamwa, P. Kundur, N. Martins, J. Paserba, P. Pourbeik, J. Sanchez-Gasca, R. Schulz, A. Stankovic, C. Taylor, and V. Vittal. Causes of the 2003 major grid blackouts in north america and europe, and recommended means to improve system dynamic performance. *Power Systems, IEEE Transactions on*, 20(4):1922–1928, 2005.

[24] A. Singh and S. Aasma. Grid failure in northern, eastern and north-eastern grid in 2012: Cause & its effect on economy of india an review. *SAMRIDDHI-A Journal of Physical Sciences, Engineering and Technology (S-JPSET 2012)*, 3(2), 2012.

[25] ENTSO-E. Report on Blackout in Turkey on March 2015, 2015.

[26] F. Vandenberghe, E. Grebe, D. Klaar, K. Kleinekorte, J.M. Rodriguez, H. Erven, C. Laffaye, H.and Sabelli, F. Kropec, T. Tillwicks, et al. Final report of the investigation committee on the 28 september 2003 blackout in italy, 2004.

[27] Y.V. Makarov, V.I. Reshetov, and N.I. Stroev, A.Voropai. Blackout prevention in the united states, europe, and russia. *Proceedings of the IEEE*, 93(11):1942–1955, 2005.

[28] S.J. Qin and T.A. Badgwell. A survey of industrial model predictive control technology. *Control engineering practice*, 11(7):733–764, 2003.

[29] V. Donde, M.A. Pai, and I.A. Hiskens. Simulation and optimization in an agc system after deregulation. *Power Systems, IEEE Transactions on*, 16(3):481–489, 2001.

[30] A.J. Wood and B.F. Wollenberg. *Power Generation, Operation, and Control.* John Wiley & Sons, Inc.

[31] C.T. Pan and C.M. Liaw. An adaptive controller for power system load-frequency control. *Power Systems, IEEE Transactions on*, 4(1):122–128, 1989.

[32] W. Chan and Y. Hsu. Automatic generation control of interconnected power systems using variable-structure controllers. In *IEE Proceedings C (Generation, Transmission and Distribution)*, volume 128, pages 269–279. IET, 1981.

[33] E.E. Ejegi, J.A. Rossiter, and P. Trodden. A survey of techniques and opportunities in power system automatic generation control. In *UKACC Int. Conf.*, pages 537–542, July 2014.

[34] E.E. Ejegi, J.A. Rossiter, and P. Trodden. Model predictive load frequency control of a two-area deregulated power system. In *Control Conference (ECC), 2015 European*, pages 1044–1049. IEEE, 2015.

[35] E.E. Ejegi, J.A. Rossiter, and P. Trodden. Generalized model for load frequency control studies in a deregulated environment, ECC, 2016 Accepted.

[36] E.E. Ejegi, J.A. Rossiter, and P. Trodden. Predictive load frequency control of an interconnected power system after deregulation. 2016 [To be submitted].

[37] E.E. Ejegi, J.A. Rossiter, and P. Trodden. Distributed model predictive load frequency control of a deregulated power system. In *UKACC Int. Conf.*, 2016.

[38] E.E. Ejegi, J.A. Rossiter, and P. Trodden. Distributed predictive control for power system load frequency control after deregulation. 2016 [To be submitted].

[39] G. Dell'Olio, M. Sforna, C. Bruno, and M. Pozzi. A pluralistic lfc scheme for online resolution of power congestions between market zones. *IEEE Transactions on Power Systems*, 20(4):2070–2077, 2005.

[40] ENTSO-E. Continental europe operation handbook - appendix 1 : Load frequency control and performance. Technical report, 2004.

[41] J. Schmutz and M. Koller. Primary Frequency Control Provided by Battery. 2013.

[42] IEEE Report. Dynamic models for steam and hydro turbines in power system studies. *IEEE Transactions on Power Apparatus and Systems*, (6):1904–1915, 1973.

[43] O. Fosha, C.and Elgerd. The megawatt-frequency control problem: a new approach via optimal control theory. *IEEE Transactions on Power Apparatus and Systems*, 4(PAS-89):563–577, 1970.

[44] P.W. Sauer. Time-scale features and their applications in electric power system dynamic modeling and analysis. In *Proceedings of the 2011 American Control Conference*, pages 4155–4159. IEEE, 2011.

[45] G. Lalor, A. Mullane, and M. O'Malley. Frequency control and wind turbine technologies. *IEEE Transactions on Power Systems*, 20(4):1905–1913, 2005.

[46] H. Banakar, C. Luo, and B.T. Ooi. Impacts of wind power minute-to-minute variations on power system operation. *IEEE Transactions on Power Systems*, 23(1):150–160, 2008.

[47] J. Aho, A. Buckspan, J. Laks, P. Fleming, Y. Jeong, F. Dunne, M. Churchfield, L. Pao, and K. Johnson. A tutorial of wind turbine control for supporting grid frequency through active power control. In *American Control Conference (ACC), 2012*, pages 3120–3131. IEEE, 2012.

[48] H. Bevrani and T. Hiyama. *Intelligent automatic generation control.* CRC press New York, 2011.

[49] H.L. Willis and L. Philipson. *Understanding electric utilities and de-regulation*, volume 27. CRC Press, 2005.

[50] I. Ibraheem, P. Kumar, and D.P. Kothari. Recent philosophies of automatic generation control strategies in power systems. *Power Systems, IEEE Transactions on*, 20(1):346–357, 2005.

[51] A.K. Srivastava, S. Kamalasadan, D. Patel, S. Sankar, and K.S. Al-Olimat. Electricity markets: an overview and comparative study. *International Journal of Energy Sector Management*, 5(2):169–200, 2011.

[52] A.M. Pirbazari. Ancillary services definitions, markets and practices in the world. In *Transmission and Distribution Conference and Exposition: Latin America (T D-LA), 2010 IEEE/PES*, pages 32–36, 2010.

[53] H. Singh and A. Papalexopoulos. Competitive procurement of ancillary services by an independent system operator. *IEEE Transactions on Power Systems*, 14(2):498–504, 1999.

[54] R.D. Christie and A. Bose. Load frequency control issues in power system operations after deregulation. *Power Systems, IEEE Transactions on*, 11(3):1191–1200, 1996.

[55] J. Kumar, K. Ng, and G. Sheble. AGC simulator for price-based operation. I. a model. *IEEE Trans. Power Sys.*, 12(2):527–532, 1997.

[56] J. Kumar, K. Ng, and G. Sheble. AGC simulator for price-based operation. II. case study results. *IEEE Transactions on Power Systems*, 12(2):533–538, 1997.

[57] E. Onaiwu. How does bilateral trading differ from electricity pooling. *Universisty of Dundee*, 2009.

[58] IEEE recommended definitions of terms for automatic generation control on electric power systems. *IEEE Std 94-1991*, pages 1–, 1991.

[59] D.B. Eidson and M.D. Ilic. Advanced generation control with economic dispatch. In *Decision and Control, 1995., Proceedings of the 34th IEEE Conference on*, volume 4, pages 3450–3458. IEEE, 1995.

[60] N. Li, L. Chen, C. Zhao, and S.H. Low. Connecting automatic generation control and economic dispatch from an optimization view. In *2014 American Control Conference*, pages 735–740. IEEE, 2014.

[61] H. Shayeghi, H.A. Shayanfar, and A. Jalili. Load frequency control strategies: A state-of-the-art survey for the researcher. *Energy Conversion and Management*, 50(2):344–353, 2009.

[62] S.K. Pandey, S.R. Mohanty, and N. Kishor. A literature survey on load-frequency control for conventional and distribution generation power systems. *Renewable and Sustainable Energy Reviews*, 25:318–334, 2013.

[63] C. Concordia and L.K. Kirchmayer. Tie-line power and frequency control of electric power systems [includes discussion]. *Power Apparatus and Systems, Part III. Transactions of the American Institute of Electrical Engineers*, 72(2), 1953.

[64] E.C. Tacker, T.W. Reddoch, O.T. Tan, and T.D. Linton. Automatic generation control of electric energy systems - a simulation study. *Systems, Man and Cybernetics, IEEE Trans.*, (4):403–405, 1973.

[65] H.G. Kwatny, K.C. Kalnitsky, and A. Bhatt. An optimal tracking approach to load-frequency control. *Power Apparatus and Systems, IEEE Transactions on*, 94(5):1635–1643, 1975.

[66] M.L. Kothari and J. Nanda. Application of optimal control strategy to automatic generation control of a hydrothermal system. In *Control Theory and Applications, IEE Proceedings D*, volume 135, pages 268–274. IET, 1988.

[67] J. Nanda and B.L. Kaul. Automatic generation control of an interconnected power system. *Proceedings of the Institution of Electrical Engineers*, 125(5):385–390, 1978.

[68] C. Concordia, L.K. Kirchmayer, and E.A. E. A. Szymanski. Efect of speed-governor dead band on tie-line power and frequency control performance. *Transactions of the American Institute of Electrical Engineers. Part III: Power Apparatus and Systems*, 76(3):429–434, April 1957.

[69] C.W. Taylor, K.Y. Lee, and D.P. Dave. Automatic generation control analysis with governor deadband effects. *IEEE Transactions on Power Apparatus and Systems*, PAS-98(6):2030–2036, Nov 1979.

[70] S.C. Tripathy, T. S. Bhatti, C.S. Jha, O. P. Malik, and G.S. Hope. Sampled data automatic generation control analysis with reheat steam turbines and governor dead-band effects. *Power Apparatus and Systems, IEEE Transactions on*, PAS-103(5):1045–1051, 1984.

[71] A. Kumar, O.P. Malik, and G.S. Hope. Discrete variable structure controller for load frequency control of multiarea interconnected power systems. In *IEE Proceedings C (Generation, Transmission and Distribution)*, volume 134, pages 116–122. IET, 1987.

[72] M. Kazemi, M.H.and Karrari and M.B. Menhaj. Decentralized robust adaptive-output feedback controller for power system load frequency control. *Electrical Engineering*, 84(2):75–83, 2002.

[73] K.A. Lee, H. Yee, and C.Y. Teo. Self-tuning algorithm for automatic generation control in an interconnected power system. *Electric Power Systems Research*, 20(2):157–165, 1991.

[74] H. Bevrani, Y. Mitani, and K. Tsuji. Sequential design of decentralized load frequency controllers using μ synthesis and analysis. *Energy conversion and management*, 45(6):865–881, 2004.

[75] J. Talaq and F. Al-Basri. Adaptive fuzzy gain scheduling for load frequency control. *Power Systems, IEEE Trans.*, 14(1), 1999.

[76] H.L. Zeynelgil, A. Demiroren, and N.S. Sengor. The application of ANN technique to automatic generation control for multi-area power system. *International journal of electrical power & energy systems*, 24(5):345–354, 2002.

[77] IEEE standard definitions of terms for automatic generation control on electric power systems. *IEEE Transactions on Power Apparatus and Systems*, PAS-89(6):1356–1364, July 1970.

[78] IEEE standard definitions in power operations terminology. *IEEE Std 858-1993*, 1993.

[79] H. Bevrani, Y. Mitani, K. Tsuji, and H. Bevrani. Bilateral based robust load frequency control. *Energy conversion and management*, 46(7):1129–1146, 2005.

[80] H. Shayeghi, H.A. Shayanfar, and O.P. Malik. Robust decentralized neural networks based lfc in a deregulated power system. *Electric Power Systems Research*, 77(3):241–251, 2007.

[81] E. Rakhshani and J. Sadeh. Practical viewpoints on load frequency control problem in a deregulated power system. *Energy Conversion and Management*, 51(6):1148–1156, 2010.

[82] K.P. Parmar, S. Majhi, and D.P. Kothari. LFC of an interconnected power system with multi-source power generation in deregulated power environment. *Int. J. of Elect. Power & Energy Sys.*, 57:277–286, 2014.

[83] W. Tan, H. Zhang, and M. Yu. Decentralized load frequency control in deregulated environments. *International Journal of Electrical Power & Energy Systems*, 41(1):16–26, 2012.

[84] W. Tan, Y. Hao, and D. Li. Load frequency control in deregulated environments via active disturbance rejection. *International Journal of Electrical Power & Energy Systems*, 66:166–177, 2015.

[85] P. Bhatt, R. Roy, and S.P. Ghoshal. Optimized multi area agc simulation in restructured power systems. *International journal of electrical power & energy systems*, 32(4):311–322, 2010.

[86] S. Debbarma, L.C. Saikia, and N. Sinha. Agc of a multi-area thermal system under deregulated environment using a non-integer controller. *Electric Power Systems Research*, 95:175–183, 2013.

[87] K. Sabahi, S. Ghaemi, and S. Pezeshki. Application of type-2 fuzzy logic system for load frequency control using feedback error learning approaches. *Applied Soft Computing*, 21:1–11, 2014.

[88] S. Bhowmik, K. Tomsovic, and A. Bose. Communication models for third party load frequency control. *IEEE Transactions on Power Systems*, 19(1):543–548, 2004.

[89] C. Zhang, L. Jiang, Q. Wu, and M. He, Y.and Wu. Delay-dependent robust load frequency control for time delay power systems. *IEEE Transactions on Power Systems*, 28(3):2192–2201, 2013.

[90] C. Peng and J. Zhang. Delay-distribution-dependent load frequency control of power systems with probabilistic interval delays. *IEEE Transactions on Power Systems*, 31(4):3309–3317, 2016.

[91] C. Seneviratne and C. Ozansoy. Frequency response due to a large generator loss with the increasing penetration of wind/pv generation-a literature review. *Renewable and Sustainable Energy Reviews*, 57:659–668, 2016.

[92] D. Apostolopoulou, A.D. Domínguez-García, and P.W. Sauer. An assessment of the impact of uncertainty on automatic generation control systems. *IEEE Transactions on Power Systems*, 31(4):2657–2665, 2016.

[93] M.H. Variani and K. Tomsovic. Distributed automatic generation control using flatness-based approach for high penetration of wind generation. *IEEE Transactions on Power Systems*, 28(3):3002–3009, 2013.

[94] H. Bevrani and P.R. Daneshmand. Fuzzy logic-based load-frequency control concerning high penetration of wind turbines. *IEEE systems journal*, 6(1):173–180, 2012.

[95] D. Qian, S. Tong, H. Liu, and X. Liu. Load frequency control by neural-network-based integral sliding mode for nonlinear power systems with wind turbines. *Neurocomputing*, 173:875–885, 2016.

[96] A.M. Ersdal, L. Imsland, K. Uhlen, D. Fabozzi, and N.F. Thornhill. Model predictive load–frequency control taking into account imbalance uncertainty. *Control Engineering Practice*, 2015.

[97] O. I. Elgerd and C.E. Fosha. Optimum megawatt-frequency control of multiarea electric energy systems. *Power Apparatus and Systems, IEEE Transactions on*, PAS-89(4):556–563, 1970.

[98] H. Shayeghi and H.A. Shayanfar. Application of ANN technique based on μ-synthesis to load frequency control of interconnected power system. *International Journal of Electrical Power & Energy Systems*, 28(7):503 – 511, 2006.

[99] J.H. Zhang, J.H. Hao, G.H. Zhang, and G.L. Hou. Application of sliding mode prediction control to agc systems considering signal delay. In *Systems and Control in Aerospace and Astronautics, 2008. ISSCAA 2008. 2nd International Symposium on*, pages 1–6. IEEE, 2008.

[100] H. Guolian, L. Junjun, and Z. Jianhua. Application of fuzzy predictive control to agc system after deregulation over communication network. In *Indust. Electronics and Applications (ICIEA), 2011 6th IEEE Conference on*, pages 2512–2517, June 2011.

[101] X. Liu, X. Kong, and X. Deng. Power system model predictive load frequency control. In *ACC*, pages 6602–6607. IEEE, 2012.

[102] A.N. Venkat, I.A. Hiskens, J.B. Rawlings, and S.J. Wright. Distributed MPC strategies with application to power system automatic generation control. *Control Systems Technology, IEEE Transactions on*, 16(6):1192–1206, 2008.

[103] J.M. Maestre and R.R Negenborn. *Distributed Model Predictive Control Made Easy.* Springer, 2014.

[104] B. Tyagi and S.C. Srivastava. A decentralized automatic generation control scheme for competitive electricity markets. *IEEE Transactions on Power Systems*, 21(1):312–320, 2006.

[105] T.C. Yang, Z.T. Ding, and H. Yu. Decentralised power system load frequency control beyond the limit of diagonal dominance. *International Journal of Electrical Power & Energy Systems*, 24(3):173 – 184, 2002.

[106] W. Tan. Decentralized load frequency controller analysis and tuning for multi-area power systems. *Energy Conversion and Management*, 52(5):2015 – 2023, 2011.

[107] Muthana T. Alrifai, Mohamed F. Hassan, and Mohamed Zribi. Decentralized load frequency controller for a multi-area interconnected power system. *International Journal of Electrical Power & Energy Systems*, 33(2):198 – 209, 2011.

[108] T.H. Mohamed, H. Bevrani, A.A. Hassan, and T. Hiyama. Decentralized model predictive based load frequency control in an interconnected power system. *Energy Conversion and Management*, 52(2), 2011.

[109] S. Saxena and Y.V. Hote. Decentralized pid load frequency control for perturbed multi-area power systems. *International Journal of Electrical Power & Energy Systems*, 81:405–415, 2016.

[110] H. Shayeghi and H.A. Shayanfar. Decentralized robust load frequency control using LMI in a deregulated multi-area power system. 2005.

[111] Y. Mi, Y. Fu, C. Wang, and P. Wang. Decentralized sliding mode load frequency control for multi-area power systems. *IEEE Transactions on Power Systems*, 28(4):4301–4309, 2013.

[112] A.N. Venkat, I.A. Hiskens, J.B. Rawlings, and S.J. Wright. Distributed output feedback MPC for power system control. In *Decision and Control, 2006 45th IEEE Conference on*, pages 4038–4045, 2006.

[113] A.M. Ersdal, L. Imsland, and K. Uhlen. Model predictive load-frequency control. 2015.

[114] Bruce H. Jia, D.and Krogh. Distributed model predictive control. In *American Control Conference, 2001. Proceedings of the 2001*, volume 4, pages 2767–2772. IEEE, 2001.

[115] R.M. Hermans, M. Lazar, and A. Jokic. Distributed predictive control of the 7-machine cigré power system. In *American Control Conference (ACC), 2011*, pages 5225–5230. IEEE, 2011.

[116] M. Ma, H. Chen, X. Liu, and F. Allgöwer. Distributed model predictive load frequency control of multi-area interconnected power system. *Int. J. of Elect. Power & Energy Sys.*, 62:289–298, 2014.

[117] R.P. Aggarwal and F.R. Bergseth. Large signal dynamics of load-frequency control systems and their optimization using nonlinear programming: I. *IEEE Transactions on Power Apparatus and Systems*, (2):527–532, 1968.

[118] Aggarwal R.P. and Bergseth F.R. Large signal dynamics of load-frequency control systems and their optimization using nonlinear programming: Ii. *IEEE Transactions on Power Apparatus and Systems*, PAS-87(2):532–538, Feb 1968.

[119] N. Cohn. Some aspects of tie-line bias control on interconnected power systems. *Power apparatus and systems, part iii. trans. of the american institute of electrical engineers*, 75(3), 1956.

[120] Y. Moon, H. Ryu, J. Lee, K. Song, and M. Shin. Extended integral control for load frequency control with the consideration of generation-rate constraints. *International journal of electrical power & energy systems*, 24(4):263–269, 2002.

[121] K.P. Parmar, S. Majhi, and D.P. Kothari. Load frequency control of a realistic power system with multi-source power generation. *Int. J of Elect. Power & Energy Sys.*, 42(1):426–433, 2012.

[122] H. Trinh and T. Fernando. *Functional observers for dynamical systems*, volume 420. Springer Science & Business Media, 2011.

[123] H. Trinh, T. Fernando, Herbert H.C. Iu, and K.P. Wong. Quasi-decentralized functional observers for the lfc of interconnected power systems. *IEEE Transactions on Power Systems*, 28(3):3513–3514, 2013.

[124] T. Fernando, K. Emami, S. Yu, H.H. Iu, and K.P. Wong. A novel quasi-decentralized functional observer approach to lfc of interconnected power systems. *IEEE Transactions on Power Systems*, 31(4):3139–3151, 2016.

[125] T.N. Pham, H. Trinh, and L.H Hien. Load frequency control of power systems with electric vehicles and diverse transmission links using distributed functional observers. *IEEE Transactions on Smart Grid*, 7(1):238–252, 2016.

[126] W. Tan. Unified tuning of pid load frequency controller for power systems via imc. *IEEE Transactions on power systems*, 25(1):341–350, 2010.

[127] S. Saxena and Y.V. Hote. Load frequency control in power systems via internal model control scheme and model-order reduction. *IEEE Transactions on Power Systems*, 28(3):2749–2757, 2013.

[128] M. Zribi, M. Al-Rashed, and M. Alrifai. Adaptive decentralized load frequency control of multi-area power systems. *International Journal of Electrical Power & Energy Systems*, 27(8):575–583, 2005.

[129] A. Rubaai and V. Udo. Self-tuning load frequency control: multilevel adaptive approach. *IEE Proceedings-Generation, Transmission and Distribution*, 141(4):285–290, 1994.

[130] R.R. Shoults and J.A. Jativa Ibarra. Multi-area adaptive lfc developed for a comprehensive agc simulator. *Power Systems, IEEE Transactions on*, 8(2):541–547, 1993.

[131] I. Vajk, M Vajta, L. Keviczky, R. Haber, J. Hetthessy, and K. Kovacs. Adaptive load-frequency control of the hungarian power system. *Automatica*, 21(2):129–137, 1985.

[132] J.A Rossiter. *Model Predictive Control: A Pratical Approach*. CRC Press, 2003.

[133] M. Moradzadeh, R. Boel, and L. Vandevelde. Voltage coordination in multi-area power systems via distributed model predictive control. *IEEE Transactions on Power Systems*, 28(1):513–521, 2013.

[134] K. Edlund, J.D. Bendtsen, and J.B. Jørgensen. Hierarchical model-based predictive control of a power plant portfolio. *Control Engineering Practice*, 19(10):1126–1136, 2011.

[135] X. Shi, J. Hu, J. Yu, T. Yong, and J. Cao. A novel load frequency control strategy based on model predictive control. In *Power & Energy Society General Meeting, 2015 IEEE*, pages 1–5. IEEE, 2015.

[136] A.M. Ersdal, L. Fabozzi, D.and Imsland, and N.F. Thornhill. Model predictive control for power system frequency control taking into account imbalance uncertainty. In *Proc. IFAC World Congr*, volume 19, pages 981–986, 2014.

[137] A. Morattab, Q. Shafiee, and H. Bevrani. Decentralized model predictive load-frequency control for deregulated power systems in a tough situation. In *PowerTech, 2011 IEEE Trondheim*, pages 1–5, 2011.

[138] S. Riverso, M. Farina, and G. Ferrari-Trecate. Plug-and-play decentralized model predictive control for linear systems. *IEEE Transactions on Automatic Control*, 58(10):2608–2614, 2013.

[139] Ralph M. Hermans, A. Jokić, M. Lazar, A. Alessio, Paul P.J. Van den B., I.A. Hiskens, and A. Bemporad. Assessment of non-centralised model predictive control techniques for electrical power networks. *International journal of control*, 85(8):1162–1177, 2012.

[140] F. Milla, M.A. Duarte-Mermoud, and N. Aguila-Camacho. Hierarchical mpc secondary control for electric power system. *Mathematical Problems in Engineering*, 2014, 2014.

[141] M.D Galus, S. Koch, and G. Andersson. Provision of load frequency control by phevs, controllable loads, and a cogeneration unit. *IEEE Transactions on Industrial Electronics*, 58(10):4568–4582, 2011.

[142] R. Nepal and T. Jamasb. Security of european electricity systems: Conceptualizing the assessment criteria and core indicators. *International Journal of critical infrastructure protection*, 6(3):182–196, 2013.

[143] J.H. Zhang, J.H. Hao, and G.L. Hou. Automatic generation controller design in deregulated and networked environment using predictive control strategy. *matrix*, 1(1):2, 2008.

[144] ENTSO-E. Continental europe operation handbook - appendix 1 : Load frequency and performance, 2004.

[145] N. Atic, D. Rerkpreedapong, A. Hasanovic, and A. Feliachi. Nerc compliant decentralized load frequency control design using model predictive control. In *Power Engineering Society General Meeting, 2003, IEEE*, volume 2. IEEE, 2003.

[146] N. Atic, A. Feliachi, and D. Rerkpreedapong. Cps1 and cps2 compliant wedge-shaped model predictive load frequency control. In *Power Engineering Society General Meeting, 2004. IEEE*, pages 855–860. IEEE, 2004.

[147] Paul Mc Namara, Rudy R Negenborn, Bart De Schutter, Gordon Lightbody, and Seán McLoone. Distributed mpc for frequency regulation in multi-terminal hvdc grids. *Control Engineering Practice*, 46:176–187, 2016.

[148] L. Dong, Y. Zhang, and Z. Gao. A robust decentralized load frequency controller for interconnected power systems. *ISA transactions*, 51(3):410–419, 2012.

[149] F. Liu, Y. Li, Y. Cao, J. She, and M. Wu. A two-layer active disturbance rejection controller design for load frequency control of interconnected power system. *IEEE Transactions on Power Systems*, 31(4):3320–3321, 2016.

[150] S. Sondhi and Y.V. Hote. Fractional order pid controller for perturbed load frequency control using kharitonov's theorem. *International Journal of Electrical Power & Energy Systems*, 78:884–896, 2016.

[151] N. Chuang. Robust h-infinity load-frequency control in interconnected power systems. *IET Control Theory & Applications*, 10(1):67–75, 2015.

[152] W. Tan and Z. Xu. Robust analysis and design of load frequency controller for power systems. *Electric Power Systems Research*, 79(5):846–853, 2009.

[153] X. Yu and K. Tomsovic. Application of linear matrix inequalities for load frequency control with communication delays. *IEEE transactions on power systems*, 19(3):1508–1515, 2004.

[154] L. Jiang, W. Yao, Q.H. Wu, J.Y. Wen, and S.J. Cheng. Delay-dependent stability for load frequency control with constant and time-varying delays. *IEEE Transactions on Power systems*, 27(2):932–941, 2012.

[155] C. Zhang, L. Jiang, Q. Wu, Y. He, and M. Wu. Further results on delay-dependent stability of multi-area load frequency control. *IEEE Transactions on Power Systems*, 28(4):4465–4474, 2013.

[156] C.C. Lee. Fuzzy logic in control systems: fuzzy logic controller. *Systems, Man and Cybernetics, IEEE Trans.*, 20(2), 1990.

[157] C. Godjevac. Comaparative study of fuzzy control, neural networks and neuro-fuzzy control. Technical report, Swiss Federal Institute of Technology in Lausanne, 1995.

[158] C.S. Chang and W. Fu. Area load frequency control using fuzzy gain scheduling of {PI} controllers. *Electric Power Systems Research*, 42(2):145 – 152, 1997.

[159] I. Kocaarslan and E. Cam. Fuzzy logic controller in interconnected electrical power systems for load-frequency control. *International Journal of Electrical Power & Energy Systems*, 27(8):542 – 549, 2005.

[160] H.J. Lee, J.B. Park, and Y.H. Joo. Robust load-frequency control for uncertain nonlinear power systems: A fuzzy logic approach. *Information Sciences*, 176(23):3520 – 3537, 2006.

[161] H. Bevrani, P.R. Daneshmand, P. Babahajyani, Y. Mitani, and T. Hiyama. Intelligent lfc concerning high penetration of wind power: synthesis and real-time application. *IEEE Transactions on Sustainable Energy*, 5(2):655–662, 2014.

[162] C.K. Shiva and V. Mukherjee. Automatic generation control of multi-unit multi-area deregulated power system using a novel quasi-oppositional harmony search algorithm. *IET Generation, Transmission & Distribution*, 9(15):2398–2408, 2015.

[163] K. Sabahi, S. Ghaemi, and M. Badamchizadeh. Designing an adaptive type-2 fuzzy logic system load frequency control for a nonlinear time-delay power system. *Applied Soft Computing*, 43:97–106, 2016.

[164] H.A. Yousef, A. Khalfan, M.H. Albadi, and N. Hosseinzadeh. Load frequency control of a multi-area power system: An adaptive fuzzy logic approach. *IEEE Transactions on Power Systems*, 29(4):1822–1830, 2014.

[165] A.P. Birch, A.T. Sapeluk, and C.S. Ozveren. An enhanced neural network load frequency control technique. 1994.

[166] V.S. Sundaram and T. Jayabarathi. Load frequency control using pid tuned ann controller in power system. In *Electrical Energy Systems (ICEES)*, pages 269–274. IEEE, 2011.

[167] N. Patel and B.B. Jain. Automatic generation control of three area power systems using ANN controllers. *International Journal of Emerging Technology and Advanced Engineering*, 3(7):278–284, 2013.

[168] S.H. Hosseini and A.H. Etemadi. Adaptive neuro-fuzzy inference system based automatic generation control. *Electric Power Systems Research*, 78(7):1230–1239, 2008.

[169] Y.L. Karnavas and D.P. Papadopoulos. Agc for autonomous power system using combined intelligent techniques. *Electric power systems research*, 62(3):225–239, 2002.

[170] S.B. Shree and N. Kamaraj. Hybrid neuro fuzzy approach for automatic generation control in restructured power system. *International Journal of Electrical Power & Energy Systems*, 74:274–285, 2016.

[171] G.A. Chown and B. Wigdorowitz. A methodology for the redesign of frequency control for ac networks. *IEEE Transactions on Power Systems*, 19(3):1546–1554, 2004.

[172] G. Gross and J.W. Lee. Analysis of load frequency control performance assessment criteria. *IEEE Transactions on power systems*, 16(3):520–525, 2001.

[173] A.P.S. Meliopoulos, G.J. Cokkinides, and A.G. Bakirtzis. Load-frequency control service in a deregulated environment. *Decision Support Systems*, 24(3):243–250, 1999.

[174] E. Nobile, A. Bose, and K. Tomsovic. Feasibility of a bilateral market for load following. *IEEE Transactions on Power systems*, 16(4):782–787, 2001.

[175] E. De Tuglie and F. Torelli. Load following control schemes for deregulated energy markets. *IEEE Transactions on Power systems*, 21(4):1691–1698, 2006.

[176] J.M. Arroyo and A.J Conejo. Optimal response of a power generator to energy, agc, and reserve pool-based markets. *IEEE Transactions on Power Systems*, 17(2):404–410, 2002.

[177] H. Holttinen, P. Meibom, A. Orths, and F. others Hulle. Design and operation of power systems with large amounts of wind power, first results of iea collaboration. In *EWEC'2006-European Wind Energy Conference & Exhibition*, pages 1–15, 2006.

[178] L. Fan, Z. Miao, and D. Osborn. Wind farms with hvdc delivery in load frequency control. *IEEE Transactions on Power Systems*, 24(4):1894–1895, 2009.

[179] J. Pahasa and I. Ngamroo. Coordinated control of wind turbine blade pitch angle and phevs using mpcs for load frequency control of microgrid. *IEEE Systems Journal*, 10(1):97–105, 2016.

[180] A. Sargolzaei, K.K. Yen, and M.N. Abdelghani. Preventing time-delay switch attack on load frequency control in distributed power systems. *IEEE Transactions on Smart Grid*, 7(2):1176–1185, 2016.

[181] S. Sönmez and S. Ayasun. Stability region in the parameter space of pi controller for a single-area load frequency control system with time delay. *IEEE Transactions on Power Systems*, 31(1):829–830, 2016.

[182] S. Wen, X. Yu, Z. Zeng, and J. Wang. Event-triggering load frequency control for multiarea power systems with communication delays. *IEEE Transactions on Industrial Electronics*, 63(2):1308–1317, 2016.

[183] S. Liu, P.X. Liu, and A. El Saddik. Modeling and stability analysis of automatic generation control over cognitive radio networks in smart grids. *IEEE Transactions on Systems, Man, and Cybernetics: Systems*, 45(2):223–234, 2015.

[184] Y. Ba and W. Li. A simulation scheme for agc relevant studies. *IEEE Transactions on Power Systems*, 28(4):3621–3628, 2013.

[185] Y. Hain, R. Kulessky, and G. Nudelman. Identification-based power unit model for load-frequency control purposes. *IEEE Transactions on Power Systems*, 15(4):1313–1321, 2000.

[186] A. Rahman, L.C. Saikia, and N. Sinha. Load frequency control of a hydro-thermal system under deregulated environment using biogeography-based optimised three-degree-of-freedom integral-derivative controller. *IET Generation, Transmission & Distribution*, 9(15):2284–2293, 2015.

[187] M. Farahani, S. Ganjefar, and M. Alizadeh. Pid controller adjustment using chaotic optimisation algorithm for multi-area load frequency control. *IET Control Theory & Applications*, 6(13):1984–1992, 2012.

[188] K. Emami, T. Fernando, H.H. Iu, B.D. Nener, and K.P. Wong. Application of unscented transform in frequency control of a complex power system using noisy pmu data. *IEEE Transactions on Industrial Informatics*, 12(2):853–863, 2016.

[189] H. Chen, R. Ye, X. Wang, and R. Lu. Cooperative control of power system load and frequency by using differential games. *IEEE Transactions on Control Systems Technology*, 23(3):882–897, 2015.

[190] T. Namerikawa and T. Kato. Distributed load frequency control of electrical power networks via iterative gradient methods. In *2011 50th IEEE Conference on Decision and Control and European Control Conference*, pages 7723–7728. IEEE, 2011.

[191] P. Kalvibool and S. Arunsawatwong. Design of load frequency regulator for power systems subject to bounded persistent disturbance considering generation rate constraint. In *Society of Instrument and Control Engineers of Japan (SICE), 2015 54th Annual Conference of the*, pages 916–921. IEEE, 2015.

[192] C. Boonchuay. Improving regulation service based on adaptive load frequency control in lmp energy market. *IEEE Transactions on Power Systems*, 29(2):988–989, 2014.

[193] T. Tsay. Load-frequency control of interconnected power system with governor backlash nonlinearities. *International Journal of Electrical Power & Energy Systems*, 33(9):1542–1549, 2011.

[194] S.J. Qin and T.A. Badgwell. An overview of industrial model predictive control technology. In *AIChE Symposium Series*, volume 93, pages 232–256. Citeseer, 1997.

[195] J.B. Froisy. Model predictive control-building a bridge between theory and practice. *Computers & chemical engineering*, 30(10):1426–1435, 2006.

[196] B.P. Gibbs, D.S. Weber, and D.W. Porter. Application of nonlinear model-based predictive control to fossil power plants. In *Proceedings of the 30th IEEE Conference on Decision and Control*, pages 1850–1856. IEEE, 1991.

[197] J.A. Rossiter, P.W. Neal, and L. Yao. Applying predictive control to a fossil-fired power station. *Transactions of the Institute of Measurement and Control*, 24(3):177–194, 2002.

[198] M. Larsson and D. Karlsson. Coordinated system protection scheme against voltage collapse using heuristic search and predictive control. *IEEE Transactions on Power Systems*, 18(3):1001–1006, 2003.

[199] A. Jain, G. Schildbach, L. Fagiano, and M. Morari. On the design and tuning of linear model predictive control for wind turbines. *Renewable Energy*, 80:664–673, 2015.

[200] V. Spudić, C. Conte, M. Baotić, and M. Morari. Cooperative distributed model predictive control for wind farms. *Optimal Control Applications and Methods*, 36(3):333–352, 2015.

[201] P. Kou, D. Liang, L. Gao, and F. Gao. Stochastic coordination of plug-in electric vehicles and wind turbines in microgrid: A model predictive control approach. *IEEE Transactions on Smart Grid*, 7(3):1537–1551, 2016.

[202] D.E. Seborg, D.A. Mellichamp, T.F. Edgar, and F.J. Doyle III. *Process dynamics and control*. John Wiley & Sons, 2010.

[203] B. Kouvaritakis and M. Cannon. *Model Predictive Control*. Springer, 2016.

[204] D.Q. Mayne and J.B. Rawlings. Model predictive control: theory and design. *Madison, WI: Nob Hill Publishing, LCC*, 2009.

[205] D.J. Chmielewski and V. Manousiouthakis. On constrained infinite-time linear quadratic optimal control. In *Proceedings of the 35th IEEE Conference on Decision and Control*, volume 2, pages 1319–1324. IEEE, 1996.

[206] P.D. Christofides, R. Scattolini, David M. de la P., and J. Liu. Distributed model predictive control: A tutorial review and future research directions. *Computers & Chemical Engineering*, 51:21–41, 2013.

[207] S. Li and Y. Zheng. *Distributed Model Predictive Control for Plant-wide Systems*. John Wiley & Sons, 2016.

[208] G. Pannocchia, J.B. Rawlings, and S.J. Wright. Fast, large-scale model predictive control by partial enumeration. *Automatica*, 43(5):852–860, 2007.

[209] B.T. Stewart, A.N. Venkat, J.B. Rawlings, S.J. Wright, and G. Pannocchia. Cooperative distributed model predictive control. *Systems & Control Letters*, 59(8):460–469, 2010.

[210] M. Scherer and G. Andersson. How future-proof is the Continental European frequency control structure? In *IEEE Eindhoven PowerTech*, pages 1–6. IEEE, 2015.

[211] J. Stoustrup. Plug & play control: Control technology towards new challenges. In *European Control Conference (ECC), 2009*, pages 1668–1683. IEEE, 2009.

[212] R. Scattolini. Architectures for distributed and hierarchical model predictive control - A review. *Journal of Process Control*, 19(5):723–731, 2009.

[213] L. Magni and R. Scattolini. Stabilizing decentralized model predictive control of nonlinear systems. *Automatica*, 42(7):1231–1236, 2006.

[214] P. Trodden and A. Richards. Distributed model predictive control of linear systems with persistent disturbances. *International Journal of Control*, 83(8):1653–1663, 2010.

[215] Y.Q. Chen and Z. Wang. Formation control: A review and a new consideration. In *2005 IEEE/RSJ International Conference on Intelligent Robots and Systems*, pages 3181–3186. IEEE, 2005.

[216] M.A. Müller and F. Allgöwer. Distributed MPC for consensus and synchronization. In *Distributed Model Predictive Control Made Easy*, pages 89–100. Springer, 2014.

[217] E. Camponogara, D. Jia, B.H. Krogh, and S. Talukdar. Distributed model predictive control. *IEEE Control Systems Magazine*, pages 44–52, 2002.

[218] M. Farina and R. Scattolini. Distributed predictive control: a non-cooperative algorithm with neighbor-to-neighbor communication for linear systems. *Automatica*, 48(6):1088–1096, 2012.

[219] S. Li, Y. Zhang, and Q. Zhu. Nash-optimization enhanced distributed model predictive control applied to the shell benchmark problem. *Information Sciences*, 170(2):329–349, 2005.

[220] A.N Venkat. *Distributed model predictive control: theory and applications*. PhD thesis, Citeseer, 2006.

[221] G. Hahn. Boiler efficiency vs. steam quality-the challenge of creating quality steam using existing boiler efficiencies. 1998.

[222] R.J. Abraham, D. Das, and A. Patra. Load following in a bilateral market with local controllers. *International Journal of Electrical Power & Energy Systems*, 33(10):1648–1657, 2011.

[223] V.B. Kenneth, D. Erik, and D. William. Dc power flow in unit commitment models. Technical report, TME Working Paper-Energy and Environment, 2014.

[224] Michael G. and Stephen B. CVX: Matlab software for disciplined convex programming, version 2.1. `http://cvxr.com/cvx`, March 2014.

[225] G. Betti, M. Farina, and R. Scattolini. Distributed predictive control for tracking constant references. In *American Control Conference (ACC), 2012*, pages 6364–6369. IEEE, 2012.

[226] M.A. Hanley and J. Ilic. Frequency instability problems in North American interconnections. *National Energy Technology Laboratory: Pittsburgh, PA, USA*, 2011.

[227] B. Delfino, F. Fornari, and S. Massucco. Load-frequency control and inadvertent interchange evaluation in restructured power systems. *IEE Proceedings-Generation, Transmission and Distribution*, 149(5):607–614, 2002.